Hydraulic Performance and Chemical Compatibility of Mineral Barriers to Mitigate Natural Contamination from Excavated Rocks

Angelica Mariko Naka Kishimoto

ABSTRACT

Natural contamination of soil and groundwater by metals and metalloids has been responsible for serious health and environmental problems all over the world. Acid drainage, with subsequent heavy metal leaching (acid rock drainage, or ARD), is usually observed in countries located in geologically active areas, such as Japan, or in countries where mining is crucial for economic development, but with limited waste management for economic reasons, such as Peru.

ARD is produced when sulfide minerals such as FeS_2, Cu_2S, PbS, ZnS, $CuFeS_2$, or FeAsS are oxidized in the presence of oxygen and percolating water. Although this phenomenon occurs naturally, mining and excavation from infrastructure construction accelerate the generation of ARD by increasing the quantity of sulfides exposed. As sulfides are only stable under reducing conditions, exposing them to the atmosphere will destabilize them causing several oxidation reactions.

In those cases, there is a need for an efficient, cost-effective, and readily available solution. To this effect, the use of minerals as a barrier appears to be a good solution, since previous studies have suggested that several of them have large specific surface area, metal adsorptive capacity, self-healing capacity, and low hydraulic conductivity. However, the performance of these minerals when exposed to strong acid leachates with high heavy metal concentrations has not been yet well studied. Therefore, the main objective of this study is to evaluate the applicability of three minerals (bentonite, zeolite, and ferrihydrite) as bottom barrier layers in containment facilities for excavated rocks with ARD potential generation.

The first part of this research aims to characterize ARD in the world and choose representative ARDs (having pH = 3 and electrical conductivity or EC = 400 mS/m as referential points) to investigate the barrier performance of bentonite, zeolite, and ferrihydrite when exposed to different types of ARDs, according to the pH and EC. ARDs in the world are complex, difficult to predict, and pose different characteristics in terms of pH, EC, sulfate, and metal concentration. Statistical tools were used in this research to describe, summarize, and interpret 817 ARDs cases collected from several countries, and the limits (maximum, minimum, interquartile range, etc.) for each parameter for every type of mine (coal, gold, etc.) were determined. Relationships between metals and pH, EC, and sulfate, were also studied.

The barrier performance of bentonite contained in a geosynthetic clay liner (GCL), a commercial product that contains Na-bentonite supported by geotextiles and/or geomembranes, zeolite (clinoptilolite type), and ferrihydrite (FeO(OH)) against artificial ARDs was evaluated in terms of hydraulic conductivity (by performing swelling and hydraulic conductivity tests) and metal retention capacity (by performing batch sorption tests). Also a simple cost analysis for the material and installation was proposed.

The hydraulic conductivity of a GCL permeated with distilled water was 1.4×10^{-11} m/s, while ARD permeation with ten different ARDs ranged between 9.5×10^{-12} and 5.0×10^{-10} m/s, which represents a maximum one order of magnitude increase. The hydraulic conductivity of zeolite permeated with water was 3.0×10^{-10} m/s, while when permeated with the most severe ARD case was 1.4×10^{-9} m/s. The hydraulic conductivity of ferrihydrite was the highest among the three species with a hydraulic conductivity value of 7.3×10^{-9} m/s in the case of permeation with water. This value remained constant after ARD permeation

with the most severe ARD case, with a value of 8.6×10^{-9} m/s.

The swell index of bentonite, which is the only material among the three materials that shows swelling capacity, was also studied. A relationship between swell index and hydraulic conductivity for future predictions was also proposed based on previous equations reported in the literature. Relationships between EC and swell index and between EC and hydraulic conductivity were also proposed. Besides, several factors that affect the hydraulic performance of GCLs against ARD were also studied such as prehydration over non-prehydration, the effect of short and long term experimental tests, and the effect of type of bentonite was also investigated.

To evaluate the metal retention capacity of bentonite, zeolite, and ferrihydrite, single, bi-metal, and ARD sorption tests were conducted. From single metal batch sorption test results, it was observed that bentonite has higher sorption capacity against metals than zeolite and ferrihydrite, except in the case of As for which ferrihydrite was more suitable. The metal retention capacity for each mineral among single metals was: Bentonite: 13.2 mg Al/g bentonite, 71.0 mg Fe/g bentonite, 93.7 mg Cu/g bentonite, 47.1 mg Zn/g bentonite, 0.6 mg As/g bentonite, and 0.01 mg Pb/g bentonite; Zeolite: 1.0 mg Al/g zeolite, 23.7 mg Fe/g zeolite, 43.1 mg Cu/g zeolite, 13.1 mg Zn/g zeolite, 0.9 mg As/g zeolite, and 1.07 mg Pb/g zeolite; Ferrihydrite: 3.1 mg Al/g ferrihydrite, 22.4 mg Cu/g ferrihydrite, 17.7 mg Zn/g ferrihydrite, 2.3 mg As/g ferrihydrite, and 0.34 mg Pb/g ferrihydrite.

Different ARD dilutions showed that increasing ARD percentage (which correlates with an increase in metal concentration) positively impacts on As sorption. From the results of bi-metal solutions, it can be inferred that although GCL has no retention capacity towards As, the presence of Fe, Cu, Al, Zn, and Pb in the ARD may retard the mobilization of As from 51 to 71% when they are in 1:1 relationship (1 mM As: 1 mM metal), but this value increases if the metal proportion increases. The low hydraulic conductivity of GCL favors long-term contact between metals and As, making precipitation of As occur. It was found, therefore, that precipitation occurs as well as ion exchange (for bentonite and zeolite) and surface complexation (for ferrihydrite) mechanisms.

Combining the hydraulic performance and chemical compatibility, the relationship between total monovalent, total divalent, total trivalent, and sum of divalent and trivalent cations against hydraulic conductivity was discussed in order to predict the hydraulic conductivity through just the concentration of target metals. Metal release prediction from experimental results was also done, by calculating the period without any leakage as well as the concentration of metals in the groundwater after one and ten years.

The approximate cost of materials, installation and transport was calculated using a simple analysis, assuming a rock containment facility of 1 ha. For GCL, it was found that the total cost will be approximately 66,000 USD, whereas for zeolite and ferrihydrite, around 840,000 and 2,400,000 USD, respectively. These values may change according to the price of materials, availability, among others.

From the overall results presented in this research, it can be inferred that using GCL, zeolite, and ferrihydrite as barriers in rock containment facilities appears to be a good solution against ARD. In terms of material cost, transportation and installation, as well as barrier performance (low hydraulic conductivity and metal retention capacity, although limited buffering capacity), GCL seems to be the best option.

ACKNOWLEDGEMENTS

This study was possible thanks to a Nikkei Scholarship granted by The Nippon Foundation (Nippon Zaidan) and a Doctoral Course Scholarship granted by the Rotary Yoneyama Memorial Foundation. I am very grateful to Nippon Zaidan, Kaigai Nikkeijin Kyokai for the support and great opportunity to study in Japan and to the Rotary Club of Kyoto South for the support and hospitality of all Rotarians and the opportunities to attend events in Kyoto and learn more about Japanese culture.

I would like to expresses my deep and sincere gratitude to my supervisor, Dr. Takeshi Katsumi, Professor of the Graduate School of Global Environmental Studies at Kyoto University, the main advisor of this research, for his patience, motivation, enthusiasm, detailed and constructive comments, and for his important guidance and support throughout these three years of PhD study.

My special thanks go to Dr. Masashi Kamon, President of the Kagawa National College of Technology, for all his advice and valuable information he has provided since I was in Peru, for believing in me, and accepting me at the Graduate School of Global Environmental Studies.

I would also like to extend my gratitude to Dr. Toru Inui, Associate Professor of the Graduate School of Global Environmental Studies at Kyoto University, for providing me with his good vision to conduct research and making me concentrate on the important matters.

Special thanks to Dr. Masaki Takaoka, Professor of the Graduate School of Engineering at Kyoto University, for his valuable suggestions and comments on the content of this dissertation.

My sincere thanks also go to Takai-sensei, Assistant Professor of the Graduate School of Global Environmental Studies at Kyoto University, for his constant support with Japanese, papers and experimental work.

Special thanks to Dr. Giancarlo Flores (my dearest senpai), Associate Professor of the Graduate School of Engineering at Kyoto University, for his continuous help, encouragement, long discussions about life, constructive comments, suggestions about research, computer assistance, and also for his funny remarks and jokes that made me smile and laugh all the time.

I would like to thank Dr. Roy Henk, Associate Professor of the Graduate School of Energy Science at Kyoto University for his guidance with statistical concepts and analysis of the database presented in this research.

Special thanks to MD Pilar Suguimoto, Assistant Professor of the Department of Global Health and Socio-Epidemiology at Kyoto University for her support with statistical analysis.

I would also like to express my deep gratitude to Dr. Takehiro Ohta, Director of the Disaster Prevention Technology Division at the Railway Technical Research Institute (RTRI), for giving me the opportunity to join his research team for an internship in 2010 and work on his project and also for allowing me to use part of the results in this dissertation. Special thanks to Mr. Takuya Urakoshi, Assistant Senior Researcher of the Geology Group at RTRI, and Tomokazu Ishihara, temporarily transferred to the Japan Railway Construction, Transport, and Technology Agency (JRTT), for the long discussions about research and their patience and support throughout the internship period.

My special thanks go to Yasumoto-san, the laboratory Assistant, and my laboratory friends (senpais and kohais) of the Environmental Infrastructure Engineering Laboratory at Kyoto University for all the fun we have had during these three years of PhD and for making me enjoy the laboratory life. Special thanks to Mogami-san, Haruka-chan, Katayama-san, Yano-chan, Sano-chan, Kihara-san and Kimura-san for their kind support and help with Japanese proof reading not only related to research but also extracurricular activities.

I would like to thank my PhD batch friends at the Graduate School of Global Environmental Studies Harris, Naoko-san, Ria, and Farah, for their important company and their encouragement since the beginning of the PhD.

I would like to express my gratitude to the Aoki family, my host family during the last year of my PhD, for taking care of me and make me feel home. Special thanks go to Mr. Aoki (my father in Japan), member of the Rotary Club of Kyoto South, for inviting me to events and giving me the opportunity to learn more about Kyoto and Japanese culture and for all his advice, suggestion, and encouragement.

Special thanks to my dear friends, the Peruvians (my dear *Perujines*) I met in Kyoto (Pilar, Cecilia, Satomi, Jimena, Giancarlo, Carlos, Akira, Manuel, and Oscar) without whom life in Kyoto would not be as fun as it has been. Together we spent birthdays, Christmases, New Year celebrations, BBQs, picnics and other excuses we made up to gather and spend time together.

I am infinitely thankful to my parents, Yoriko and Tatsunori, my two sisters in Peru (Agnes and Monica), and my sister and brother in England (Andrea and Jonathan) for their unconditional love, advice, care and emotional support, as well as their visits (thanks Andrea and Jonathan for coming to Japan several times and spoiling me during your stay!), phone calls, generous presents, and emails that made me feel closer to home. Without their encouragement it would have been impossible for me to finish this work.

And last but not least, I would like to thank Yoshihiro, my husband, for all his love, patience, and encouragement. Although living and working in Tokyo since we started dating, his every-day phone calls after his job and effort to come to Kyoto and visit me every weekend meant a lot to me. Thanks to him, my last four years in Japan were amazing and my understanding of Japanese culture and Japanese skills increased very much as well.

TABLE OF CONTENTS

LIST OF FIGURES

LIST OF TABLES

LIST OF ABBREVIATIONS

AMD:	Acid Mine Drainage
ARD:	Acid Rock Drainage
ASTM:	American Society for Testing and Materials
CEC:	Cation Exchange Capacity
DPH-GCL:	Dense-Prehydrated Geosynthetic Clay Liner
EC:	Electrical Conductivity
GCL:	Geosynthetic Clay Liner
ICP:	Inductively Coupled Plasma
ICP-MS:	Inductively Coupled Plasma – Mass Spectrometry
k:	Hydraulic Conductivity
MSB:	Multi Swellable Bentonite
NA:	Not Available / Not Applicable
NS:	No Sorbent
ORP:	Oxidation Reduction Potential
PC:	Polypropylene Carbonate
pH:	Potential Hydrogen
PVF:	Pore Volume of Flow
SEM:	Scanning Electron Microscopy
TMC:	Total Monovalent Cations
TDC:	Total Divalent Cations
TTC:	Total Trivalent Cations
TDTC:	Sum of Total Divalent and Trivalent Cations
XRD:	X-Ray Diffraction

1 INTRODUCTION

1.1 General Remarks

Excavated soils and rocks are generated in large quantities worldwide every year from economically essential practices such as construction and mining. Reusing or recycling of these materials would reduce the use of new resources by utilizing otherwise wasted materials. This would save space in landfills, which would be particularly beneficial in countries with limited space such as Japan, and decrease the environmental impact in countries where mining is economically important, such as Peru.

The Japanese government has encouraged industries and consumers to follow the "3R Concept", which consists of "reduce", "reuse", and "recycle", in order to contribute to sustainable development. Reusing materials will reduce the amount of disposed of by-products and waste and also reduce the amount of natural resources used. In 1991, the "Law for the Promotion of the Utilization of Recyclable Resources" was established. According to this law, the following items generated by the construction industry are considered to be recyclable by-products: (1) steel slag discharged from iron and steel manufacturing; (2) coal ash from electric power plants; and (3) waste cement-concrete, waste asphalt-concrete, waste wood, waste sludge, etc. In addition, in 2000, the "Basic Law for Establishing the Recycling-based Society" was issued. The purpose of this Law is to make possible the policies to transform Japan into a "Resource Recycling Society". Under this, individual laws were established to encourage different industries to use specific recyclable materials. In the case of construction industry this law was called "Law for the Recycling of Construction Materials". Moreover, in 2002, the "Soil Contamination Countermeasures Law", related to the influence on the reuse of surplus soils generated from construction works, has been established.

According to the data collected from the Japan Ministry of Land, Infrastructure, and Transport, different types of waste are generated every year from construction works (Table 1-1). Table 1-2 shows the amount of waste disposed in landfills, and so the differences in mass between Table 1-1 and Table 1-2 correspond to reused material. Beneficial reuse (recycling) of waste asphalt concrete and cement concrete is currently high (98 to 99%). However, only 45% of waste sludge is reused, while 30% of this material is disposed. In addition, surplus soil, which is not categorized as waste, has been generated in large quantities (around 141 million m^3) in 2008, of which 30% (42 million m^3) was reused in construction sites. Figure 1-1 presents the estimated material flow of surplus soil in Japan. It shows the amount of this material disposed in landfill sites (legally and illegally dumped), as well as the use of new material. The use of new soil materials extracted from mountains or river beds is around 32 million m^3, which results in a negative impact on the environment (Katsumi et al. 2008c; Katsumi et al. 2010).

Mining activities also produce huge amounts of liquid, solid, and gaseous waste or by-products from mining, mineral processing, and metallurgical extraction. Mine solid wastes constitute the highest proportion of waste produced by the industry, with 15,000 to 20,000 Mt approximately generated annually (Lottermoser 2007). Waste from mining operations can be classified as mining waste, processing waste, metallurgical waste, and mine water (Table 1-3).

Table 1-1 Generation of waste from construction works (unit: 10,000 ton)

Year	1995	2000	2002	2005
Asphalt concrete	3,570	3,010	2,970	2,610
Cement concrete	3,650	3,530	3,510	3,220
Wood waste	630	480	460	470
Sludge	980	830	850	750
Mixed waste	950	480	340	290
Others	140	150	140	360
Total	9,910	8,480	8,270	7,700

Table 1-2 Landfill amount of waste from construction works (unit: 10,000 ton)

Year	1995	2000	2002	2005
Asphalt concrete	680	50	40	40
Cement concrete	1,290	130	90	60
Wood waste	390	80	50	40
Sludge	840	490	270	190
Mixed waste	850	440	220	210
Others	90	100	100	60
Total	4,150	1,280	700	600

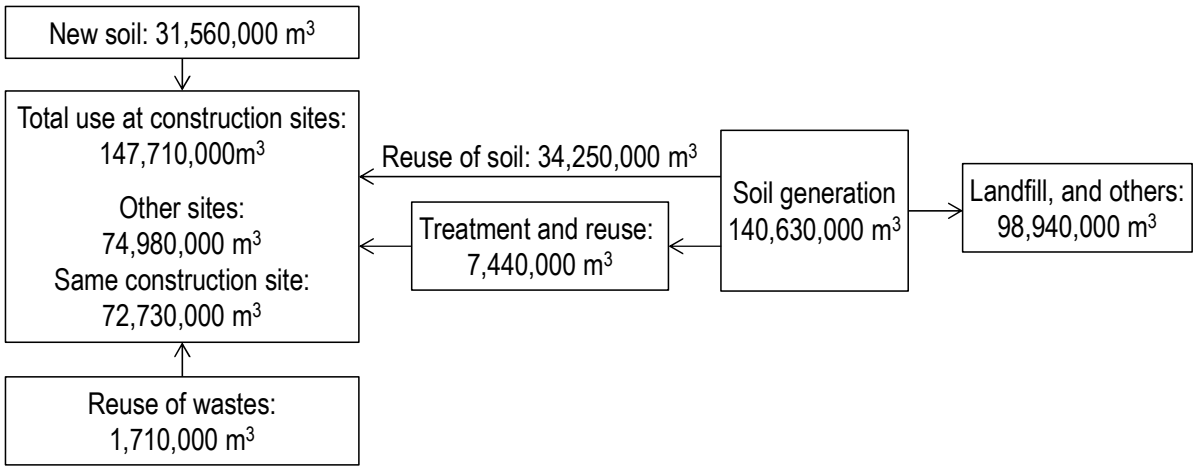

Figure 1-1 Volume of generated surplus soil and its reuse in 2008

Table 1-3 Mine waste (Lottermoser 2007)

Waste	Characteristics	Particle size
Mining waste	Materials from surface or underground mining operations to access and mine ore. They do not contain (if contains, very low concentration) ore minerals, industrial minerals, metals, coal or mineral fuels.	Sedimentary, metamorphic or igneous rocks, soils and loose sediments. The particle size range from clay size particle to boulder size fragments.
Processing waste	Residue after washing the ore, gravity, magnetic, electrical or optical separation, crushing and sizing, grinding and milling.	Tailings, sludges and waste water. The particle size range from colloidal to coarse, gravel size
Metallurgical waste	Residues of the hydrometallurgy, pyrometallurgy and electrometallurgy	Atmospheric emissions, roasted ore, slag, ash, flue dust, waste water.
Mine water	Any surface water and subsurface groundwater present at a mine site used for dust suppression, mineral processing, coal washing, and hydrometallurgical extraction.	---

The physical and chemical properties of mine waste or rocks excavated from mining depend on several factors, including mineralogy and geochemistry, the type of mining, and particle size. Some mine waste has the potential to be reused, such as for backfilling the mine reclamation and rehabilitation of mined areas, road construction, complete extraction (caused by unfavorable economics, inefficient processing, technological limitation, or mineralogical factors), and by the agricultural and building industries (clay-rich soil wastes can improve sandy soils or be used as the raw materials for brick manufacturing). However, an economically feasible and effective method of disposal must be found for the majority of waste. Disposal usually involves dumping the solid waste at the surface next to the mine (Lottermoser 2007).

To the author's best knowledge, no specific laws and/or regulations exist on the reuse of excavated materials coming from construction and mining. However, when recycled materials are used in geotechnical applications, such as embankments, the potential for pollution or natural contamination should be considered. Some by-product materials, such as industrial waste (coal ash, slag, and scrap tire) and municipal solid waste (MSW) incinerator ash may contain toxic chemicals (heavy metals, boron, fluorine, among others). In addition, some of them have the potential to induce an adverse environmental

effect even following treatment prior to the geotechnical application. Thus, the characterization of soil and waste becomes a very important source of information in order to judge whether or not a certain type of soil and/or waste would be environmentally compatible. For this purpose, leaching (or elution) and composition (human availability) tests are conducted and the results are used to determine whether the leaching level exceeds the environmental standards. If it does, necessary measures should be taken in order to prevent a negative environmental impact (Katsumi et al. 2008a; Katsumi 2010).

Natural contamination of soil and groundwater by metals and metalloids derived from waste rock and mine tailings has caused serious health and environmental problems in many countries. Acid rock drainage (ARD), with subsequent heavy metal leaching, which are not degradable by simple mechanisms and will remain present for a long time, is usually observed in countries located in geologically active areas, such as Japan (Ohta et al. 2006), or in countries where mining is crucial for economic development with limited waste management due to economic reasons, such as Peru.

ARD is produced when sulfide minerals such as FeS_2, Cu_2S, PbS, ZnS, $CuFeS_2$, or FeAsS are oxidized in the presence of oxygen and percolating water. Although this phenomenon occurs naturally, mining and infrastructure construction excavation accelerate the generation of ARD by increasing the quantity of sulfides exposed. Exposing these rocks to the atmosphere destabilizes them and, therefore, oxidation will occur. Sulfide oxidation and host rock dissolution do not end until the mineral is fully weathered, which can take hundreds of thousands of years.

In recent years, many parties, including governments, have started to become aware of natural contamination when excavated soils are reused in geotechnical applications. In Japan, particularly, several types of metals such as As and Pb are present in higher concentrations compared to the average level in the world (Table 1-4). This is because Japan is located in a geologically active area, which favors the accumulation of these elements. Moreover, in mountainous areas of Japan, there are several rock formations which may contain pyrite (FeS_2) and other minerals that contain high amounts of As and Pb.

Table 1-4 Compositions of metals naturally contained in the geologic strata (Katsumi et al. 2010)

	Global average (Clarke number) (mg/kg)	Average of element composition of crust at the continents (mg/kg)	Average of element composition of upper crust of Japan (mg/kg)	Average of element composition of river sediments in Japan (mg/kg)
As	1.8	1	6.5 – 7.1	9.32
Pb	13	8	16.9	23.1
F	625	625	---	---
B	10	10	---	---
Hg	0.08	0.08	---	0.054
Cd	0.2	0.098	---	0.158
Cr	100	185	84	65.2

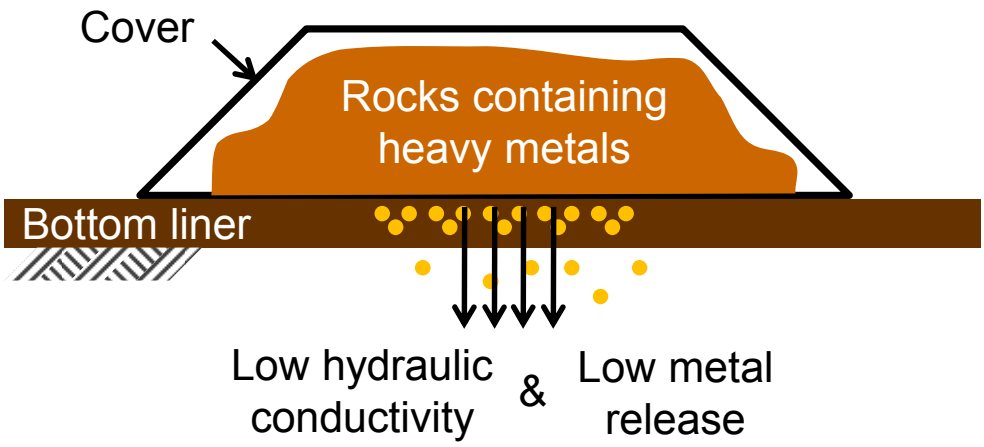

Figure 1-2 Rock containment facility to prevent natural contamination

Thus, acid drainage with subsequent As and Pb leaching becomes an important issue (Tabelin and Igarashi 2009; Tabelin et al. 2010; Tabelin et al. 2012a; Tabelin et al. 2012b; Tatsuhara et al. 2012; Igarashi et al. 2013). To prevent this environmental problem from spreading, constructing an adsorption layer is considered a relatively new and cost-effective measure, and it is the method studied by the author. This method places a layer of material (geosynthetic clay liners (GCLs) that contain bentonite, zeolite, or ferrihydrite, for example) that has adsorption capacity against heavy metals, as shown in Figure 1-2. This will help keep the groundwater clean and will guarantee health and environmental security and, if the area was not to be used for human water consumption but for crop irrigation, food security as well.

In the past, remediation technologies were focused on physical covers to reduce the production of acids by limiting infiltration of water and oxygen (Lange et al. 2010a). However, recent research has suggested that potentially toxic elements, particularly As, Se, and in some cases Ni and Zn, are mobile even under neutral pH-conditions (Rowe 2006; Lange et al. 2010a; Shackelford et al. 2010). Moreover, the reductive dissolution of As-bearing minerals has resulted in the release of As (Rowe 2006). As a result, disposal of excavated of rocks from construction and mining is moving towards storage of hazardous materials in a lined containment facility (Lange et al. 2007). So, GCLs or bentonite, as well as other mineral materials such as zeolite and ferrihydrite represent a potentially attractive means of controlling contaminants.

GCLs play an important role in providing cost effective barriers for environmental protection in a wide range of applications, including recent applications in the mining industry (Lange et al. 2007, 2009, 2010a). The low permeability and high attenuation capacity offered by the Na-montmorillonite in GCLs suggests that they may be particularly beneficial for this type of application. However, like all engineering materials, they need to be carefully and correctly placed and protected from damage in order to maintain long-term performance. There are several factors that can affect the performance of GCLs, including, but not limited to: the effect of the degree of saturation with certain chemicals; the effect of freeze-thaw cycles; the effect of subzero temperatures on the permeability of saturated and unsaturated GCLs; the potential for internal

erosion of GCLs; the susceptibility of GCLs to shrinkage and desiccation; the diffusion of ions through GCLs; the leakage through GCLs; and the interaction between GCLs and acid rock drainage (Rowe 2006; Shackelford et al. 2010).

Previous studies have suggested that GCLs have potential as barrier materials for the containment of metal-bearing wastes because of their capability to retard the movement of metals or high metal attenuation capacity (Lange et al. 2005; Rowe 2006). Thus, it is important to examine the sequence of the reactions that are occurring, as well as the mechanism of metal attenuation, such as the role of sorption onto Na-bentonite and sorption onto Fe hydroxides including the effect of reducing conditions on the long-term stability of this hydroxide, as well as factors that cause changes in GCLs performance, in order to guarantee a long-term durability of the GCLs.

Several studies can be found in the literature that focus on the mechanical properties of the GCLs, but very few regarding the chemical changes that occur within the GCLs, especially when permeated with solutions containing high concentrations of metals and metalloids (Lange et al. 2007; Shackelford et al. 2010). In addition, many issues related to metal interactions with GCLs are often explained using data exclusively from sorption experiments on Na-bentonite (with only a few of them using Na-bentonite taken directly from GCLs), cation exchange capacity (80 – 100 meq/100 g), and surface area (800 m^2/g) of Na-montmorillonite. In addition, for the majority of studies, this information is obtained after experiments performed under single or equimolar multi-metal permeants. Previous studies have demonstrated that the chemical composition of solutions greatly affects the order in which metals are retained into GCLs (Lange et al. 2005, 2007). Thus, it can be inferred that the behavior of a single metal batch test cannot be simply extended or applied to ARD cases, because metal behaviors may differ when combined.

Zeolite and ferrihydrite also represent low-cost and readily available materials as potential sorbents for the removal of heavy metals in solutions. Zeolite is widely geographically distributed and ferrihydrite is usually part of clays, soils, and sediments. Zeolite, similar to bentonite, has a cage-like structure suitable for ion exchange due to isomorphous replacement of Al^{3+} with Si^{4+} in the structure, which leads to a deficiency of positive charge. This is balanced by innocuous cations that are exchangeable with certain cations such as lead, cadmium, zinc, and manganese. Clinoptilolite is the most abundant natural zeolite, and although zeolites from different regions show different behavior, previous studies have reported that this mineral generally shows preference for metals in the following order: $Pb^{2+} > Cd^{2+} > Cs^{+} > Cu^{2+} > Co^{2+} > Cr^{3+} > Zn^{2+} > Ni^{2+} > Hg^{2+}$ (Erdem et al. 2004). Research on ferrihydrite has shown that this material has high potential to remove arsenic, lead, and cadmium from contaminated water because of its large surface areas and abundance of binding sites.

Even though bentonite, zeolite, and ferrihydrite are found to have an intermediate to high capacity to retain certain metals, they have not been tested against a complex mixture of heavy metals. So, in order to evaluate their potential to treat ARD problems, it is important to understand to what extent metals can be retained into these minerals, as well as to evaluate the competition of metals and elucidate the mechanism of how metals become retained within the structure or surface of these minerals. This study becomes even more important when projecting the long-term fate of metals within these mineral barriers, as many factors such as

pH, electrical conductivity, redox potential, saturation, temperature, among others that influence these mechanisms may change over time.

1.2 Objectives

The main objective of this study is to evaluate the applicability of GCL, zeolite, and ferrihydrite as bottom barrier layers in containment facilities for excavated rocks and soils with ARD potential generation. In order to do so, this main objective was subdivided in four parts: (i) to characterize ARDs in the world; (ii) to study the hydraulic performance of GCL (bentonite), zeolite, and ferrihydrite against different ARDs; (iii) to evaluate the chemical compatibility of these minerals against the same ARDs; and (iv) to estimate the field application potential of these mineral barriers.

For the characterization of ARDs, several ARD compositions from different publications were collected and analyzed using statistical tools. For studying hydraulic performance, ten ARDs from the database generated from the collected data (with pH ranging from 2.6 to 10 and electrical conductivity ranging from 40 to 1000 mS/m) were selected to test the swelling capacity (only for GCL or bentonite) and hydraulic conductivity of GCL, zeolite, and ferrihydrite. For the study of the chemical compatibility, batch sorption tests on bentonite, zeolite, and ferrihydrite at different single metal concentrations, bi-metal concentration, and the ten selected ARDs were conducted. For the field application potential of GCL, zeolite, and ferrihydrite, hydraulic conductivity and metal release prediction after 1 and 10 years, as well as simple cost analysis were done.

Even though previous studies conducted by other research teams have shown that bentonite, zeolite, and ferrihydrite have metal ion attenuation capacity, their barrier performance when exposed to strong acid leachates with high heavy metals concentration remains unknown. So, this study aims to provide information about the behavior of these minerals when subjected to extreme conditions of pH and metal content in terms of hydraulic performance and chemical compatibility.

1.3 Outline of the Research

This research thesis has been divided in 7 chapters: Chapter 1 aims to clarify the objectives and to outline the contents of this research. Chapter 2 reviews the sources and origins of heavy metals and ARD, as well as their treatment methods, focused on the construction of bottom liners and their barrier performance in terms of hydraulic conductivity and sorption of heavy metals into bentonite, zeolite, and ferrihydrite. Chapter 3 describes the ARDs in the world based on the 817 ARD compositions collected from different publications by using the statistical softwares R and SPSS. Chapter 4 presents the results of hydraulic conductivity tests of GCL against 10 different ARDs selected from the database analyzed in Chapter 3. A comparison of the hydraulic performance of GCL with zeolite and ferrihydrite was also presented. Chapter 5 shows the results of batch sorption tests on bentonite against different metals, including varying

concentrations and combinations, and complex metal systems (natural rock leachates and artificial ARDs). A comparison of the chemical compatibility of bentonite with zeolite and ferrihydrite was also presented. Chapter 6 presents the practical implications of this research. This chapter utilizes the results obtained in the previous chapter in order to predict the hydraulic conductivity and the metal retention in mineral barriers. The costs of applying this technology in the field are also estimated. Chapter 7 summarizes the results of this research and suggests areas for further research and possible applications of the results, both in the laboratory and in the field.

1.4 Originality of the Research

Although ARDs differ in terms of metal concentration and pH, this research aims to understand ARDs in the world in terms of pH, metal concentration, and relationships among parameters. It intends also to clarify to what extent and/or in which cases GCL, zeolite, and ferrihydrite can be used to as bottom liner in containments for rocks with potential of ARD generation. This research presents the result of the barrier performance of these minerals against 10 different ARDs carefully selected and studied in order to quantify the effect of pH and electrical conductivity in physical (hydraulic conductivity) and chemical properties (sorption capacity). One of the ARDs used in this research has very high metal concentrations (the pH was 3 and the EC was around 1000 mS/m), especially Fe. The artificial ARD corresponds to the composition of an acidic lake caused by the discharge of acid rock drainage from an Fe rich (more than 4000 mg/L) Pb-Zn-(Cu) deposit located in Cerro de Pasco, Peru. This composition was selected as an example to demonstrate how serious this problem can be in terms of metal concentration and pH not only to the environment, but also to people's health and safety. The long-term nature of the hydraulic conductivity experiments makes this work also different from previous research. Nine-month tests are important to verify the tendencies of hydraulic conductivity and metal release over time, which are critical issues for long-term soil material storage or to contain rocks. Besides, sorption with single, bi-metal, and multiple metal batch sorption test aims to provide information about the compatibility and capacity of bentonite, zeolite, and ferrihydrite to sorb certain contaminants, as well as the role of metals present in ARD in the immobilization of As, especially when minerals are not able to retain it. Moreover, the relationship between swelling and hydraulic conductivity is a useful tool to predict the hydraulic conductivity without conducting experiments, especially for field applications. In addition, metal transport through these minerals was calculated and the relationship between total monovalent cations, total divalent cations, total trivalent cations, and sum of divalent and trivalent cations against hydraulic conductivity was also established, which will be useful for future predictions. A simple cost analysis was also conducted in order to determine the total cost of material, installation, and transport of each material in the field.

2 LITERATURE REVIEW

2.1 General Remarks

Metals and metalloids contaminating soils and groundwater are worldwide environmental problems that started during the industrial revolution and have accelerated dramatically since then. Heavy metals present in soils and groundwater include Cd, Cu, Pb, Hg, Cr, Ni, Zn, Mn, Mo, Se, B, and As, all of which represent risks to human health and the environment, especially because they are not degradable by natural processes. There are three main pathways through which heavy metals can come into contact with living organisms (Bradl 2005). The first way is through atmosphere deposition to water and soil; secondly through drinking contaminated water or using it for cooking and crop irrigation; and thirdly through accumulation in the food chain.

This chapter gives a general introduction into heavy metal sources, focusing on the acid rock drainage (ARD), which represents one of the cases with extreme conditions of pH and heavy metal concentration. In addition, several remediation techniques are described, emphasizing the use of low-cost adsorbents and locally available materials (bentonite, zeolite, and ferrihydrite) that have been already reported in the literature to have intermediate to high removal capability for certain metal ions, but have not yet been tested under ARD conditions.

2.2 Sources and Origins of Heavy Metals

Sources of heavy metals in the environment can be classified by origin: natural or anthropogenic. This section provides general information about the different heavy metal sources, such as rock types (magmatic, sedimentary, and metamorphic), soil formation, and human activities (agriculture, mining, among others).

2.2.1 Natural Sources

The principal natural sources of heavy metals in the environment are rocks and soils. The primary rocks (magmatic or igneous rocks) are formed from magma cooling. Magma, which is molten rock, contains a large variety of different chemicals, including heavy metals. They are incorporated as trace elements into the crystal lattice of the primary minerals. The second type is sedimentary rocks, which are the result of physical or chemical weathering. In case of physical weathering, particles (sediments) are formed; in the case of chemical weathering, the rocks are dissolved into ions. Metamorphic rocks constitute the third rock type, which are the result of chemical alterations of magmatic, sedimentary or metamorphic rocks due to an increase in temperature and pressure.

The other source of metal and the most important element for the terrestrial ecosystem is soil. It constitutes the end of the weathering processes of consolidated rocks. Its formation is influenced by the climate, soil organisms, topography, type of parent rock, and time. Therefore, the natural concentrations of

heavy metals vary significantly from one ore to another. During the soil development, different layers are developed, which constitute the soil profile (Figure 2-1).

The first layer is called the O-horizons and consists of decomposed organic matter. The underlying A horizon is composed of minerals and organic matter and is subjected to leaching by rainwater filtration. The underlying B horizon is characterized by a large content of clay minerals and Fe oxyhydroxydes, which are able to absorb heavy metals. Finally, the C horizon is composed of partially weathered parent rock, which is followed by unaltered parent rock. The soil composition varies according to the parent rock. If a soil is derived from basalt, which is a rock enriched in Cr, Co, and Ni, this soil is expected to contain high concentration of those elements.

2.2.2 Anthropogenic Sources

Heavy metals are released into the environment through many human activities. It occurs at three different stages: at the beginning of the production chain whenever ores are mined; during the use of products containing them; and at the end of the production chain (Bradl 2005). The main anthropogenic sources of heavy metals are agricultural activities (use of pesticides, fungicides, and fertilizers), metallurgical activities (mining, smelting, metal finishing, and others), energy production and transportation, microelectronic products, and waste disposal.

One recent environmental concern is related to the disposal of excavated rocks from construction and mining operations, especially due to their potential release of heavy metals. These activities involve the

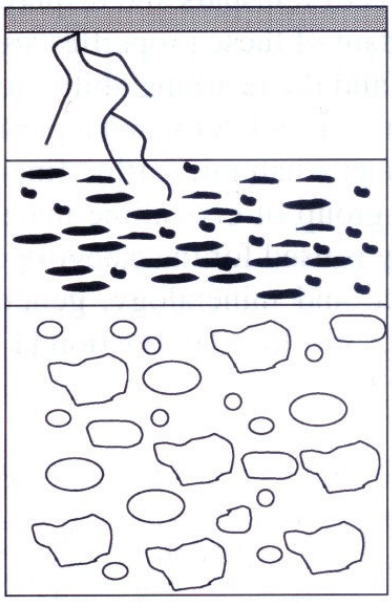

Figure 2-1 Soil horizons (Bradl 2005)

transport of large amounts of waste rocks which still contain traces of heavy metals that have not removed from the ore-bearing rock. These rocks, when disposed of without proper treatment, become an important source of toxic and hazardous substances (heavy metals) into the environment. Pyrite, for example, will weather in the tailing due to oxidizing environmental conditions and thus create acid that mobilizes heavy metals from the waste rock. This phenomenon is called ARD.

2.3 Acid Rock Drainage (ARD)

ARD, also referred to as acid mine drainage (AMD) is characterized by low pH values, high concentration of heavy metals and other toxic elements. ARD is produced when sulfide minerals such as FeS_2, Cu_2S, PbS, ZnS, $CuFeS_2$ or FeAsS are oxidized in the presence of water and air.

Even though this phenomenon occurs naturally, mining and excavation accelerate the generation of ARD by increasing the quantity of sulfides exposed. Since sulfides are only stable under strongly reducing conditions, exposing them to oxidizing conditions will destabilize these rocks and make them oxidize through a variety of mechanisms. Among sulfide minerals, pyrite is the most abundant and thus has been extensively studied from all scientific angles and there is a vast range of literature about it.

Several chemical reactions are commonly used to describe pyrite's oxidation mechanisms. In the abiotic and biotic direct oxidation processes, oxygen directly oxidizes pyrite (Lottermoser 2007):

$$FeS_{2(s)} + \frac{7}{2}O_{2(g)} + H_2O \rightarrow Fe^{2+} + 2SO_4^{2-} + 2H^+ + \text{energy} \quad (2.1)$$

The dissolved Fe^{2+}, SO_4^{2-}, and H^+ represent an increase in the total dissolved solids and acidity of the water and, unless neutralized, induce a decrease in pH. If the surrounding environment is sufficiently oxidizing, much of the ferrous iron will oxidize to ferric ions, according to the following reaction:

$$Fe^{2+} + \frac{1}{4}O_2 + H^+ \rightarrow Fe^{3+} + \frac{1}{2}H_2O \quad (2.2)$$

At pH values between 2.3 and 3.5, ferric ions precipitate as $Fe(OH)_3$ and jarosite, leaving little Fe^{3+} in solution while simultaneously lowering pH:

$$Fe^{3+} + 3H_2O \rightarrow Fe(OH)_{3(s)} + 3H^+ \quad (2.3)$$

Any Fe^{3+} from Equation (2.2) that does not precipitate from solution through Equation (2.3) may be used to oxidize additional pyrite, according to the following reaction:

$$FeS_{2(s)} + 14Fe^{3+} + 8H_2O \rightarrow 15Fe^{2+} + 2SO_4^{2-} + 16H^+ \quad (2.4)$$

All the equations assume that the oxidized mineral is pyrite and the oxidant is oxygen. Additional oxidants and sulfide minerals have different reaction pathways, stoichiometries, and rates, but research on these variations is limited.

ARDs around the world differ in acidity and metal concentrations. They usually represent a threat to groundwater and surface water at mining sites because of their extremely low pH and high metal content.

Lottermoser (2007) described five field indicators of ARD :

- pH values less than 5.5: low pH values are found due to the oxidation of sulfide minerals.
- Disturbed or absence of fauna or flora: caused by to the low pH and high metal concentrations.
- Precipitated mineral efflorescences covering stream beds and banks: yellow-red-brown precipitation (iron hydroxides).
- Discolored, turbid or exceptional clear water: the turbidity of ARD water decreases downstream as the Fe and Al flocculate and salts precipitate with increasing pH. As a result, acid water appears very clear.
- Abundant algae and bacterial slimes: the elevated levels of sulfate favor the growth of green or brown algae.

The most common elements found in ARD from metallic mine wastes are sulfur, iron, copper, zinc, silver, gold, cadmium, arsenic, and uranium (Ripley et al. 1996). Considering that there is no typical composition of ARD, classification of ARD is difficult to achieve. Mine water composition depends on the mined ore and chemicals additives from mineral processing. Morin and Hunt (1997) proposed a classification of the ARDs according to the pH (Table 2-1).

Several factors affect the chemistry of ARD. The initial chemistry depends on geological and geochemical controls including the type and abundance of metal-bearing sulfides in ore and wall rock, kinetic rates of ore and wall rock dissolution, permeability of the ore deposit or mine tailings, and the ability of the host rock to buffer acidity (Plumlee et al. 1992; Strömberg and Banwart 1994).

Limited information about the typical composition of water effluents according to the type of mine is available in the literature. Therefore, detailed studies on the metal composition, pH, electrical conductivity, and sulfate concentration for different type of mines are presented in Chapter 3, using a database with information collected from several publications. An approach to characterize sulfide and coal mine operations was done by Gazea et al. (1996) and the results are presented in Table 2-2.

Table 2-1 Classification of ARD according to the pH (after Morin and Hunt (1997))

Class	Characteristic
Extremely acid	pH < 1: Rocks enriched in pyrite and depleted in acid buffering materials
Acid	pH < 5.5: Oxidation of Fe-rich sulfides. Commonly found at base metals, gold and coal mines
Neutral to alkaline	pH 6 – 10: Acid producing and acid buffering keep a pH balance or abundant Fe-rich sulfides are absent
Saline	pH highly variable: Associated with the mining of coal and industrial minerals

Table 2-2 Typical mine drainage composition (after Gazea et al. (1996))

	Coal mines (mg/L, except pH)	Cu-Pb-Zn mixed sulphide mines (mg/L, except pH)
pH	2.6 – 6.3	2 – 7.9
Fe	1 – 473	8.5 – 3200
Zn		0.04 – 1600
Al	1 – 58	
Mn	1 -130	0.4
Cu		0.005 – 76
Pb		0.02 – 90

2.4 Heavy Metal Treatment Methods

To mitigate contamination by heavy metals, many remediation technologies have been proposed. Three of the traditional available clean–up technologies are: excavation or removal of polluted soil and proper disposal; stabilization of toxic metals in soil by adding chemical agents or forcing an anaerobic environment; and phytoremediation, or use of plants to extract heavy metals from soil or prevent the spread of contamination. Other new technologies propose electrokinetic methods, soil flushing and washing, and the use of industrial by–products like fly ashes and slags, taking advantage of their high adsorption capacity toward metals. However, since most heavy metal treatment technologies are usually found to be inadequate, difficult, time consuming, environmentally destructive, or expensive, this problem is left untreated majority of the time (Akcil and Koldas 2006).

In the case of excavated rocks with potential for heavy metal leaching, there are several requirements listed (Bradl 2005) that are important to be considered. First, the site for rock disposal should be selected according to its geological and hydrogeological characteristics (low permeability underground such as clay, large distance to groundwater levels, no karst, no earthquakes or volcanic activities, no mass movements, etc.). Second, the site has to be equipped with barrier systems both on the base and the top of the deposit in order to prevent spreading of contaminants from the mineral and the leachate into the environment. Third, leachate and gas collection system should allow for collection and transfer of gas and leachate to treatment plants for heavy metal removal. Finally, the site should be constantly monitored by air sampling devices and wells sunk outside its periphery.

Regarding barrier systems for deposit on the base (bottom liner), geosynthetic clay liner (GCL) seems to be a good alternative. Previous studies suggest that, due to its low hydraulic conductivity, large specific surface area, and high attenuation capacity, Na-bentonite present GCLs can be used to attenuate toxic substances present in ARD (Lange et al. 2007, 2010a), such as heavy metals. These metals can be immobilized in GCLs through many adsorption mechanisms: cation exchange; surface complexation; surface-induced precipitation; surface co-precipitation; colloid formation at surface; and diffusion into

particle micropores. In addition, a recent mixture has been proposed consisting of limestone (40 to 75 weight percent), clay (10 to 35 weight percent), and magnesium oxide or magnesium hydroxide (10 to 30 weight percent) that can efficiently control ARD, that supports the important role of clay in the attenuation of heavy metals present in ARD (Barnes 2008). As briefly mentioned before, due to its large cation exchange capacity (between 80 and 150 meq/100g), high surface area (around 800 m^2/g) and ability for interlayer swelling, Na-montmorillonite, the principal mineral component of Na-bentonite used in many GCLs, has a great affinity for cation or metal ions. However, most of the studies that have been conducted to examine the engineering performance of GCLs are in presence of salt solutions and municipal solid waste leachates. So, the performance of this material in presence of metal-rich leachates and low pH values is not well investigated and will be the subject of this research.

One of the main functions of GCLs applied to the containment systems in landfill or impoundments is the barrier function. Therefore, an index that can evaluate the difficulty posed to liquid to pass through a GCL is necessary. In this research the physical (hydraulic conductivity value) and chemical (metal sorption or release) performance are evaluated for a GCL. The physical performance is detailed in Chapter 4 and the chemical performance in Chapter 5.

2.5 Geosynthetic Clay Liner (GCL)

GCL is a thin (typically 5-10 mm) commercial hydraulic barrier that has been extensively used since the mid-1980s in both landfill liners and final covers because of their relatively low cost, easy installation, and excellent barrier performance to water. It consists of a layer of dry powdered clay supported by geotextiles and/or geomembranes, held together by needling, stitching, or chemical adhesives (Figure 2-2and Figure 2-3). The clay usually used in GCLs is bentonite as this has a very low permeability to liquid and gases and a high potential to swell when hydrated.

Figure 2-2 Geosynthetic clay liner

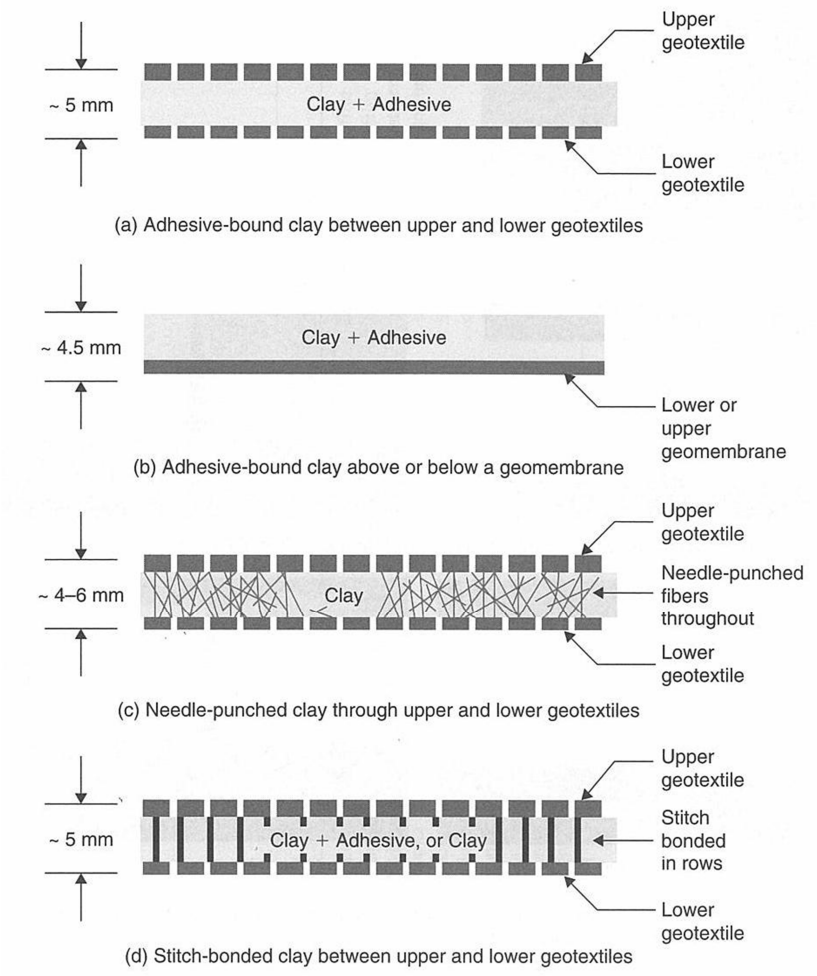

Figure 2-3 Cross sections of currently available GCLs (Koerner and Koerner 2010)

Clays have a layer structure of two-layer minerals and of three-layer minerals (Figure 2-4). Bentonite belongs to the smectite group, one of the most important and common mineral groups in soils, along with kaolin and illite group. Smectites belong to the three-layer minerals and are composed of units consisting of two silica tetrahedral sheets with a central alumina octahedral sheet (Figure 2-4). As the lattice has an unbalanced charge because of isomorphic substitution of alumina for silica in the tetrahedral sheet, and of iron and magnesium for alumina in the octahedral sheet, the attractive force between the unit layers in the stacks is weak and thus, cations (e.g. Na, K, Ca, Mg) and polar molecules are able to enter between the layers and cause the layer to expand (Bradl 2005).

Bentonites can be classified into sodium bentonites (Na-bentonites) or calcium bentonites (Ca-bentonites), depending on the dominant exchangeable cation that is present. Ca-bentonites are naturally occurring bentonites, while natural Na-bentonites are relatively rare. However, in order to take advantage of the better swelling performance of Na-bentonites, Ca-bentonites are activated with soda (sodium carbonate or sodium hydroxide) and, thus, the primary calcium ions are exchanged by sodium ions (so-called active bentonite) (Egloffstein 2001).

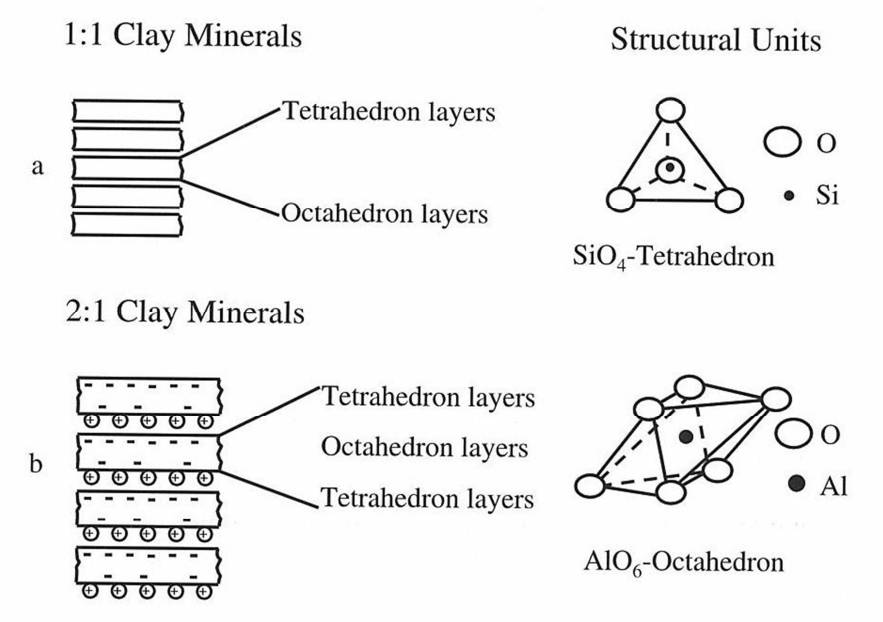

Figure 2-4 Layer structures of two and three layer minerals (Bradl 2005)

The higher swell capacity of Na-bentonites compared to Ca-bentonites is attributed to the formation of thicker hydrated shells around the clay particles due to sodium's higher water binding capacity (Figure 2-5). This phenomenon hinders the flow of water through these electrostatically bounded overlapping hydrate shells. However, if the permeant solution contains high concentration of calcium or magnesium ions, the Na-bentonites change their sodium ions for calcium or magnesium ions, resulting in an increase of the permeability by about one order of magnitude (Egloffstein 2001; Blight 2009). In addition, as a consequence of the ion exchange, a reduction in the distances between the montmorillonite flakes and a loss of water of approximately 6–12% has been reported. Moreover, the micro structure is changed from smaller, finely distributed clay mineral flakes to larger clay mineral crystals, which results in a higher permeability (Egloffstein 2001). This exchange is a natural process that could only be prevented if the permeant solution had very high sodium content, which is very rare in nature.

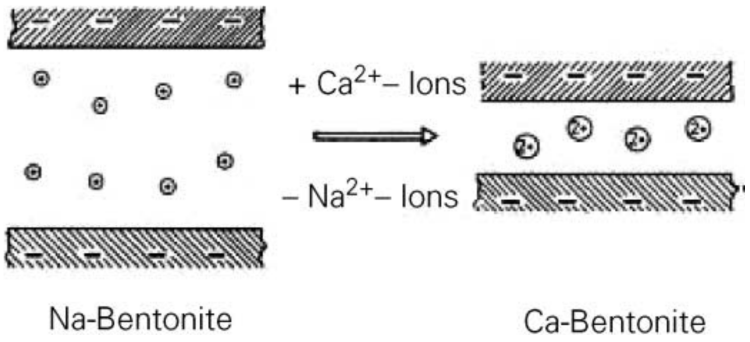

Figure 2-5 Change from sodium to calcium bentonite (Jasmund and Lagaly 1993)

Limited research has studied the impact of ARD in GCL performance. To the best knowledge of the author there were six main studies regarding the change in the barrier performance (hydraulic performance and/or chemical compatibility) of GCL after ARD permeation, which are summarized in Table 2-3. Shackelford et al. (2010) reported on the hydraulic conductivity of two granular bentonite GCLs (standard GCL and contaminant resistant GCL) considered as a liner component for tailing impoundments at a zinc and copper mine. GCLs were permeated with: groundwater (GW) recovered from a mining site; process water (PW) with a chemical composition similar to the water expected from operation of the impoundment; and a simulated leachate (SL) with a chemical composition simulating a severe case of acidic leachate if oxidation of the impounded tailings occurred after closure of the facility. The hydraulic conductivity values for both GCLs permeated with GW were 1.7×10^{-11} m/s, which is between the range reported for GCLs permeated with water or low ionic strength liquids. However, they observed dramatic increase in the hydraulic conductivity values after PW and SL permeation, regardless of whether or not the GCL specimens were prehydrated or not prior to permeation. Lange et al. (2010a) evaluated the metal attenuation capacity and hydraulic conductivity of a granular bentonite GCL. This study aimed to evaluate the potential for GCL to serve as barrier in holding ponds in which ARD waters that have been treated with lime (TARD). They tested the performance of GCL against ARD, TARD, and landfill leachate. They reported removal efficiencies greater than 80% in the TARD for metals that have been shown to be difficult to precipitate. An increase in the hydraulic conductivity was observed with the TARD (1.4×10^{-11} m/s to 3.5×10^{-11} m/s), ARD (1.4×10^{-11} m/s to 7.5×10^{-11} m/s), and landfill leachate (1.4×10^{-11} m/s to 4.4×10^{-11} m/s). The research team concluded that GCLs may be suitable for short-term containment (< 4 years) in an active-passive treatment system for ARD. Lange et al (2010b) studied the relationship between trace elements and clay at a micron scale in order to describe and predict interfacial processes controlling metal retention and release. They found the development of metal-attenuating crystalline phases that may have a significant long-term impact on metal mobility. They observed, for example, the formation of gypsum and pyrite. It was also reported that solution composition plays an important role in metal uptake behavior, considering that Fe oxides phases were important in sequestering metals such as Ni, Mn, and Zn. Hornsey et al. (2010) summarize a number of factors that should be taken into consideration when incorporating geosynthetics into a modern mining operation. Strongly alkaline or strongly acid pH and elevated temperatures are the greatest threats to long-term performance. Extremely high and low pH values promote polymer hydrolysis and ligand substitution reactions, resulting in loss of polymer strength. High temperatures increase the rate at which these adverse reactions occur, but also directly affect geotextile and geomembrane strength and elongation. They reported that for GCLs, both the geotextiles and the bentonite undergo dissolution reactions at extreme values of pH, elevated ionic strength, and temperature which negatively impact the barrier performance of GCL. Lange et al. (2009) investigated the diffusive transport of Al, As, Cd, Ca, Cl, Cu, Fe, K, Mg, Mn, Ni, SO_4, Sr, and Zn through granular bentonite GCL from four water conditions associated with mining and landfill wastes: ARD water; pH neutral water with elevated As, typical of those associated with carbonate-associated gold mine tailings; ARD water that had been treated with lime (TARD); and landfill leachate (LL). Results from this research showed that although

solution composition had some effect on the metal diffusion coefficient, sorption on the GCL was the dominant control on metal mobility. Lange et al. (2007) presented the result of metal attenuation in granular bentonite GCL. They tested ARDs and neutral-pH gold mine waters (GMW). Metal distribution within the permeated GCLs was used to determine the mechanisms involved in early (100% sorption) and later times (approaching equilibrium). The results obtained from this research team confirmed the retention of metals and the precipitation of ferrihydrite and gypsum (identified by XRD analysis) at later times. The authors mentioned that these precipitates, being more thermodynamically stable than other amorphous forms, can have a significant impact on the behavior of the contaminant transport process within the GCL.

Table 2-3 Summary of previous research on the impact of ARD in GCL

	Hydraulic conductivity test			Other tests	Compilation from other research
	Time	Permeant	Result		
Shackelford et al. (2010)	0.1 hours to 57 days (max. 39 PVF)	Groundwater Process water Simulated ARD pH 2.5	k/k_w 2.3 to 3.9 orders of magnitude increment	×	Predicted k from Kolstad (2000)
Lange et al. (2010a)	21 PVF	ARD pH 3 Treated ARD pH 5.8 Landfill leachate pH 5	k/k_w 2.5 to 5.3 times increment	Soil digestion (cation content analysis)	×
Lange et al. (2010b)	×	ARD pH – 3 As-rich Au mine tailings MSW leachate	×	Micro-analysis, μXRD, μXRF	×
Hornsey et al. (2010)	×	×	×	×	Factors affecting GCL performance: high T, salinity, and extreme pH
Lange et al. (2009)	×	ARD pH 2.6 Gold mine tailings pH 6.8 Landfill leachate pH 5.4 Treated ARD pH 5.8	×	Diffusion test, Sorption test	×
Lange et al. (2007)	21 PVF	Gold mine tailings pH 6.8 ARD pH 3.3	k/k_w 3.5 to 11 times increment	XRD analysis: (ferrihydrite and gypsum formation)	×

Hydraulic conductivity values of 5×10^{-11} and 1.3×10^{-10} m/s were obtained after permeation of GMW and ARD waters respectively.

2.6 Hydraulic Conductivity

Since the primary function of GCLs is use as a barrier to liquids and gases, hydraulic properties are very important. Hydraulic conductivity (k) is an index that measures the movement rate of water through permeable soil media. It is the constant of proportionality in Darcy's Law and as such is defined as the flow volume per unit cross-sectional area of porous medium under the influence of a unit hydraulic gradient, which may be expressed as:

$$v = ki \tag{3.1}$$

where

v = discharge velocity, which is the quantity of water flowing in unit time through a unit gross cross-sectional area of soil at right angles to the direction of flow

k = hydraulic conductivity (or the coefficient of permeability)

i = hydraulic gradient

Hydraulic conductivity is generally expressed in cm/s or m/s in SI units and depends on several factors: fluid viscosity, pore size distribution, grain-size distribution, void ratio, roughness of mineral particles, and degree of soil saturation (Das 2009). In clayey soils, structure plays an important role in hydraulic conductivity. Other factors that affect the permeability of clays are the ionic concentration and the thickness of layers of water held to the clay particles (Das 2009). The typical ranges of hydraulic conductivity values for soils are summarized in Table 2-4.

The hydraulic conductivity of barrier materials such as GCLs is difficult to measure because the level of hydraulic conductivity is extremely low. Figure 2-6 shows the measures involved in hydraulic conductivity tests, as well as the difficulties that can arise (shadowed in green). Hydraulic conductivity tests for materials

Table 2-4 Typical range of hydraulic conductivity values for soils

Type of soil	Range of hydraulic conductivity
Gravelly soil	$> 1\times10^{-2}$ m/s
Sandy soil	1×10^{-2} m/s – 1×10^{-4} m/s
Silt	1×10^{-4} m/s – 1×10^{-8} m/s
Clayey soil	$< 1\times10^{-7}$ m/s
Bentonite layer in GCLs	1×10^{-11} m/s – 5×10^{-11} m/s

with levels of permeability take a long time. So, in this case, a large hydraulic gradient is applied to shorten the testing period, which may cause sidewall leakage and create significant difference between the top and the bottom of the specimen. Other problems are related to the physico-chemically sensitiveness of clays, such as the type of liquid use in the first step of saturation (first exposure effect), as well as the permeant solutions.

Therefore, the factors to be considered when conducting hydraulic conductivity test with GCLs are the type of permeameter, the effective stress, the hydraulic gradient, the size of the specimen, the type and the chemistry of permeant, and the termination criteria (Katsumi 2010).

Two standard laboratory tests are used to determine the hydraulic conductivity of soil, the constant-head test and the falling-head test. In this research, a falling headwater-constant tailwater was used. A typical scheme of the falling-head permeability test is shown in Figure 2-7. Water from a stand pipe flows through the soil. The initial head difference h_1 at time = 0 is recorded, and water is allowed to flow through the soil specimen until the final head difference at time $t = t_2$ is h_2.

The rate of flow of the water through the specimen at any time t can be given by:

$$q = k\frac{h}{L}A = -a\frac{dh}{dt} \tag{3.2}$$

where

q = flow rate

a = cross-sectional area of the standpipe

A = cross-sectional area of the soil specimen

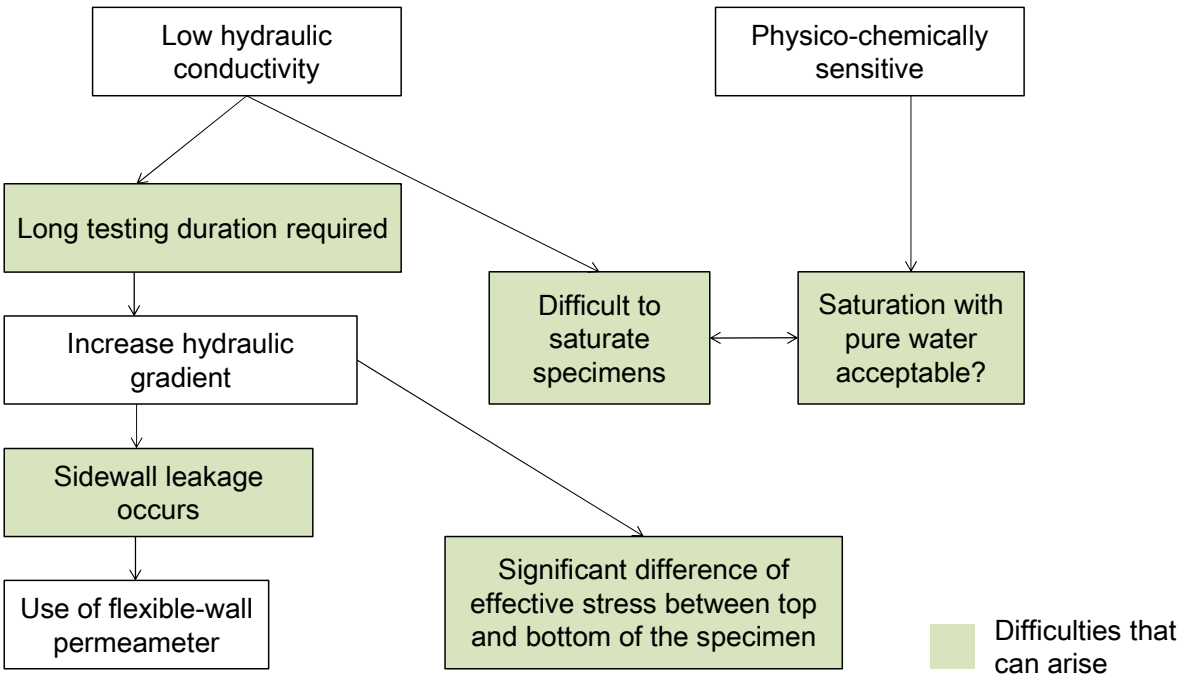

Figure 2-6 Difficulties and measurement involved with hydraulic conductivity test (Katsumi 2010)

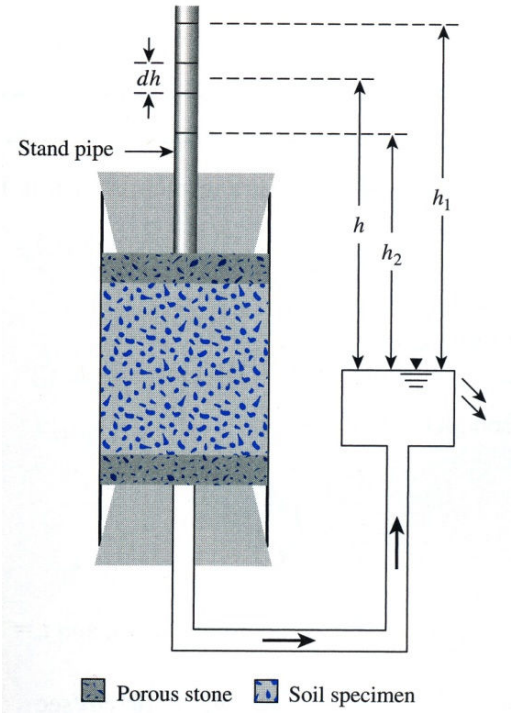

Figure 2-7 Falling-head hydraulic conductivity test (Das 2009)

Rearrangement of the Equation (3.2) gives

$$dt = \frac{aL}{Ak}\left(-\frac{dh}{h}\right) \tag{3.3}$$

Integration of the left side of Equation (3.3) with limits of time from 0 to t and the right side with limits of head difference from h_1 to h_2 gives

$$t = \frac{aL}{Ak}\ln\frac{h_1}{h_2} \tag{3.4}$$

or

$$k = \frac{aL}{At}\ln\frac{h_1}{h_2} \tag{3.5}$$

Even though the hydraulic conductivity of GCLs is proved to be very low, some studies have shown that increases in permeability of GCLs can arise by the replacement of the original Na cations in the bentonite by Ca and Mg combined with the effects of desiccation of the clay during dry seasons. In one study, the measured permeability of Na-bentonite GCL when installed ranged from 1 to 2.5 mm/y. However, after 12-18 months service, it had increased to 440 to 30,000 mm/y, which means that all liquids can infiltrate through it or, in other words, that the GCL is no longer effective as a hydraulic barrier (Benson et al. 2007; Blight 2009).

2.7 Chemical Compatibility

Sorption mechanisms have an important role in reducing the transport of heavy metals in the environment (Bradl 2005). It is due to the materials present in soils and aquifers, such as clay minerals, organic matter, and metal oxy-hydroxides that can sorb chemicals. There are various processes indicated by the general term sorption, which are illustrated in Figure 2-8. The term adsorption refers to the adherence of a chemical to the surface of the solid, without the development of a three-dimensional molecular arrangement; absorption suggests that the chemical is taken up into the solid; and exchange involves replacement of one chemical for another one at the solid surface.

Previous studies suggest that ion exchange is the mechanism that explains the metal sorption process on bentonite, although other types of reactions, such as precipitation and dissolution may also occur. Ion exchange processes are equilibrium processes in which the occupation of a cation exchanger depends on the kind and concentration of the cations available for the exchange. Moreover, the size and the charge of the cations are important. For instance, bivalent cations are more easily exchanged against monovalent cations than vice versa (Egloffstein 2001).

The ion exchange of monovalent sodium ions against bivalent ions reduces the spaces between the silicate layers (Katsumi 2010). When this phenomenon occurs, the diffuse sodium ion double layer at the surfaces of the clay minerals turns into a central bivalent cation layer. The increase of the inner-crystalline attraction by the bivalent ions leads to a certain reduction of volume and a change of the micro structure from smaller, finely distributed clay mineral flakes to larger clay mineral crystals (Egloffstein 2001). This phenomenon leads to an increase of permeability.

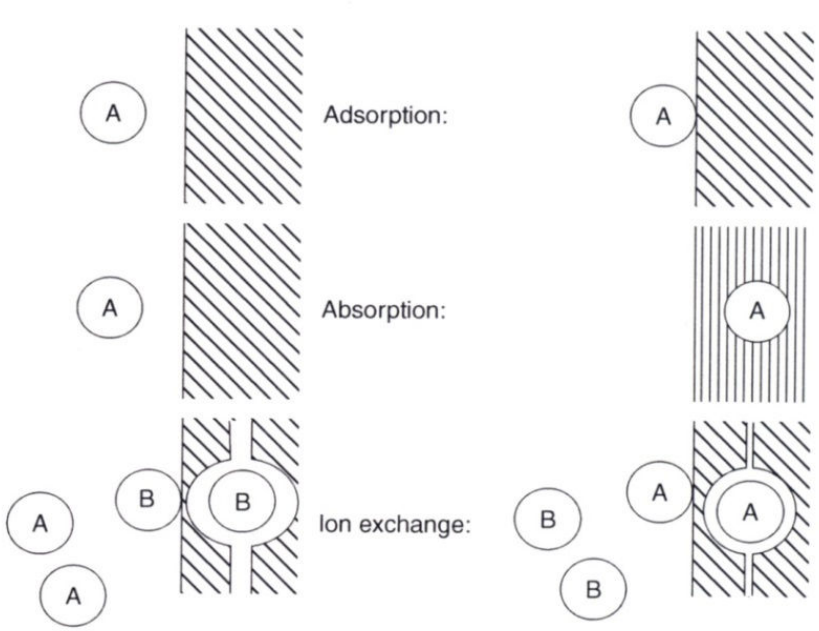

Figure 2-8 Different sorption processes (Appelo and Postma 2009)

The presence of complex species in solution can impact on the transport of metals through GCLs. Transport of heavy metals in bentonite can be generally described by the advection-dispersion equation. Rowe et al. (2004) have described the procedure for modeling contaminant transport in landfill liner systems. If a GCL is part of that liner system, the contaminant transport through the saturated GCL can be represented by a slightly modified form of the advection/dispersion equation for a single reactive solute:

$$n_t = \frac{\partial c}{\partial t} = \left(n_t D_t \frac{\partial^2 c}{\partial z^2} - n_t \bar{v} \frac{\partial c}{\partial z} \right) - \rho K_d \frac{\partial c}{\partial t} \tag{3.6}$$

where c = concentration in the GCL at depth z and time t [ML^{-3}]; n_t = total porosity of the GCL [–]; D_t = diffusion coefficient deduced from total porosity [L^2T^{-1}]; $\bar{v}$ = average linearized groundwater velocity [LT^{-1}]; ρ = dry density [ML^{-3}]; K_d = partitioning coefficient [$M^{-1}L^3$]. Solving the partial differential equation given above allows an estimate of the concentration c, at any time t, and depth z, in the GCL.

Lange et al. (2009) investigated the diffusive transport of four types of waters associated with mining and landfill wastes and observed that the receptor concentration remained very low ($c/c_0 < 0.1$) for the duration of the test. These results show that, although GCLs consist of a very thin layer (typically 5-10 mm) and solution composition has some effect on the metal diffusion coefficient, metals were significantly retarded within GCL and, thus, sorption to the GCL was the dominant control on metal mobility. However, the limitation due to the bentonite buffering capacity has to be also taken into consideration. Figure 2-9 shows a scheme of the metal retention mechanisms in GCLs. It can be seen that when water is permeated through a GCL, the water can hydrate the cations (e.g. Na) present in the interlayers, which results in an expansion of the bentonite layers. In case of ARD permeation, several mechanisms such as ion exchange, precipitation and/or co-precipitation can occur.

Abollino et al. (2003) reported that the primary mechanisms controlling metal mobility in GCLs are: the cation exchange in the interlayers resulting from the interactions between ions and negative permanent charge; the formation of inner-sphere complexes through Si–O^- and Al–O^- groups at the clay particle edges; limited anion exchange (30 meq/100 g) where the anions typically attach to the clay structure by substitution of hydroxides at the edges of gibbsite sheets; and precipitation. These mechanisms are pH dependent because in acidic conditions the hydrogen ion competes with the heavy metals towards the superficial sites. Additionally, most silanol and aluminol groups are protonated and it becomes more difficult to form complexes with bivalent and trivalent ions present in solution. Thus, low pH may increase the mobility of metals. In addition, other physical and chemical parameters such as redox conditions, presence of other cations in solution, and temperature may also influence heavy metal sorption.

2.7.1 Cation Exchange/Unspecific Sorption

Cation exchange / unspecific sorption occurs when a cation retains its outer hydration shell of water molecules and is attracted to a negatively charged bentonite surface through a combination of hydrogen bonding and electrostatic long-range Coulombic forces. The binding energies are relatively weak. Cation

exchange processes are reversible, diffusion controlled, stoichiometric, and selective. Heavy metals are exchanged better at bentonite surfaces occupied by monovalent cations than those occupied by divalent cations. This type of sorption can be expressed as:

$$\underline{S}OH + M^{2+} \rightarrow SOHM^{2+} \quad (3.7)$$

where S is the mineral surface

The presence of many cations (many with charges +2 or +3), complex anions, and ligands, in typical mine waters often results in metal ion activity differing from what single metal sorption tests would suggest. In cation exchange, or non-specific adsorption, the adsorbent shows preference for some ions, typically dependent on the cation charge or valence, size of hydrated cation and the cation concentration. Cations that have high sorption energy are more attracted to the exchange surface. This sorption energy is a function of the cation charge and, thus, in trivalent (i.e. Al^{3+}) and divalent (i.e. Ca^{2+}) cations is much higher than that in monovalent (i.e. K^{+}, Na^{+}) cations. As a consequence, an exchangeable cation of Al or Ca stays close to the clay particle and does not interfere in the cohesion between aggregated particles. The valence of an exchangeable cation also determines the double layer thickness. High valence of the dominant exchangeable cation leads to thinner the double layer. When the valence of the cations is equal, the cation with the smallest hydrated radius is more strongly sorbed. In the case of monovalent cations, K is more strongly sorbed than Na because it has a smaller hydrated diameter and hence is more strongly attracted to the negative charge of the bentonite. Similar to monovalent cations, the magnesium ion is more weakly attracted to bentonite due to the larger hydrated diameter of Mg compared to Ca. The non-hydrated and hydrated diameters of several metals are reported in Table 2-5.

Table 2-5 Effective diameters of non-hydrated and hydrated ions (Kielland 1937; Shannon 1976)

	Non-hydrated (pm)	Hydrated (pm)
Na	100	550
K	160	300
Mg	90	800
Ca	140	600
Fe	100	600
Cu	114	600
Zn	110	600
Al	80	900
Pb	238	590
As	68	---

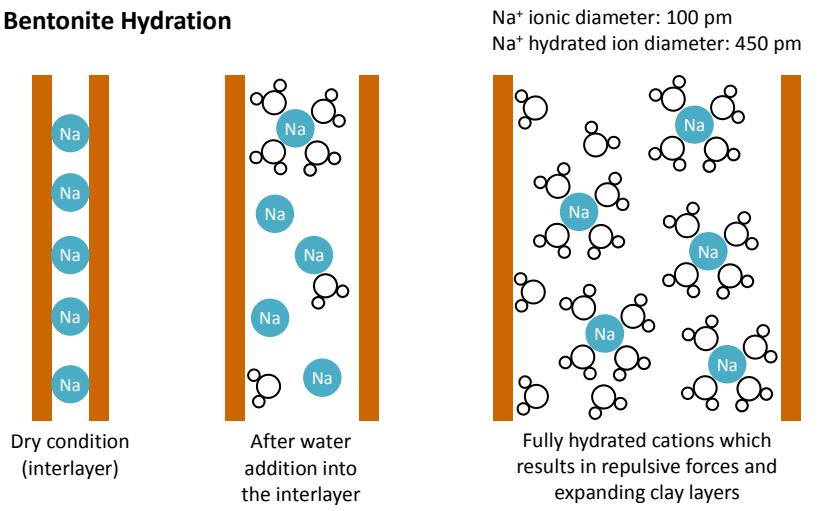

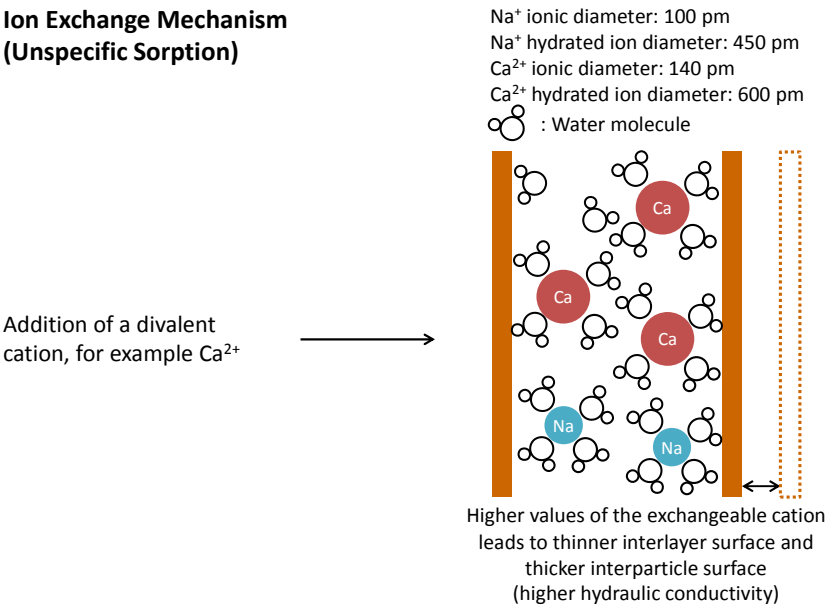

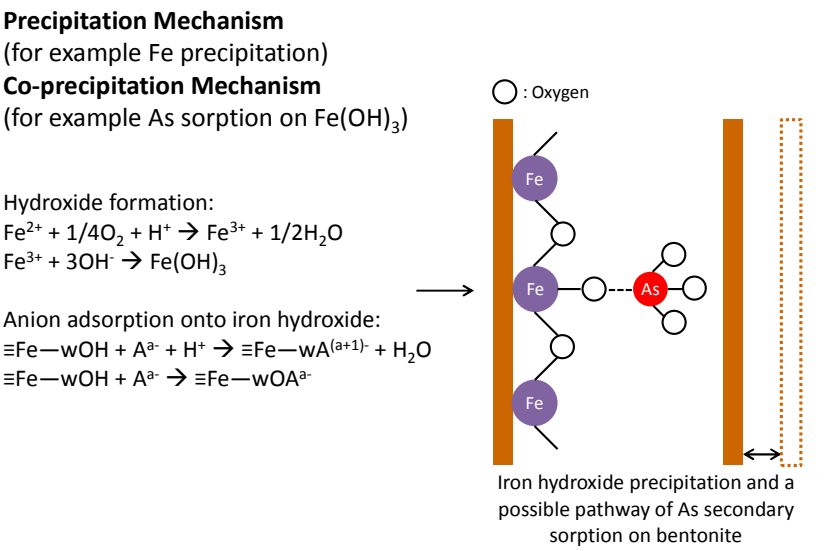

Figure 2-9 Metal retention mechanism in bentonite

2.7.2 Specific Sorption

Specific sorption occurs through the loss of water hydration around the cations and the formation of direct chemical bonds with the mineral surface, typically with surface oxygen atoms. Depending on the number of surface oxygen atoms to which the cations bind, it can be monodentate (one), bidentate (two), or tridentate (three, but rarely occurs). This type of sorption can be expressed as:

$$\underline{S}OH + M^{2+} \rightarrow \underline{S}OM^{+} + H^{+} \text{ (monodentate)} \quad (3.8)$$

$$2\underline{S}OH + M^{2+} \rightarrow (\underline{S}O)_2M + 2H^{+} \text{ (bidentate)} \quad (3.9)$$

where $\underline{S}$ is the mineral surface

2.7.3 Surface Precipitation

Sorption densities exceeding a monolayer of sorbed cations can form a solid surface layer of the metal, usually as a hydroxide or oxide phase. This is called surface precipitation and it is the result of a continued sorption, first from mononuclear sorbed ions to multinuclear sorption complexes and finally to homogeneous surface precipitates. This mechanism can be expressed as:

$$\underline{S}OMOH^{2+} + M^{2+} + H_2O \rightarrow \underline{S}OMOH^{2+} + M(OH)_2(s) + 2H^{+} \quad (3.10)$$

where $\underline{S}$ is the mineral surface

2.7.4 Co-precipitation

Besides homogeneous surface precipitation, there are other types of precipitation such as the one that incorporate other aqueous metal species. One type of precipitate occurs through dynamic dissolution of the solid surface and formation of a new heterogeneous solid phase that includes both material from the substrate and aqueous metal species. This co-precipitation phenomenon occurs among aluminum bases substrates, ferrihydrite, among others.

3 CHARACTERIZATION OF ACID ROCK DRAINAGE

3.1 General Remarks

The pollution of surface and groundwater caused by the inflow of ARD generated from excavated sites poses a serious environmental problem in Japan. The ground under cities such as Osaka and Tokyo contains sand and marine mud sediments that commonly contain pyrite. When the underground environment in these cities is altered, by the construction of tunnels for example, pollution by acid water originating from the mudstone may arise (Ohta et al. 2005; Ohta et al. 2006). This is because the pyrite is exposed to groundwater in an oxidized environment. Thus, the groundwater becomes acid due to sulfate generated by the decomposition of the pyrite. It may cause severe corrosion of pipelines or other infrastructure placed deep underground and the pollution of groundwater (Ohta et al. 2008; Ohta et al. 2010). Moreover, there have also been studies about the potential pollution of groundwater around road and rail tunnel projects in Japan in places where hydrothermally altered rocks containing high amount of As, Pb, B and Se is present as well as the mechanisms and main factors affecting their mobilization (Tabelin and Igarashi 2009; Tabelin et al. 2010; Tabelin et al. 2012a; Tabelin et al. 2012b).

However, information on ARD generated from excavated sites is still limited and, thus, difficult to know the extent of the problem in terms of pH and metal concentration. Conversely, there is a great deal of information and data about ARD coming from mining activities. Thus, it was decided to collect ARD composition from mining sites in order to characterize the ARD and assess the risk of potential environmental mobility of toxic metals contained in excavated rocks. Due to the fact that in mining sites metals tend to be concentrated, the pH, sulfate, and metal concentrations is more severe than the observed around construction places. Therefore, the expected ARD from construction operations, which is the target of the present research, is less complex than the one expected from mining sites.

ARDs in the world are complex and difficult to predict as there is no typical ARD with two having the same composition and characteristics. Moreover, studies on ARDs are usually based on leachates coming from one place or mine. There is no database that gives an idea on the possible ranges of pH and metal release. This makes the development of remediation technologies even more difficult to achieve and therefore it becomes necessary to study or analyze ARDs from different types of mines, different countries, and different characteristics.

A database of ARDs, if proper analyzed, becomes a valuable scientific tool for the estimation of water chemistry between monitoring events and the future. Statistical approaches can be successfully used to describe, summarize and interpret cases collected and make an empirical water chemistry model for future predictions. According to Morin et al. (1995) these predictions become useful for:

- Estimating future water-treatments costs.
- Refining water-retention times in ponds to obtain a particular range of concentration.
- Determining the acceptable degree of failure in water-quality control technologies such as clay covers.
- Negotiating closure bonds with government agencies.

- Reducing the frequency of intense monitoring programs.

In this research, 817 cases of ARDs were collected and analyzed. Considering that data on ARD coming from construction sites is less available, AMD (acid mine drainage) compositions were collected. The author cannot assure that this database includes all possible cases of ARD in the world. However, reliability of the analysis increases with the number of samples and the number of years monitored and thus numerous ARDs from different type of mines and different countries were selected from more than 80 publications. The results presented in this section are original and valuable and propose to be an approach to chemically characterize ARDs in the world, find relationships between parameters to easily estimate ARDs potential generation in the future.

Mining companies usually report water chemistry around the mine, but interpretation and analysis of the resulting data are done either poorly or not at all. Therefore, this research intends to demonstrate an approach to understand the behavior of metals and relationship between parameters in ARDs in order to use them for future predictions.

The best way to predict the chemistry of ARDs is by considering each variables or factors that contributes to this. According to Morin et al. (1995), in the case of ARDs, physical (e.g. water and air, temperature, etc.), chemical (e.g. pH, chemical complexation, etc.), and biological (e.g. bacterial activities, etc.) factors determine the chemistry of ARD. If each variable or parameter could be described and predicted, ARD can also be predicted through deterministic modeling. There is also a stochastic modeling which uses statistical tools to predict water chemistry. Empirical modeling, which identifies patterns and cycles in measured data, can be also used; potential patterns include statistically normal distributions of values or their logarithms. A normal or logarithm distributions can be summarized using statistical tools such as the mean and standard deviation (Morin et al. 1995).

3.2 Characteristic Parameters of ARDs

There are several important parameters such as Eh, hardness, alkalinity, acidity, total dissolved solids, dissolved oxygen, turbidity, temperature, and salinity that provide information about the quality of the water in case of ARD contamination potential. Table 3-1 shows selected parameters critical to mine waters, obtained from Brownlow (1996), Drever (1997), Appelo and Postma (2009), and Flicklin and Moisier (1999).

The purpose of the ARD database in the current research is to select ARDs that can provide information about the impact of pH and EC into the barrier performance of minerals. The database analysis in this section consists on the description of pH, electrical conductivity (EC), sulfate, and 10 metal concentrations (Al, As, Cu, Fe, Pb, Zn, Ca, K, Na, and Mg). Also, relationship between parameters such as sulfate and EC, pH, and EC, etc. were investigated as an attempt to predict certain parameters using parameters that can be easily measured in the field such as EC and pH.

Description of each parameter was conducted using statistical tools such as histograms and box plots. A histogram (Figure 3-1), also called distribution graph, is a graphical representation of the distribution of

the data. It is particularly useful when there are a large number of observations. A histogram is usually depicted as a bar chart (rectangles), with one bar representing the count of how many measurements fall within a single and discrete interval (bin). The width of the rectangles represents the class intervals and the height of a rectangle is also equal to the frequency density of the interval. The area of each rectangle is proportional to the corresponding frequencies and the total area of the histogram is equal to the number of data.

A box-and-whisker plot (sometimes called simply a box plot) is a histogram-like graphical representation of data, invented by the American mathematician John Tukey. It shows the lowest value, highest value, median value, and the size of the first and third quartile (Figure 3-2).

Table 3-1 Important parameters to mine waters

Parameter	Explanation
Eh	Reduction-oxidation potential of a solution. Expressed as volts (V).
pH	Negative logarithm of hydrogen activity
Electrical conductivity (EC)	Ability to conduct electrical current, depending on the amount of charged ions in solution. For freshwater, the conductivity is approximately related to the quantity of total dissolved solids. Expressed as μS/cm.
Hardness	Sum of the ions which can precipitate as "hard particles" from water. It is expressed as mg $CaCO_3$ L^{-1} and related to the sum of calcium and magnesium ions.
Alkalinity	Capacity of a solution to neutralize acid. In most natural waters, alkalinity is equal to the molality concentrations of bicarbonate and carbonate ions. Other ions such as ammonia, borate, silicic acid, bisulfides, organic anions, and hydroxide ions can combine with hydrogen and contribute to alkalinity. Expressed as mg $CaCO_3$ or HCO_3^- L^{-1}.
Acidity	Capacity of a solution to donate protons. A number of dissolved ions (H^+, Fe^{2+}, HSO_4^-), gases (CO_2, H_2S), humic and fulvic acids, and suspended matter (metal hydroxides, clays), may contribute to an acidity value. Mine waters generally have very low organic acid contents. Expressed as mg $CaCO_3$ or HCO_3^- L^{-1}.
Total dissolved solids (TDS)	Amount of dissolved solids. Determine by evaporating and weighing the dry residue. Expressed as mg/L.
Dissolved oxygen	Amount of dissolved oxygen. Expressed as mg/L.
Temperature	Expressed in Celsius degree.
Salinity	Amount of total dissolved solids. Freshwater has <1000 or 1500 mg/L TDS, brackish water have 1000 to 10000 mg/L TDS, saline waters have 10000 to 100000 mg/L TDS, whereas brines have even higher salinities.

To create a box-and-whisker plot, a box (represented with a square) with ends at the quartiles Q1 and Q3 is drawn. Then, the statistical median is placed as a horizontal line in the box. It is also possible to indicate the mean. Finally, "whiskers" at 1.5 IQR are drawn. If there is no data or observation corresponding to the upper or lower fence, the maximum and minimum observation fence is plotted as shown in Figure 3-2 (right). It is also possible to show outliers, which are observations that are more extreme than the upper and lower fences (plus minus 1.5 IQR).

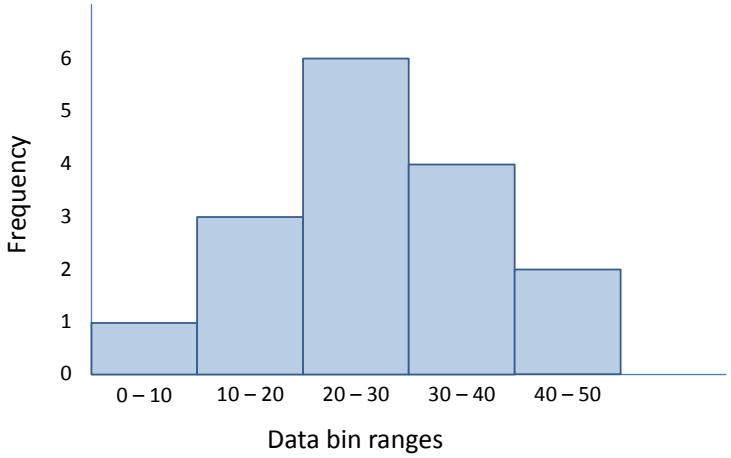

Figure 3-1 Elements of an histogram

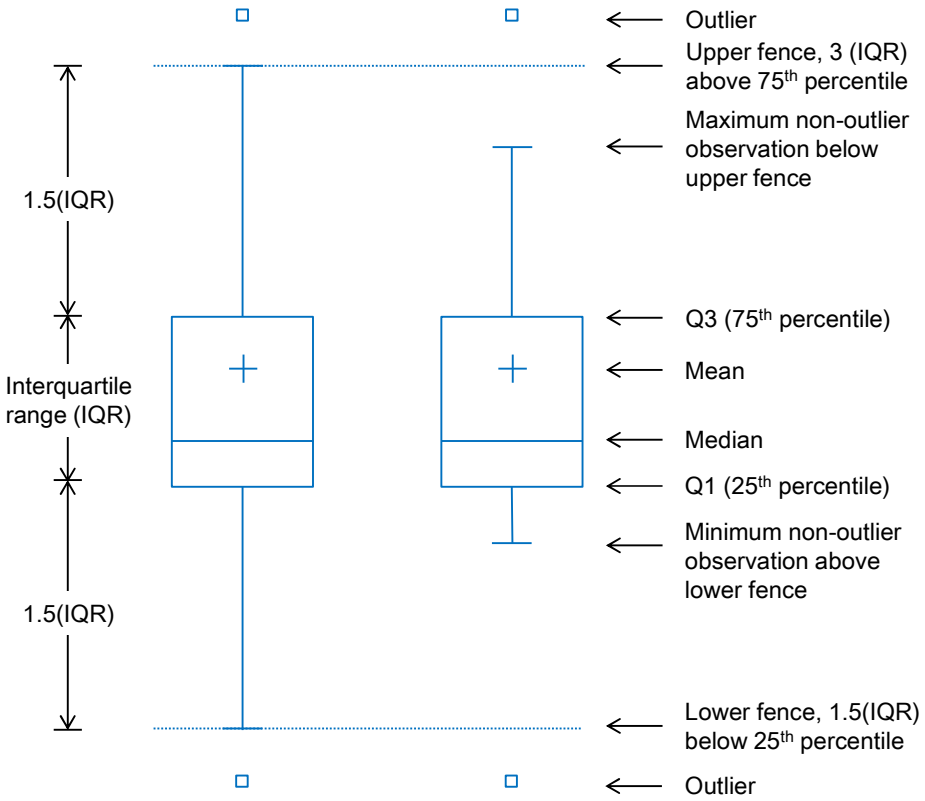

Figure 3-2 Box plot elements a) ideal case (left) and b) with no data at 1.5 IQRs (right)

3.2.1 Evaluation of pH

The original database contains 817 cases of which 754 cases around the world reported pH values. The median reported pH concentration was 4.5 with an IQR from 3.1 to 6.8. The average pH value was 4.9 with a standard deviation of 2.1. The minimum reported pH value was -2.5 and the maximum was 10.4. Figure 3-3 shows the pH values of the collected data.

From the database it was observed that the pH varies according to the type of mine. Figure 3-4 and Table 3-2 show the median, mean, maximum ,and minimum pH values according to the type of mine. The highest average value was 5.5 for gold mines, whereas the minimum was 3.3 for sulfide mines.

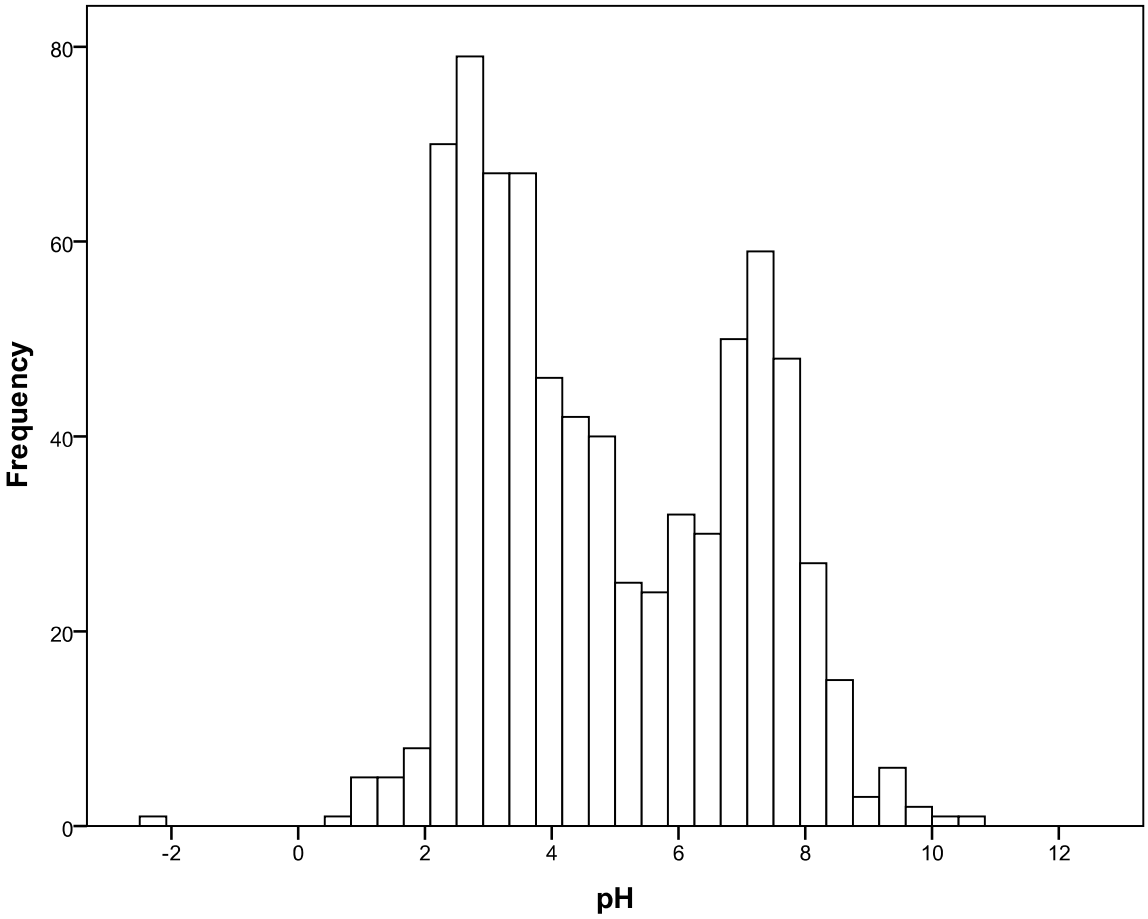

Figure 3-3 pH ranges of the database

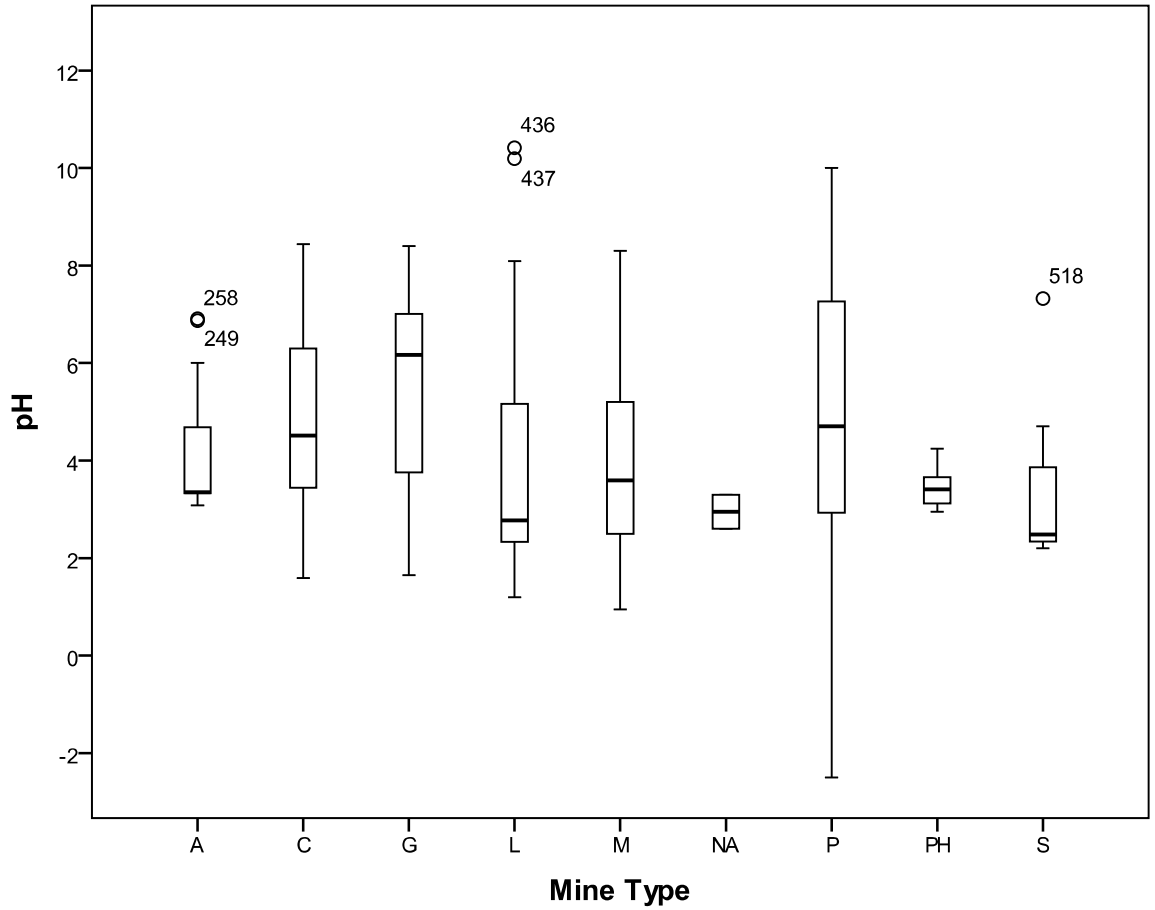

Figure 3-4 pH range at different types of mine

Table 3-2 Average of pH at different types of mine

Type	Cases	Average	Std. Error
Type A	11	4.20	0.62
Type C	219	4.86	0.14
Type G	91	5.48	0.21
Type L	33	3.81	0.36
Type M	50	4.09	0.29
Type na	2	2.95	1.44
Type P	328	5.07	0.11
Type PH	10	3.43	0.65
Type S	10	3.30	0.65

Type A: arsenic, C: coal, G: gold, L: leachate, M: metal, na: not available, P: polymetallic, PH: phosphate, S: sulfur

3.2.2 Evaluation of EC

The original database contains 817 cases of which 457 cases around the world reported EC. Of these, 457 cases had concentrations of EC greater than zero. The median reported EC was 116 mS/m with an IQR from 47.3 to 419 mS/m. The average EC was 302 mS/m with a standard deviation of 427 mS/m. The minimum reported EC was 1.6 mS/m and the maximum was 2600 mS/m. Figure 3-5 shows the concentration of EC for non-zero cases.

The EC varies according to the type of mine. Figure 3-6 and Table 3-3 show the median, mean, maximum, and minimum EC according to the type of mine. The highest average value was 462 mS/m for leachates, whereas the minimum was 51.8 mS/m for arsenic mines.

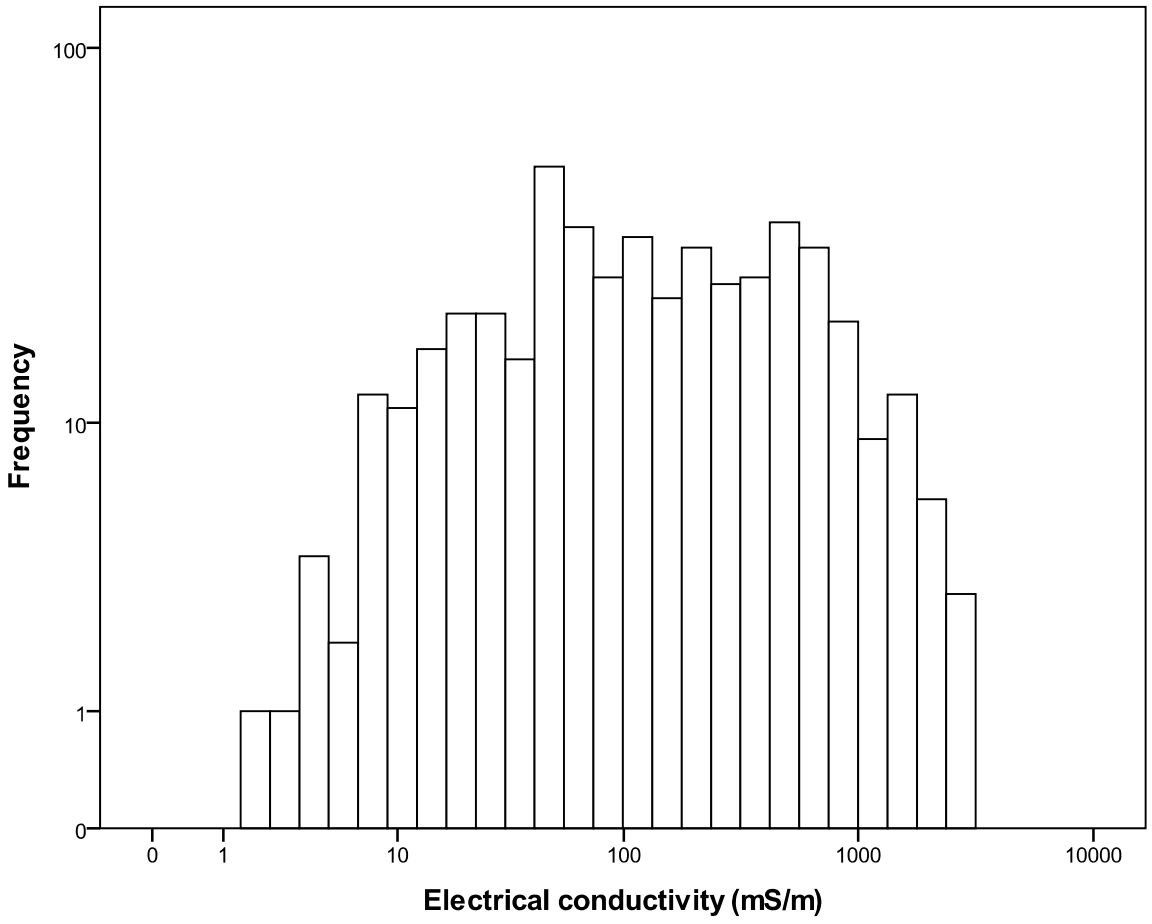

Figure 3-5 Electrical conductivity range from the database

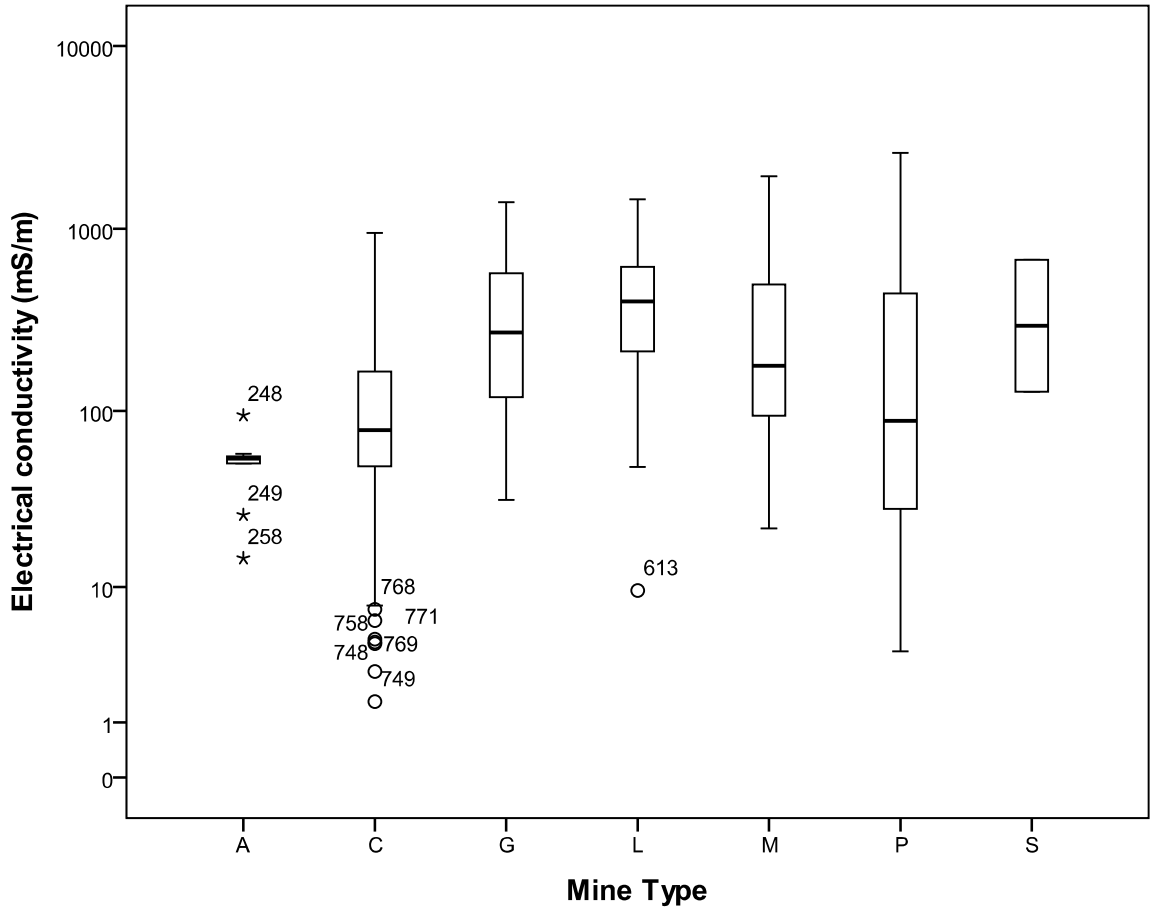

Figure 3-6 Electrical conductivity range at different types of mine

Table 3-3 Average EC at different types of mine

Type	Cases	Average (mS/m)	Std. Error (mS/m)
Type A	10	51.79	132.04
Type C	103	147.41	41.14
Type G	64	390.53	52.19
Type L	33	462.30	72.69
Type M	13	372.40	115.81
Type P	232	329.69	27.41
Type S	2	402.19	295.26

Type A: arsenic, C: coal, G: gold, L: leachate, M: metal, na: not available, P: polymetallic, PH: phosphate, S: sulfur

3.2.3 Evaluation of Sulfate Concentration

The original database contains 817 cases of which 495 cases around the world reported SO_4. Of these, 495 cases had concentrations of SO_4^{2-} greater than zero. The median reported SO_4 concentration was 668 mg/L with an IQR from 150 to 2588 mg/L. The average SO_4 concentration was 4755 mg/L with a standard deviation of 34896 mg/L. The minimum reported SO_4 concentration was 1 mg/L and the maximum was 760000 mg/L. Figure 3-7 shows the Log of the concentration of SO_4 for non-zero cases.

The concentration of sulfate varies according to the type of mine. Figure 3-8 and Table 3-4 show the median, mean, maximum, and minimum concentration of sulfate according to the type of mine. The highest average value was 15308 mg/L for phosphate mines, whereas the minimum was 190 mg/L for arsenic mines.

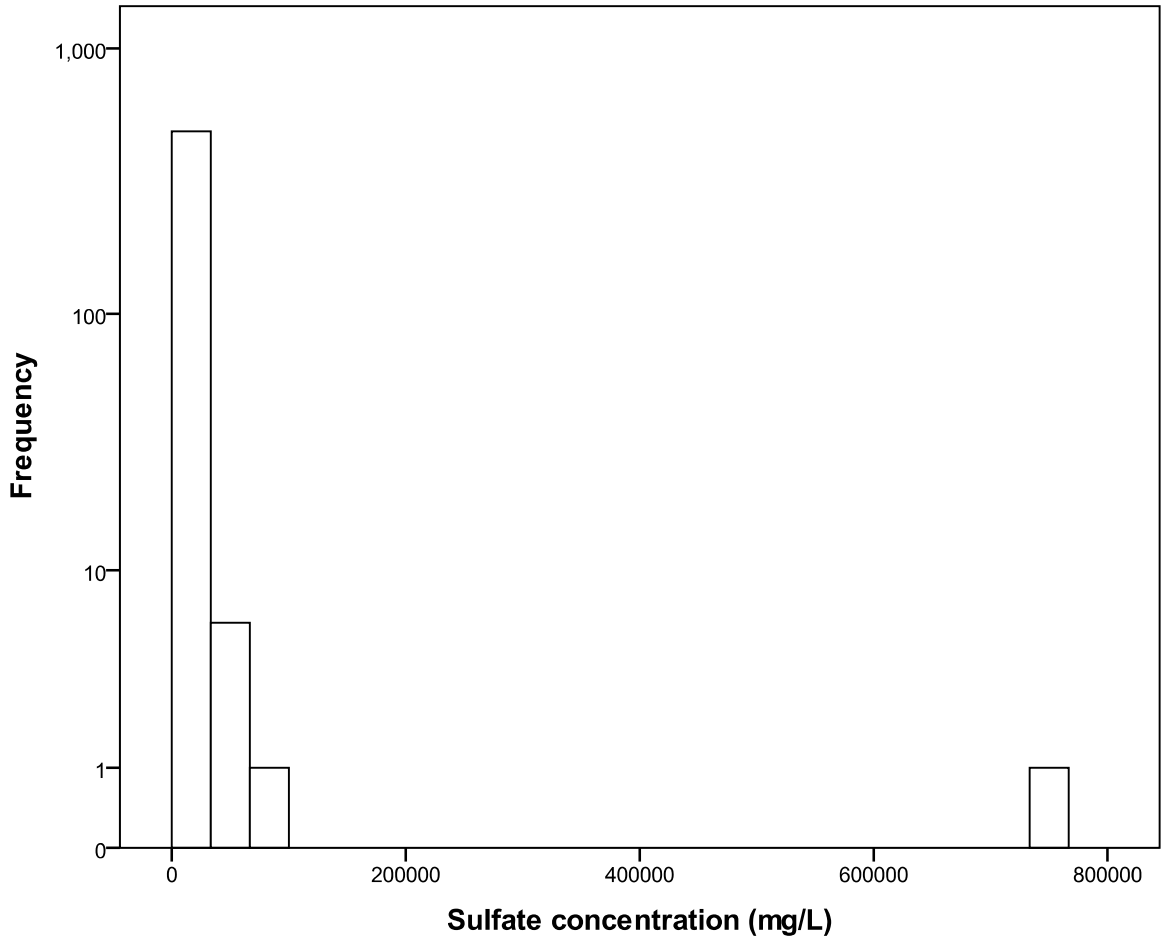

Figure 3-7 Sulfate concentration range from the database

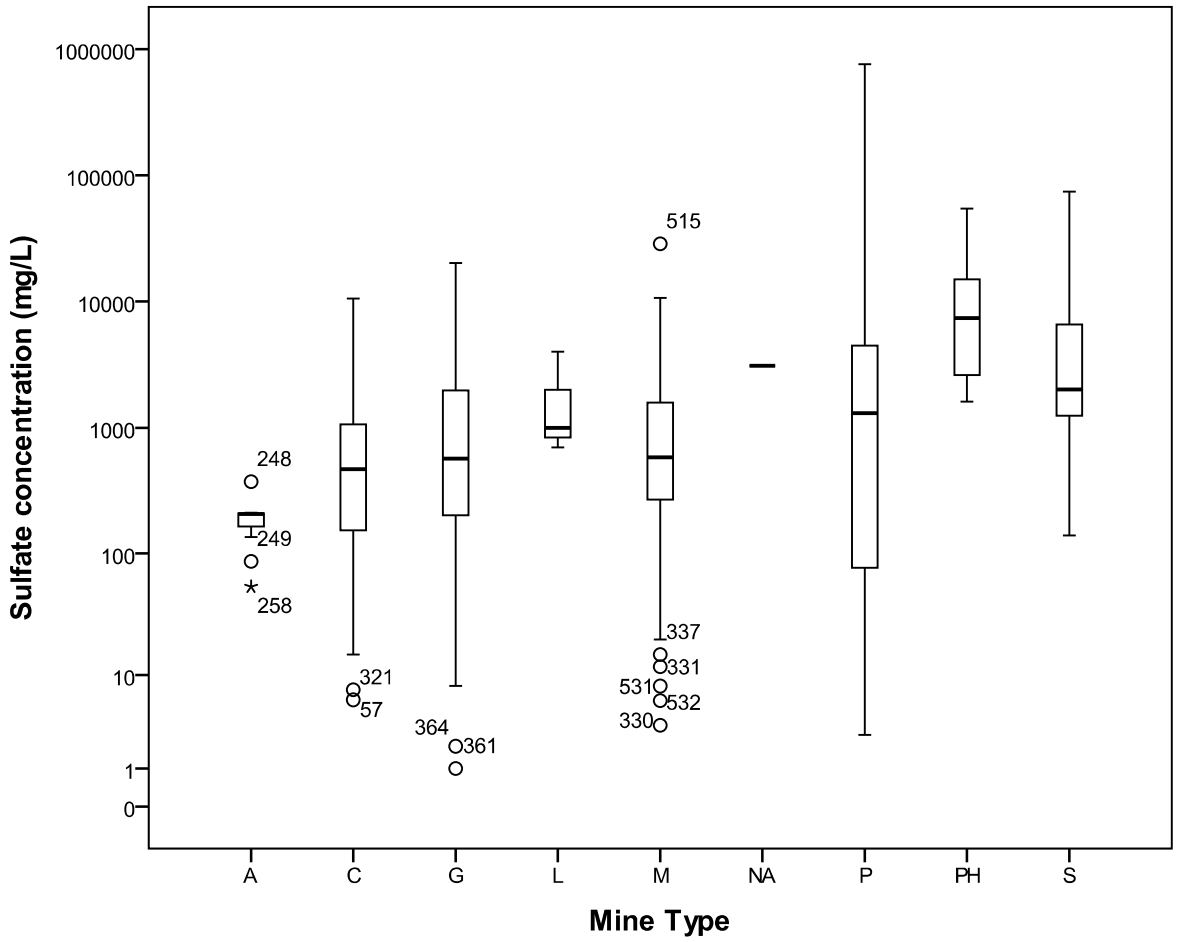

Figure 3-8 Sulfate concentration range at different types of mine

Table 3-4 Average of sulfate concentration at different types of mine

Type	Cases	Average (mg/L)	Std. Error (mg/L)
Type A	11	190.4	10533.7
Type C	108	988.1	3361.8
Type G	81	1747.5	3881.8
Type L	3	1900.0	20170.5
Type M	36	2217.0	5822.7
Type na	1	3102.0	34936.4
Type P	236	7447.5	2278.7
Type PH	10	15308.3	11047.8
Type S	9	11536.7	11645.5

Type A: arsenic, C: coal, G: gold, L: leachate, M: metal, na: not available, P: polymetallic, PH: phosphate, S: sulfur

3.2.4 Aluminum Concentration

The original database contains 817 cases of which 450 cases around the world reported Al. Of these, 445 cases had concentrations of Al greater than zero. The median reported Al concentration was 10.9 mg/L with an IQR from 1.7 to 80.0 mg/L. The average Al concentration was 160 mg/L with a standard deviation of 471 mg/L. The minimum reported Al concentration was 0.007 mg/L and the maximum was 4050 mg/L. Figure 3-9 shows the concentration of Al for non-zero cases.

The concentration of Al varies according to the type of mine. Figure 3-10 and Table 3-5 show the median, mean, maximum, and minimum concentration of Al according to the type of mine. The highest average value was 1018 mg/L for phosphate, whereas the minimum was 4.8 mg/L for arsenic mines.

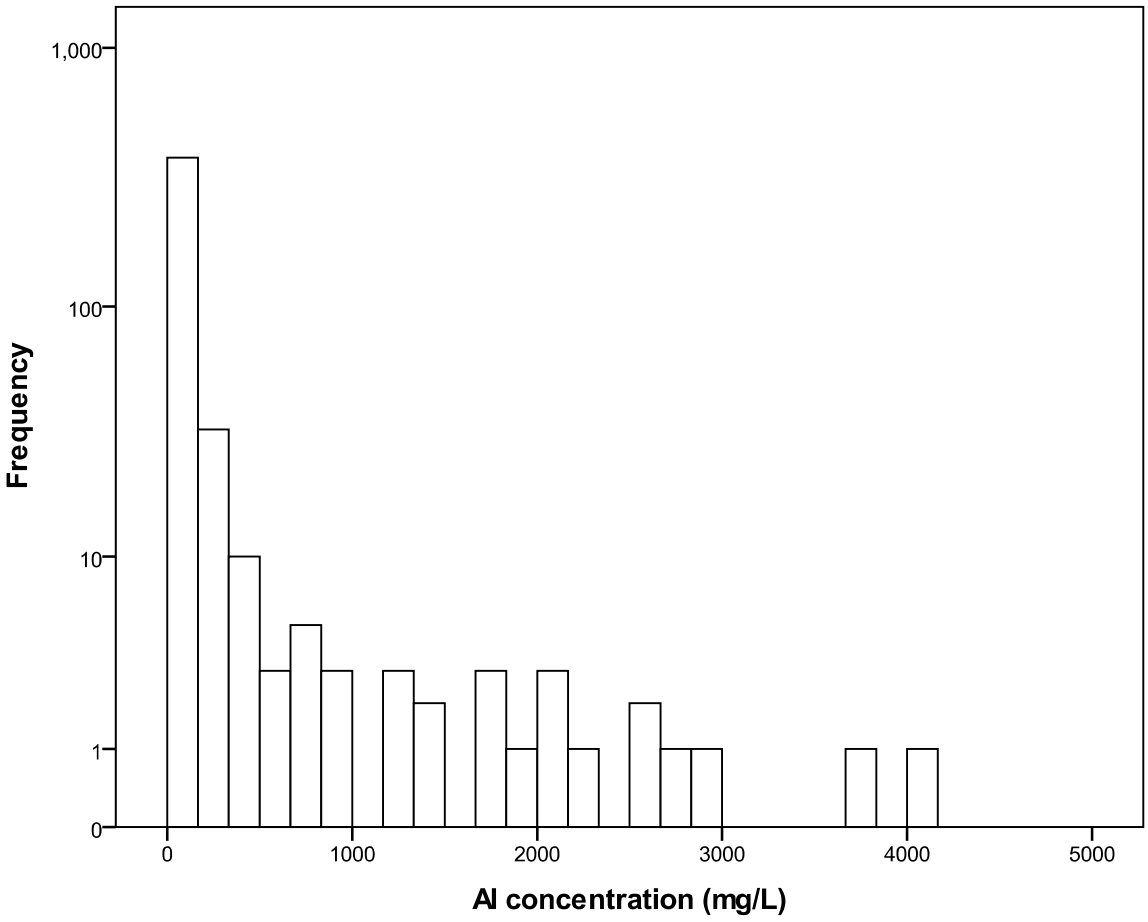

Figure 3-9 Aluminum concentration range from the database

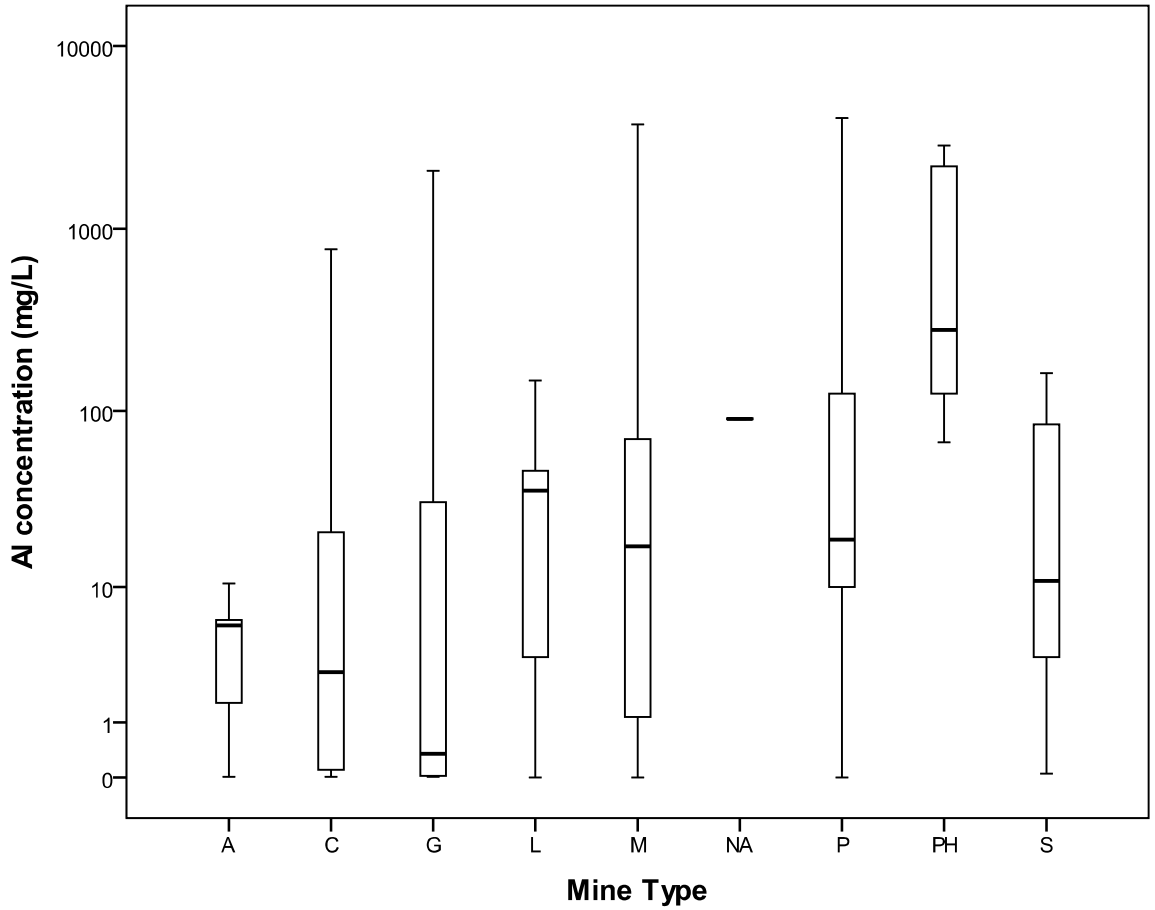

Figure 3-10 Aluminum concentration range at different types of mine

Table 3-5 Average concentration of Al according to the type of mine

Type	Cases	Average (mg/L)	Std Error (mg/L)
Type A	11	4.76	135.00
Type C	110	33.86	42.69
Type G	29	226.80	83.15
Type L	11	38.73	135.01
Type M	37	153.26	73.61
Type na	2	90.50	316.62
Type P	231	189.28	29.46
Type PH	10	1017.66	141.60
Type S	9	46.54	149.26

Type A: arsenic, C: coal, G: gold, L: leachate, M: metal, na: not available, P: polymetallic, PH: phosphate, S: sulfur

3.2.5 Arsenic Concentration

The original database contains 817 cases of which 507 cases around the world reported As. Of these, 498 cases had concentrations of As greater than zero. The median reported As concentration was 0.01 mg/L with an IQR from 0.001 to 0.3 mg/L. The average As concentration was 4.0 mg/L with a standard deviation of 27.8 mg/L. The minimum reported As concentration was 0.0001 mg/L and the maximum was 471 mg/L. Figure 3-11 shows the the concentration of As for non-zero cases.

The concentration of As varies according to the type of mine. Figure 3-12 and Table 3-6 show the median, mean, maximum, and minimum concentration of As according to the type of mine. The highest average value was 84.2mg/L for phosphate mines, whereas the minimum was 0.03 mg/L for coal mines.

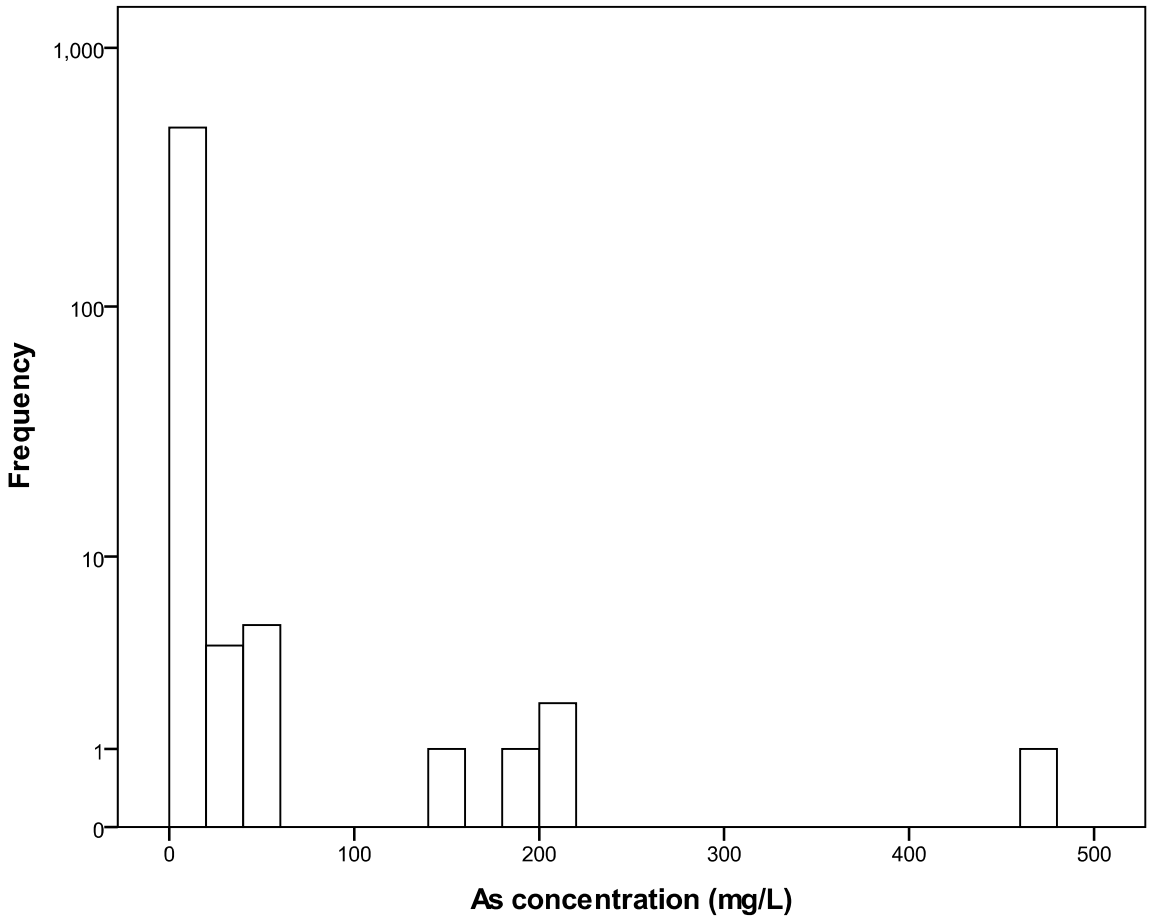

Figure 3-11 Arsenic concentration range from the database

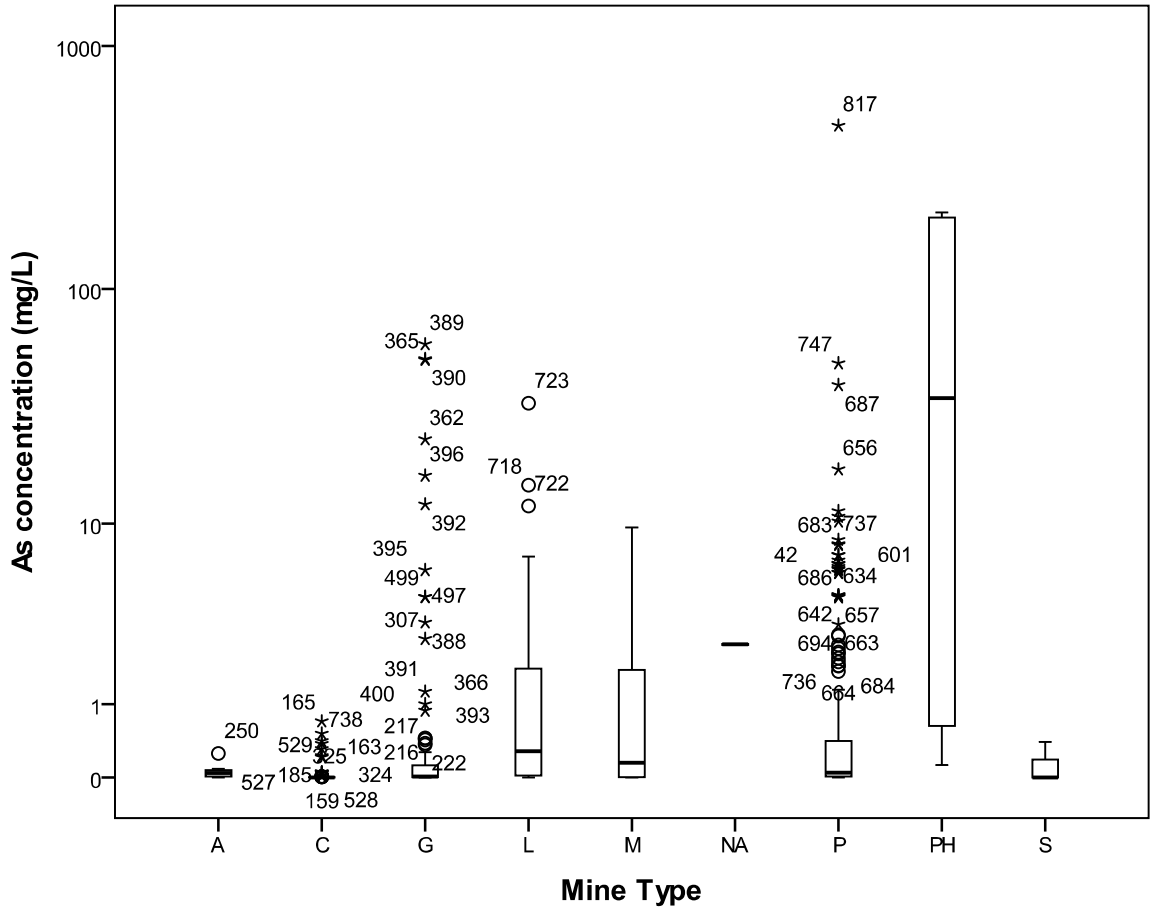

Figure 3-12 Arsenic concentration range at different types of mine

Table 3-6Average concentration of As according to the type of mine

Type	Cases	Average (mg/L)	Std. Error (mg/L)
Type A	11	0.06	7.60
Type C	115	0.03	2.35
Type G	99	2.44	2.53
Type L	20	3.14	4.94
Type M	18	1.18	5.63
Type na	2	2.51	17.81
Type P	220	3.52	1.70
Type PH	10	84.20	7.97
Type S	3	0.13	14.54

Type A: arsenic, C: coal, G: gold, L: leachate, M: metal, na: not available, P: polymetallic, PH: phosphate, S: sulfur

3.2.6 Copper Concentration

The original database contains 817 cases of which 598 cases around the world reported Cu. Of these, 585 cases had concentrations of Cu greater than zero. The median reported Cu concentration was 0.5 mg/L with an IQR from 0.02 to 6.0 mg/L. The average Cu concentration was 26.9 mg/L with a standard deviation of 205 mg/L. The minimum reported Cu concentration was 0.000 mg/L and the maximum was 4760 mg/L. Figure 3-13 shows the concentration of Cu for non-zero cases.

The concentration of Cu varies according to the type of mine. Figure 3-14 and Table 3-7 show the median, mean, maximum, and minimum concentration of Cu according to the type of mine. The highest average value was 44 mg/L for polymetallic mines, whereas the minimum was 0.02 mg/L for arsenic mines.

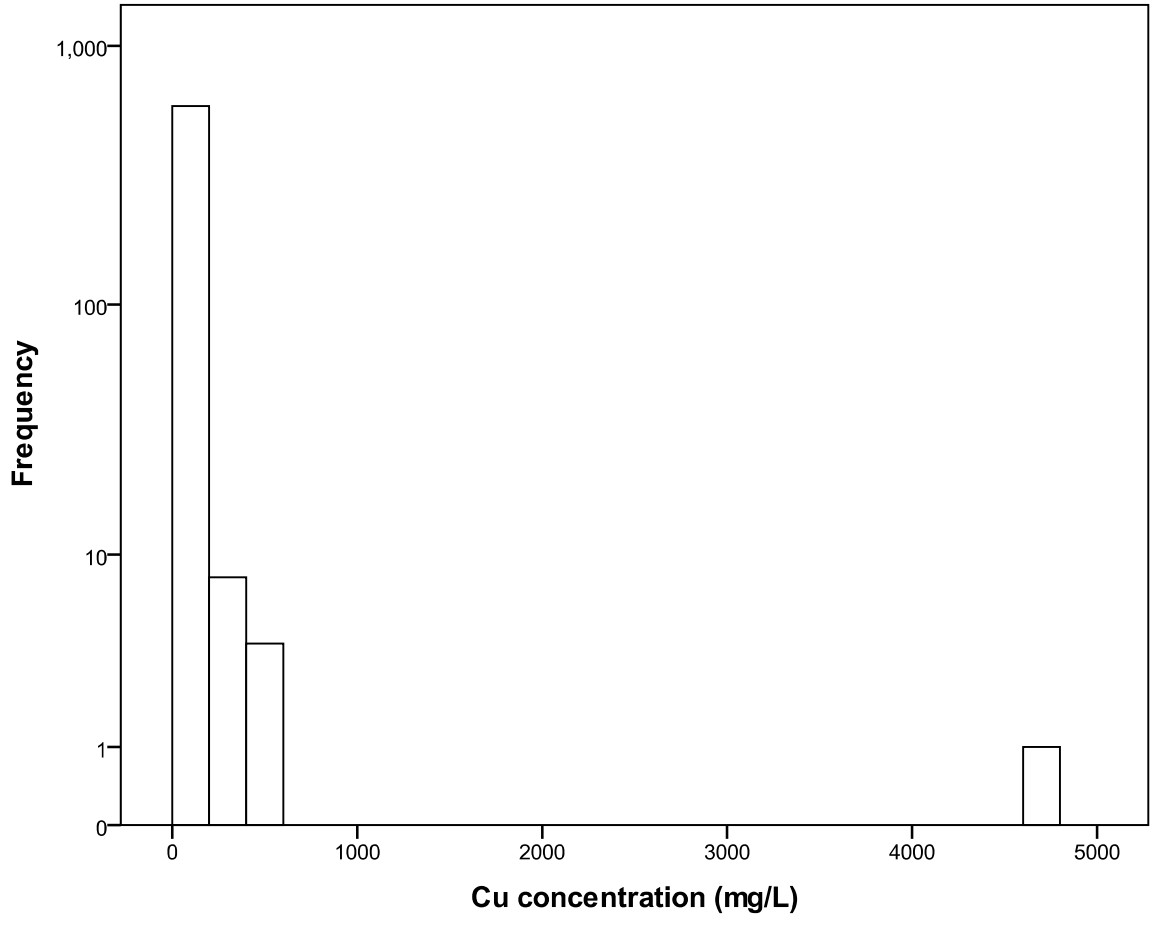

Figure 3-13 Copper concentration range from the database

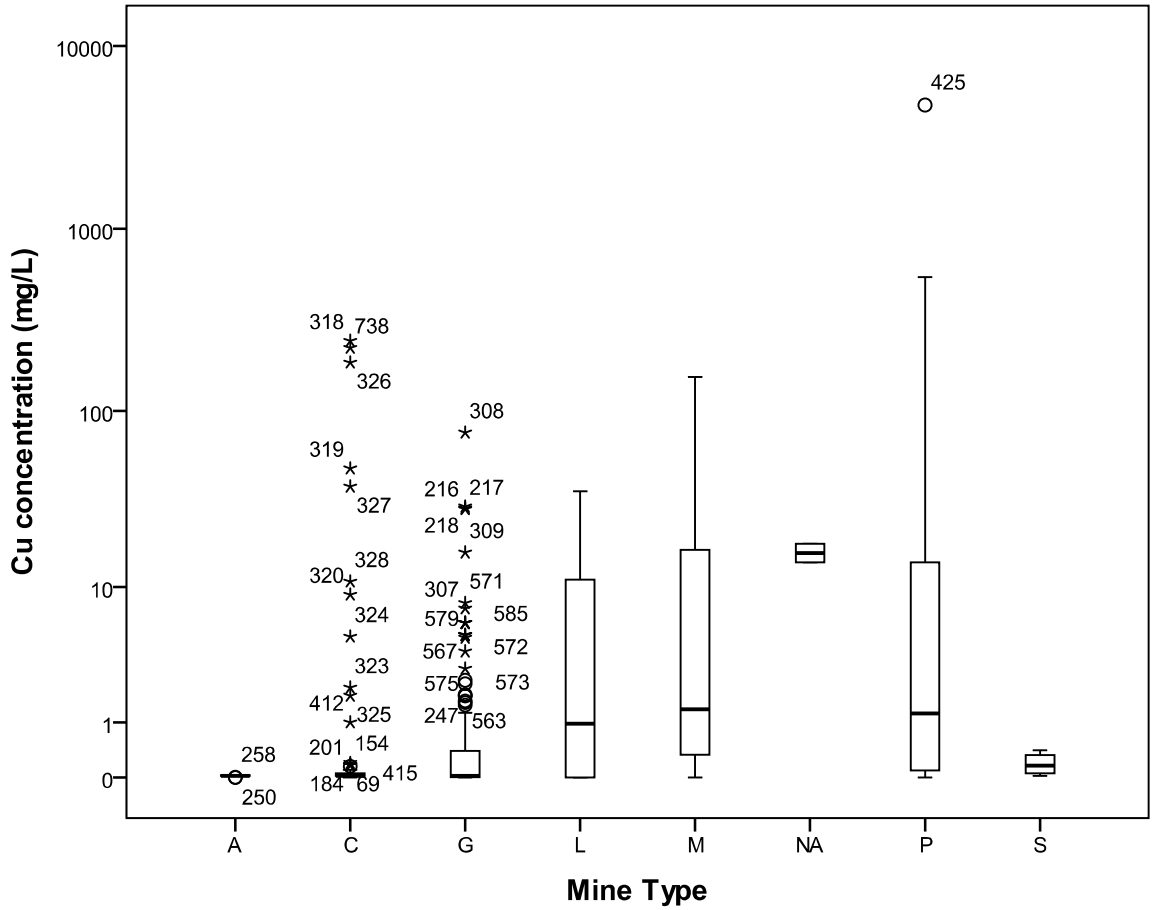

Figure 3-14 Copper concentration range at different types of mine

Table 3-7 Average concentration of Cu according to the type of mine

Type	Cases	Average (mg/L)	Std. Error (mg/L)
Type A	10	0.02	64.10
Type C	76	10.12	23.25
Type G	118	2.26	18.66
Type L	31	6.02	36.41
Type M	44	20.18	30.56
Type na	2	16.00	143.34
Type P	310	43.84	11.51
Type S	7	0.19	76.62

Type A: arsenic, C: coal, G: gold, L: leachate, M: metal, na: not available, P: polymetallic, PH: phosphate, S: sulfur

3.2.7 Iron Concentration

The original database contains 817 cases of which 631 cases around the world reported Fe. Of these, 621 cases had concentrations of Fe greater than zero. The median reported Fe concentration was 15.0 mg/L with an IQR from 0.9 to 253 mg/L. The average Fe concentration was 665.4 mg/L with a standard deviation of 5142 mg/L. The minimum reported Fe concentration was 0.0100 mg/L and the maximum was 124000 mg/L. Figure 3-15 shows the concentration of Fe for non-zero cases.

The concentration of Fe varies according to the type of mine. Figure 3-16 and Table 3-8 show the median, mean, maximum, and minimum concentration of Fe according to the type of mine. The highest average value was 4305 mg/L for phosphate mines, whereas the minimum was 2.1 mg/L for arsenic mines.

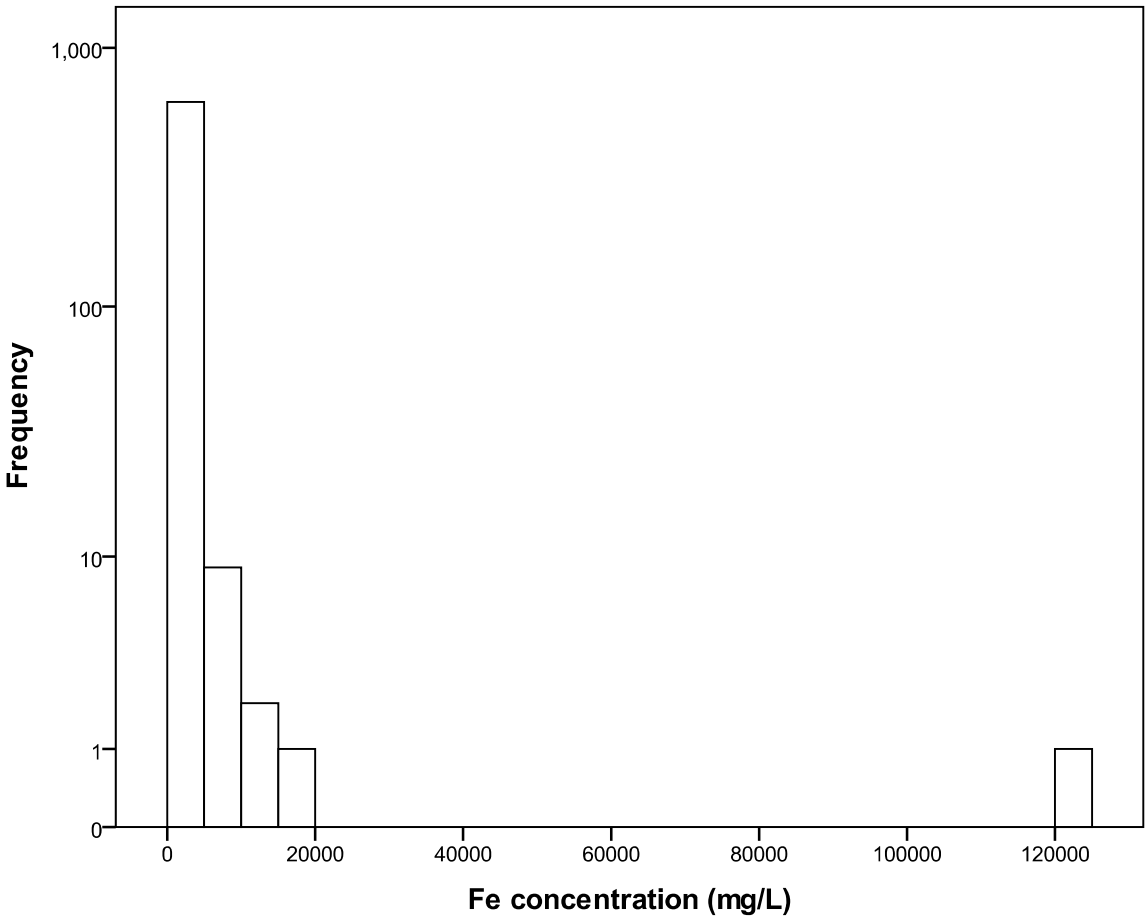

Figure 3-15 Iron concentration range from the database

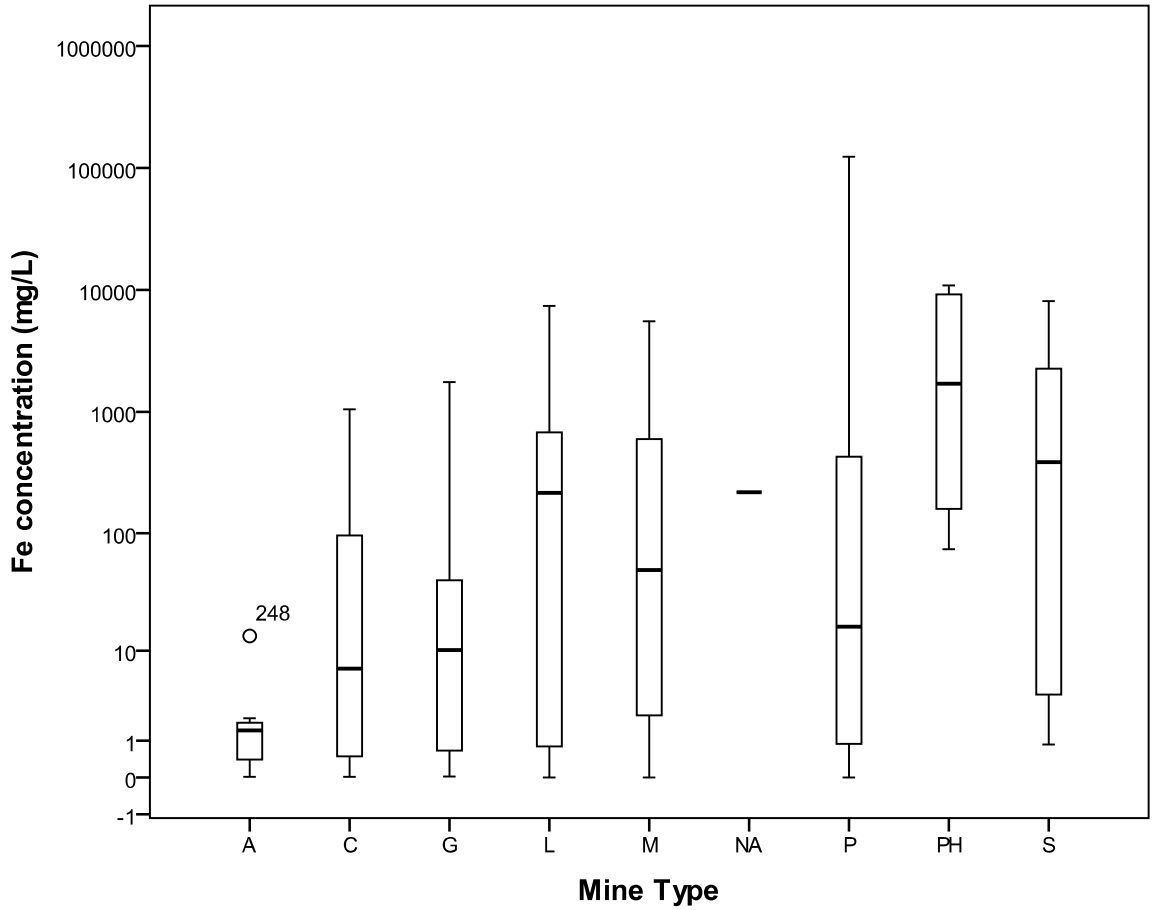

Figure 3-16 Iron concentration range at different types of mine

Table 3-8 Average concentration of Fe according to the type of mine

Type	Cases	Average (mg/L)	Std. Error (mg/L)
Type A	11	2.14	1536.33
Type C	152	85.39	413.30
Type G	75	145.72	588.37
Type L	30	644.01	930.29
Type M	40	525.10	805.66
Type na	2	218.00	3603.01
Type P	301	951.44	293.70
Type PH	10	4304.93	1611.32
Type S	10	1907.98	1611.32

Type A: arsenic, C: coal, G: gold, L: leachate, M: metal, na: not available, P: polymetallic, PH: phosphate, S: sulfur

3.2.8 Lead Concentration

The original database contains 817 cases of which 415 cases around the world reported Pb. Of these, 402 cases had concentrations of Pb greater than zero. The median reported Pb concentration was 0.06 mg/L with an IQR from 0.005 to 0.5 mg/L. The average Pb concentration was 1.5 mg/L with a standard deviation of 7.3 mg/L. The minimum reported Pb concentration was 0.00001 mg/L and the maximum was 73.0 mg/L. Figure 3-17 shows the concentration of Pb for non-zero cases.

The concentration of Pb varies according to the type of mine. Figure 3-18 and Table 3-9 show the median, mean, maximum, and minimum concentration of Pb according to the type of mine. The highest average value was 2.4 mg/L for polymetallic mines, whereas the minimum was 0.02 mg/L for coal mines.

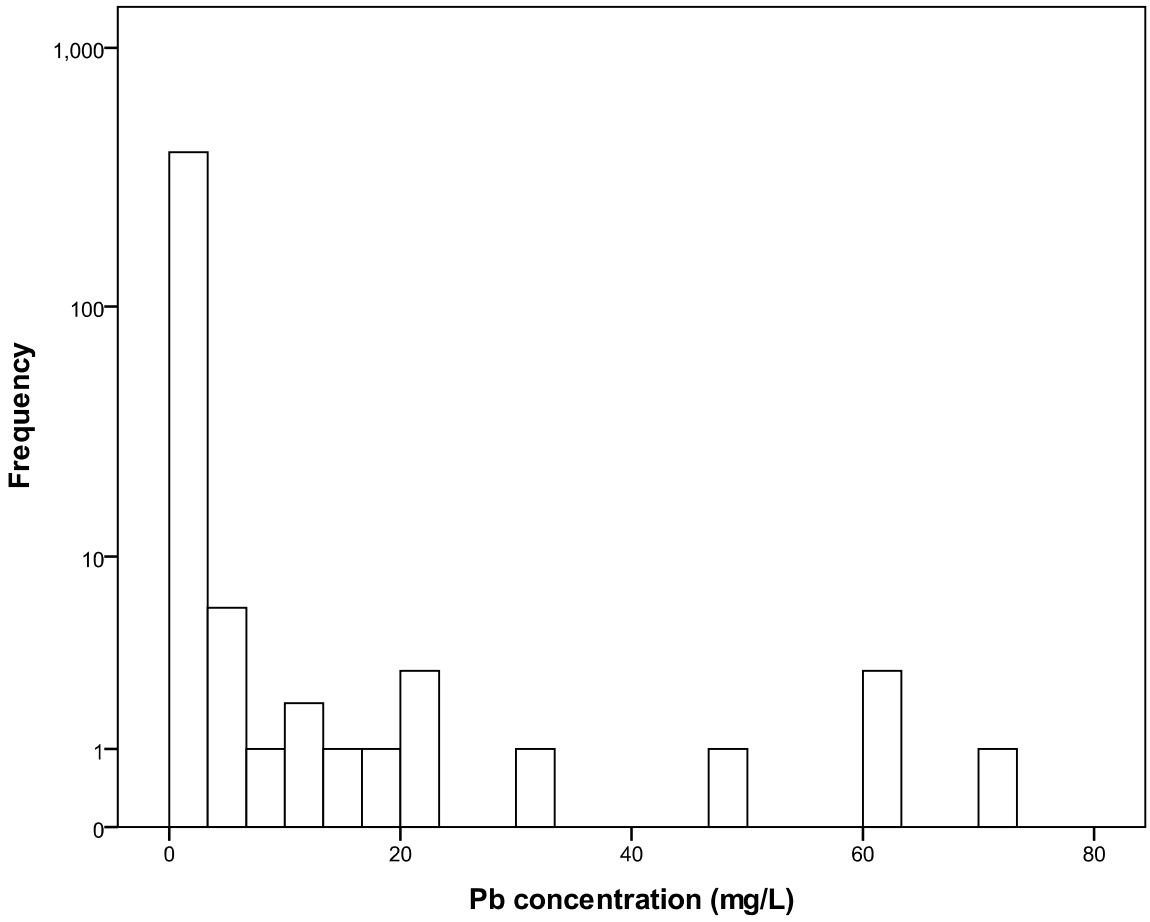

Figure 3-17 Lead concentration range from the database

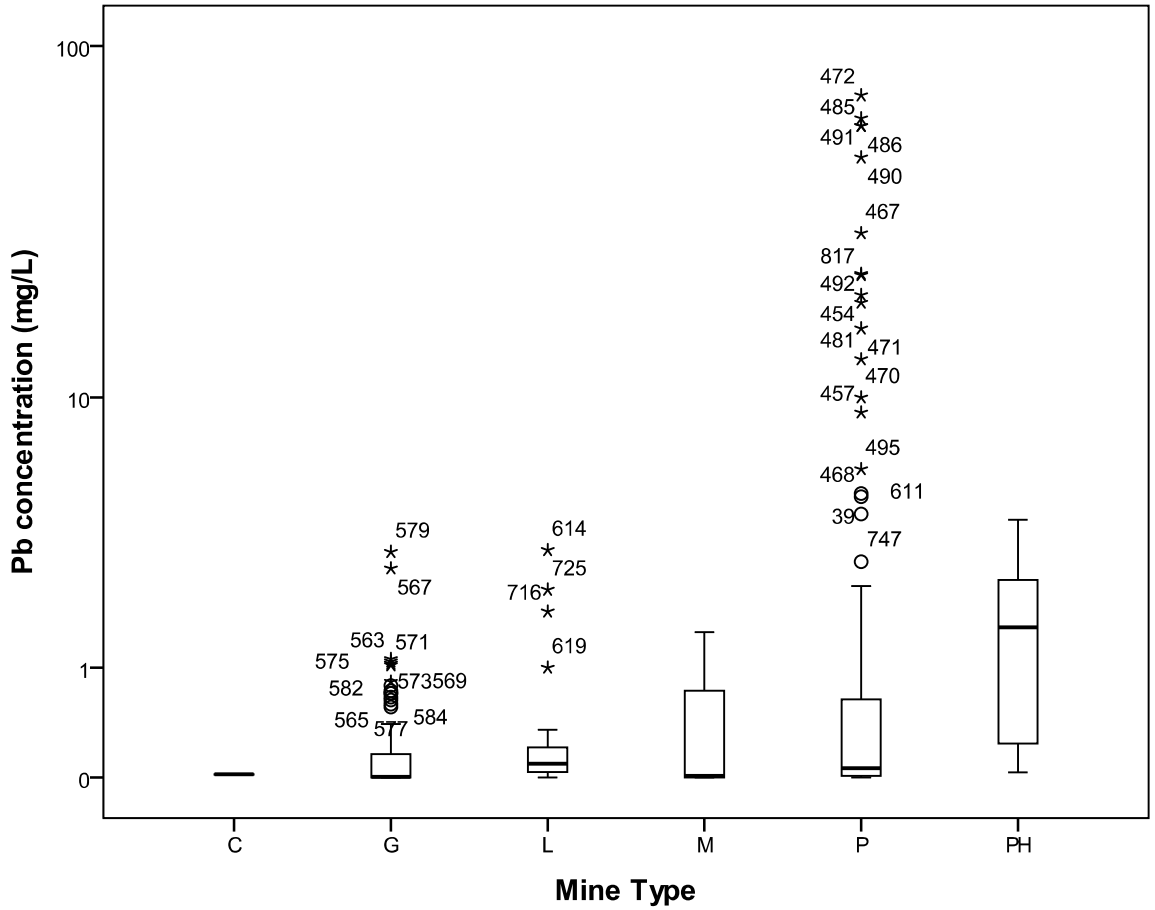

Figure 3-18 Lead concentration range at different types of mine

Table 3-9 Average concentration of Pb according to the type of mine

Type	Cases	Average (mg/L)	Std. Error (mg/L)
Type C	4	0.02	3.60
Type G	113	0.20	0.68
Type L	31	0.36	1.29
Type M	24	0.34	1.47
Type P	233	2.38	0.47
Type PH	10	1.62	2.27

Type A: arsenic, C: coal, G: gold, L: leachate, M: metal, na: not available, P: polymetallic, PH: phosphate, S: sulfur

3.2.9 Zinc Concentration

The original database contains 817 cases of which 607 cases around the world reported Zn. Of these, 602 cases had concentrations of Zn greater than zero. The median reported Zn concentration was 5.2 mg/L with an IQR from 0.2 to 71.0 mg/L. The average Zn concentration was 437 mg/L with a standard deviation of 2711 mg/L. The minimum reported Zn concentration was 0 mg/L and the maximum was 37700 mg/L. Figure 3-19 shows the Log of the concentration of Zn for non-zero cases.

The concentration of Zn varies according to the type of mine. Figure 3-20 and Table 3-10 show the median, mean, maximum, and minimum concentration of Zn according to the type of mine. The highest average value was 814 mg/L for polymetallic mines, whereas the minimum was 1.4 mg/L for sulfide mines.

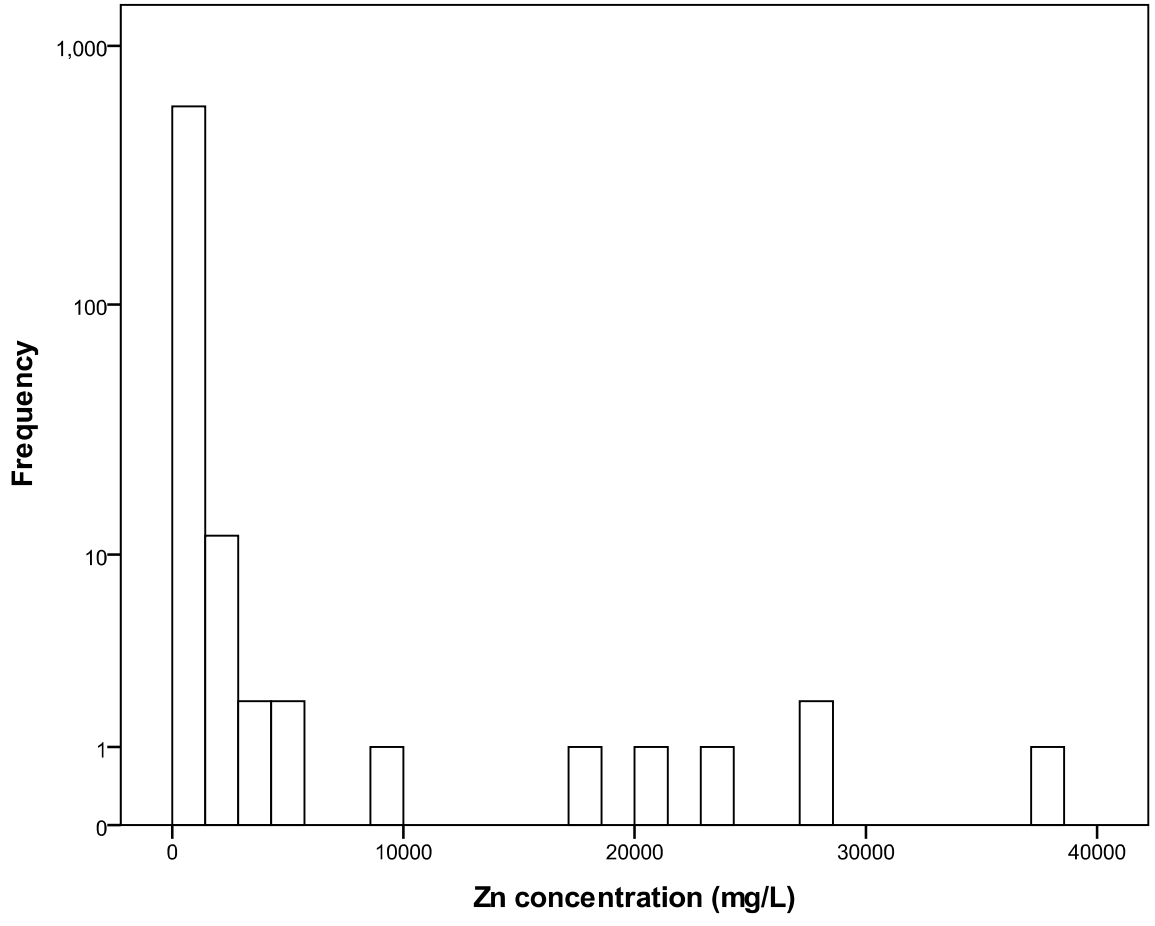

Figure 3-19 Zinc concentration range from the database

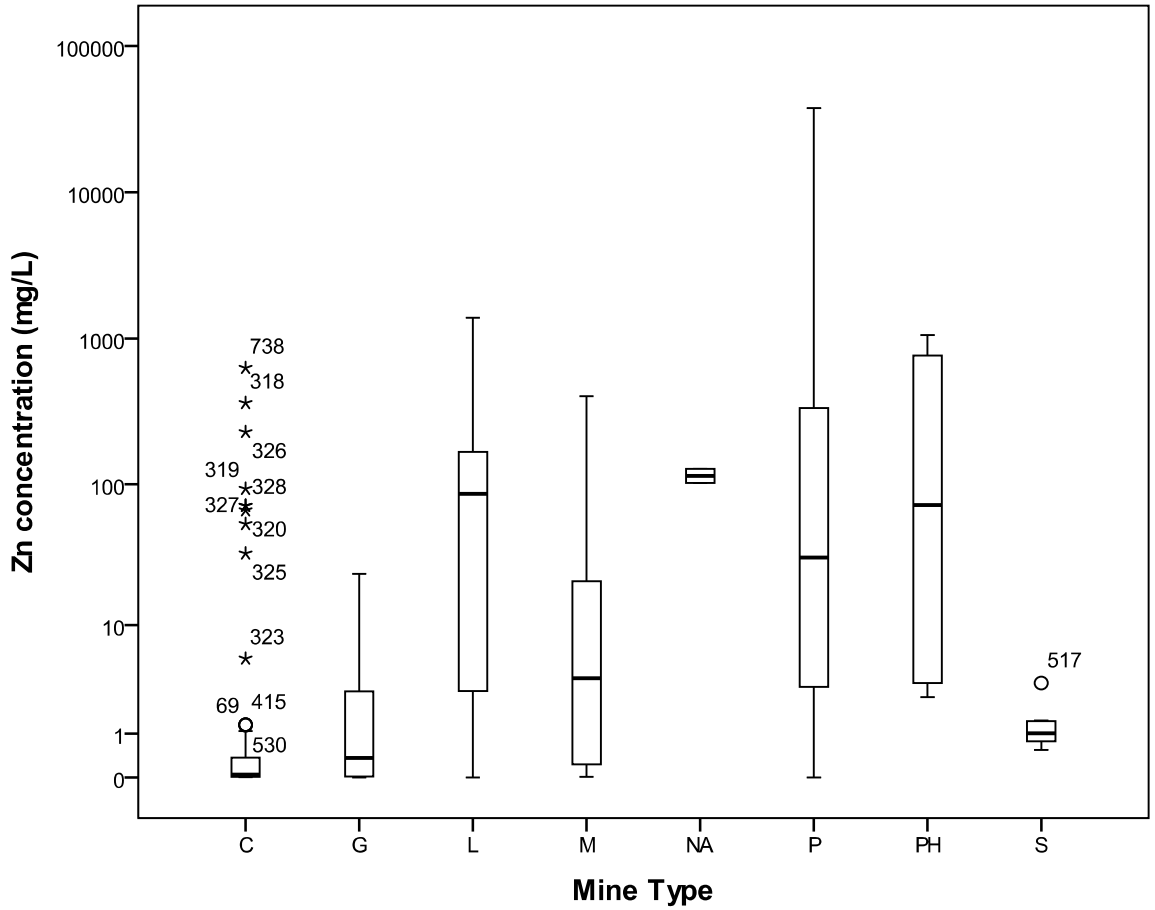

Figure 3-20 Zinc concentration range at different types of mine

Table 3-10 Average concentration of Zn according to the type of mine

Type	Cases	Average (mg/L)	Std. Error (mg/L)
Type C	88	18.49	286.43
Type G	111	2.98	255.04
Type L	33	184.98	467.74
Type M	49	23.13	383.85
Type na	2	115.00	1899.98
Type P	307	814.34	153.35
Type PH	10	359.28	849.70
Type S	7	1.34	1015.58

Type A: arsenic, C: coal, G: gold, L: leachate, M: metal, na: not available, P: polymetallic, PH: phosphate, S: sulfur

3.2.10 Calcium Concentration

The original database contains 817 cases of which 461 cases around the world reported Ca. Of these, 461 cases had concentrations of Ca greater than zero. The median reported Ca concentration was 96.0 mg/L with an IQR from 29.3 to 215 mg/L. The average Ca concentration was 152 mg/L with a standard deviation of 165 mg/L. The minimum reported Ca concentration was 0.05 mg/L and the maximum was 974 mg/L. Figure 3-21 shows the concentration of Ca for non-zero cases.

The concentration of Ca varies according to the type of mine. Figure 3-22 and Table 3-11 show the median, mean, maximum, and minimum concentration of Ca according to the type of mine. The highest average value was 268 mg/L for leachates, whereas the minimum was 26.1 mg/L for arsenic mines.

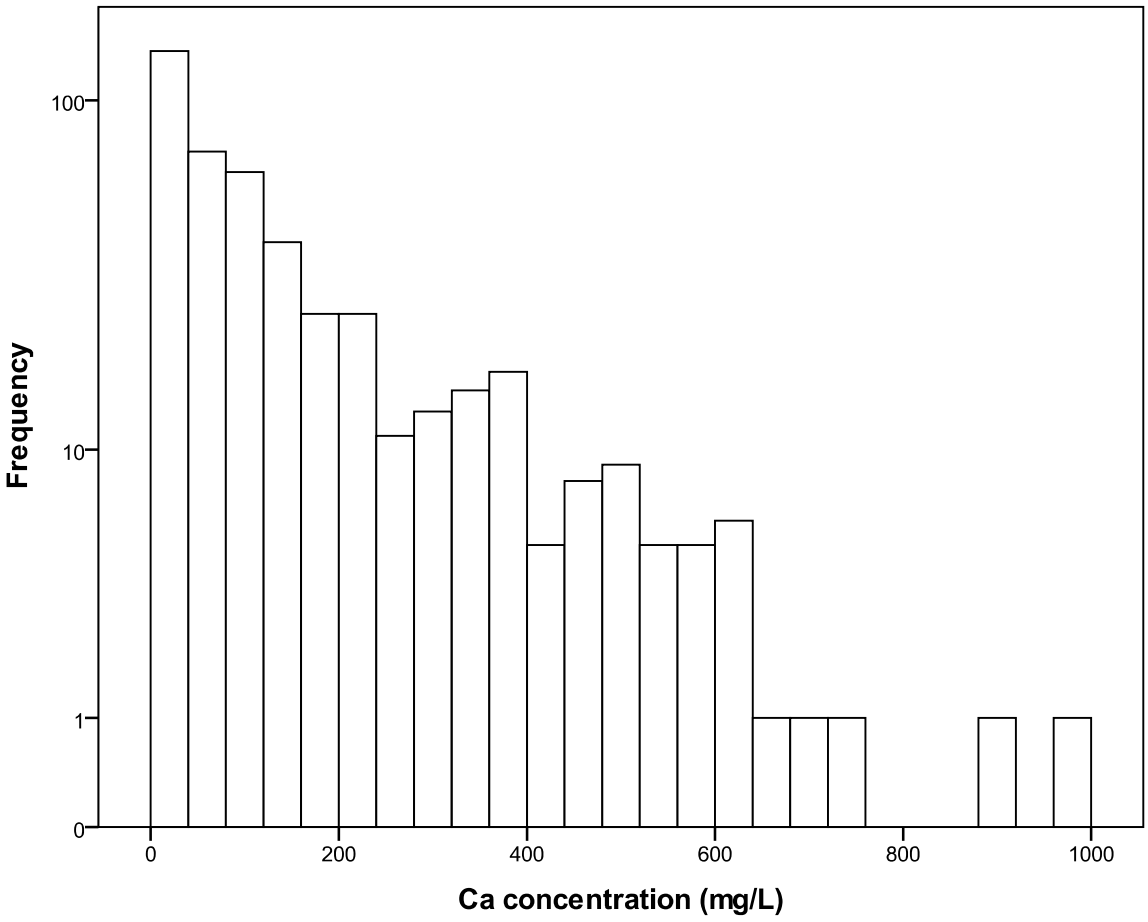

Figure 3-21 Calcium concentration range from the database

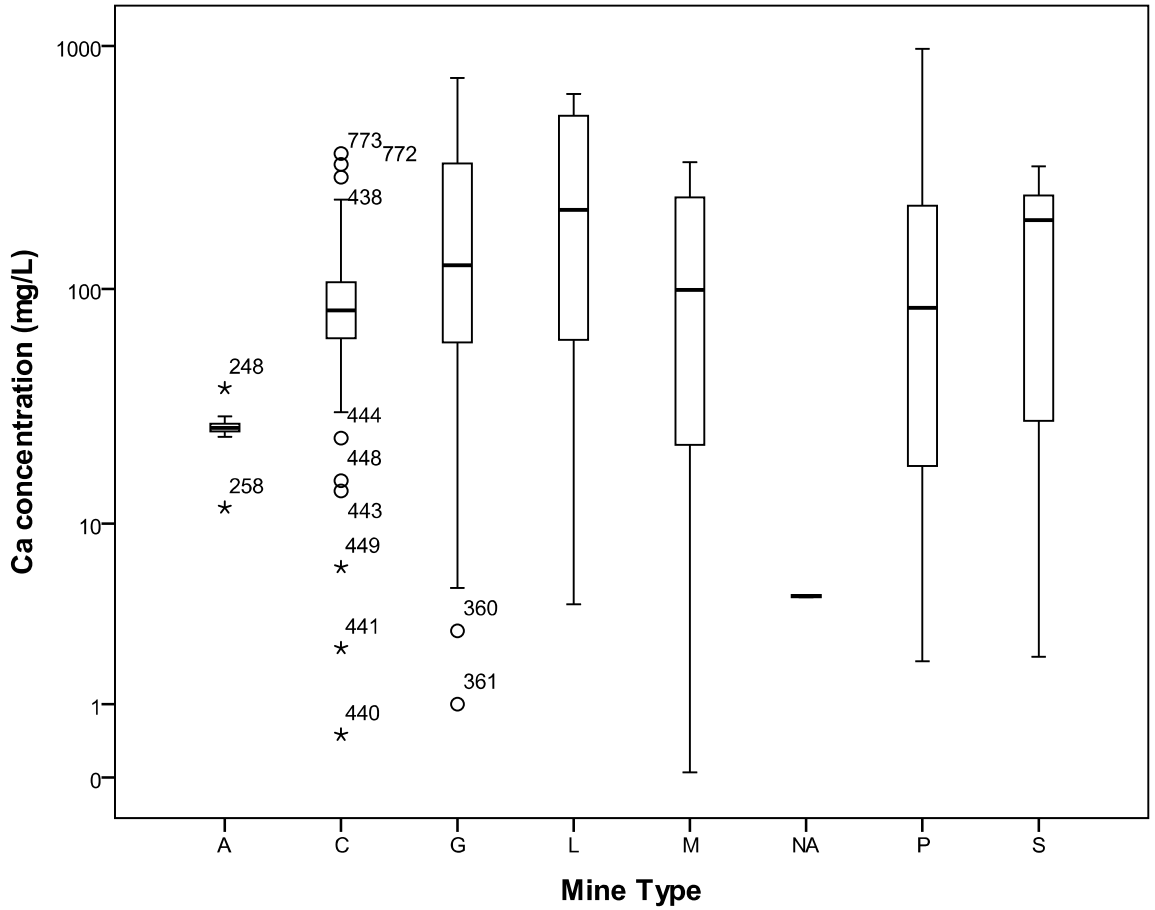

Figure 3-22 Calcium concentration range at different types of mine

Table 3-11 Average concentration of Ca according to the type of mine

Type	Cases	Average (mg/L)	Std. Error (mg/L)
Type A	11	26.13	48.18
Type C	72	98.66	18.82
Type G	86	198.27	17.22
Type L	30	268.51	29.16
Type M	28	136.53	30.18
Type na	2	4.56	112.92
Type P	226	145.48	10.62
Type S	1	164.51	65.20

Type A: arsenic, C: coal, G: gold, L: leachate, M: metal, na: not available, P: polymetallic, PH: phosphate, S: sulfur

3.2.11 Potassium Concentration

The original database contains 817 cases of which 322 cases around the world reported K. Of these, 317 cases had concentrations of K greater than zero. The median reported K concentration was 2.4 mg/L with an IQR from 1.0 to 5.0 mg/L. The average K concentration was 10.0 mg/L with a standard deviation of 53.8 mg/L. The minimum reported K concentration was 0.009 mg/L and the maximum was 667 mg/L. Figure 3-23 shows the concentration of K for non-zero cases.

The concentration of K varies according to the type of mine. Figure 3-24 and Table 3-12 show the median, mean, maximum, and minimum concentration of K according to the type of mine. The highest average value was 20.0 mg/L for gold mines, whereas the minimum was 1.0 mg/L for arsenic mines.

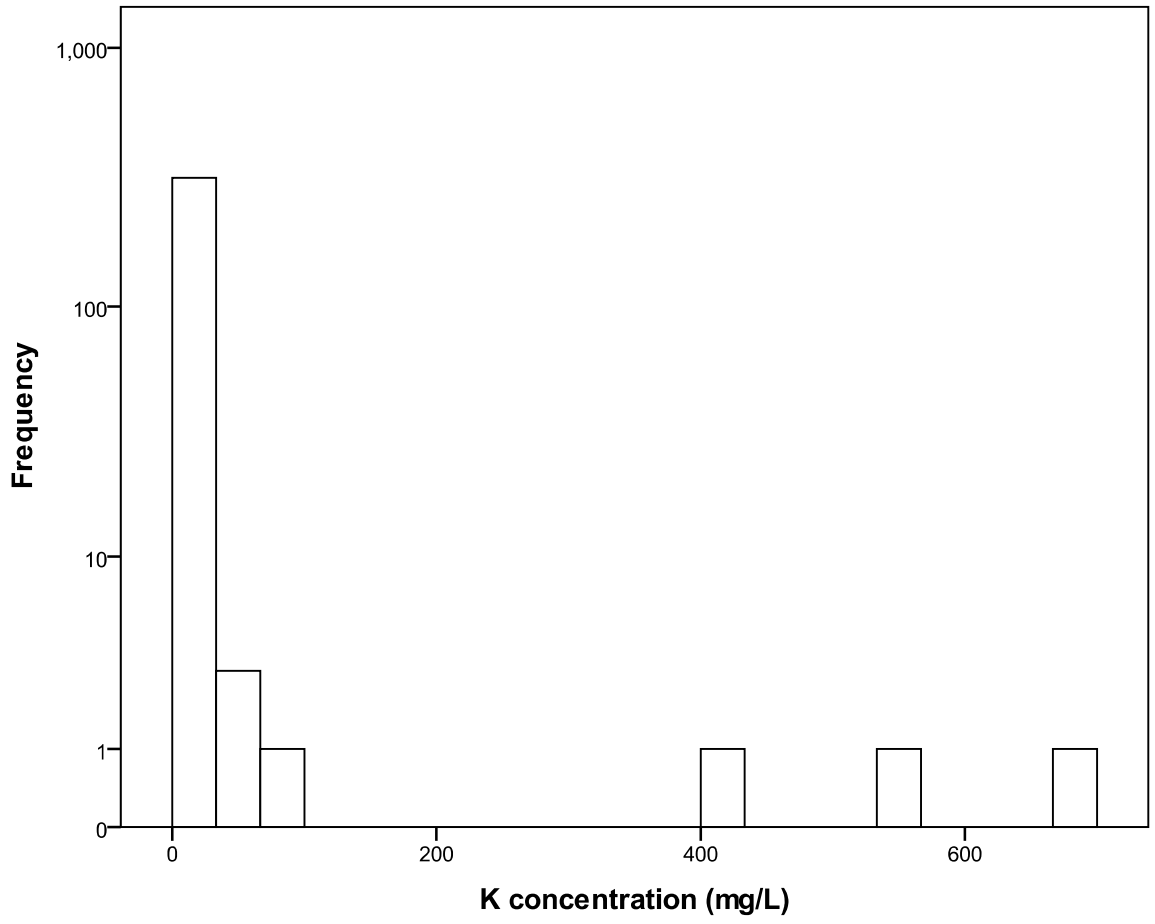

Figure 3-23 Potassium concentration range from the database

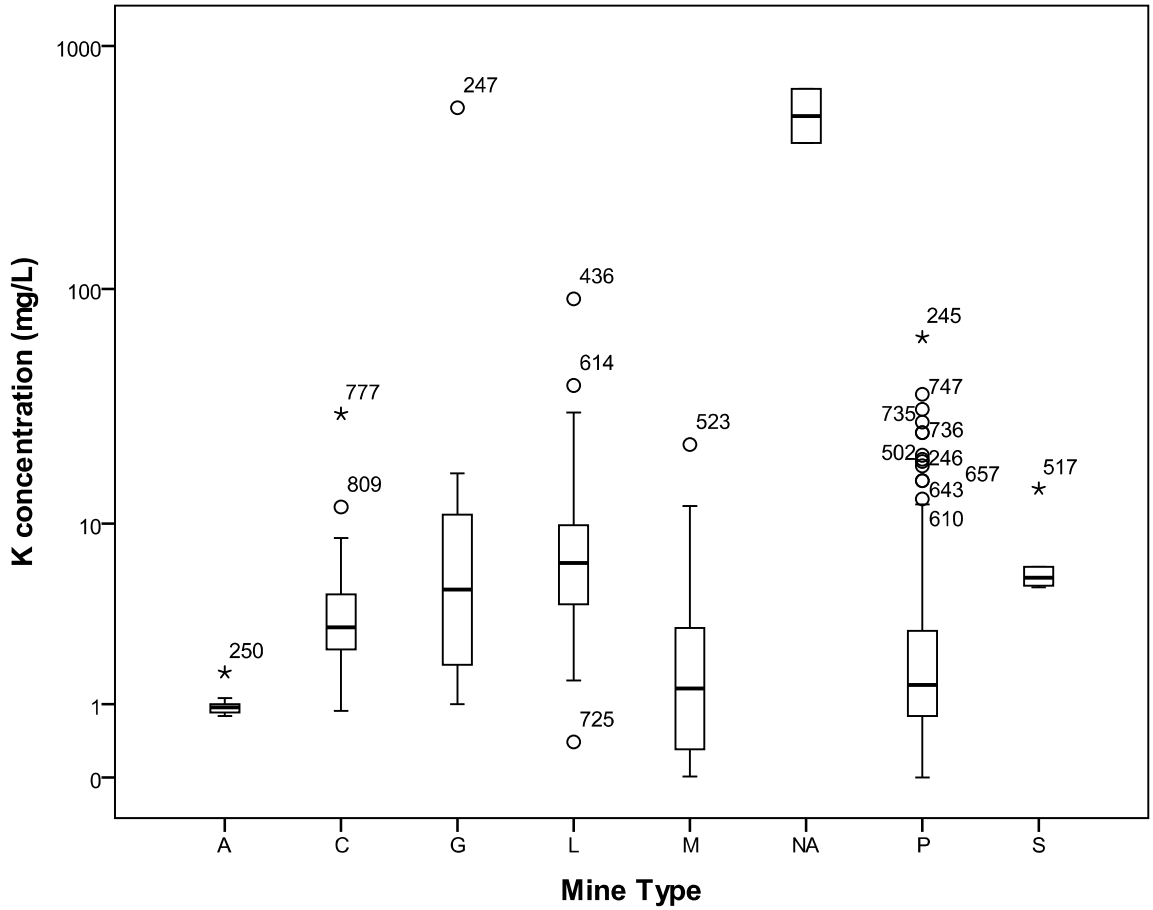

Figure 3-24 Potassium concentration range at different types of mine

Table 3-12 Average concentration of K according to the type of mine

Type	Cases	Average (mg/L)	Std. Error (mg/L)
Type A	11	0.99	10.11
Type C	57	4.02	4.44
Type G	41	19.99	5.23
Type L	25	12.20	6.70
Type M	27	2.91	6.45
Type na	2	533.50	23.70
Type P	153	3.93	2.71
Type S	6	7.00	13.68

Type A: arsenic, C: coal, G: gold, L: leachate, M: metal, na: not available, P: polymetallic, PH: phosphate, S: sulfur

3.2.12 Magnesium Concentration

The original database contains 817 cases of which 423 cases around the world reported Mg. Of these, 423 cases had concentrations of Mg greater than zero. The median reported Mg concentration was 38.0 mg/L with an IQR from 11.0 to 149 mg/L. The average Mg concentration was 218 mg/L with a standard deviation of 628 mg/L. The minimum reported Mg concentration was 0.1 mg/L and the maximum was 7792 mg/L. Figure 3-25 shows the concentration of Mg for non-zero cases.

The concentration of Mg varies according to the type of mine. Figure 3-26 and Table 3-13 show the median, mean, maximum, and minimum concentration of Mg according to the type of mine. The highest average value was 333 mg/L for polymetallic mines, whereas the minimum was 7.3 mg/L for arsenic mines.

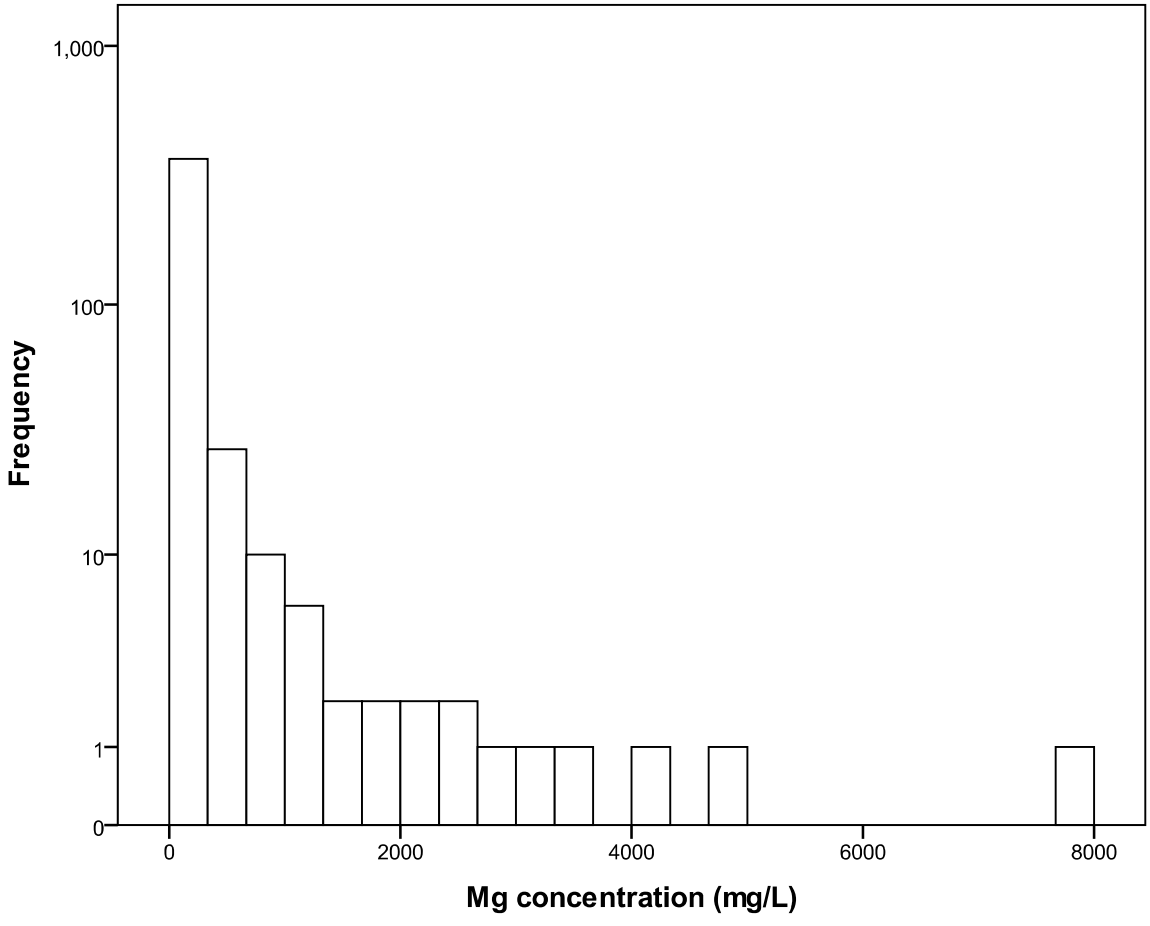

Figure 3-25 Magnesium concentration range from the database

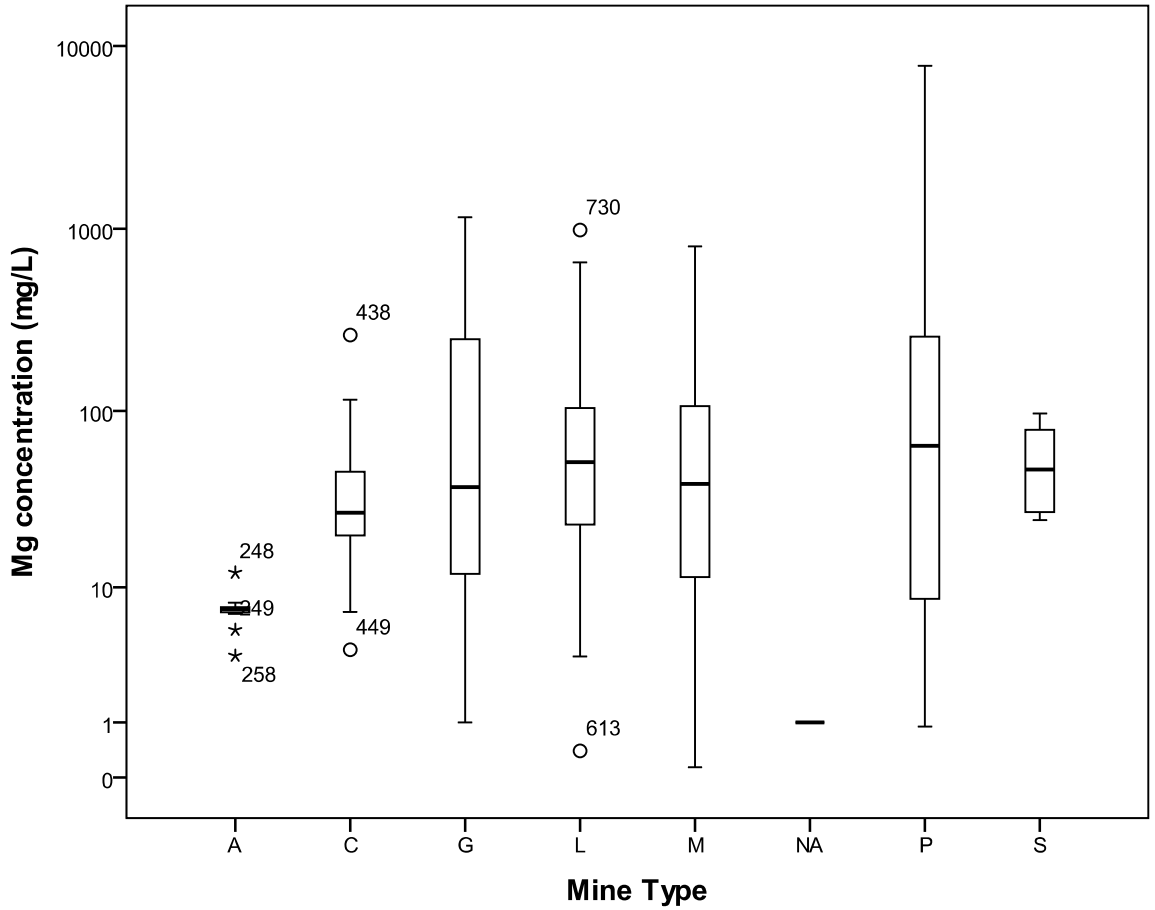

Figure 3-26 Magnesium concentration range at different types of mine

Table 3-13 Average concentration of Mg according to the type of mine

Type	Cases	Average (mg/L)	Std. Error (mg/L)
Type A	11	7.33	186.81
Type C	75	38.02	71.54
Type G	46	171.73	91.35
Type L	30	117.18	113.12
Type M	28	100.54	117.09
Type na	2	1.00	438.10
Type P	225	332.57	41.30
Type S	6	55.64	252.94

Type A: arsenic, C: coal, G: gold, L: leachate, M: metal, na: not available, P: polymetallic, PH: phosphate, S: sulfur

3.2.13 Sodium Concentration

The original database contains 817 cases of which 366 cases around the world reported Na. Of these, 366 cases had concentrations of Na greater than zero. The median reported Na concentration was 16.4 mg/L with an IQR from 5.9 to 31.4 mg/L. The average Na concentration was 66.8 mg/L with a standard deviation of 211 mg/L. The minimum reported Na concentration was 0.01 mg/L and the maximum was 2400 mg/L. Figure 3-27 shows the concentration of Na for non-zero cases.

The concentration of Na varies according to the type of mine. Figure 3-28 and Table 3-14 shows the median, mean, maximum, and minimum concentration of Na according to the type of mine. The highest average value was 198 mg/L for gold mines, whereas the minimum was 5.6 mg/L for arsenic mines.

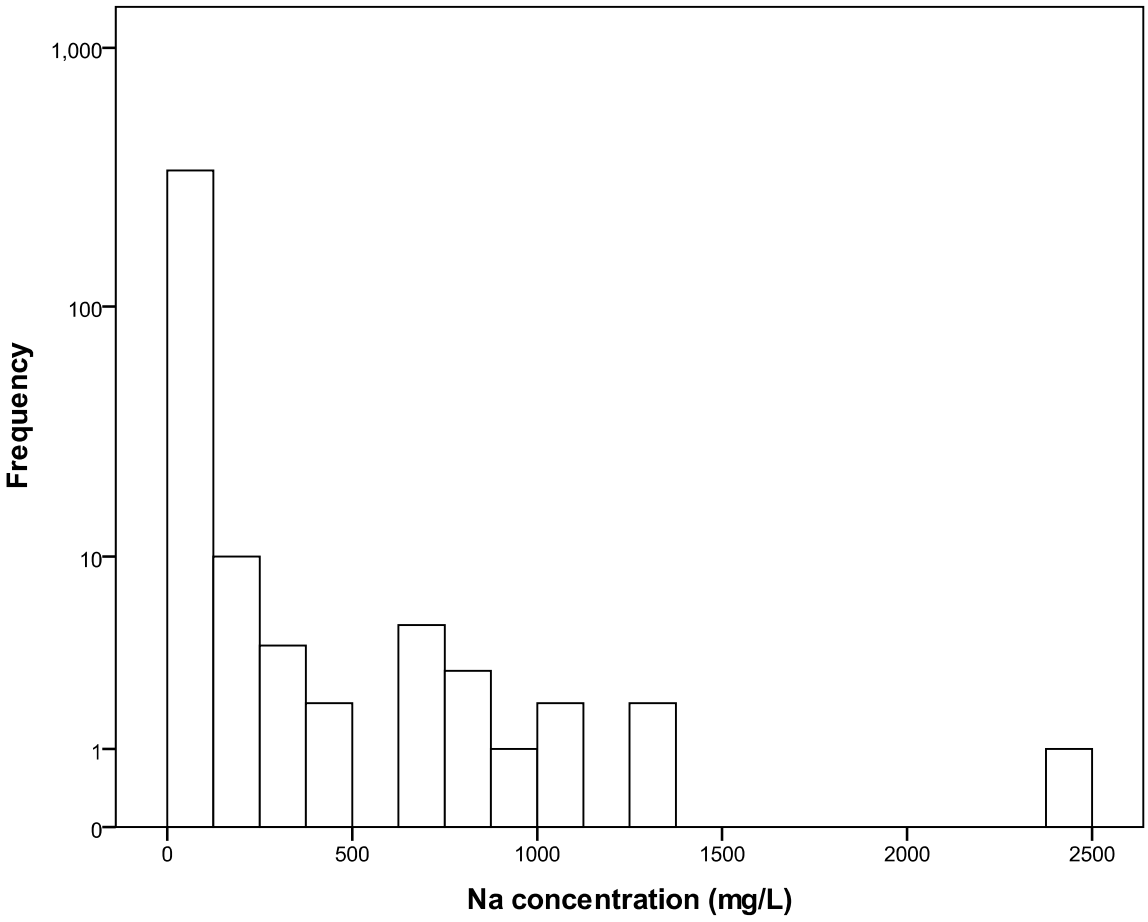

Figure 3-27 Sodium concentration range from the database

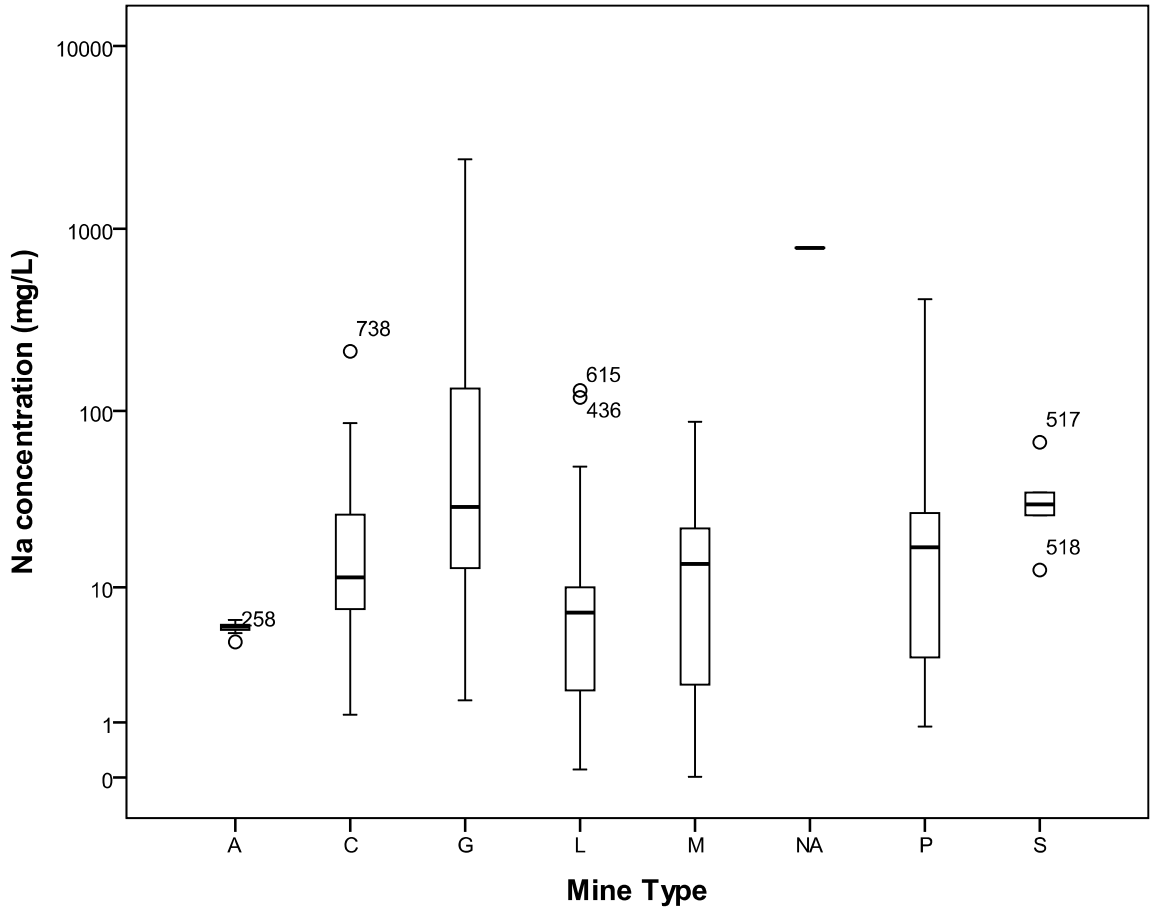

Figure 3-28 Sodium concentration range at different types of mine

Table 3-14 Average concentration of Na according to the type of mine

Type	Cases	Average (mg/L)	Std. Error (mg/L)
Type A	11	5.60	58.01
Type C	58	22.07	25.26
Type G	82	197.86	21.24
Type L	27	17.01	37.02
Type M	28	18.22	36.36
Type na	2	787.00	136.04
Type P	152	27.29	15.60
Type S	6	33.68	78.54

Type A: arsenic, C: coal, G: gold, L: leachate, M: metal, na: not available, P: polymetallic, PH: phosphate, S: sulfur

3.3 Relationship between Parameters

The first major task in this approach to empirical modeling is to reduce a water-chemistry database with thousands of numbers to a more manageable level using, for example, statistical tools. The variables with highest influence for water chemistry include pH, time, sulfate, flow rate, temperature, and rock type. As constituents dissolved in ARDs are numerous, there is no typical composition of ARDs and, thus, classification of ARDs based on their constituents is difficult to achieve. Several classification schemes of ARDs have been proposed using one or several water parameters such as major cations and anions, pH, pH and Fe^{2+} and Fe^{3+} concentration, pH versus combined metals, alkalinity versus acidity, alkalinity vs. acidity and sulfate concentration. However these classifications have several limitations such as (a) classifications do not include waters with neutral pH and extraordinary salinities; (b) do not consider water with elevated concentration of arsenic, antimony, mercury, cyanide compounds, etc.; (c) do not consider iron, manganese and aluminum that which are present in major concentrations in ARDs; (d) routine water analysis do not include determinations of Fe^{2+} and Fe^{3+} (Lottermoser 2007).

Predicting ARD is an important aspect of mining, mineral processing activities, and construction. However, it is a very complex task and represents a major challenge for scientists and operators. There are simple mathematical models and computational tools which help predict the chemistry of ARDs. The predicted concentrations of individual metals, metalloids, and anions of ARDs obtained from computational geochemical models should be compared with actual site measurements. Geochemical modeling programs of waters are also able to calculate the mineral saturation indices and to identify minerals that will probably form. At low pH values, metals are mobilized and present at concentrations that favor precipitation of secondary minerals. Precipitation and adsorption are also important process in ARDs and computational software can predict this phenomenon (Lottermoser 2007).

Up to now, the effectiveness of a remedial alternative usually cannot be quantified or predicted and, thus, remediation has been experimental. Therefore, research is required to achieve the best and appropriate remediation available at a given time for a given site (Nordstrom 2004). Having a database of ARD from different sites, countries, and type of mines can help understand the composition of ARDs, tendencies, relationship between parameters, etc.

3.3.1 Relationship between Metals and pH

Problems with ARD usually start when ground and surface water come into contact with excavated materials or minerals under oxic conditions and dissolve several components of the ore mineral. These processes are controlled by the Eh-pH conditions. If sulfide minerals are present, the acidity that is formed can be able to dissolve other metals. Considering that metal, coal and other types of mines are so diverse in their mineral composition, ARD discharge in each construction site or mine is unique. If carbonate minerals are present, they can neutralize the acidity, leading to neutral to alkaline water.

It is commonly accepted that sulfide minerals, especially the oxidation of pyrite, are the initial reactions in the formation of ARD which produces protons (see Chapter 2, Section 2.3). Pyrite oxidation is

a complex process that occurs rapidly and releases acid into the water. For that reason, pyrite weathering is the strongest acid-producing process of all oxidation processes that occur in nature (Stumm and Morgan 1996). If no buffering minerals are present, the pH can be extremely acidic with a value as low as -3.6 (Stumm and Morgan 1996; Nordstrom and Alpers 1999; Nordstrom et al. 2000). The reaction is exothermic and therefore air and water temperature can reach higher temperatures than usual (Nordstrom 2004).

Oxidation of pyrite and other sulfides is the major contribution of hydrogen ion in ARD, associated with the release of sulfate, heavy metals, metalloids, and other elements. Due to its important role in several reactions that led to the formation to ARD, the pH has been considered as the "master variable" (Stumm and Morgan 1996). The variation in concentration of the metals is also affected by the pH, as shown from Figure 3-29 to Figure 3-42. A clear inverse linear relationship was determined for EC-pH (Figure 3-29), sum of metal-pH (Figure 3-30), sulfate-pH (Figure 3-31), Al-pH (Figure 3-33), Cu-pH (Figure 3-14), Fe-pH (Figure 3-36), and Zn-pH (Figure 3-38) systems for the whole range of pH, except for the bicarbonate-pH (Figure 3-32), in which a direct linear relationship was observed. In general, it can be said that at low pH values, more metals are found in solution (Figure 3-30). Oxidation of pyrite (FeS_2, a sulfide mineral) is the major contributor of acidity. The oxidation of each sulfide mineral consists of several reactions that have different oxidation rates and create acid together with metal and sulfate release into water. ARD water are particularly characterized by high sulfate (>1000 mg/L), high Al and Fe (>100 mg/L), and elevated Cu, Cr, Ni, Pb and Zn (>10 mg/L). Ca, K, Mg and Na may also occur in strongly elevated concentrations. Although these alkaline metals are not of environmental concern, they may limit the use of water because of its hardness (Lottermoser 2007).

In case of As, a different tendency to other heavy metals is observed. The dissolution of As salts will lead to As release and dissolution. Arsenolite (As_2O_3) is a high solubility phase that readily liberates As into water (Williams 2001). In addition, scorodite ($FeAsO_4 \cdot 2H_2O$) is a common As mineral which is formed during the oxidation of arsenopyrite-rich wastes. Scorodite solubility is strongly controlled by pH (Krause and Ettel 1988). It is very soluble at very low pH, its solubility decreases at pH 4 and then the solubility increases at pH higher than 4. This tendency is observed in Figure 3-34; from this, it is probable that arsenopyrite (or scorodite resulting from its oxidation) was present in the ARDs collected.

Low pH is not a universal characteristic of ARDs. The pH can be alkaline, with anions and cations ranging from less than 1 mg/L to several 100,000 mg/L (Lottermoser 2007). In acid waters, sulfate is the principal anion, and iron, manganese, and aluminum are the major cations, whereas in alkaline waters, sulfate and bicarbonate (Figure 3-32) are principal anions, and concentrations of calcium, magnesium, and sodium are generally elevated relative to iron and aluminum (Lottermoser 2007). According to Lottermoser (2007), neutral to alkaline mine waters with high metal, metalloid, and sulfate concentrations can be caused by:

- Drainage from tailings repositories containing residues of alkaline leach processes or neutralized acid tailings.
- Drainage from non-sulfidic ores or wastes.

- Drainage from sulfidic ores or wastes that have been completely oxidized during pre-mining weathering.
- Drainage from pyrite-rich ores and wastes with abundant acid neutralizing minerals such as carbonate.
- Drainage from sulfide ores or waste depleted in acid producing sulfides (e.g. pyrite, pyrrhorite) and enriched in non-acid producing sulfides (e.g. galena, spharelite, arsenopyrite, chalcocite, covellite, stibnite).

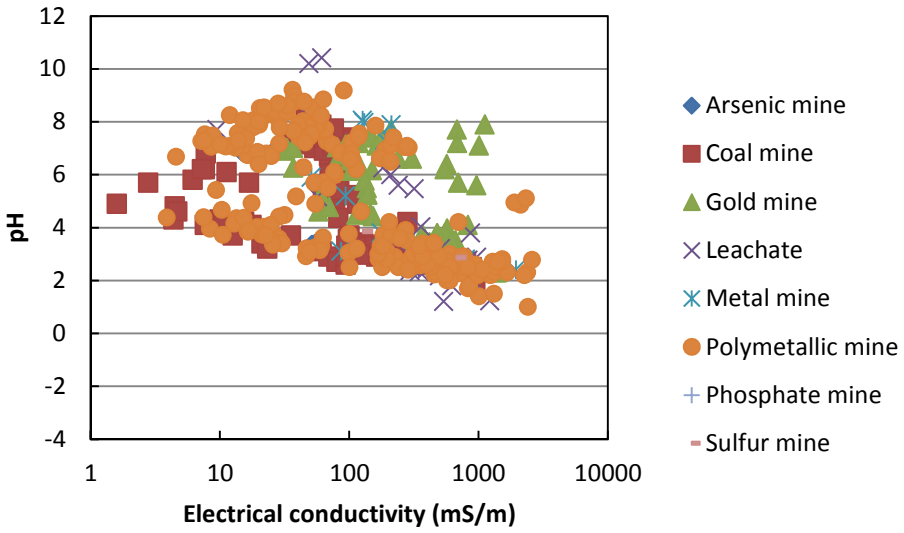

Figure 3-29 Electrical conductivity at different pH values

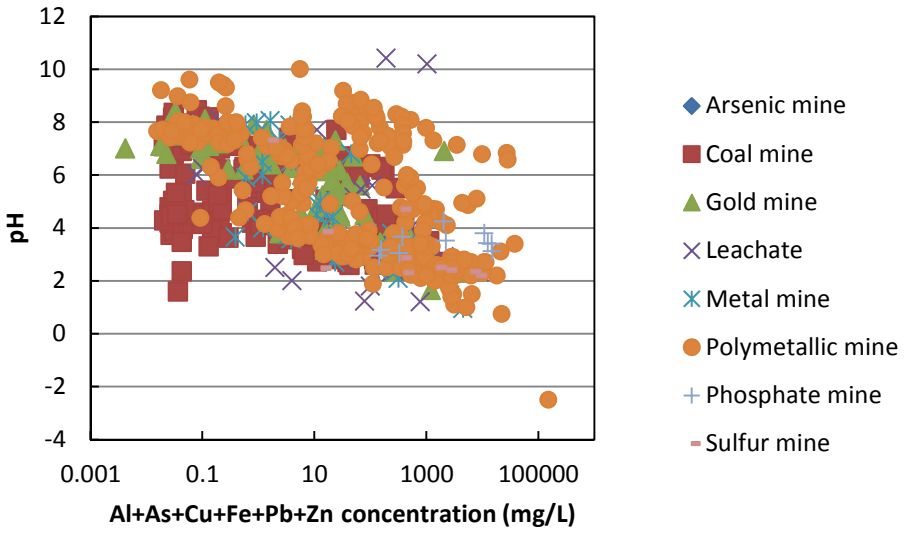

Figure 3-30 Relationship between Sum of metal and pH

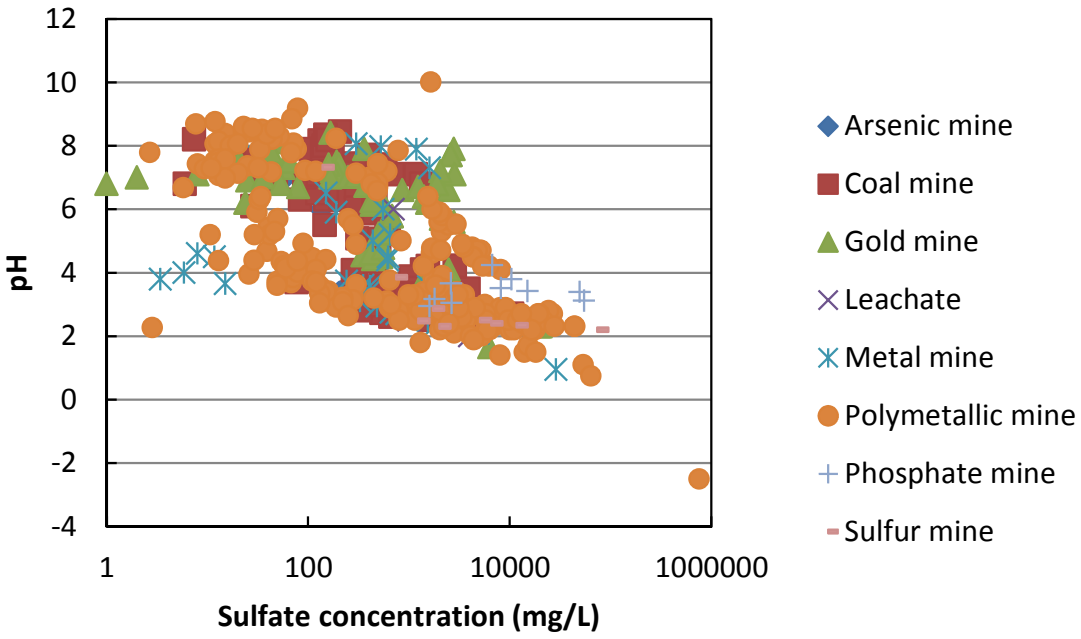

Figure 3-31 Sulfate concentration at different pH values

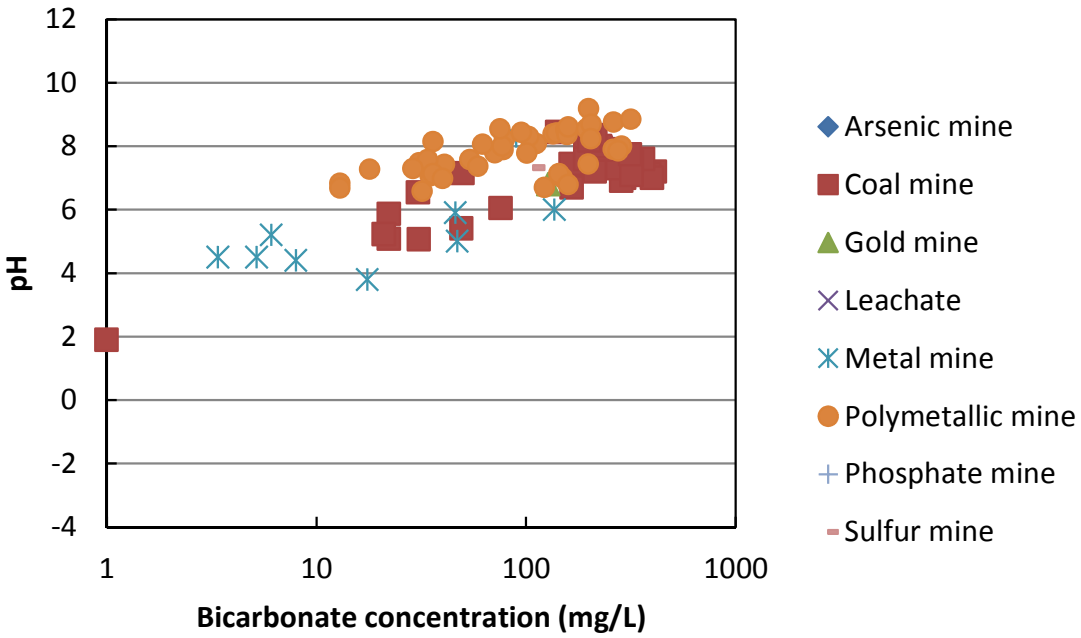

Figure 3-32 Bicarbonate concentration at different pH values

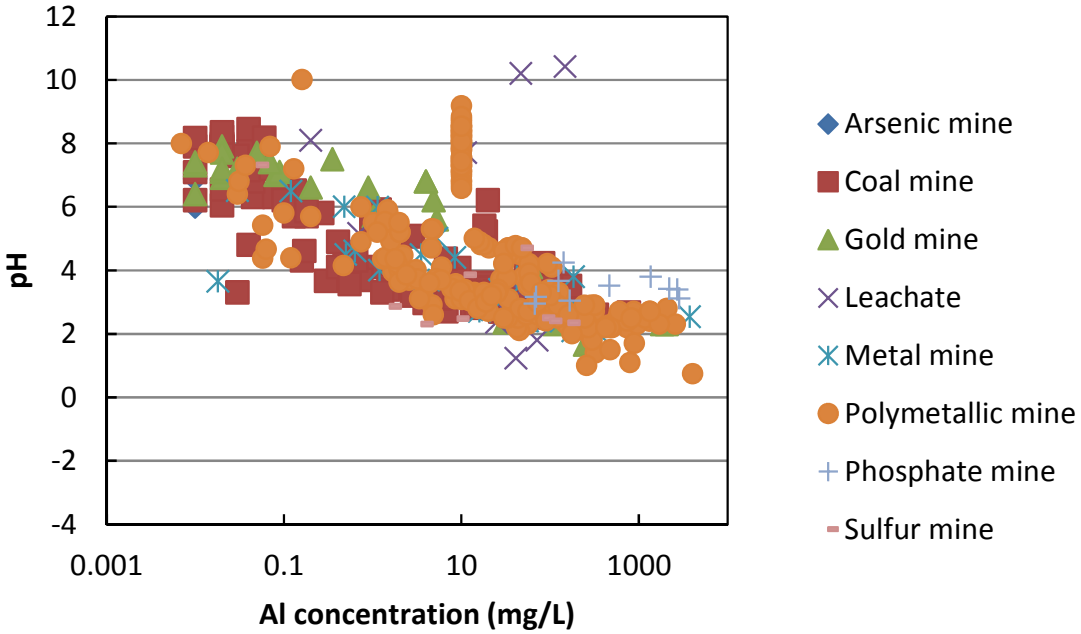

Figure 3-33 Al concentration at different pH values

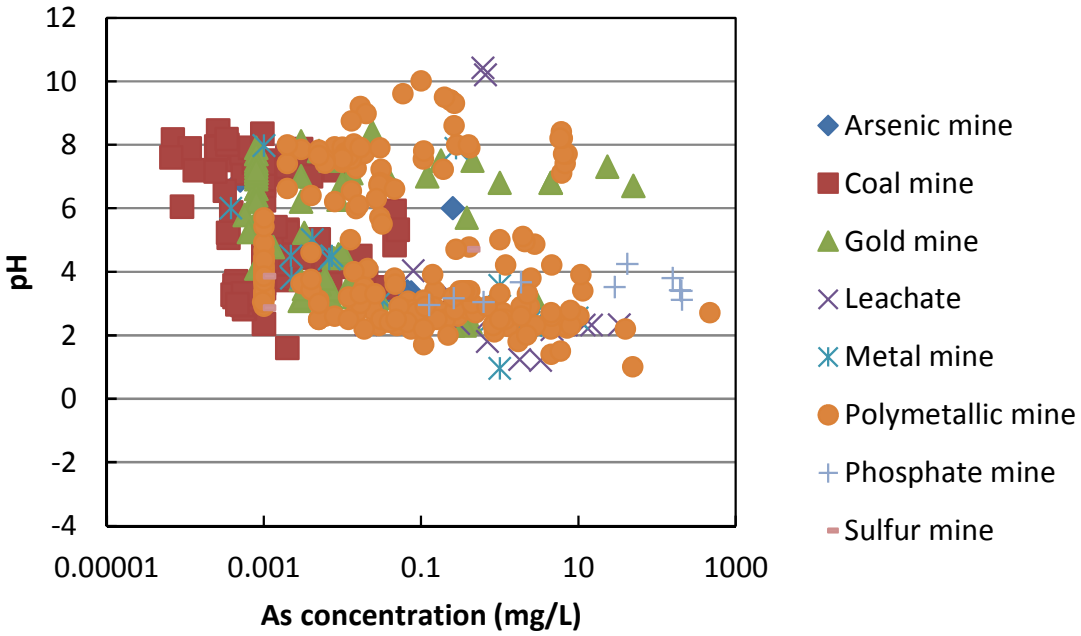

Figure 3-34 As at different pH values

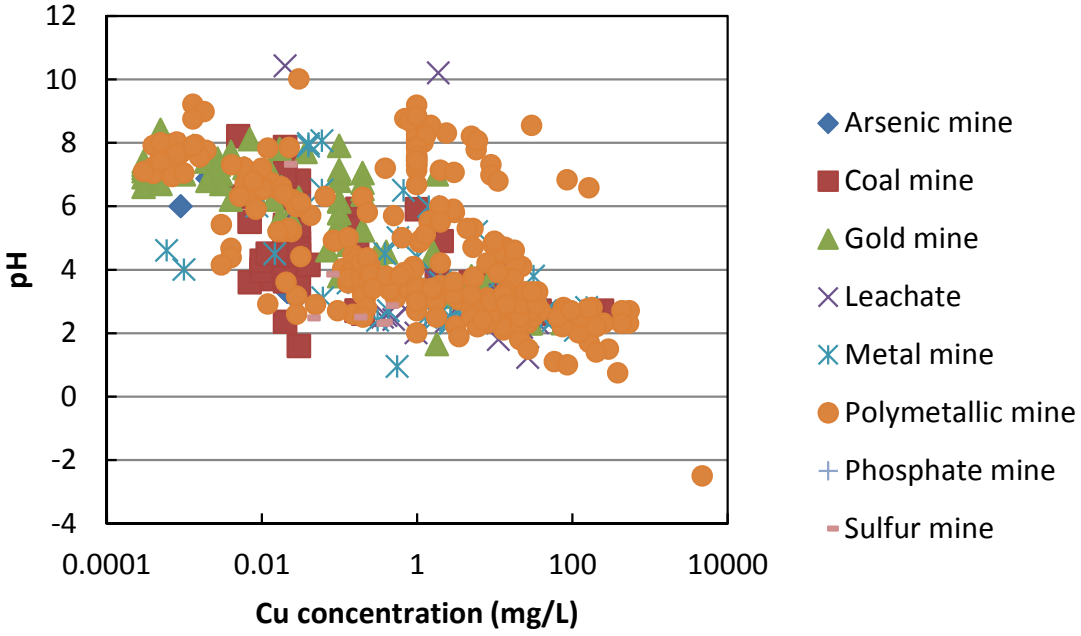

Figure 3-35 Cu concentration at different pH values

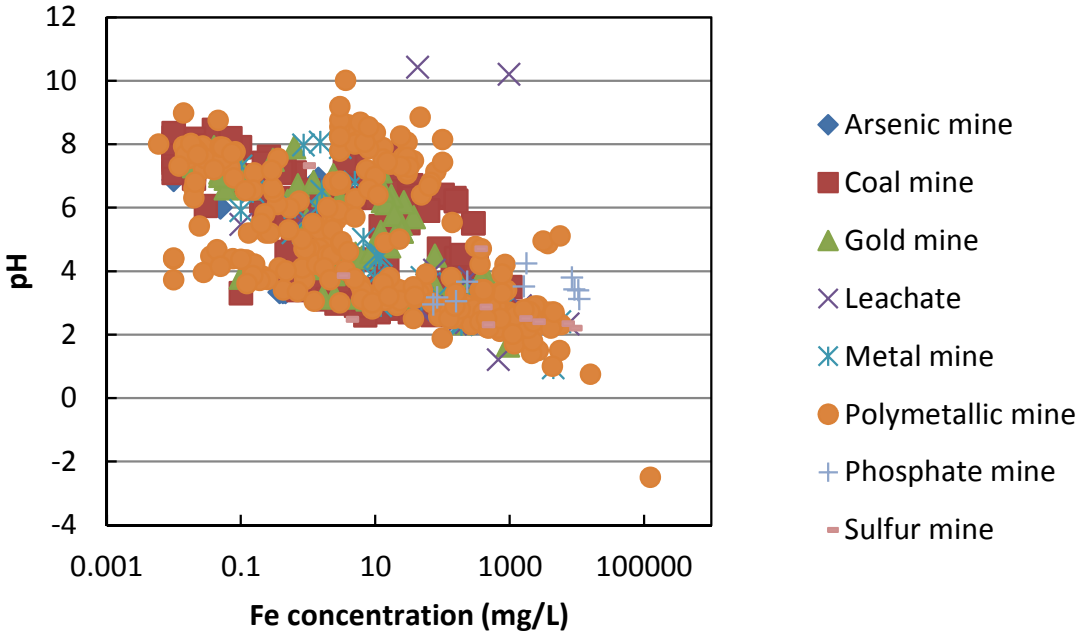

Figure 3-36 Fe concentration at different pH values

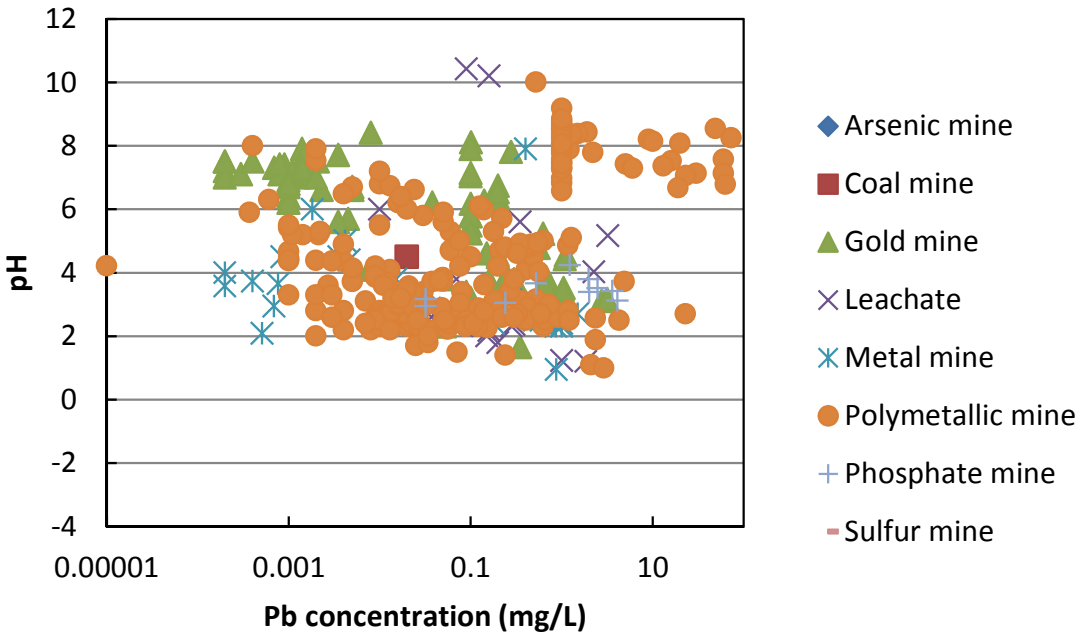

Figure 3-37 Pb concentration at different pH values

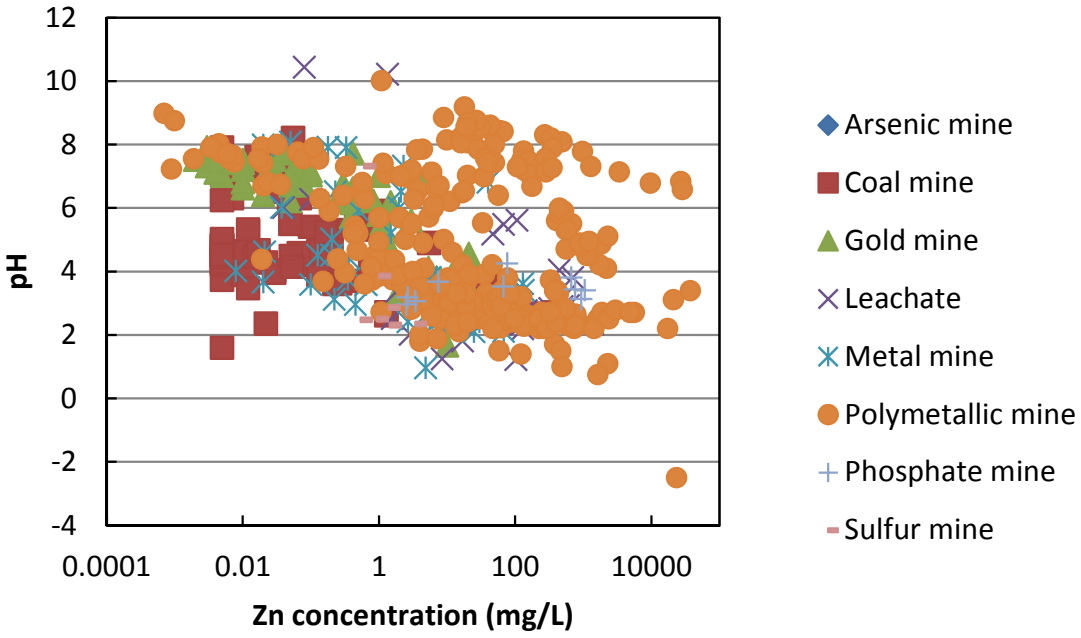

Figure 3-38 Zn concentration at different pH values

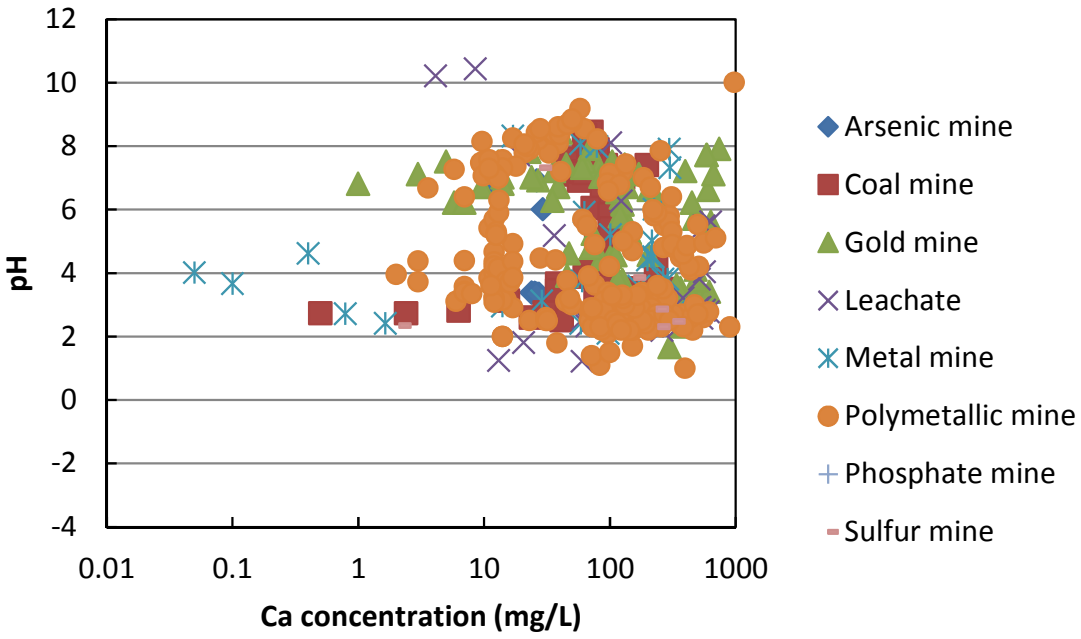

Figure 3-39 Ca concentration at different pH values

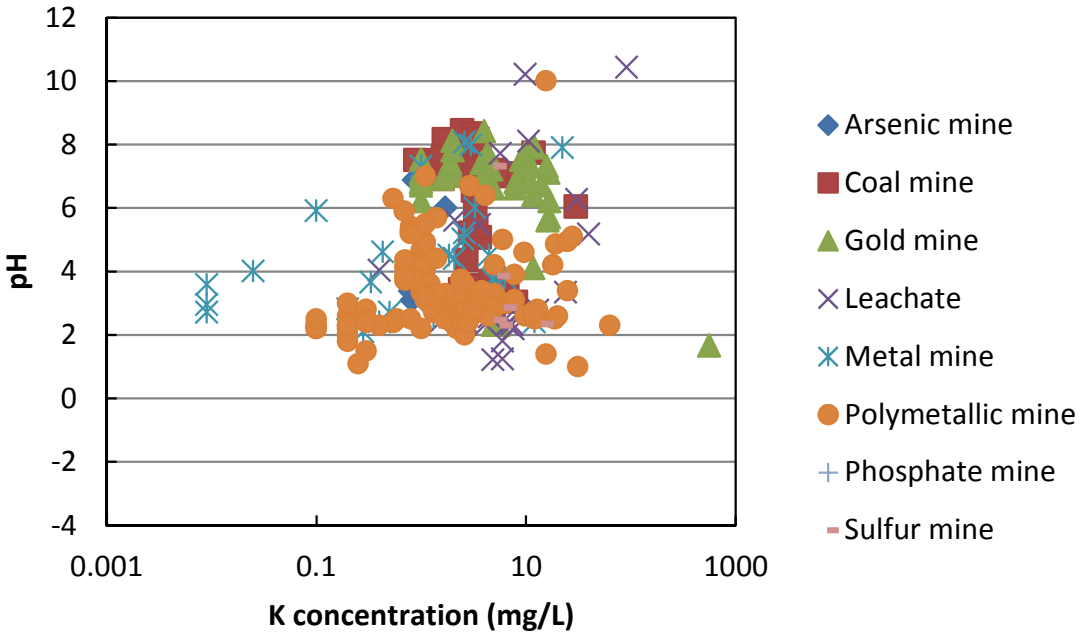

Figure 3-40 K concentration at different pH values

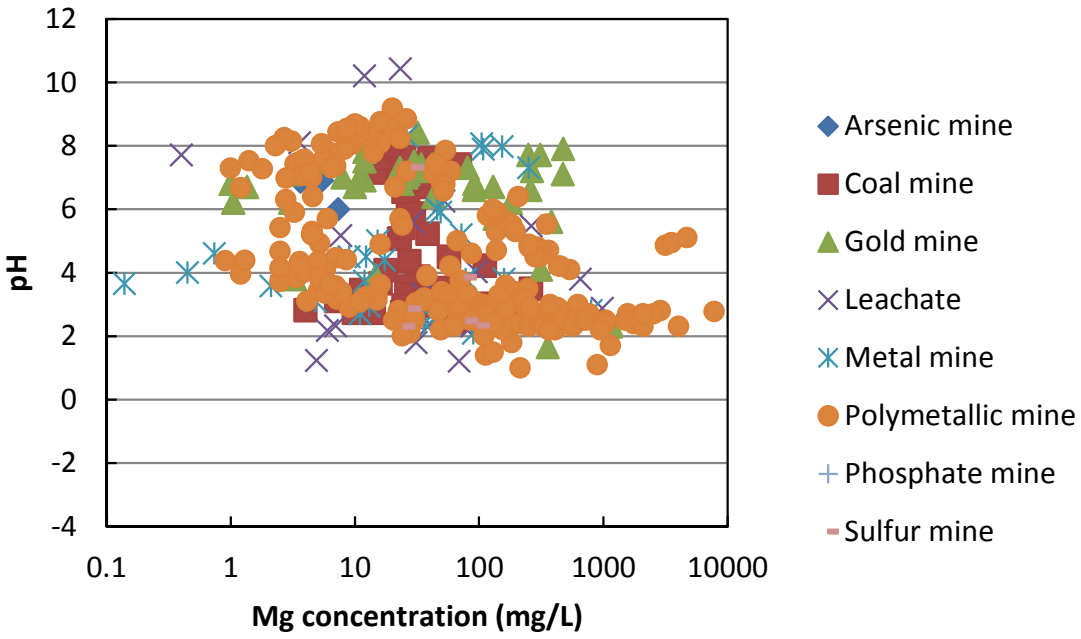

Figure 3-41 Mg concentration at different pH values

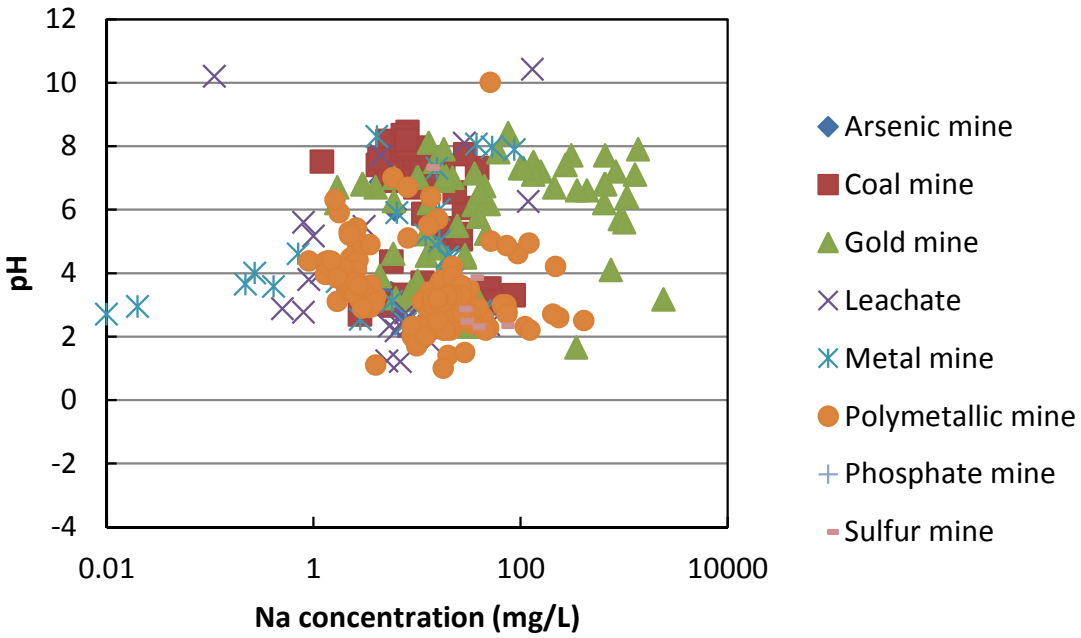

Figure 3-42 Na concentration at different pH values

Gulec et al. (2005) studied the composition of 12 ARDs for metallic mine wastes. They found that the most abundant species were Fe, Zn, Cu, and Ca, with the most abundant metals mined from sulfide ores being Fe, Zn, and Cu. Moreover, the average ratios for Fe:Zn, Fe:Cu, and Zn:Cu were 5, 7, and 24, respectively. Maximum and minimum metal ratios reported by these authors were 0 and 13 for Fe:Zn, 0 and 25 for Fe:Cu, and 1 and 206 for Zn:Cu, respectively. A positive linear relationship between Fe, Zn, and Cu was also found in the database analysis, as shown in Figure 3-43, Figure 3-44, and Figure 3-45. These relationships are most probably closely related to the metal composition of the ore minerals. Examples of minerals and composition of these minerals are presented in Table 3-15.

Important information can be obtained by looking at the metal composition in solution. For example Wolkersdorfer (2008) mentioned that if mine water has elevated concentration of Fe, Zn, Cu, Pb, and Cd, pyrite, spharelite, galena, and chalcopyrite are relevant minerals in the ore deposit and therefore, it is likely that they are released from a Pb-Zn mine. Similar to heavy metals, waters rich in metalloid concentration such as As may indicate that this is released from arsenopyrite (FeAsS), enargite or tennantite. Uranium mines, as well as hydrothermal gold deposits tend to present high As concentration (Wolkersdorfer 2008).

Correlation between parameters was done using the information collected in the database using the Pearson Product Moment Correlation (PPMC) coefficient. PPMC is a measure of the strength of the linear relationship between two sets of data. It is referred to as Pearson's correlation or simply as the correlation coefficient. The symbol for Pearson's correlation is "ρ" for population and "r", for sample. Pearson's r can range from -1 to 1, where r = -1 indicates a perfect negative linear relationship between variables, r = 0 indicates no linear relationship between variables, and r = 1 indicates a perfect positive linear relationship between variables. Table 3-16 shows the results of the correlation between EC, pH, sulfate and metals (Al, As, Cu, Fe, Pb, Zn, Ca, K, Mg, and Na) in the database. The correlation coefficients, r, higher than 0.5

Table 3-15 Sulfide mineral and composition

Mineral	Composition
Pyrite	FeS_2
Marcasite	FeS_2
Chalcopyrite	$CuFeS_2$
Covellite	CuS
Chalcocite	Cu_2S
Sphalerite	ZnS
Galena	PbS
Millerite	NiS
Pyrrhotite	$Fe_{1-x}S$ (where $0<x<0.2$)
Arsenopyrite	FeAsS
Cinnabar	HgS
Stibnite	Sb_2S_3

(shadowed in green color in Table 3-16) were the ones for EC-sulfate (0.86), EC-Al (0.63), EC-Ca (0.56), EC-Cu (0.56), EC-Fe (0.78), EC-Mg (0.68), sulfate-Al (0.80), sulfate-Cu (0.98), sulfate-Fe (0.99), sulfate-Mg (0.73), Al-Cu (0.63), Al-Fe (0.74), As-Fe (0.59), As-Pb (0.83), and Cu-Fe (0.97).

Table 3-16 Correlation between parameters

Parameter		EC	pH	SO_4	Al	As	Ca	Cu	Fe	K	Mg	Na	Pb	Zn
EC	PC		-0.482**	0.861**	0.633**	0.198**	0.561**	0.559**	0.785**	0.147*	0.684**	0.170**	-0.107	0.058
	N		454	316	286	318	335	348	420	248	295	290	260	346
pH	PC			-0.234**	-0.299**	-0.092	-0.183**	-0.227**	-0.222**	-0.062	0-.200**	0.125*	0.211**	-0.080
	N			479	431	450	444	544	610	305	404	348	365	555
SO_4	PC				0.798**	0.369**	0.373**	0.981**	0.989**	0.046	0.732**	0.001	-0.042	0.347**
	N				387	303	411	384	459	283	370	322	316	405
Al	PC					0.414**	0.241**	0.630**	0.736**	-0.022	0.545**	-0.082	-0.034	0.012
	N					268	351	341	436	265	353	266	271	343
As	PC						0.124*	0.099*	0.588**	0.053	0.158**	0.015	0.828**	0.482**
	N						314	411	384	285	293	305	292	404
Ca	PC							0.108*	0.230**	0.025	0.492**	0.306**	-0.101	0.006
	N							376	433	322	420	365	339	382
Cu	PC								0.968**	-0.033	0.358**	-0.066	-0.026	0.368**
	N								474	256	338	299	400	564
Fe	PC									0.013	0.409**	-0.064	-0.010	0.347**
	N									295	395	341	355	496
K	PC										0.015	0.332**	0.090	0.006
	N										321	318	223	259
Mg	PC											0.050	-0.038	0.046
	N											324	301	341
Na	PC												0.148*	-0.027
	N												265	302
Pb	PC													0.073
	N													407

PC: Pearson correlation

N: number of cases

** Correlation is significant at the 0.01 level (2-tailed)

* Correlation is significant at the 0.05 level (2-tailed)

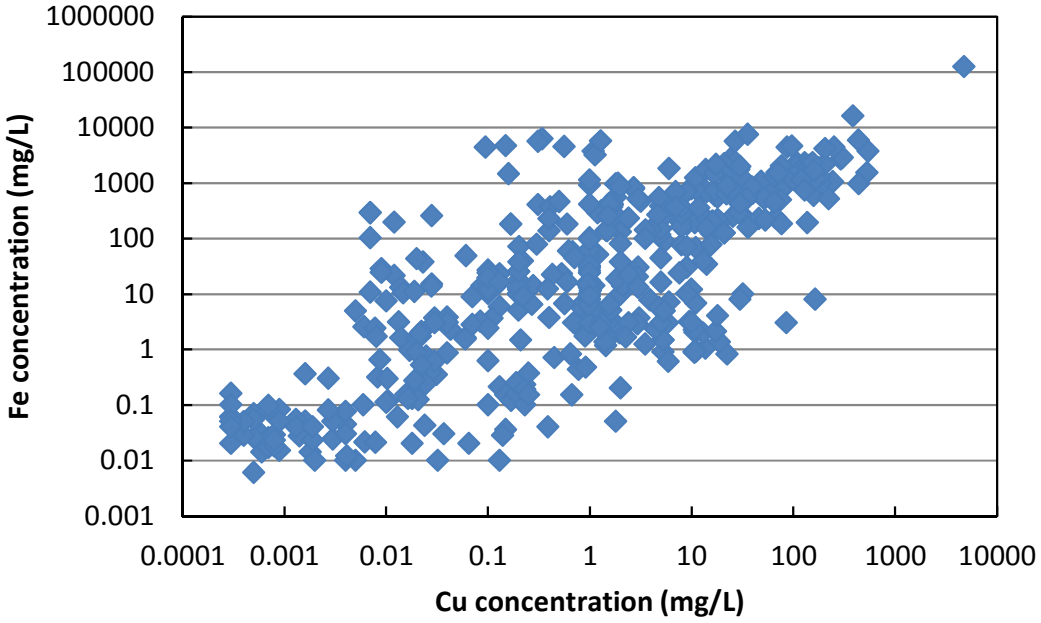

Figure 3-43 Relationship between Fe and Cu

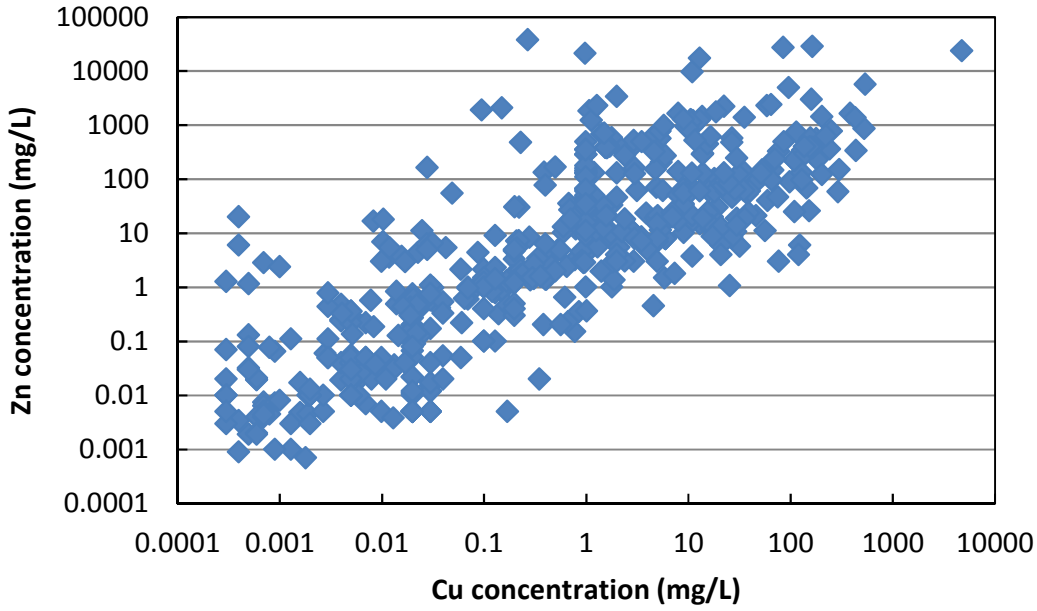

Figure 3-44 Relationship between Zn and Cu

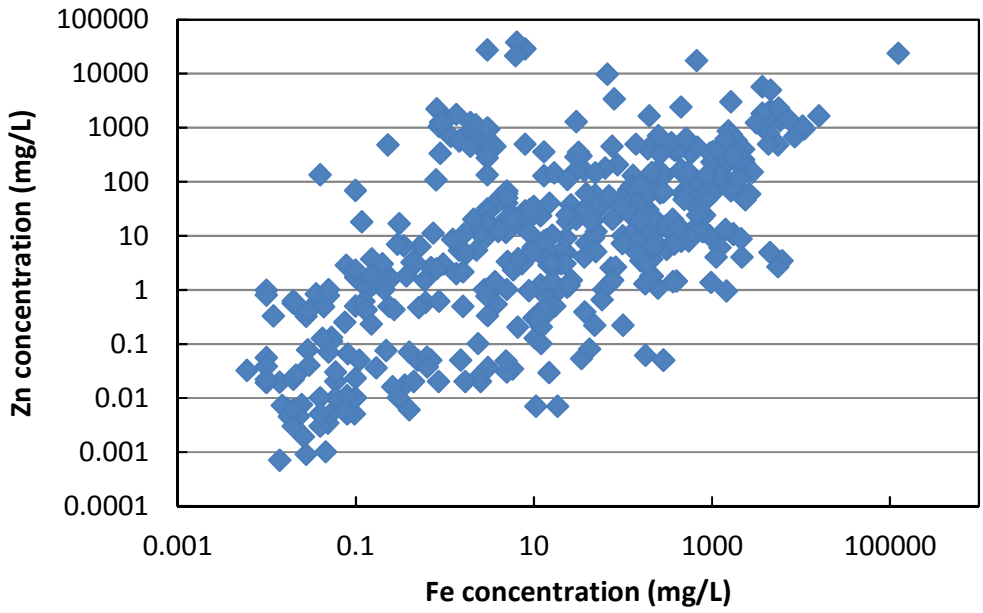

Figure 3-45 Relationship between Zn adn Fe

3.3.2 Evaluation of pH, Electrical Conductivity, and Sulfate Concentration

Both sulfate (SO_4^{2-}) and electrical conductivity (EC) are useful indicators of ARD contamination. Sulfate is an end product of pyrite oxidation and, unlike pH, sulfate and EC are extremely sensitive to ARD even when dilutions have occurred. ARD usually contain extremely high sulfate concentrations which exceed those of heavy metals. Strongly elevated sulfate concentrations exist because very few natural processes remove sulfate from ground and surface waters. Only the precipitation of secondary sulfate minerals may reduce the concentration of sulfate in solution (Lottermoser 2007).

EC and sulfate are closely associated considering that EC is sensitive to sulfate ions and ARD waters carry significant concentrations of sulfate which exceed those of iron and heavy metal. Although sulfate is difficult to measure directly in the field, EC measurement is ideal for routine water screening. Table 3-17 and Table 3-18 show the correlations (Pearson Correlation) between EC and SO_4 and other parameters (pH, Al, As, Cu, Fe, Pb, Zn, Ca, K, Mg, and Na) classified according to the type of mine (A: arsenic mines, C: coal mines, G: gold mines, L: leachate, M: metal mines, P: polymetallic mines, PH: phosphate mines, and S: sulfur mines). These results show that EC can be used to predict sulfate concentration in majority of the cases (the Pearson correlation ranges between 0.893 and 0.999) and other key metals, as shown in Figure 3-46 to Figure 3-56, especially for Al, Cu, Fe, Zn, Ca, Mg and Na.

The Pearson correlation between sulfate and EC was calculated for each type of mine (Table 3-17). For arsenic mines, the relationship between sulfate and EC in terms of Pearson correlation was 0.994, for coal mines, it was 0.962, for gold mines, it was 0.759, for leachate, it was 0.999, for metal mines, it was 0.955, and for polymetallic mines, it was 0.893. The Pearson correlation between sulfate and pH for each type of mine ranges from -0.28 (polymetallic mines) to -0.82 (arsenic mines). The correlation for

sulfate-Al ranges from 0.39 (metal mines) to 0.98 (gold mines); the correlation for sulfate-As from -0.03 (gold mines) to 0.81 (phosphate mines); the correlation for sulfate-Cu from 0.14 (metal mines) to 0.99 (polymetallic mines); the correlation for sulfate-Fe from 0.78 (arsenic mines) to 0.99 (polymetallic mines); the correlation for sulfate-Pb from -0.03 (gold mines) to 0.99 (leachate); the correlation for sulfate-Zn from -0.04 (metal mines) to 0.89 (sulfur mines); the correlation for sulfate-Ca from 0.14 (metal mines) to 0.79 (arsenic mines); the correlation for sulfate-K from 0.01 (coal mines) to 0.99 (sulfur mines); the correlation for sulfate-Mg from 0.54 (metal mines) to 0.96 (gold mines); and the correlation for sulfate-Na from 0.04 (gold mines) to 0.93 (sulfur mines).

The Pearson correlation between EC and other parameters is presented in Table 3-18. The correlation between EC and pH for each type of mine ranges from -0.52 (polymetallic mines) to -0.82 (arsenic mines). The correlation for EC-Al ranges from 0.04 (metal mines) to 0.97 (arsenic mines); the correlation for EC-As from -0.01 (metal mines) to 0.67 (coal mines); the correlation for EC-Cu from 0.18 (metal mines) to 0.93 (coal mines); the correlation for EC-Fe from 0.54 (leachate) to 0.94 (metal mines); the correlation for EC-Pb from 0.07 (gold mines) to -0.11 (polymetallic mines); the correlation for EC-Zn from 0.06 (polymetallic mines) to 0.96 (coal mines); the correlation for EC-Ca from -0.05 (metal mines) to 0.91 (coal mines); the correlation for EC-K from -0.31 (leachate) to 0.37 (polymetallic mines); the correlation for EC-Mg from 0.39 (metal mines) to 0.97 (arsenic mines); and for EC-Na from -0.32 (leachate) to 0.55 (arsenic mines).

Table 3-17 Correlation between sulfate and other elements classified by type of mine

Mine Type		EC	pH	Al	As	Ca	Cu	Fe	K	Mg	Na	Pb	Zn
A	PC	0.994**	-0817**	0.940**	0.050	0.793**	0.758*	0.780**	-0.359	0.949**	0.401		
	N	10	11	11	11	11	10	11	11	11	11	0	0
C	PC	0.962**	-0474**	0.935**	0.588**	0.456**	0.815**	0.863**	0.007	0.594**	0.436**		0.619**
	N	68	107	81	63	72	23	108	57	72	58	1	42
G	PC	0.759**	-0484**	0.981**	-0.032	0.380**	0.936**	0.939**	0.126	0.963**	0.038	-0.035	0.290*
	N	63	81	26	62	81	80	66	40	41	77	79	75
L	PC	0.999*	-0.660				0.964					0.992	0.883
	N	3	3	0	0	0	3	0	0	0	0	3	3
M	PC	0.955**	-0441**	0.393*	0.168	0.138	0.142	0.829**	0.202	0.537**	0.300	0.445	-0.040
	N	13	36	30	14	28	32	26	27	28	28	17	35
P	PC	0.893**	-0.278**	0.825**	0.111	0.445**	0.985**	0.994**	0.222**	0.707**	0.159	-0.088	0.342**
	N	157	221	220	140	212	228	228	141	211	141	206	232
PH	PC		-0.146	0.902**	0.811**			0.828**				0.686*	0.862**
	N	0	10	10	10	0	0	10	0	0	0	10	10
S	PC	1.000**	-0.284	0.979**		-0.524	0.480	0.842**	0.994**	0.590	0.934**		0.893**
	N	2	9	8	2	6	7	9	6	6	6	0	7

Mine type A: arsenic, C: coal, G: gold, L: leachate, M: metal, P: polymetallic, PH: phosphate, S: sulfur; PC: Pearson correlation; N: number of cases; ** Correlation is significant at the 0.01 level (2-tailed); * Correlation is significant at the 0.05 level (2-tailed)

Table 3-18 Correlation between EC and other elements classified by type of mine

Mine Type		pH	SO_4	Al	As	Ca	Cu	Fe	K	Mg	Na	Pb	Zn
A	PC	-0.816**	0.994**	0.966**	0.628	0.876**	0.809**	0.759*	-0.383	0.974**	0.546		
	N	10	10	10	10	10	9	10	10	10	10	0	0
C	PC	-0.513**	0.962**	0.826**	0.671**	0.910**	0.928**	0.872**	0.050	0.703**	0.390**		0.960**
	N	103	68	74	62	57	11	92	57	57	57	0	23
G	PC	-0.462**	0.759**	0.703**	0.606**	0.665**	0.699**	0.661**	0.320	0.888**	0.422**	0.069	0.336**
	N	64	63	23	46	63	63	63	23	23	63	63	63
L	PC	-0.619**	0.999*	0.102	0.652**	0.258	0.604**	0.544**	-0.308	0.398*	-0.322	-0.082	0.576**
	N	33	3	11	26	30	31	30	25	30	27	31	33
M	PC	-0.573*	0.955**	0.040	-0.008	-0.054	0.181	0.938**	0.272	0.393	0.267		0.293
	N	13	13	9	6	13	10	12	12	13	13	0	12
P	PC	-0.519**	0.893**	0.779**	0.204**	0.723**	0.636**	0.847**	0.374**	0.711**	0.322**	-0.113	0.060
	N	229	157	157	166	160	222	211	119	160	118	166	213
PH	PC												
	N	0	0	0	0	0	0	0	0	0	0	0	0
S	PC	-1.000**	1.000**	-1.000**		1.000**	1.000**	1.000**	1.000**	-1.000**	-1.000**		1.000**
	N	2	2	2	2	2	2	2	2	2	2	0	2

Mine type A: arsenic, C: coal, G: gold, L: leachate, M: metal, P: polymetallic, PH: phosphate, S: sulfur; PC: Pearson correlation; N: number of cases; ** Correlation is significant at the 0.01 level (2-tailed); * Correlation is significant at the 0.05 level (2-tailed)

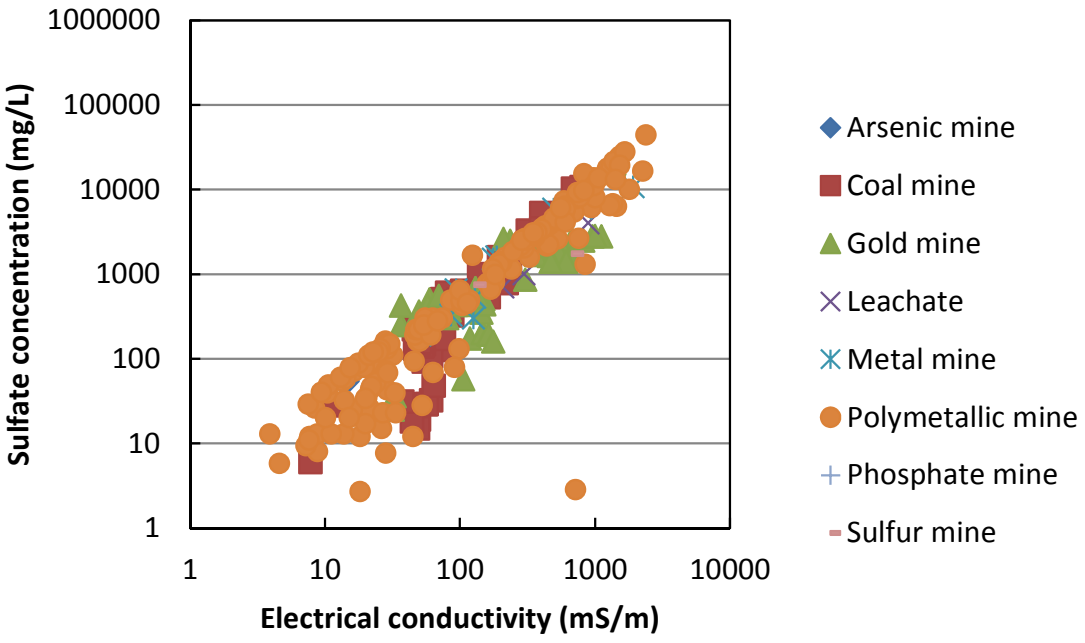

Figure 3-46 Sulfate and electrical conductivity relationship at different mine type

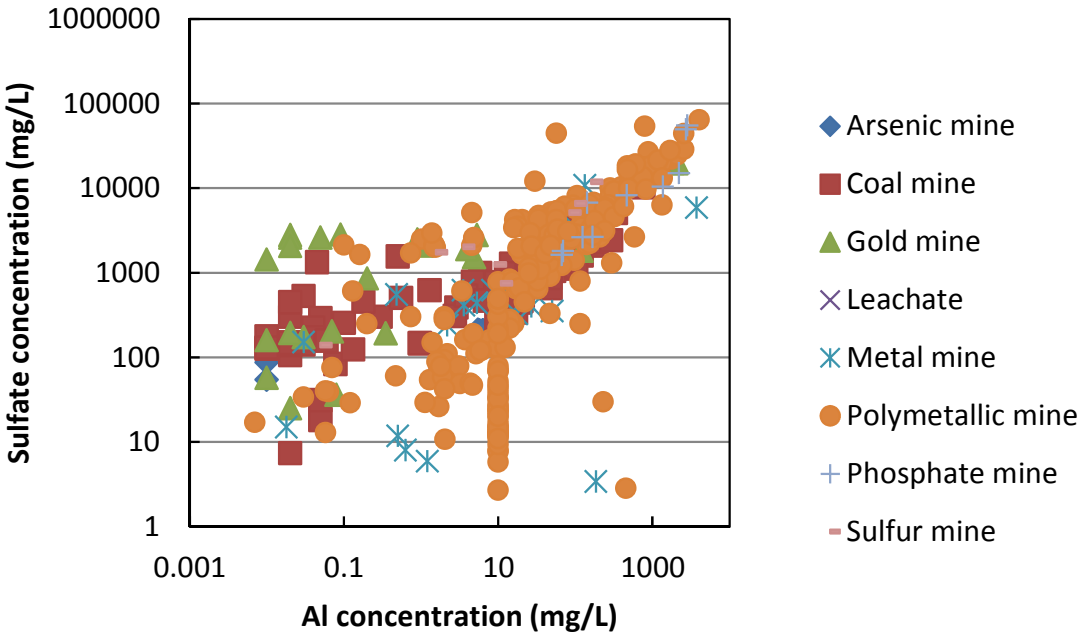

Figure 3-47 Sulfate and Al relationship at different mine type

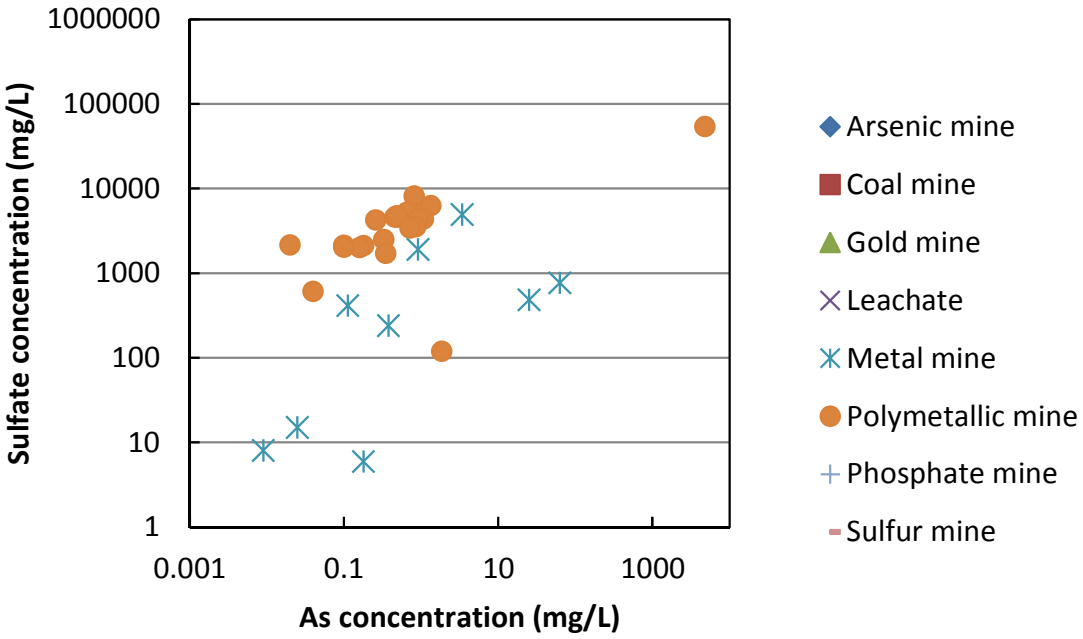

Figure 3-48 Sulfate and As relationship at different mine type

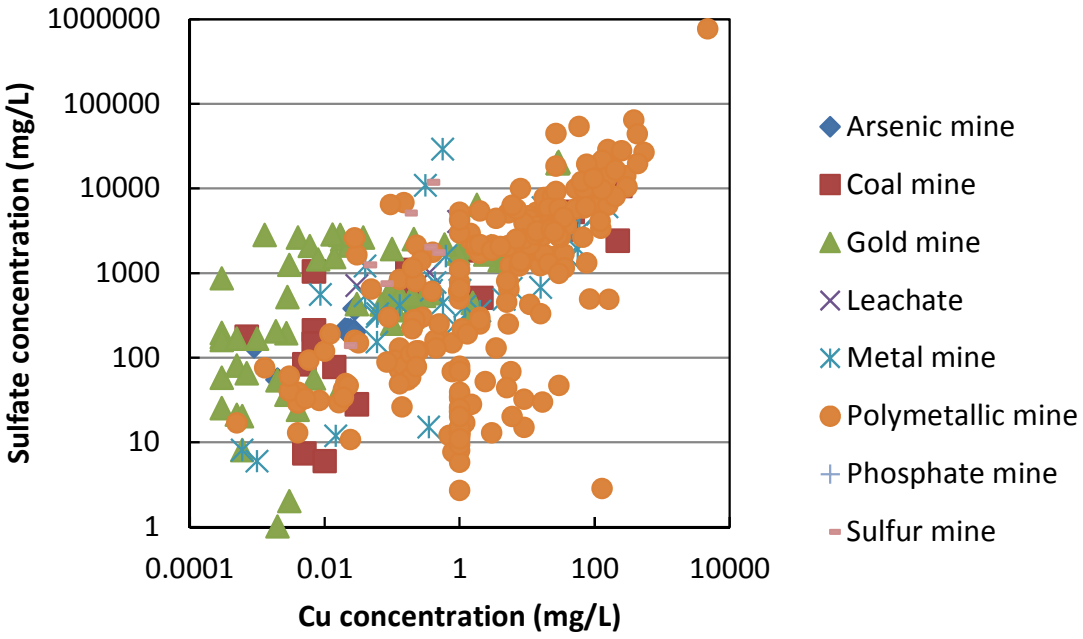

Figure 3-49 Sulfate and Cu relationship at different mine type

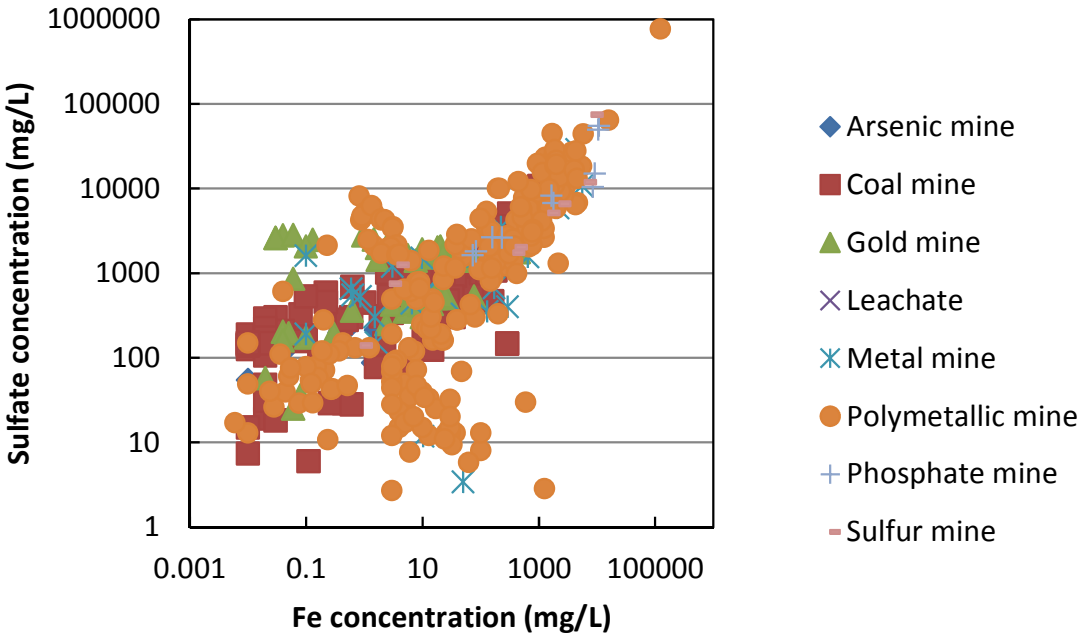

Figure 3-50 Sulfate and Fe relationship at different mine type

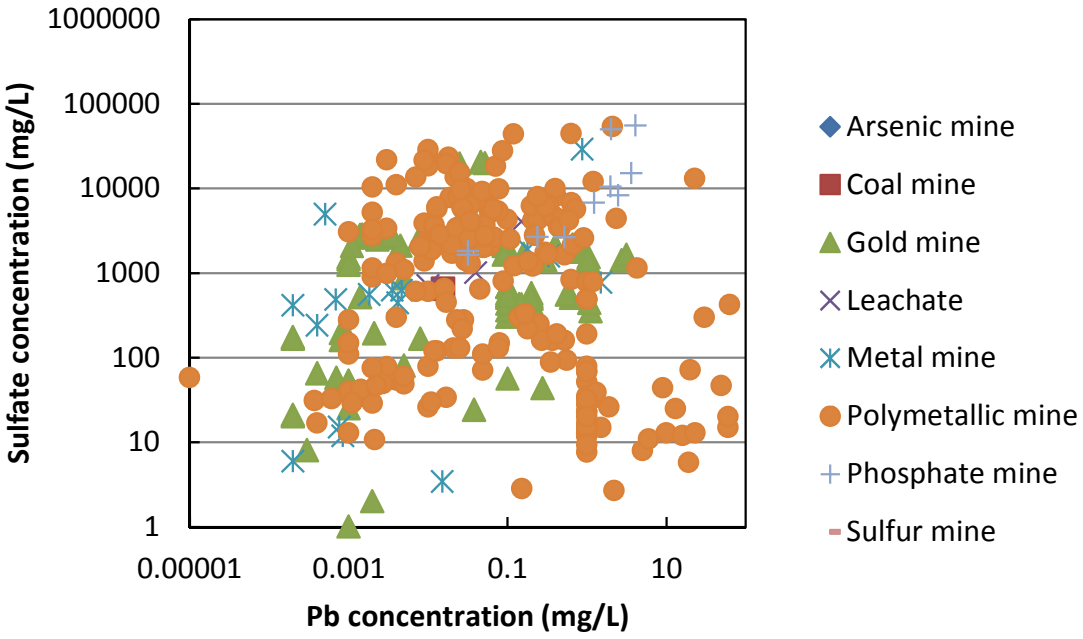

Figure 3-51 Sulfate and Pb relationship at different mine type

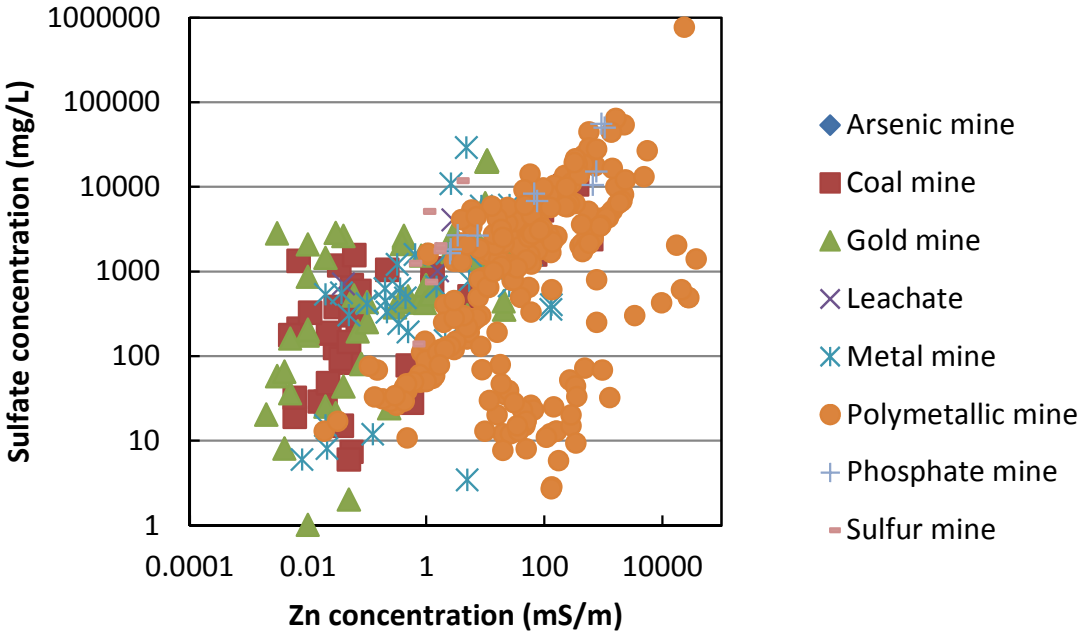

Figure 3-52 Sulfate and Zn relationship at different mine type

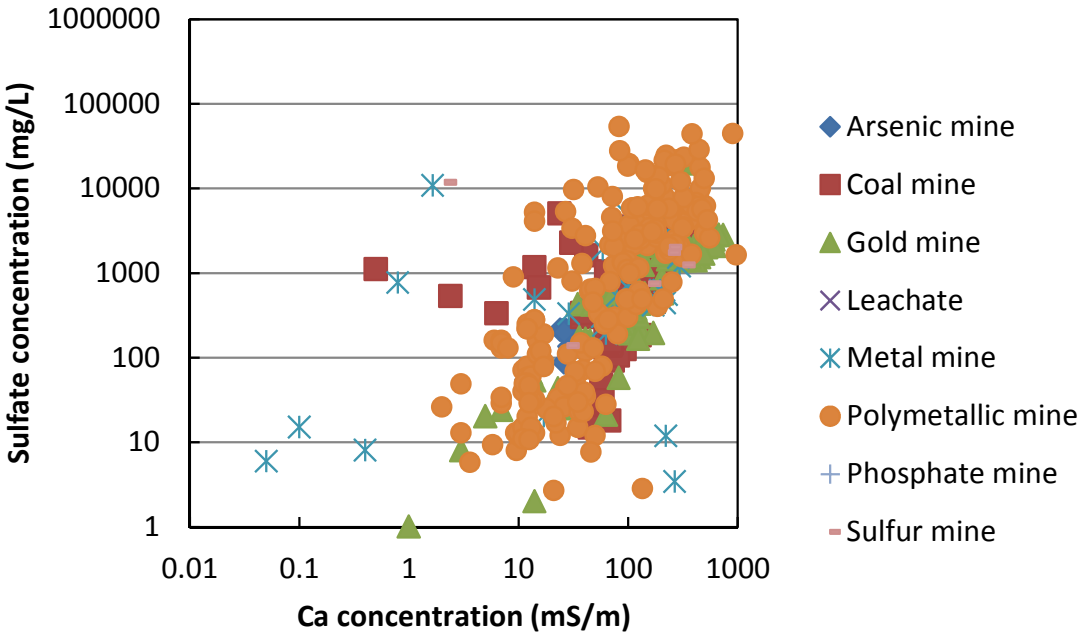

Figure 3-53 Sulfate and Ca relationship at different mine type

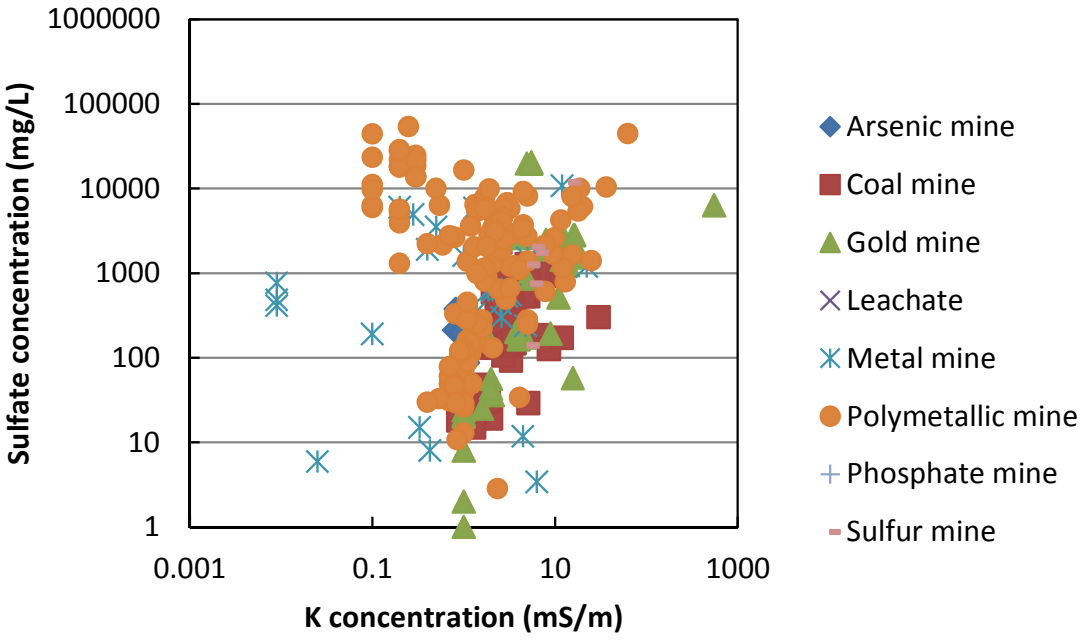

Figure 3-54 Sulfate and K relationship at different mine type

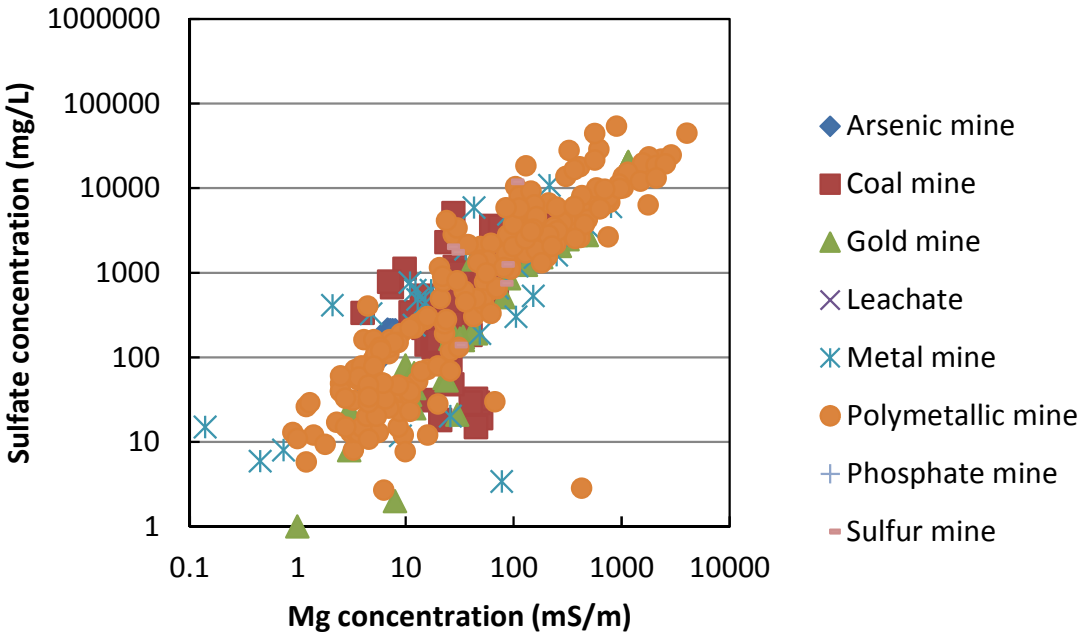

Figure 3-55 Sulfate and Mg relationship at different mine type

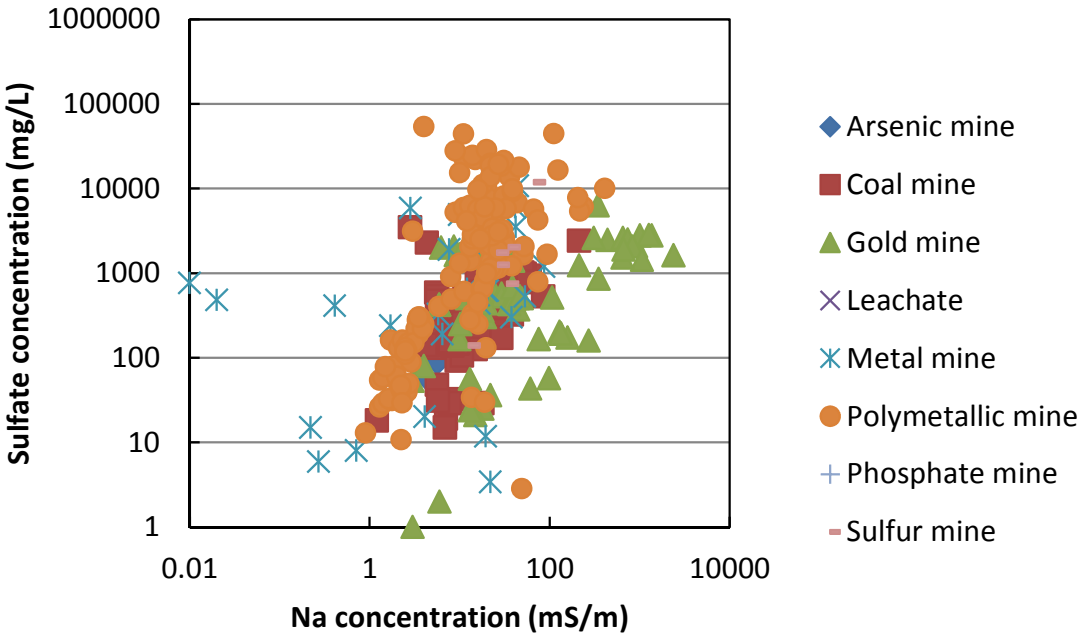

Figure 3-56 Sulfate and Na relationship at different mine type

3.4 Summary and Conclusions for this Chapter

ARD generated from excavated rocks represents a threat to the quality of both surface and ground water. Information about ARD composition from excavated sites is still very limited, whereas there is a great deal of information and data about ARD coming from mining activities. Even though ARDs expected from mine sites tend to be much more severe in terms of pH, EC, and metal concentration than ARDs from construction sites, using mining site data, it is possible to characterize ARDs and, thus, look for proper mitigation systems.

ARDs in the world are complex, difficult to predict, and pose different characteristics in terms of pH, EC, sulfate, and metal concentration. A database of ARDs represents a valuable scientific tool for the prediction of water chemistry in the future. Statistical tools were used in this chapter to describe, summarize, and interpret 817 ARDs cases collected from several countries, and the limits (maximum, minimum, mean, interquartile range, Pearson correlation, among others) for each parameter for every type of mine were determined. The parameters used for the characterization were pH, EC, sulfate concentration, and metal concentration (Al, As, Cu, Fe, Pb, Zn, Ca, K, Mg, and Na). Eight types of mines were established, according to the information provided by the authors of each research, which includes arsenic, coal, gold, leachate, metal, polymetallic, phosphate, and sulfur mines.

The minimum, maximum, and average values for the pH, EC, metal concentration of the ARD compositions of the database were calculated. The average pH value was 4.9±2.1, for EC, it was, 302±427 mS/m, for sulfate, it was 4755 mg/L±34896 mg/L; for Al, it was 159 mg/L±471 mg/L, for As, it was 4.0±27.8 mg/L, for Cu, it was 26.9±205 mg/L, for Fe, it was 665±5142 mg/L, for Pb, it was 1.5±7.3mg/L, and for Zn, it was 437±2711 mg/L.

Predicting ARD composition or chemistry is important in order to establish or design an effective mitigation system. The oxidation of pyrite is the major contribution of hydrogen ions in ARDs, which will lead to the release of other metals and metalloids. A clear inverse linear relationship was determined for EC-pH, sum of metal-pH, sulfate-pH, Al-pH, Cu-pH, Fe-pH, and Zn-pH systems for the whole range of pH, except for the bicarbonate-pH (bicarbonate buffers acidity by consuming protons), in which a direct linear relationship was observed. In general, it can be said that at low pH values, more metals are found in solution. Besides, the oxidation of sulfide minerals is particularly characterized by high sulfate (>1000 mg/L), high Al and Fe (>100 mg/L), and elevated Cu, Pb and Zn (>10 mg/L). Ca, K, Mg and Na may also occur in strongly elevated concentrations.

In the case of As, a different tendency to other metals was observed. There are several mineral sources of As such as arsenolite (As_2O_3), scorodite ($FeAsO_4 \cdot 2H_2O$), and arsenopyrite (FeAsS). Due to the direct relationship observed between As and sulfate, it can be said that arsenopyrite was one of the mineral sources of As. Scorodite solubility is strongly controlled by pH and it is known that the solubility is higher at low pH and decreases at pH 4 and then the solubility increases at pH 4. Thus, the relationship obtained between pH and As can be probably explained by the mineral source.

A direct linear relationship between EC and sulfate was observed, which constitutes a useful tool for ARD indication. This becomes an important finding as EC can be easily measured in the field compared to

sulfate concentration. The Pearson correlation between sulfate and EC was calculated for each type of mine. For arsenic mines, the relationship between sulfate and EC in terms of Pearson correlation was 0.994, for coal mines, it was 0.962, for gold mines, it was 0.759, for leachate, it was 0.999, for metal mines it was 0.955, and for polymetallic mines, it was 0.893.

Besides, the relationship between sulfate against pH and metal concentration in terms of Pearson correlation was also established, which indicates that metals can also be predicted indirectly by measuring the EC in the field. The Pearson correlation between sulfate and pH for each type of mine ranges from -0.28 (polymetallic mines) to -0.82 (arsenic mines). The correlation for sulfate-Al ranges from 0.39 (metal mines) to 0.98 (gold mines); the correlation for sulfate-As from -0.03 (gold mines) to 0.81 (phosphate mines); the correlation for sulfate-Cu from 0.14 (metal mines) to 0.99 (polymetallic mines); the correlation for sulfate-Fe from 0.78 (arsenic mines) to 0.99 (polymetallic mines); the correlation for sulfate-Pb from -0.03 (gold mines) to 0.99 (leachate); the correlation for sulfate-Zn from -0.04 (metal mines) to 0.89 (sulfur mines).

The Pearson correlation between EC against pH and metal concentration for each type of mine ranges from -0.52 (polymetallic mines) to -0.82 (arsenic mines). The correlation for EC-Al ranges from 0.04 (metal mines) to 0.97 (arsenic mines); the correlation for EC-As from -0.01 (metal mines) to 0.67 (coal mines); the correlation for EC-Cu from 0.18 (metal mines) to 0.93 (coal mines); the correlation for EC-Fe from 0.54 (leachate) to 0.94 (metal mines); the correlation for EC-Pb from 0.07 (gold mines) to -0.11 (polymetallic mines); and the correlation for EC-Zn from 0.06 (polymetallic mines) to 0.96 (coal mines).

Considering that ARDs differ in terms of pH, EC, metal concentration, among others, the database provided in this chapter can be used to determine the average values of the main parameters of ARDs in general and according to the type of mine. For this research in particular, this database was used not only to characterize ARDs in the world, but also to strategically choose certain ARD cases (e.g. low pH and high EC, low pH and low EC, high pH and low EC, high pH and high EC, among others) to test the barrier performance of GCL, zeolite, and ferrihydrite in the subsequent chapters.

4 HYDRAULIC CONDUCTIVITY OF MINERAL BARRIERS AGAINST ACID ROCK DRAINAGE

4.1 General Remarks

Even though the performance of geosynthetic clay liners (GCLs) when dealing with acid rock drainage (ARDs) has been suggested to be good, there are some factors, such as saturation of the buffering capacity of bentonite and changes in pH among others, potentially affecting and degrading their overall performance. Although numerous studies have been conducted to determine the effects of a variety of chemicals solutions on the hydraulic performance of GCLs, most of them have used single inorganic salts or organic solutions as permeant liquids. Very few have focused on the hydraulic performance of GCLs subjected to permeation with ARDs, which are mixtures of several metals and metalloids. This chapter seeks to provide a systematic study of the change in swell index and hydraulic conductivity in a needle punched GCL caused by ARD permeation. A GCL was tested against ten artificial ARDs, each of them having different EC and pH values. The compositions of these ARDs mimic real ARDs that are presented in the database (Appendix A). The barrier performance of the most critical case among them was used to test zeolite and ferrihydrite. Moreover, the most critical ARD case was also evaluated for zeolite and ferrihydrite in order to compare their performance.

4.2 Materials and Methods

4.2.1 Mineral Materials

Bentonite, zeolite, and ferrihydrite are mineral materials available in many countries, which might make them suitable for remediation techniques or barrier in embankments filled with rocks coming either from construction or mining activities. The performance of all of them have been investigated in previous research, but not under extreme conditions related to pH and heavy metal content.

4.2.1.1 Bentonite

The bentonite used for the tests was obtained from a needle-punched GCL (Bentofix® NSP 4900). This GCL contains powered sodium bentonite sandwiched between woven and non woven geotextiles, with a unit mass of 4670 g bentonite/m^2. Bentonite contained in this GCL had a water content of approximately 10.0%, a specific gravity of 2.85, and a smectite content of 80%. The bentonite was also characterized by X-ray diffraction (XRD) and the result is presented in Figure 4-1. Comparing this spectrum with a theoretical bentonite spectrum, it was verified that the bentonite sample corresponds to a beidellite type. The cation exchange capacity (CEC) of the bentonite was also determined, based on the Japan Bentonite Manufacturers Association Standard and the value was 45 mol(+)/kg.

Before conducting the tests, bentonite was ground to 100% passing a 100 mesh US. Standard Sieve

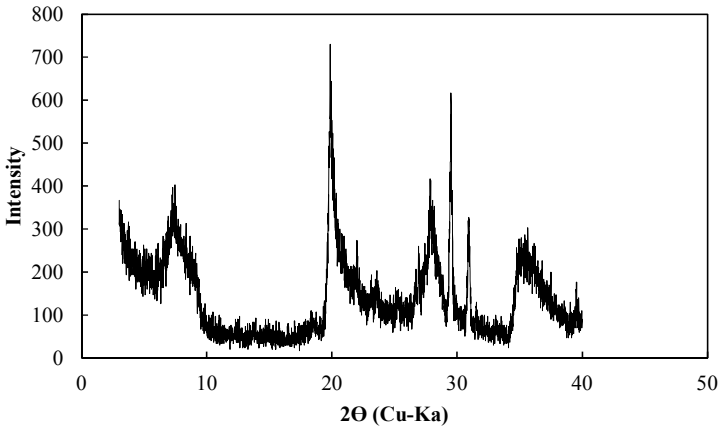

Figure 4-1 XRD spectrum of the bentonite used in the experiments

and a minimum of 65% passing a 200 mesh US. Standard Sieve, and then dried for 24 hours in a drying oven at 105±5 °C. After bentonite was dried to constant mass, it was allowed to cool to room temperature in a desiccator.

4.2.1.2 Zeolite

The zeolite used for the tests was provided by Mitsui Mineral Development Engineering Co., Ltd. (MINDECO) and has a particle size of 0.5 mm sieve pass. It was dried for 24 hours in an oven at 105±5 °C before conducting the experiments and, after being dried to constant mass, it was allowed to cool to room temperature in a desiccator and kept there until it was used. The zeolite sample was characterized by X-ray diffraction (XRD) and the result is presented in Figure 4-2. Comparing the spectrum with the theoretical zeolite spectrum, it was verified that the zeolite sample corresponds to a zeolite of a clinoptilolite type. The cation exchange capacity (CEC) of the zeolite was also determined, based on the Japan Bentonite Manufacturers Association Standard. The CEC obtained was 31 mol(+)/kg.

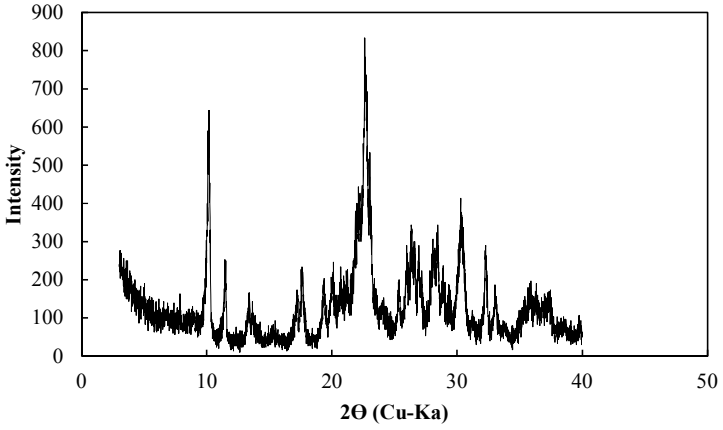

Figure 4-2 XRD spectrum of the zeolite (clinoptilolite) used in the experiments

4.2.1.3 Ferrihydrite

The ferrihydrite, FeO(OH), used for all experiments was a commercial powder material obtained from Nacalai Tesque. Before conducting the tests, ferrihydrite was dried for 24 hours in a drying oven at 105±5 °C. After being dried to constant mass, it was allowed to cool to room temperature in a desiccator and kept there until it was used.

4.2.2 Artificial Acid Rock Drainage

In order to understand and characterize ARD around the world, a database of 817 cases reported by different authors were collected and analyzed. This research is focused on 10 elements: As, Al, Cu, Fe, Pb, Zn, Ca, K, Mg, and Na. Discussion about pH and electrical conductivity (Figure 4-3), as well as sulfate concentration were also done in Chapter 3. The database is presented in Appendix A.

From Figure 4-3 it can be said that at low pH values, more metals are found in solution. Ten ARDs were selected from the database presented in Appendix A. Several studies did not report electrical conductivity values of ARDs and therefore ionic strength (I) based on the concentration was calculated for every ARD composition, according to the following formula:

$$I = \frac{1}{2}\sum_{i=1}^{n} c_i z_i^2 \tag{4.1}$$

Figure 4-3 shows that the majority of the data is concentrated between 0.001 and 0.1 M of ionic strength values. Considering that at around I = 0.1 M there are pH values around 10, this value of ionic

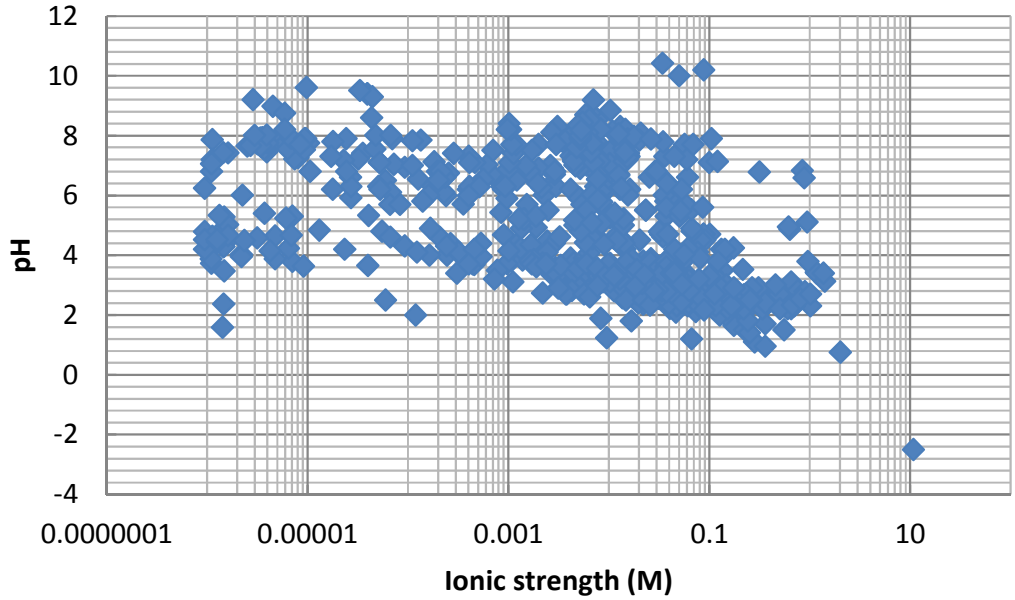

Figure 4-3 ARD classified according to the pH and ionic strength

strength was selected as a target point to study the performance of mineral barriers at different pH values. When ARDs of I = 0.1 M were artificially prepared in the laboratory, the EC values were around 400 mS/m and therefore this value was selected to evaluate the impact of pH on barrier performance of minerals. From the database statistical analysis conducted in Chapter 3, it can be seen that the average value of EC is around 400 mS/m, which makes this value worthy of study.

Although the statistical analysis done in Chapter 3 showed the average pH value to be approximately 5, the target pH value for conducting experiments was set to pH = 3. This is because the average value of the pH from the database was clearly influenced by high pH values in certain mines. It is known that low pH values have detrimental effects on mineral barriers and thus, pH 3 was chosen to study the effect of different EC values in the barrier performance of minerals materials.

A summary of the cases that were studied is shown in Table 4-1. The artificial ARDs were prepared by mixing $FeSO_4 \cdot 7H_2O$, $Al_2(SO_4)_3 \cdot 16H_2O$, $CuSO_4 \cdot 5H_2O$, $ZnSO_4 \cdot 7H_2O$, $Na_2HAsO_4 \cdot 7H_2O$, $PbNO_3/PbCl_2$, K_2SO_4, Na_2SO_4, $CaSO_4$, and $MgSO_4$, all of them of GR grade (Guaranteed Reagent) and provided by Nacalai Tesque. The pH was adjusted using H_2SO_4 or NaOH. After mixing the chemicals in the proportions specified in Table 4-2, precipitation was observed and therefore it was necessary to filter the mixture before conducting experiments. In some cases, after pH adjustment, the EC increased and thus dilution of the ARD was held, which slightly changed the target metal composition of the ARD. The concentration of each metal in solution was measured by ICP (ICPS – 800 Shimadzu) and reported as real concentration. Comparison of the data presented in Table 4-2 and Appendix A shows that some target and real ARD compositions differ one from the other which can be attributed to both precipitation and dilution.

Table 4-1 pH and EC of ten artificial ARDs used in experiments

ARD	pH	EC (mS/m)
248	3.008	74.8
406	3.002	37
625	3.007	406
747	3.007	1011
512	3.024	403
718	3.018	398
684	2.598	407
222	5.723	401
220	8.032	405
246	10.014	398

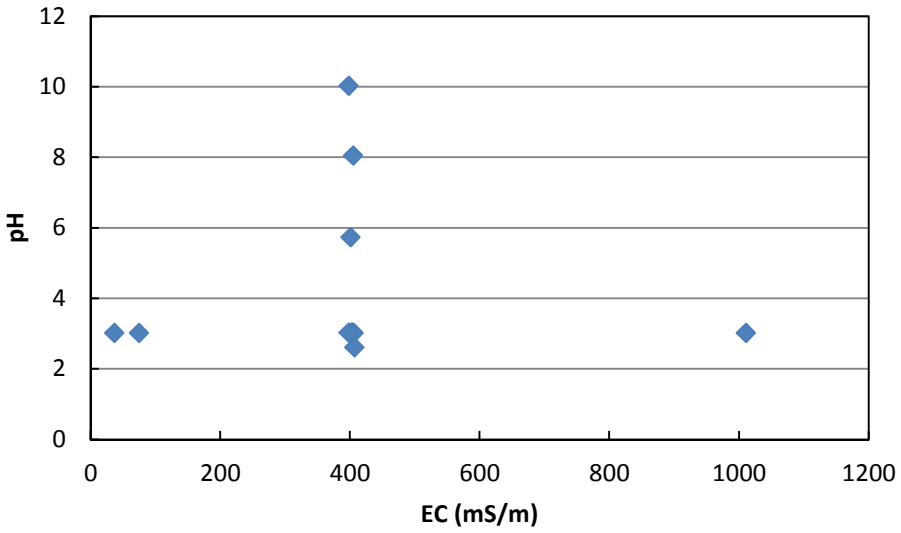

Figure 4-4 pH and EC of the ARDs tested

Table 4-2 Metal concentration of elements present in the artificial ARD

	ARD 248	ARD 406	ARD 625	ARD 512	ARD 747	ARD 718	ARD 684	ARD 222	ARD 220	ARD 246
Na	9.76	0.00	23.58	14.24	45.54	9.76	140.78	386.61	327.07	35.43
Mg	96.94	0.00	168.15	0.03	230.89	96.94	292.13	87.10	180.67	0.13
Al	0.10	0.01	24.33	123.63	272.42	0.10	12121.44	0.18	0.16	0.47
K	6.04	0.29	4.01	1.07	31.50	6.04	6.07	16.10	11.37	11.50
Ca	79.07	0.00	157.88	0.02	448.01	79.07	321.05	325.11	298.14	807.64
Fe	1304.02	1.87	777.76	1598.44	4591.14	1304.02	94128.81	1.02	0.03	0.00
Cu	12.02	0.95	0.98	0.08	96.33	12.02	9762.40	0.00	0.00	0.00
Zn	133.40	5.00	64.86	70.04	536.37	133.40	4.81	0.11	0.00	0.00
As	0.65	0.15	0.72	9.59	1.85	0.65	1.13	0.30	0.36	0.40
Pb	0.28	0.00	0.26	0.55	2.30	0.28	0.27	0.16	0.14	0.20

Unit: mg/L

4.2.3 Swelling Test

A swelling test with the clay mineral component of GCLs is a standard method for the evaluation of the swelling properties of the clay inside the GCL in reagent water. The main purpose of this test is to estimate the hydraulic conductivity of geosynthetic clay liners (ASTM 2009c). In this research, the bentonite swell index was evaluated for water and different concentration of single metal solutions, bi-metal solutions, different dilutions of artificial ARDs, from 0% or water, 2%, 4%, 8%, 20%, 40%, 80%, and 100% of ARD (Figure 4-5), as well as different pH solutions with different metal concentration.

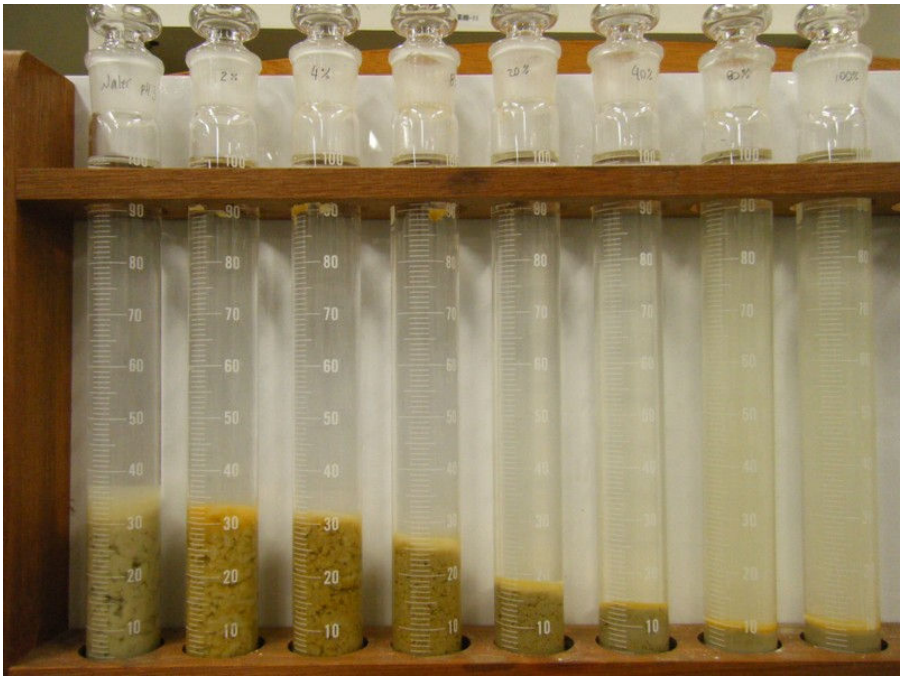

Figure 4-5 Swelling test of different ARD dilutions

The experiments were performed according to the ASTM D 5890 "Standard Test Method for Swell Index of Clay Mineral Component of Geosynthetic Clay Liners". Two grams of dry powdered bentonite were dusted into a 100 mL graduated cylinder filled with 90 mL of permeant solution. Then, the graduated cylinder was filled up to 100 mL with the same permeant solution. The cylinder was covered or capped and allowed to stand undisturbed for 24 hours. After this period, the volume level (in milliliters, mL) of the bentonite was recorded.

4.2.4 Hydraulic Conductivity Test

Hydraulic conductivity tests on GCL samples of 60 mm in diameter were conducted according to the ASTM D 5084 "Standard Test Methods for Measurement of Hydraulic Conductivity of Saturated Porous Materials Using a Flexible Wall Permeameter" and the ASTM D 7100 "Standard Test Method for Hydraulic Conductivity Compatibility Testing of Soils with Aqueous Solutions". This test method is applicable to soils with hydraulic conductivity less than approximately 1×10^{-8} m/s and it is used to measure one-dimensional flow of aqueous solutions (permeant such as landfill leachates, liquid wastes and byproducts, single and mixed chemicals, etc.) through initially saturated soils under an applied hydraulic gradient and effective stress (ASTM 2009b, a). The method described in those standards provides for different systems or permeameters. In order to minimize sidewall leakage, a falling headwater–constant tailwater system was employed in this research. A typical diagram of this system is presented in Figure 4-6. Pictures of the equipments used in these experiments are presented Figure 4-7 and Figure 4-8.

The interaction between some liquid permeants and some clayey soils have resulted in significant increases in hydraulic conductivity of the soils compared to the hydraulic conductivity of the same soil

permeated with water (ASTM 2009b). This test method is used in this research to evaluate the effect of prehydration, pH, EC and long term interactions (9 months) on the hydraulic conductivity of GCL and compare the barrier performance of GCL with other readily available materials. Three cases were studied using this method: water permeation; ARD permeation of GCL prehydrated with water; and ARD permeation. Table 4-3 summarizes the cases that were considered in this study.

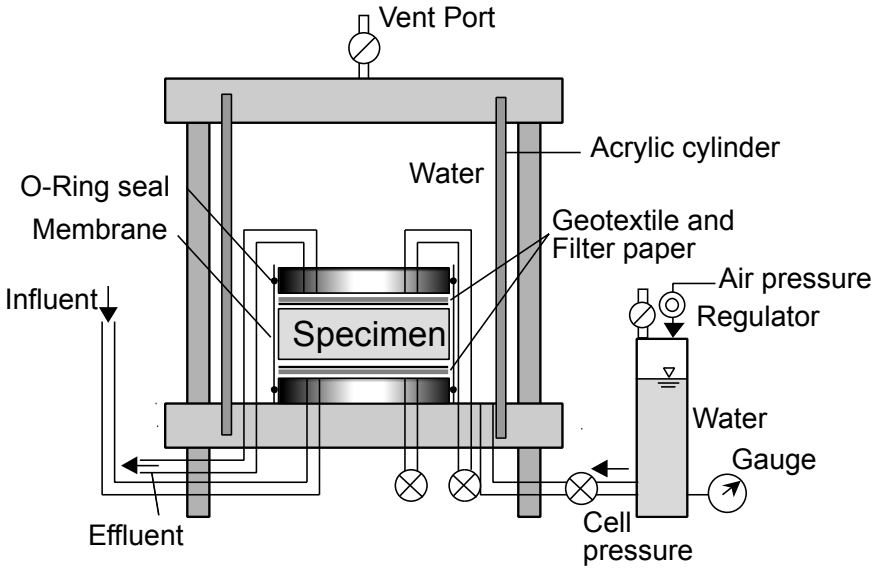

Figure 4-6 Schematic view of a flexible-wall permeameter

Figure 4-7 Equipment used to evaluate the hydraulic conductivity

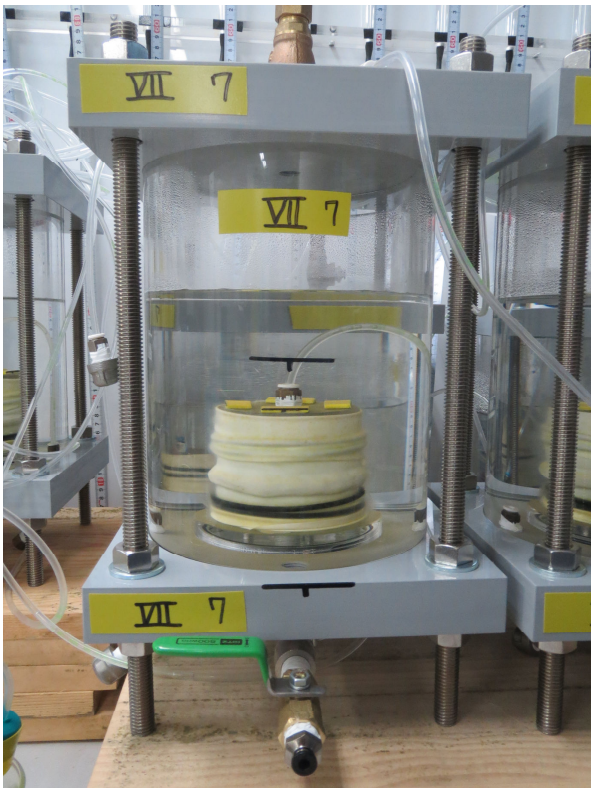

Figure 4-8 System used to measure the hydraulic conductivity of GCL

Table 4-3 Cases tested for the hydraulic conductivity test

	GCL	Zeolite	Ferrihydrite
ARD	ARD 248, 406, 625, 512, 747, 684, 222, 220, 246	ARD 747	ARD 747
Prehydrated	ARD 248, 406, 625, 512, 747, 684, 222, 220, 246	NA	NA
Not prehydrated	ARD 747	ARD 747	ARD 747
Short term test	ARD 248, 406, 625, 512, 747, 684, 222, 220, 246	ARD 747	ARD 747
Long term test	ARD 747	---	---

NA: not applicable

The test specimen was placed between filter papers, geotextiles, and plastic caps (cap and pedestal) with holes to connect the tubes, and confined by a latex membrane on the sides. The cell was filled with water and a cell pressure of 30 kPa, and a hydraulic gradient of 90±5 cm was applied. The thickness of the GCL was measured regularly using a cathetometer. The thickness of the zeolite and ferrihydrite was adjusted to 2 cm and prepared by compaction in a consolidation machine using optimum water content

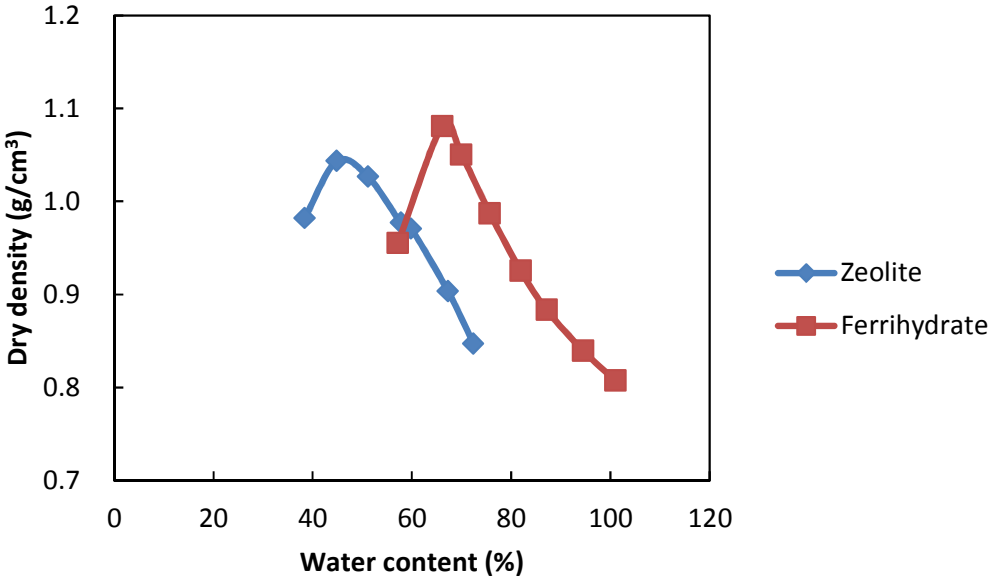

Figure 4-9 Compaction test results of zeolite and ferrihydrite

(45% for zeolite and 66% for ferrihydrite, as shown in Figure 4-9) and applying 40 kPa of pressure (20 kPa for 24 hours and 40 kPa for 24 hours). The optimum water content was calculated from compaction test results, following the procedures described in ASTM 698 (2007). This factor is important, as the thickness may easily vary with the testing conditions and accurate thickness values are necessary for accurate calculation of the hydraulic conductivity. The temperature was fixed to 25°C during the duration of the experiment.

One of the critical issues reported by Daniel et al. (1997) is the loss of bentonite along the edges when the GCLs sandwiched between geotextiles are trimmed, as shown in Figure 4-10. In order to avoid the loss of bentonite, water is applied along the area to be cut. Moreover, after cutting the GCLs water is applied along the edges if necessary and the uncut fibers are cut.

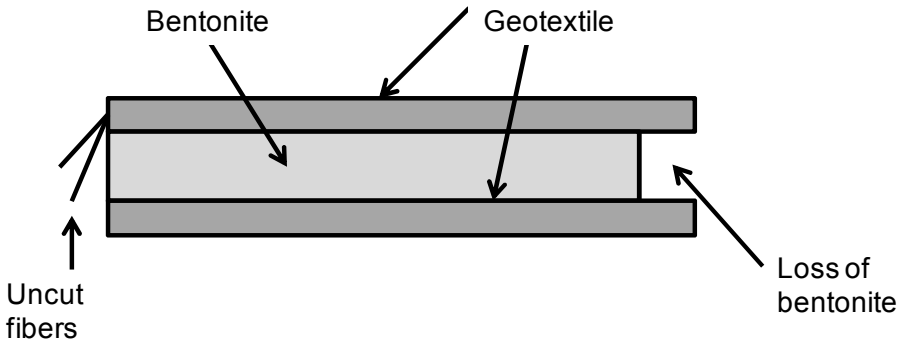

Figure 4-10 Loss of bentonite from the edge of the GCL

Experiments were conducted using distilled water and artificial ARD solutions as permeants. The GCL permeated with water was non-prehydrated and, thus, water was directly permeated from the influent port. Two types of prehydration were performed on the GCLs before ARD permeation: (a) GCLs were prehydrated for a period of 7 days, by placing them into containments with water, and applying 30 kPa of pressure, according to the scheme presented in Figure 4-6; (b) GCLs were prehydrated once the GCL was already placed in the system by permeating water for one month. Thickness of GCL was measured regularly (using a cathetometer), and analysis of the effluent was conducted every month in some cases and every week (one to three times per week) in others, according to the flow rate. Effluents analysis includes electrical conductivity (EC), pH, and volume of effluent measurements. Metal concentration of effluents was analyzed by ICP (ICPS – 800 Shimadzu).

General criteria to terminate hydraulic conductivity test was described by Katsumi et al. (2007), according to whom three points need to be satisfied; (1) the hydraulic conductivity value is stable over time, (2) the volumetric flow ratio is approximately 1, and (3) 2 or more pore volumes of flow are permeated into the GCL. In addition, chemical equilibrium has to be considered. Therefore, the hydraulic conductivity values are determined after the ratios of outflow to inflow of electrical conductivity (EC), pH, and metal content were 1, which indicates chemical equilibrium between outflow and inflow. This termination criteria is consistent with Shackelford et al. (1999) and is based on simple chemical indicator parameters that provide reliable and accurate hydraulic conductivity values. They suggested that the electric conductivity ratio of the influent and effluent fall within 0.9 – 1.1 before the test is terminated. For zeolite and ferrihydrite, the same termination criteria were applied.

4.3 Swelling Tests Results

The swelling test is a simple and easy but very useful test because it provides information about hydraulic conductivity. If the bentonite swell index is high, the hydraulic conductivity is expected to be low, and vice versa. Conducting hydraulic conductivity tests on barrier materials or materials with low or extremely low levels of hydraulic conductivity takes an extremely long time. Therefore, by checking the swell index of the bentonite when exposed to different kind of solutions, an idea can be obtained about the barrier performance of this mineral. Changes in the swell index with metal concentration are presented in Figure 4-11 for each ARD. Figure 4-11 shows the effect of different dilutions of ARD in the swell index, as well as the initial and final pH. The swell index for distilled water was 33.0 mL/2g bentonite. This value decreased as the EC, corresponding to concentration of ARD in the solution, increased. As Jo et al. (2004) indicated, when the concentration of metals in solution increases, water moves out of the mineral interlayer and, then, reduction in swell volume occurs. Figure 4-12 summarizes all the data collected from each ARD and their respective dilutions. It presents the effect of EC in the swell index and shows a possible exponential relationship between EC and swell index:

$$\text{Swell index} = 35.235e^{-0.002(\text{initial EC})} \quad (4.2)$$

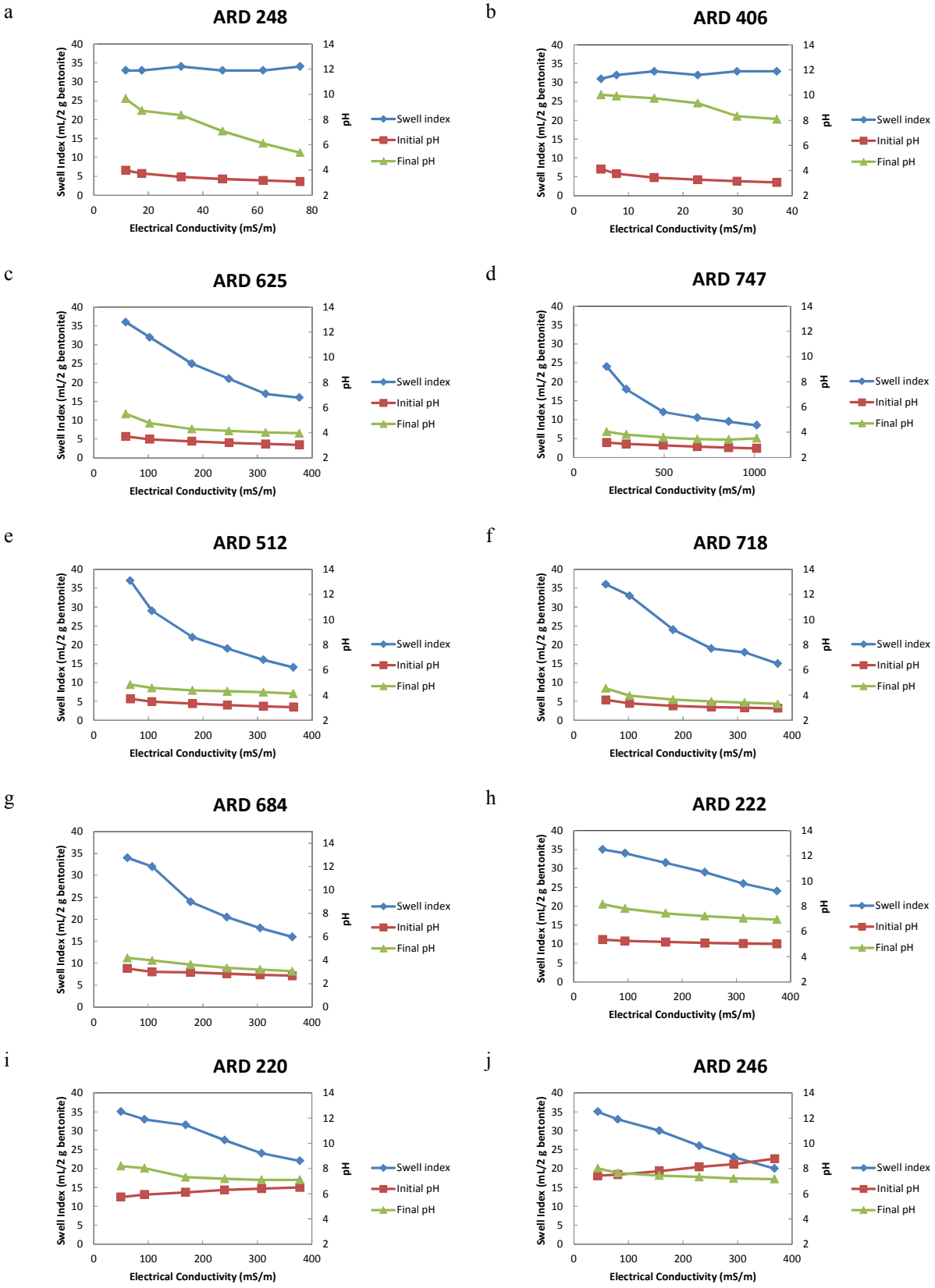

Figure 4-11 Results of free swelling tests using different dilutions of ARD

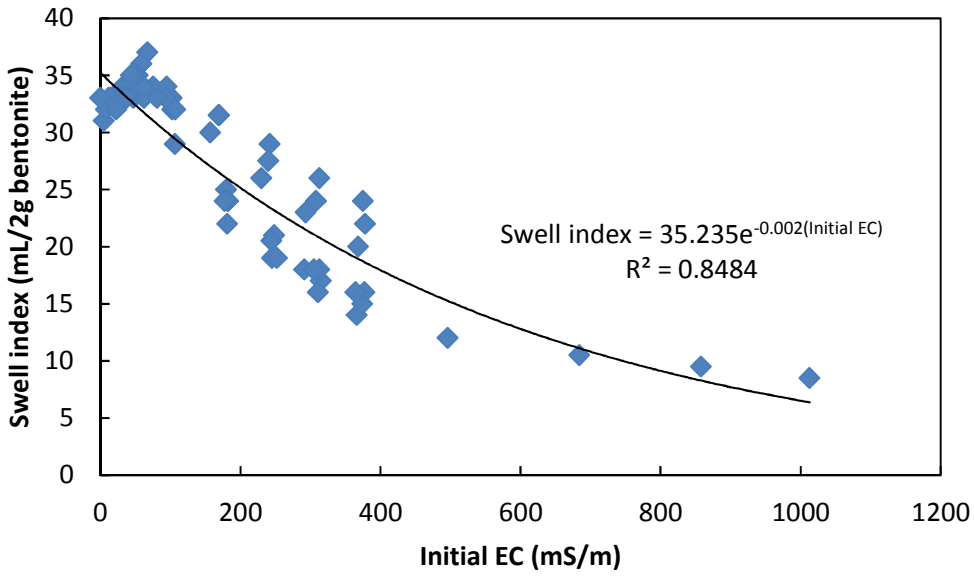

Figure 4-12 Relationship between EC and swell index

The data of each ARD and its respective dilution are summarized in Figure 4-13. This figure shows that there is no clear and single relationship between pH and swell index. From this figure it can be said that there is a positive linear relationship between pH 2.5 to 4 and a positive linear relationship between pH 5 and 5.5 (all values corresponding to ARD 222). From pH 5.5 to 6.5 (all values corresponding to ARD 220) it was observed a negative linear relationship, as well as from pH 7.5 to 8.5 (all values corresponding to ARD 246).

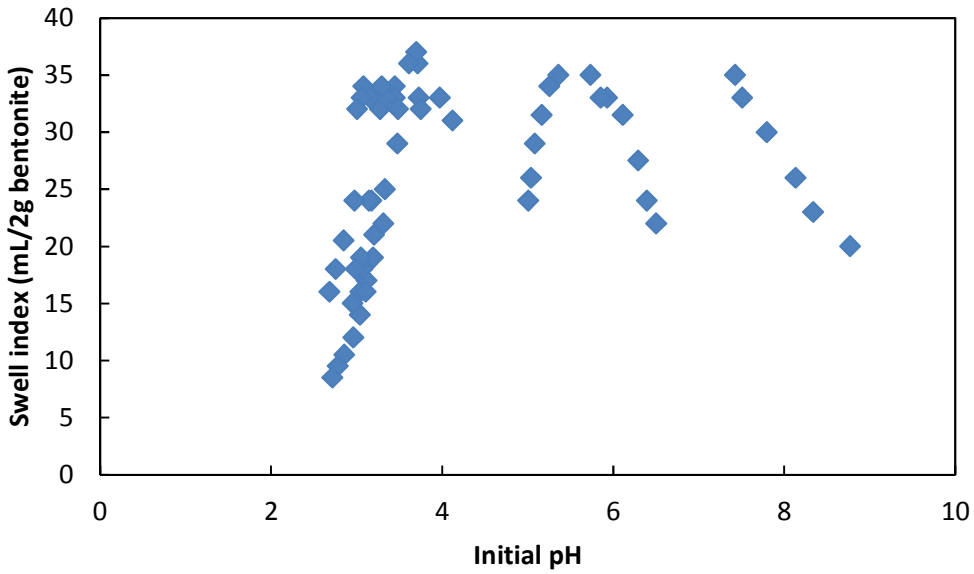

Figure 4-13 Relationship between pH and swell index

4.4 Hydraulic Conductivity of 10 Selected ARDs from the Database

This section reports on the result of GCL against ten selected cases of ARD obtained from the database (presented in Appendix A and discussed in Chapter 3) considering their pH and EC. GCLs were prehydrated with water before ARD permeation by letting water pass for around 5 pore volume of flow (PVF). The PVF was calculated by dividing the cumulative amount of effluent collected during the test (m^3) by the volume of voids in the specimen (m^3). The hydraulic conductivity of GCL against all ARD cases was constant and around 1×10^{-11} m/s, except for ARD 747, in which the hydraulic conductivity gradually increased, mainly due to the high metal concentration (Table 4-4, Figure 4-14). From these results, it can be said that for ARDs with EC values equal to or lower than 400 mS/m, GCLs seem to provide an efficient hydraulic barrier.

Table 4-4 Hydraulic conductivity values for each ARD

ARD	Hydraulic conductivity after ARD permeation, *k* (m/s)
248	1.16×10^{-11}
406	1.07×10^{-11}
625	1.17×10^{-11}
747	9.64×10^{-11}
512	1.28×10^{-11}
718	1.26×10^{-11}
684	$9.52\times10\text{-}^{12}$
222	1.19×10^{-11}
220	1.12×10^{-11}
246	1.32×10^{-11}

4.5 Relationship between Hydraulic Conductivity, pH, and EC

Figure 4-15 and Figure 4-16 summarize the variation of hydraulic conductivity at different pH and EC values. Even though there is not an evident relationship between pH and hydraulic conductivity, it seems that there is an exponential relationship between EC and hydraulic conductivity, which can be used for future prediction of hydraulic performance of a GCL by simply measuring the EC.

Figure 4-17 and Figure 4-18 show the hydraulic conductivity change at different pH values when the EC was kept constant at 400 mS/m and at different EC when the pH was fixed at pH 3, respectively. It seems that the hydraulic conductivity for ARDs with EC = 400 mS/m was kept constant at all pH values. However, it was observed that at pH = 3, the hydraulic conductivity gradually increases with EC increment.

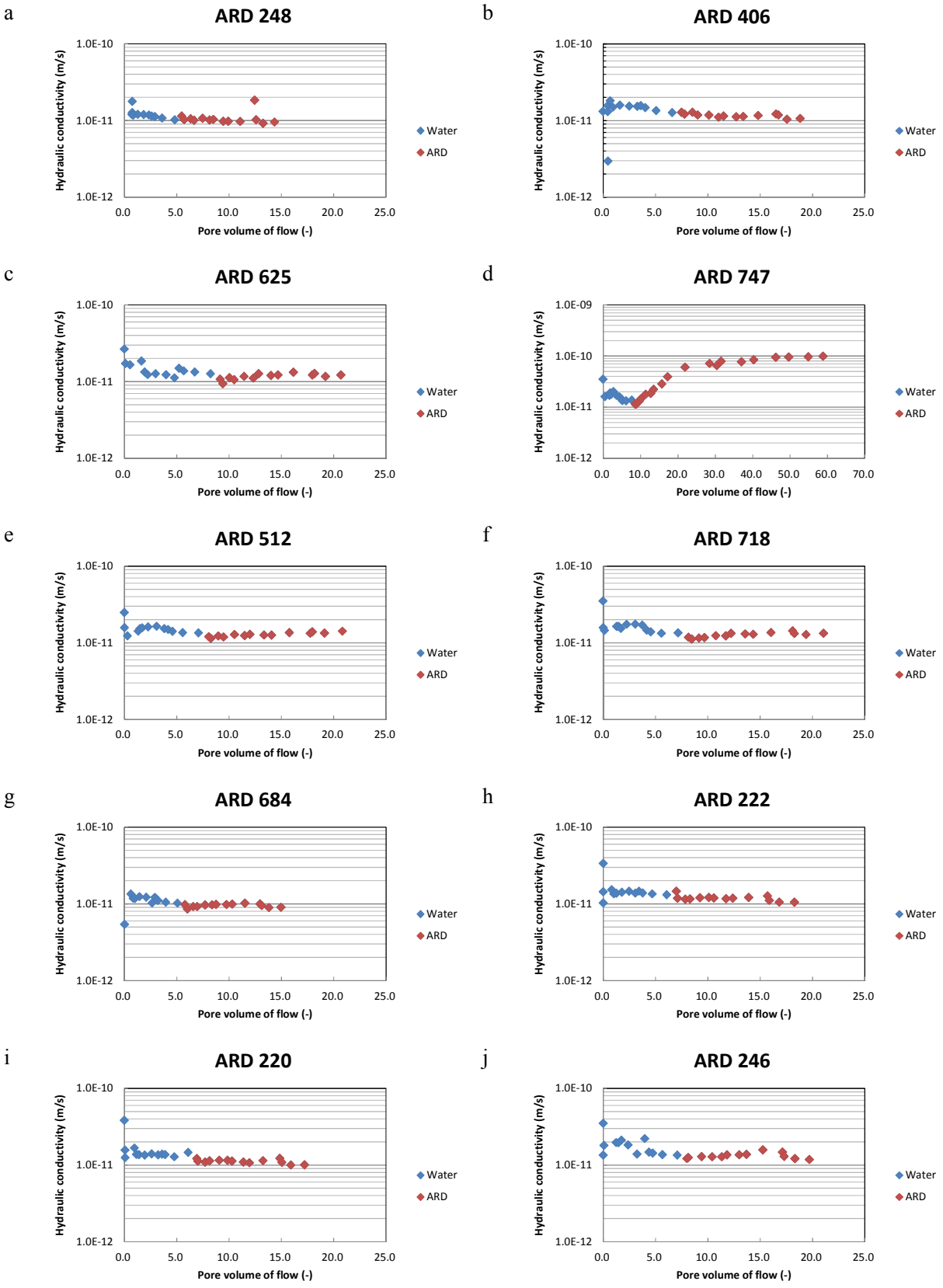

Figure 4-14 Hydraulic conductivity of 10 artificial ARDs

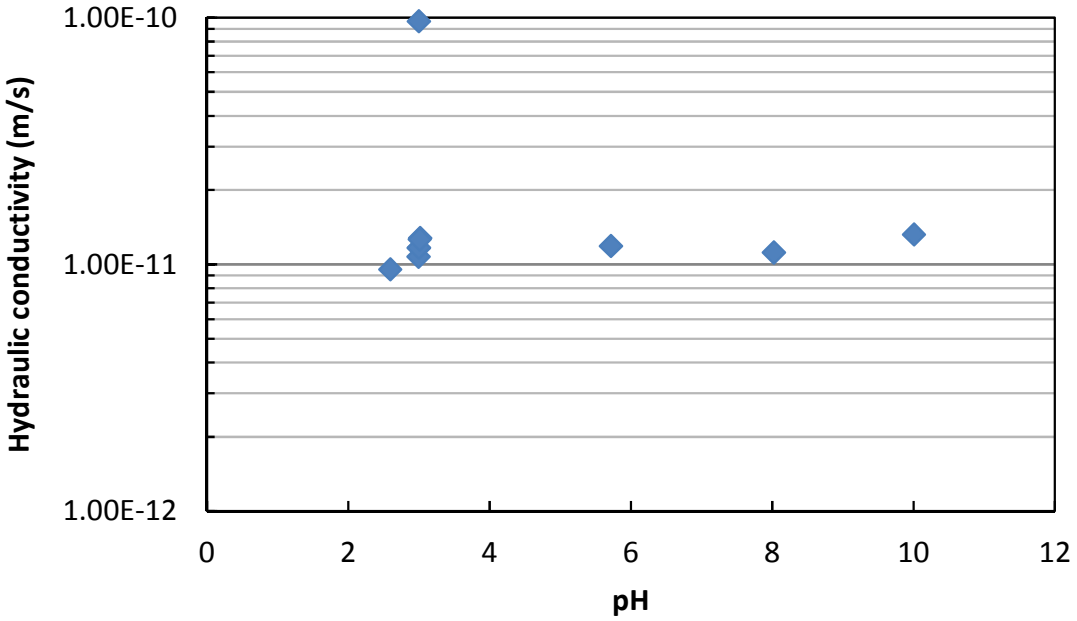

Figure 4-15 Hydraulic conductivity at different pH values

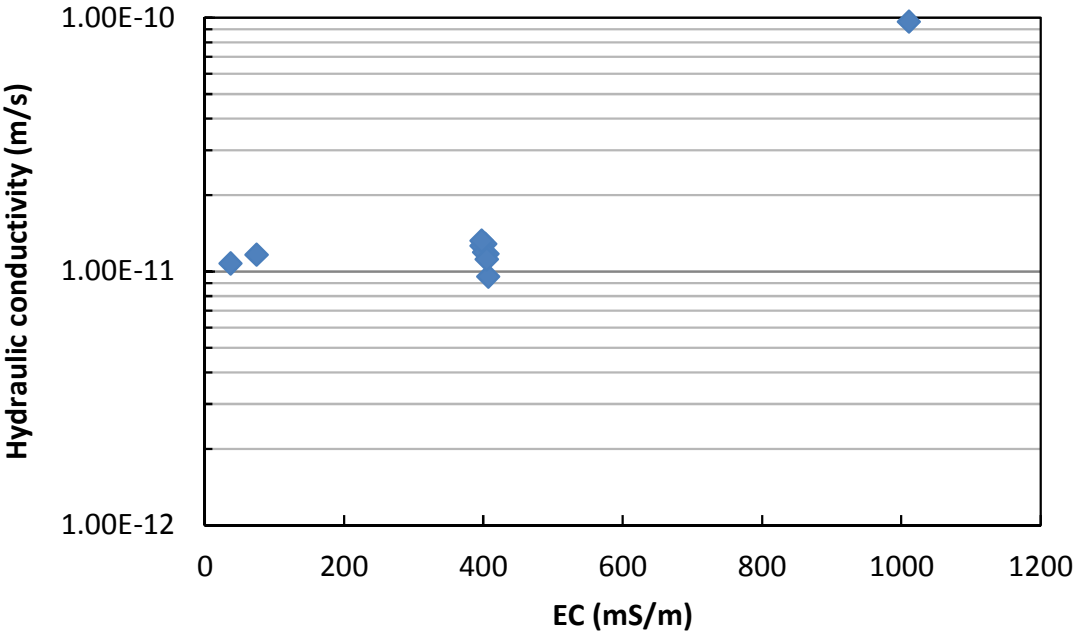

Figure 4-16 Hydraulic conductivity at different EC values

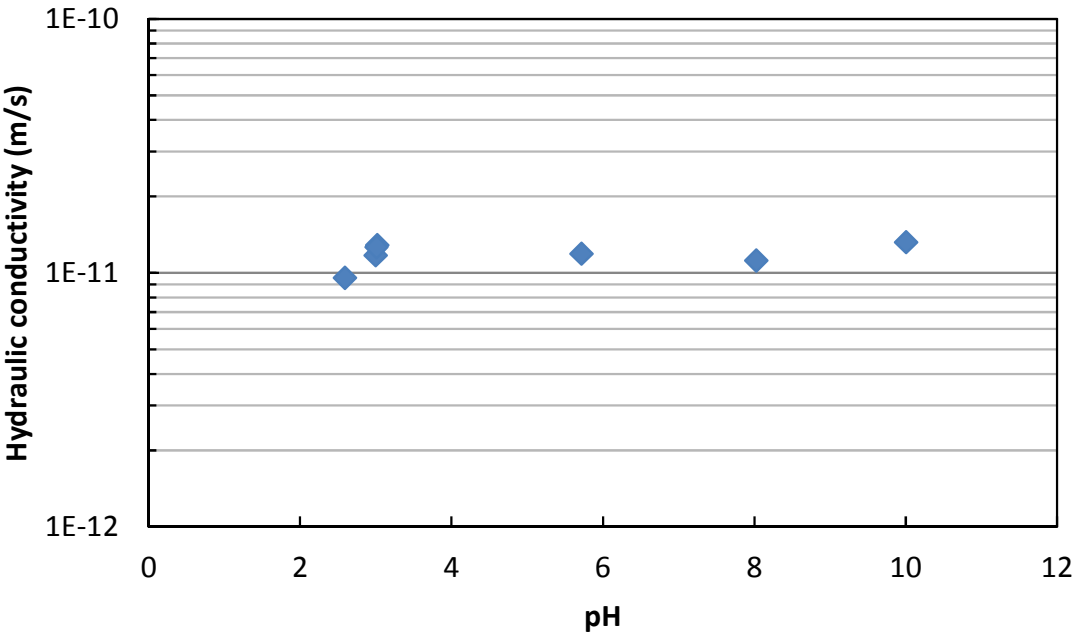

Figure 4-17 Hydraulic conductivity at different pH values, when the EC is fixed at 400 mS/m

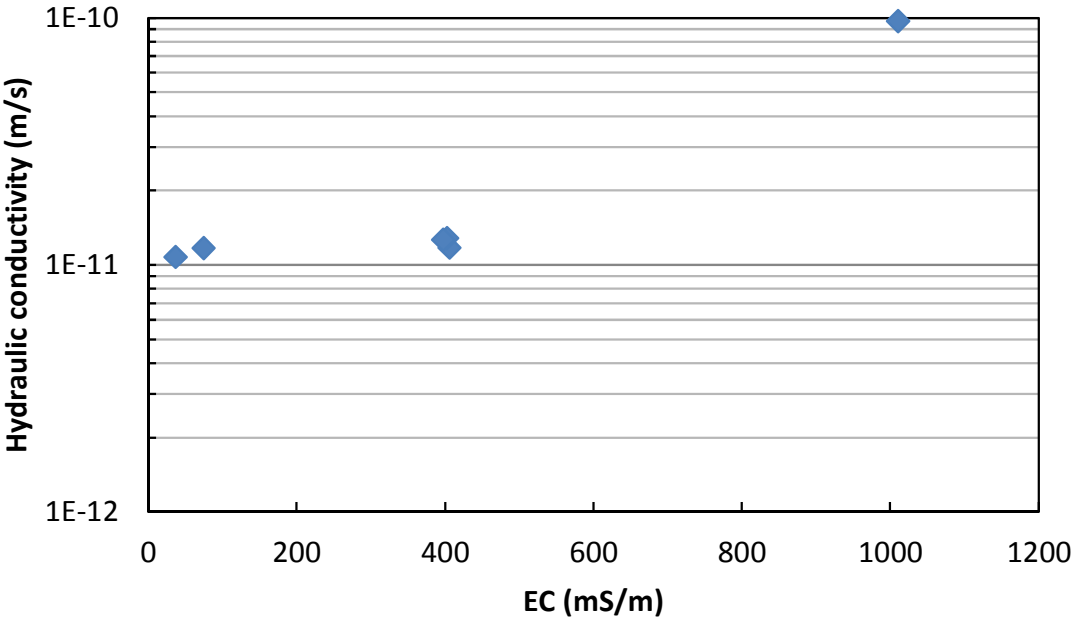

Figure 4-18 Hydraulic conductivity at different EC values, when the pH is fixed at 3

4.6 Relationship between Hydraulic Conductivity and Swell Index

Figure 4-19 shows the relationship between hydraulic conductivity and swell index of bentonite for the 10 ARDs studied. Figure 4-20 and Figure 4-21 present the variation in hydraulic conductivity at different pH when the EC was kept constant and at different EC when the pH was kept at 3, respectively.

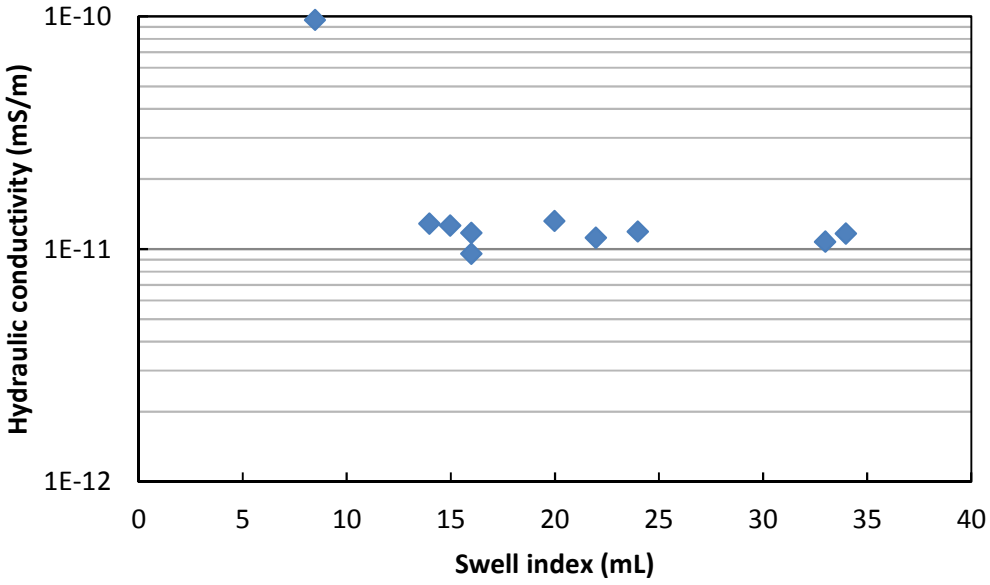

Figure 4-19 Hydraulic conductivity at different swell index

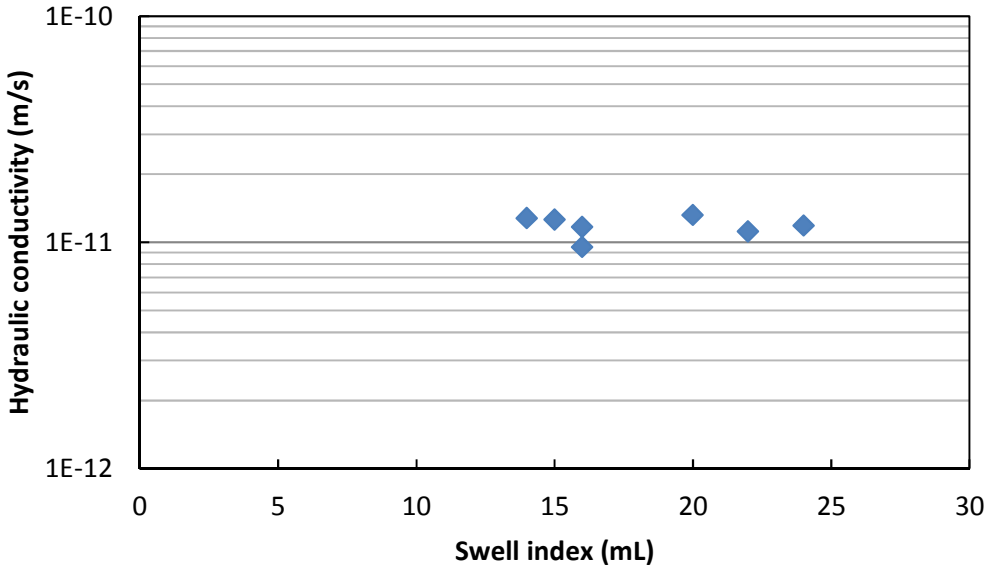

Figure 4-20 Hydraulic conductivity at different swell index when the EC was fixed at 400 mS/m

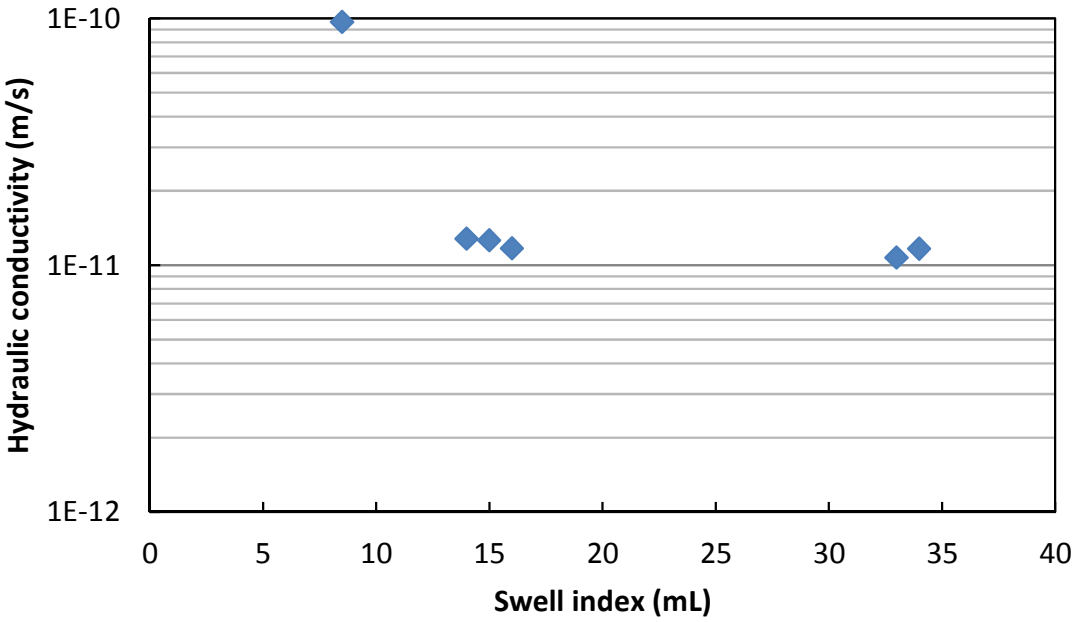

Figure 4-21 Hydraulic conductivity at different swell index when the pH was fixed at 3

4.7 Factors Affecting the Hydraulic Performance of GCLs

The GCLs' extremely low levels of hydraulic conductivity are attributed to the swelling of the bentonite contained in them. Since swelling is sensitive to chemicals, chemical compatibility becomes a critical subject when GCLs are applied to waste rock containment bottom liners. Many researchers have reported that permeation with chemical solutions will result in an increase in hydraulic conductivity. These effects can be explained by the changes in soil fabric and are categorized into (1) the dissolution of the clay particles and the chemical compounds resulting from strong acid and base solutions, (2) the restriction of the development of a diffuse double layer, and (3) the restriction of osmotic swelling for smectite clay (Katsumi 2010).

Besides mechanical properties of the GCLs, chemical changes and interactions that occur within the GCLs when permeated with solutions with low pH and high metal concentrations should be also taken into consideration. The large cation exchange capacity (CEC = 80 – 100 meq/100 g) and surface area (800 m^2/g) of sodium montmorillonites cause GCLs to have an affinity towards ions present in solutions. Many issues related to metal interactions with GCLs are often explained using data exclusively from sorption experiments on bentonite, performed under single or equimolar multi-metal permeants. However, some previous studies have shown that the chemical composition of solutions greatly affects the order in which metals are retained in GCLs (Lange et al. 2005, 2007). Thus, it can be inferred that the behavior of a single metal batch test cannot be simply extended or applied to ARD cases, because metal behaviors may differ when they are combined.

Table 4-5 Effect of different parameters in the hydraulic and metal retention performance

Parameters	Hydraulic conductivity	Metal retention
Type of bentonite	○	---
pH	○	○
Metal concentration and metal ion type	○	○
Short and long term performance evaluation	○	---
Bentonite buffering capacity	---	○
Metal precipitation	○	○

○: Studied parameters

So, in order to understand to what extent hydraulic conductivity and metal transport are affected by ARD permeation and how the metals are retarded or retained into bentonite, this chapter presents a thorough discussion using all the results obtained, as well as comparison with results of other previous research. Table 4-5 shows the parameters that are discussed in this chapter (hydraulic conductivity) and the next chapter (metal retention).

Numerous studies have been done on the impact of municipal solid waste (MSW) leachate on GCLs' performance using different kinds of inorganic salt solutions such as NaCl, LiCl, $CaCl_2$, $MgCl_2$, as well as alkali solutions, acid solutions, MSW leachate, and sea water solutions (Petrov and Rowe 1997; Jo et al. 2004; Touze-Foltz et al. 2006; Katsumi et al. 2008b). However, limited research has been conducted on the impact of ARD in GCLs' performance (Hornsey et al. 2010; Lange et al. 2010a; Shackelford et al. 2010).

Using GCLs in waste rock containment facilities for materials with ARD generation potential may not be a simple matter of transferring common technology used in landfills due to the extreme ranges in leachate characteristics observed in ARDs, in terms of acidity and heavy metal concentration, compared to MSW leachates. Gates et al. (2009) have reported that leachates of excessive ion strength (> 0.3 M), usually found in ARD cases, elevated temperatures (> 60 ºC) and strong acid (pH < 3) or alkaline solutions (pH > 12) may have detrimental effects on the hydraulic conductivity of GCLs, lowering their barrier performance. Hornsey et al. (2010) stated that bentonite inside GCLs undergoes dissolution at extreme pH, pore structure and loss of gel at elevated salinity, and shrinkage at elevated temperatures.

Therefore, evaluation of the performance and chemical compatibility of GCLs with ARDs becomes necessary before their field application in order to ensure long-term performance and prevent groundwater pollution. The potential use of GCLs in waste rock containment with ARD generation potential can be judged in terms of hydraulic conductivity and metal immobilization. According to previous studies, there are many factors that affect these parameters, such as low pH and high heavy metal concentrations; ARD composition and type of ions present (cations and anions); type of bentonite (Ca-bentonite, Na-bentonite,

granular or powdered bentonite, and smectite content) used in the GCLs; hydraulic conductivity change over time due to clogging; metal competition; and ion uptake mechanisms (ion exchange and precipitation). These parameters will be discussed in this section in order to study to what extent ARD solutions impact GCLs performance and to evaluate if some relationships between parameters found for MSW leachate apply or fit also to GCL-ARD cases.

4.7.1 Effect of Prehydration over Non-Prehydration

Figure 4-22 and Figure 4-23 present the effect of water prehydration in the hydraulic conductivity of GCL against ARD 747. The experiments were run simultaneously for 9 months and it was observed that the hydraulic conductivity of the non prehydrated case was higher than the prehydrated one. At the same PVF (around 150 PVF), it is observed that the hydraulic conductivity was five times higher without prehydration (5.0×10^{-10} m/s) compared to the prehydrated case (1.4×10^{-10} m/s). This result suggests that the prehydration of GCL positively impacts the hydraulic conductivity of GCL and therefore prehydration is suggested to be done prior to ARD permeation.

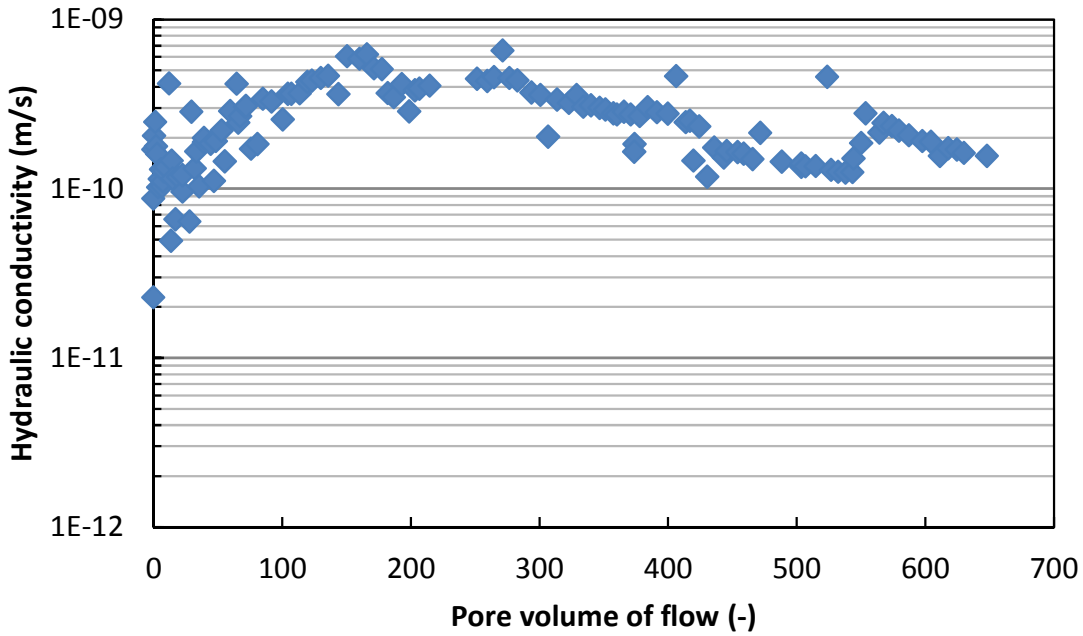

Figure 4-22 Hydraulic conductivity of GCL permeated with ARD 747 without prehydration

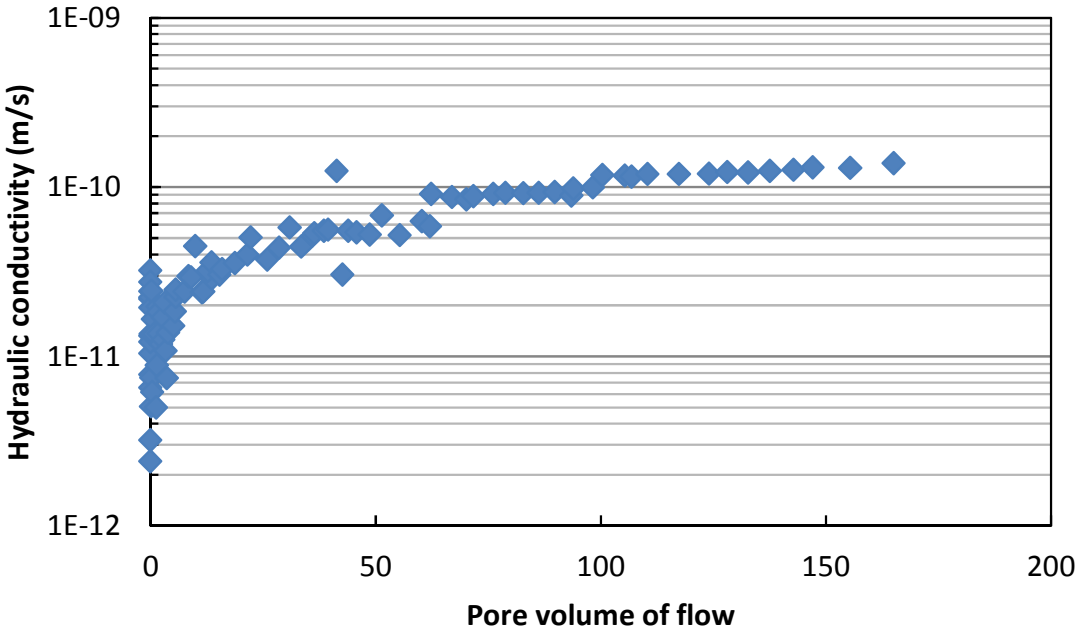

Figure 4-23 Hydraulic conductivity of GCL permeated with ARD 747 with prehydration

4.7.2 Effect of Short and Long Term Performance Evaluation

Short term hydraulic conductivity evaluations (e.g. around 20 PVF) provide accurate hydraulic conductivity values until the equilibrium has been reached (usually based on an electrical conductivity ratio of influent and effluent between 0.9 – 1.1). However, the hydraulic conductivity of GCLs may change over time especially due to metal precipitation, as shown in Figure 4-22.

According to this test which was run for 9 months, the hydraulic conductivity of the ARD permeated case gradually increased over time, until around 150 PVF. After this point, it stabilized, reaching an average permeability value of 5.0×10^{-10} m/s. Around 300 PVF it started decreasing again due to the effect of physical clogging, mainly attributed to iron precipitation (ARD with high Fe concentration). The presence of a red/orange layer of iron hydroxide in the GCL proves this hypothesis (Figure 4-24).

A reduction in hydraulic conductivity values was also reported by Katsumi et al. (2008) for long-term evaluation (1 to 7 years) of hydraulic conductivity of GCLs permeated with high ionic strength (I) solutions (especially for I > 0.5).

Although limited studies have been done on long-term performance of GCLs permeated with ARD solutions, change in hydraulic conductivity over time becomes an important issue, considering that GCLs show promise for long-term containments. Long-term performance analysis will allow prediction and understanding of the phenomenon that will occur after some time of ARD permeation and its influence on the GCLs performance as lining systems in waste rock containment facilities.

Figure 4-24 GCL after hydraulic conductivity test: water permeation (left), ARD permeation (right)

4.7.3 Effect of Gypsum and Ferrihydrite Precipitation

Figure 4-22 presented in the previous section shows the effect of long term study of the hydraulic conductivity. The experiments were run for 9 months and it was observed that the hydraulic conductivity decreased over time because of the clogging effect, mainly caused by iron precipitation. GCLs (bentonite) have high affinity toward cations, but relatively weak affinity for anions. Arsenic, which is an oxyanion, is one of the most toxic components present in ARDs, which suggest that special attention should be given to mobile metals that cannot be sorbed by GCLs. It is possible to say that great amount of As could be retained into GCLs mainly due to the high concentration of Fe present in ARD (discussed in Chapter 5). Moreover, Lange et al. (2007) proposed an hypothesis of As retention due to the gypsum precipitation observed in XRD analysis after ARD permeation through GCLs. In case of As retention onto iron oxides, the following series of equations can be considered as the immobilization mechanism.

Iron hydroxide formation:

$$Fe^{2+} + 1/4\ O_2 + H^+ \rightarrow Fe^{3+} + 1/2\ H_2O \quad (4.3)$$

$$Fe^{3+} + 3OH^- \rightarrow Fe(OH)_3 \quad (4.4)$$

Anion adsorption onto iron hydroxide at pH < IEP (isoelectronic point):

$$FeOH + H_2AsO_4^- \rightarrow FeH_2AsO_4^- + OH^- \quad (4.5)$$

$$FeH_2AsO_4^- \rightarrow FeHAsO_4^{2-} + H^+ \quad (4.6)$$

Analysis using μXRD and μXRF techniques made by Lange et al. (2010b) on bentonite permeated with ARD showed that Fe-oxides also played a significant role in sequestering a range of metals such as Ni, Mn, and Zn. This increases the overall sorption capability of the GCL and confirms that solution composition is important in metal uptake behavior.

4.7.4 Effect of Type of Bentonite

Bentonites are classified into sodium bentonites (Na-bentonites) and calcium bentonites (Ca-bentonites), depending on the dominant exchangeable cation that is present. Ca-bentonites are much more available worldwide than Na-bentonites. However, the latter is known to have the lowest permeability of any naturally occurring geological material (Koerner and Koerner 2010). Therefore, Ca-bentonite is usually activated with soda (sodium carbonate or sodium hydroxide) so that the primary calcium ions are exchanged with sodium ions (so-called active bentonite), decreasing the permeability to that of the naturally occurring Na-bentonite (Egloffstein 2001).

The swell index of Na-bentonite is associated with the presence of montmorillonite (smectite) and depends on the valence of the cations and the ionic concentration between the crystalline layers. If monovalent cations, such as Na^+, are present in the interlayer region, numerous layers of water molecules are retained electrostatically. Thus, less mobile water is available for flow, the swell volume is large, and the hydraulic conductivity is low. If polyvalent cations, such as Ca^{2+}, Mg^{2+}, and heavy metal ions replace the Na^+ cations due to their higher charge, bentonite shrinks. This occurs because the volume of bound water decreases until the interlayer spacing reaches four layers of water molecules. Accordingly, a smaller fraction of the water will be bound, a larger fraction will be mobile, and the hydraulic conductivity would increase (Jo et al. 2001; Shackelford et al. 2010).

A decrease in swell index of a powdered bentonite (Bentofix® NSP 4900) from 32 mL/2 g bentonite (deionized water) to 8.5 mL/2 g bentonite was observed after ARD 747 permeation (pH = 3, EC = 1010 – 1192 mS/m). This decrease in swelling volume correlated with an increase in hydraulic conductivity of one order of magnitude (5.0×10^{-10} m/s) compared to the water permeation case (1.4×10^{-10} m/s).

A relationship between hydraulic conductivity and free swell index for a powdered bentonite was found by Katsumi et al. (2007) for inorganic salts (Figure 4-25). This relationship was explored using 40 types of inorganic permeant solutions. According to the study, the permeability of a bentonite can be approximately given as a simple function of the free swell:

$$\log\left(\frac{y}{c}\right) = \exp(a(x-b)) \tag{4.7}$$

where x is the free swell index of the bentonite (mL/2 g solid), y is the hydraulic conductivity of the bentonite in m/s, a is -0.31, b is 8.69 mL/2 g solid, and c is 3.09×10^{-11} m/s, which is the hydraulic conductivity at x to infinity. These parameters are dependent on the effective stress confining the bentonite, which was fixed to 29.4 kPa. On applying this equation to the bentonite and artificial ARD systems, the same tendency was found, but slightly different results. Therefore, an adjusted model from Katsumi et al. (2007) was proposed to better fit the experimental results (Figure 4-26). In this adjusted model, the value of a is -0.6, b is 8.37 mL/2g solid, and c is 1.15×10^{-11} m/s. This adjusted equation has an error between 0.4 and 19.2% (Table 4-6) and therefore, it constitutes a useful tool to easily estimate the barrier performance of GCLs against ARDs, as free swell index can be evaluated much more rapidly than hydraulic conductivity.

An exponential relationship between hydraulic conductivity and electrical conductivity was proposed in Figure 4-27. More evidences such as theoretical explanation or experimental results (or data from other

research) are necessary to confirm or support this relationship. It is useful to have a relationship between EC and hydraulic conductivity because EC is easy to measure in the field (by using simple equipment, an EC meter), and, by having this, an estimate of the hydraulic conductivity (at least the order of magnitude) can be obtained.

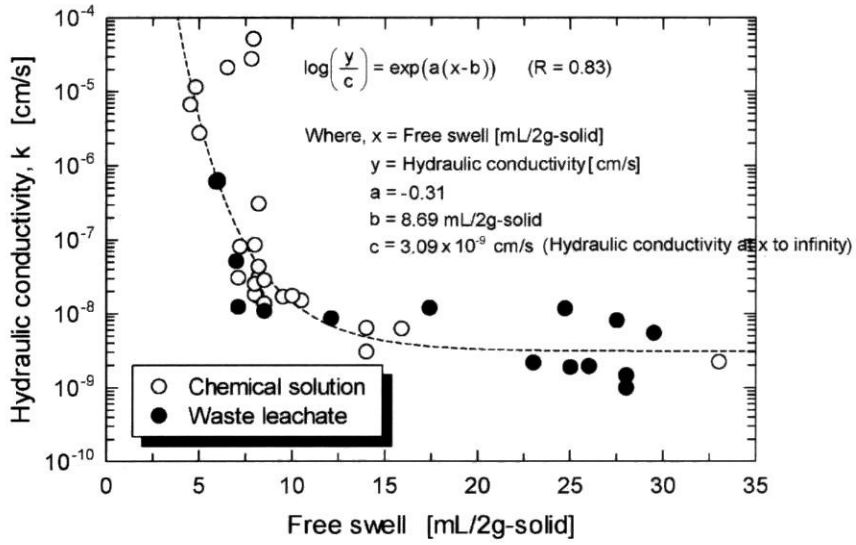

Figure 4-25 Relation between the hydraulic conductivity and the free swell (Katsumi et al. 2007)

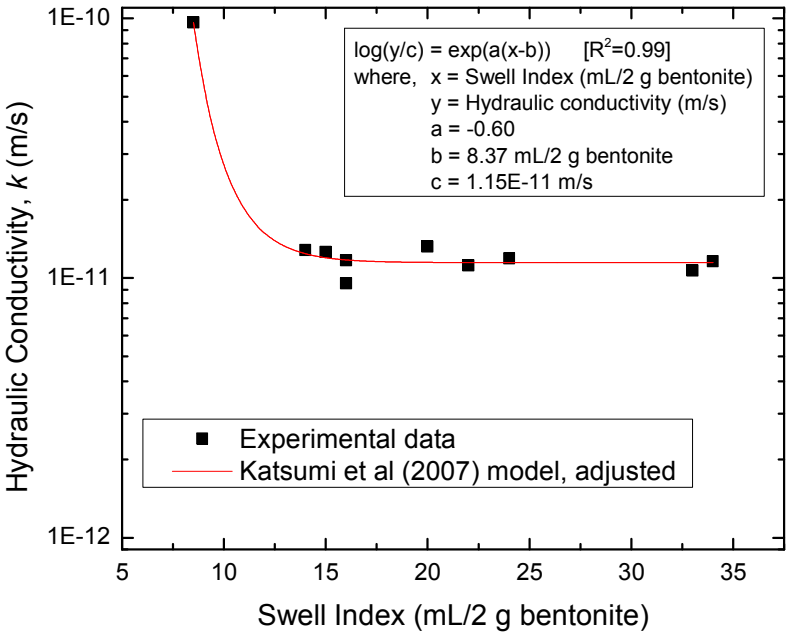

Figure 4-26 Model adjusted from Katsumi et al. (2007)

Table 4-6 Experimental and theoretical hydraulic conductivity using two models

ARD	Swell index	k (m/s)	k_1 (Katsumi et al. 2007)	Error percentage of k_1	k_2 (Katsumi et al. 2007, adjusted)	Error percentage of k_2
248	34	1.16×10^{-11}	3.09×10^{-11}	62.4	1.15×10^{-11}	0.9
406	33	1.07×10^{-11}	3.09×10^{-11}	65.4	1.15×10^{-11}	7.0
625	16	1.17×10^{-11}	3.92×10^{-11}	70.1	1.18×10^{-11}	0.6
747	8.5	9.64×10^{-11}	3.55×10^{-10}	72.9	9.68×10^{-11}	0.4
512	14	1.28×10^{-11}	4.82×10^{-11}	73.4	1.24×10^{-11}	2.9
718	15	1.26×10^{-11}	4.28×10^{-11}	70.6	1.20×10^{-11}	4.9
684	16	9.52×10^{-12}	3.92×10^{-11}	75.7	1.18×10^{-11}	19.2
222	24	1.19×10^{-11}	3.15×10^{-11}	62.2	1.15×10^{-11}	3.5
220	22	1.12×10^{-11}	3.21×10^{-11}	65.1	1.15×10^{-11}	2.7
246	20	1.32×10^{-11}	3.31×10^{-11}	60.1	1.15×10^{-11}	14.5

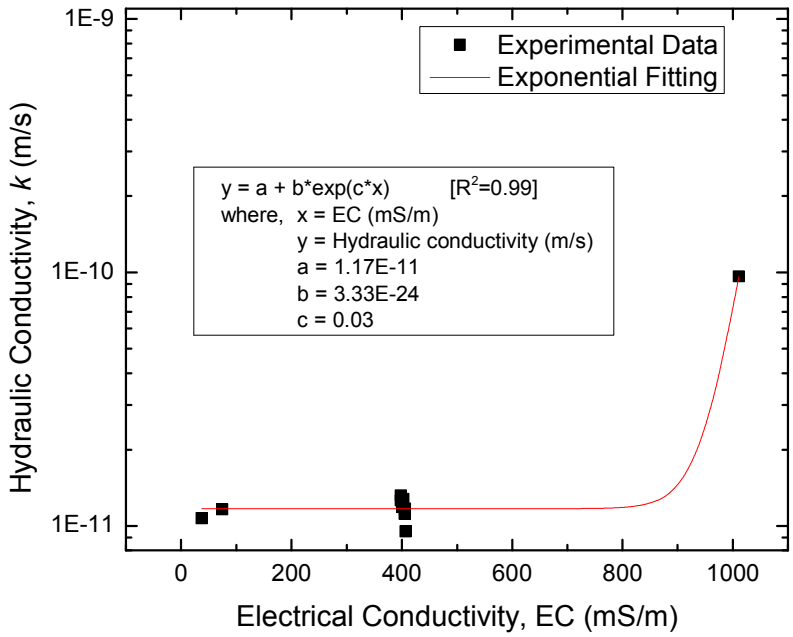

Figure 4-27 A possible relationship between EC and hydraulic conductivity

Another GCL classification can be made by the state of the bentonite used to produce GCLs: granular (aggregated) or powdered. Powder bentonites have a higher degree of processing than granular bentonites in terms of pulverizing, sieving, and size fractioning the mineral.

Previous research have shown that both GCLs are affected by chemical solutions, but that the powdered

bentonite are more compatible than the granular bentonite, particularly with strong chemical solutions (Katsumi 2010). Vangpaisal and Bouazza (2003) observed that powdered bentonites generally hydrate uniformly from the outer surfaces of the GCL toward the center, resulting in rapid development of an effective seal against further water movement. In addition, pores of powdered bentonite are small (high specific surface area) even when the swelling is limited by acid or high metal concentration solutions and therefore lower hydraulic conductivity is observed (Katsumi 2010). On the other hand, in granulated bentonites, the outer surfaces of each individual granule wets first and therefore particles within aggregates wet slowly (Vangpaisal and Bouazza 2003). Besides, pores of the granules are not blocked due to the low swelling caused by aggressive chemicals and therefore higher hydraulic conductivity values are expected (Katsumi 2010).

Experiments conducted by Shackelford et al. (2010) on granular bentonite GCLs show that the hydraulic conductivity increases by three orders of magnitude after ARD permeation, compared to the water permeation case. In this research using powdered bentonite, an increase of one order of magnitude in hydraulic conductivity was observed after permeation with ARD 747, with higher ionic strength but

Table 4-7 Hydraulic conductivity comparison between two types of GCLs

	Shackelford et al. (2010)	This research (ARD 747)
ARD composition	Al (31 mg/L) As (0.6 mg/L) Cd (4.3 mg/L) Ca (270 mg/L) Co (1.3 mg/L) Cu (51 mg/L) Fe (410 mg/L) Mg (1400 mg/L) Mn (180 mg/L) Ni (1.5 mg/L) SO_4 (6900 mg/L) Zn (1800 mg/L)	Al (259.2 mg/L) Fe (4330.2 mg/L) Cu (86.9 mg/L) Zn (493.1 mg/L) As (49.1 mg/L) Pb (2.9 mg/L) K (31.8 mg/L) Na (413.9 mg/L) Ca (397.0 mg/L) Mg (214.0 mg/L)
pH	2.5	3.0
Ionic strength	356 mM	504 mM
Type of Na-bentonite	Granular	Powdered
k for water permeation	1.7×10^{-11} m/s	1.4×10^{-11} m/s
k for ARD permeation with prehydration	7.9×10^{-9}	1.1×10^{-10} m/s
k for ARD permeation without prehydration	3.9×10^{-8}	5.0×10^{-10} m/s

slightly higher pH than reported by Shackelford et al. (2010). Information about the ARD composition, pH, ion strength, type of bentonite used, and hydraulic conductivity results in both study cases are detailed in Table 4-7. From these results it can be said that the hydraulic conductivity of both granular and powdered bentonite are similar in the water permeation case. However, hydraulic conductivity values greatly differ after ARD permeation.

Similar to the relationship based on swell index to predict hydraulic conductivity, Kolstad et al. (2004) proposed an estimation of the hydraulic conductivity for non-prehydrated granular bentonite based on the ionic strength and the ratio of the monovalent and divalent cations:

$$\frac{\log K_c}{\log K_{DI}} = 1.085 - 1.097I + 0.03981I^2 RMD \tag{4.8}$$

where K_c is the hydraulic conductivity to the inorganic chemical solution, *KDI*, the hydraulic conductivity to deionized water, *I*, the ionic strength (between 0.05 and 5 M), and *RMD* is the ratio of the concentrations of monovalent and divalent cations in the permeant solution (for *RMD* < 2.0 $mM^{1/2}$). The *I* and the RMD are calculated with the following equations:

$$I = \frac{1}{2}\sum_{i=1}^{n} c_i z_i^2 \tag{4.9}$$

$$RMD = \frac{M_M}{\sqrt{M_D}} \tag{4.10}$$

where c_i and z_i are the concentration of and the valence of the *i*th ion, respectively. M_M is the total molarity of monovalent ions and *MD* is the total molarity of divalent cations in the solution. According to Shackelford et al. (2010) this correlation among *k*, *I*, and *RMD* proposed by Kolstad et al. (2004) provided reasonable estimates of *k* in most granular bentonite cases. Another important consideration of GCLs is the mineralogical composition of the bentonite, which in the end will determine the hydraulic performance. Guyonnet et al. (2009) have demonstrated that low smectite content results in a higher hydraulic conductivity. For example, they observed a two-order of magnitude higher hydraulic conductivity when the smectite content was less than 30% in weight. Smectite content higher than 70% in weight may provide good barrier performance in terms of hydraulic conductivity.

4.7.5 Effect of pH

It can be assumed that, in general, pH < 3 will have detrimental effects on GCLs performance mainly due to dissolution of smectite (Gates et al. 2009). Alumina in the octahedral layers of the montmorillonite can be dissolved by hydrolysis, resulting in exchange of Al^{3+} for Na^+ in the exchange complex and a decrease in the volume of bound water (Norrish and Quirk 1954).

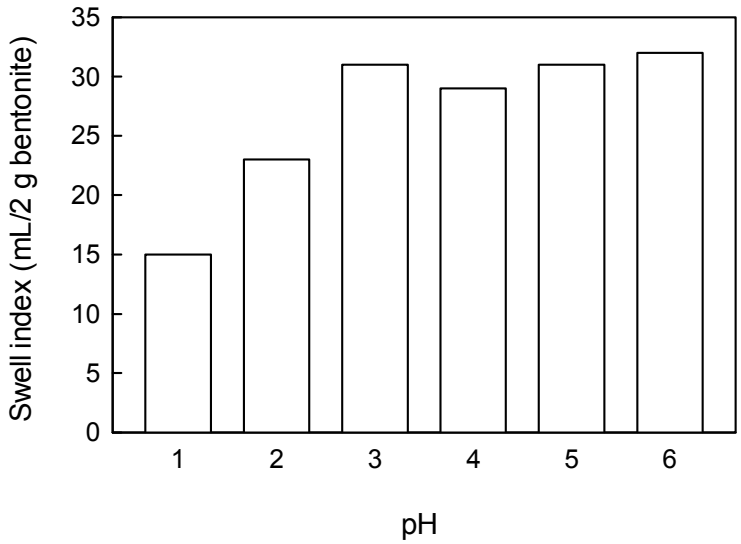

Figure 4-28 Swell index at different pH (water acidified using $H_2SO_{4(cc)}$)

The volume of bound water, discussed in the previous section, may also decrease due to the destruction of the structure of montmorillonite. From Figure 4-28, it can be observed that swell index was smallest (15 mL/2 g bentonite) in strong acid (pH = 1) solutions, but increased rapidly with increasing pH up to pH = 3. Swell index was then approximately constant (30 mL/ 2 g bentonite) until the pH reached 6. Similar results were obtained by Jo et al. (2001). Ruhl and Daniel (1997) have reported a two-order of magnitude increase in GCLs hydraulic conductivity values after pH = 1 solution permeation.

4.7.6 Effect of Metal Concentration and ARD Composition

When the concentration of cations in the bulk solution increases, water moves out of the interlayer region due to the gradient in free energy induced by the elevated concentration in the bulk pore water (Jo et al. 2001). Moreover, an ion exchange of monovalent sodium ions against high amount of bivalent ions present in ARDs may reduce the spaces between the silicate layers (Katsumi 2010), changing the surfaces of the clay minerals into a central bivalent cation layer.

As a consequence of the presence of aggressive drainages with high amounts of divalent or higher valence cations, a rapid increase in hydraulic conductivity will occur. Some studies suggest that this effect can be minimized if the first liquid to permeate the GCL is water (Shan and Lai 2002; Katsumi 2010; Shackelford et al. 2010). For example in case of ARD 747, it was observed a five-fold reduction in the hydraulic conductivity value when the GCL was prehydrated with water before ARD permeation. Shackelford et al. (2010) have found a one-order of magnitude difference in water prehydrated and ARD permeated case compared to non-prehydrated and ARD permeated cases.

4.8 Comparison of Hydraulic Performance of Bentonite with Zeolite and Ferrihydrite

Apart from GCLs, there are other materials that are readily available and may well present a possible solution for ARD mitigation. Zeolite and ferrihydrite were studied against the more critical ARD (ARD 747) in order to determine their performance against ARD. The results of the hydraulic conductivity test of the three materials are presented in Figure 4-29 (water permeation) and Figure 4-30 (ARD permeation with ARD 747). A summary of hydraulic conductivity values is presented in Table 4-8.

The hydraulic conductivity of GCL permeated with distilled water (control) was constant, with an average of 1.4×10^{-11} m/s. The hydraulic conductivity value of the GCL permeated with ARD 747 was around 5.0×10^{-10} m/s, 10 times higher compared to water permeation case. The hydraulic conductivity of zeolite permeated with water was 3.0×10^{-10} m/s and this value increased one order of magnitude when it was permeated with ARD 747, with an average a value of 1.4×10^{-9} m/s. The hydraulic conductivity of ferrihydrite is the highest among the three species with a hydraulic conductivity value of 7.3×10^{-9} m/s. The hydraulic conductivity of this material when permeated with ARD 747 does not show any change, with an average value of 8.6×10^{-9} m/s.

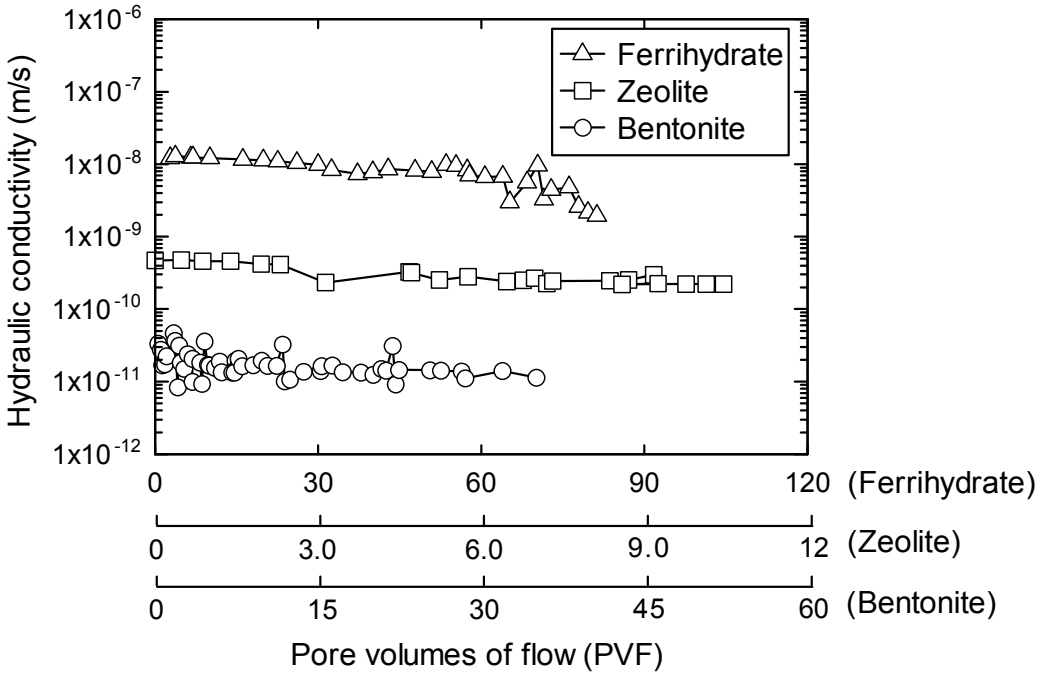

Figure 4-29 Hydraulic conductivity of minerals permeated with water (control)

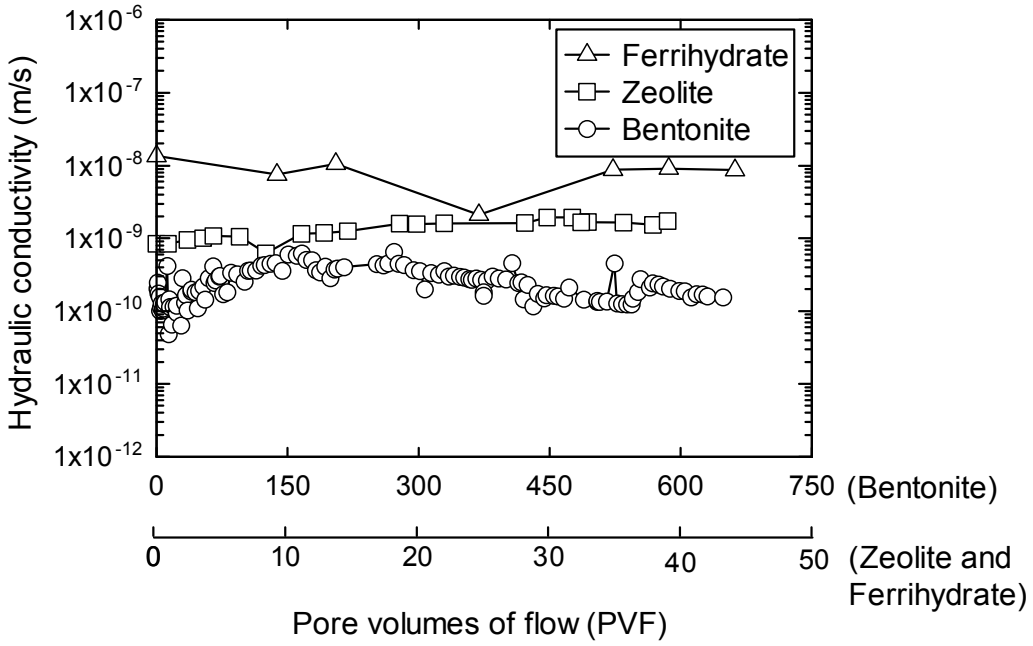

Figure 4-30 Hydraulic conductivity of minerals permeated with ARD

Table 4-8 Hydraulic conductivity of different specimens permeated with water and ARD 747

Specimen	Permeant solution	
	Water	ARD
GCL	1.4×10^{-11} m/s	$9.6\times10^{-11} - 5.0\times10^{-10}$ m/s (depending on the prehydration)
Zeolite	3.0×10^{-10} m/s	1.4×10^{-9} m/s
Ferrihydrite	7.3×10^{-9} m/s	8.6×10^{-9} m/s

4.9 Summary and Conclusions for this Chapter

Three materials that can be potentially used as an barrier layer, GCL, zeolite, and ferrihydrite, were proposed and evaluated in this chapter. Ten ARDs were selected from the database presented in Chapter 3 according to the pH and EC: 7 ARDs have EC values of 400 mS/m 2 ARDs have EC values lower than 400 mS/m (EC = 37 and 74.8 mS/m), and 1 ARD case has EC higher than 400 mS/m (EC = 1011 mS/m); 6 ARDs have pH values of 3, 1 ARD has pH lower than 3 (pH = 2.6), and 3 ARDs have pH higher than 3 (pH = 5.7, 8.0, and 10.0).

The barrier performance of GCL was tested against 10 selected ARDs, whereas the barrier

performance of zeolite and ferrihydrite was conducted only for the most severe case of ARD (ARD 747) in terms of low pH and high EC. According to experimental results, GCL, zeolite, and ferrihydrite appear to be suitable for ARD mitigation, as the hydraulic conductivity remained low enough to be used in rock containment facilities with ARD potential generation.

For GCL, the hydraulic conductivity was tested against 10 ARDs and the hydraulic conductivity values range between 9.5×10^{-12} and 5.0×10^{-10} m/s, which represents a 1 order magnitude maximum compared to the water permeation case (1.4×10^{-11} m/s). Moreover, for values lower than or equal to 400 mS/m of EC, almost no change in hydraulic conductivity was observed compared to water permeation, even at different pH values. This is an indicator of the efficiency of the GCL at this range. Even though at EC = 1011 mS/m, an increase of one order of magnitude in the hydraulic conductivity was observed, this values is low enough to be used in rock containments facilities.

The hydraulic conductivity of zeolite permeated with water was 3.0×10^{-10} m/s, while when permeated with ARD 747 (the most severe case of this study), 1.4×10^{-9} m/s. Similar to GCL, a 1 order of magnitude increment in the hydraulic conductivity was observed for the most severe ARD case. Moreover, the hydraulic conductivity of ferrihydrite was the highest among the three minerals with a hydraulic conductivity value of 7.3×10^{-9} m/s in the case of permeation with water. This value remained constant after ARD 747 (the most severe case presented in this research) permeation, with a value of 8.6×10^{-9} m/s.

The swell index of bentonite, which is the only material among the three materials that shows swelling capacity, was also studied in this section. The swelling test is a simple test that provides important information about the hydraulic conductivity. If the swell volume is high, the clay layers tend to expand and, thus, it is more difficult for the liquid to flow through the material. As a result, the hydraulic conductivity is very low. The swell index of the water was around 33 mL/2 g bentonite and this value tends to decrease as the pH decreases or the EC increases. The lowest swell index observed was 8.5 mL/2g bentonite, for ARD 747 (most severe case of ARD).

A possible exponential relationship was obtained between EC and swell index and between EC and hydraulic conductivity. Besides, a relationship between hydraulic conductivity and swell index was observed for GCL. An equation for the relationship between swell index and hydraulic conductivity was first proposed by Katsumi et al (2007) for GCL against alkaline metals. This was adjusted for ARD cases according to the experimental values and the difference between the predicted hydraulic conductivity values and the real ones decreased from 60 – 76% to 0.9 – 19.2%.

Several factors that affect the hydraulic performance of GCLs against ARD were also studied. The effect of prehydration over non-prehydration, the effect of short and long term experimental tests, and the effect of type of bentonite was also studied. It was observed that the hydraulic conductivity of GCL prehydrated with water was 5 times lower than the non-prehydrated case which suggests that a prehydration of GCL before field application is beneficial. Long term experimental results were important and necessary to conduct in order to guarantee long term performance in the field. It was observed that, after 300 PVF of ARD permeation, the hydraulic conductivity of GCL started to decrease due to the precipitation of metals present in ARD. Precipitation was possible in the case of GCL because the low

hydraulic conductivity favors precipitation to occur. After a 9-month experiment, the GCL was removed and orange-red precipitation was observed which confirms the precipitation of iron. The effect of the type of bentonite was studied in comparison with previous research. This research was focused only on powdered bentonite whereas previous research related to GCL-ARD were conducted using granular bentonite. For granular bentonite, an increase up to three orders of magnitude in the hydraulic conductivity using an ARD with ionic strength of 356 mM was observed. In this research, only a one order of magnitude increase in the hydraulic conductivity for an ARD with 504 mM of ionic strength was observed.

Among the three materials tested in this research against ARDs, GCL showed the best barrier performance with a hydraulic conductivity between 9.6×10^{-11} – 5.0×10^{-10} m/s. Besides, considering that GCL is a commercial material that is easy to transport and install, it can be suitable for bottom liners in rock containment facilities. However, zeolite and ferrihydrite also showed a good performance against ARD, with hydraulic values of 1.4×10^{-9} m/s and 8.6×10^{-9} m/s respectively. After establishing a proper thickness for these two materials, they can also be successfully used as absorption layer for rock containment facilities.

5 CHEMICAL COMPATIBILITY OF MINERAL BARRIERS AGAINST ACID ROCK DRAINAGE

5.1 General Remarks

This chapter seeks to provide a systematic and chemical study of the factors and mechanisms that lead to the metal retention and release from geosynthetic clay liners (GCLs) when permeated with acid rock drainage (ARD). For this purpose, the effluents of 10 ARDs after hydraulic conductivity were analyzed in terms of pH, electrical conductivity, and metal concentration. Moreover, single metal sorption test, bi-metal sorption test and sorption with ARD were conducted in order to understand the interactions between heavy metals and GCLs as well as competition among metals. The performance of GCL was compared to the chemical compatibility of zeolite and ferrihydrite.

5.2 Materials and Methods

5.2.1 Mineral Materials

The materials used were bentonite, zeolite, and ferrihydrite, which are mineral materials available in several countries that might be suitable for remediation techniques or barrier containments for rocks coming from construction or mining activities. While their performance has been investigated in previous research, they have not been studied under extreme conditions related to pH and heavy metal content.

5.2.1.1 Bentonite

The bentonite used for the tests was obtained from a needle-punched GCL (Bentofix® NSP 4900). This GCL contains powdered sodium bentonite sandwiched between woven and non woven geotextiles, with a unit mass of 4670 g bentonite/m^2. Bentonite contained in this GCL had a water content of approximately 10.0%, a specific gravity of 2.85, and a smectite content of 80%. Before tests, bentonite was ground to 100% passing a 100 mesh US. Standard Sieve with a minimum of 65% passing a 200 mesh US. Standard Sieve and then dried for 24 hours in a drying oven at 105±5 °C. After bentonite was dried to constant mass, it was allowed to cool to room temperature in a desiccator.

5.2.1.2 Zeolite

Zeolite was provided by Mitsui Mineral Development Engineering Co., Ltd. (MINDECO) and had a particle size of 0.5 mm sieve pass. It was dried for 24 hours in an oven at 105±5 °C before conducting the experiments, and after being dried to constant mass, it was allowed to cool to room temperature in a desiccator and kept there until it was used.

5.2.1.3 Ferrihydrite

The ferrihydrite, FeO(OH) was a commercial powder material obtained from Nacalai Tesque. Before

conducting the tests, ferrihydrite was dried for 24 hours in a drying oven at 105±5 °C. After being dried to constant mass, it was allowed to cool to room temperature in a desiccator and kept there until it was used.

5.2.2 Heavy Metal Solutions

Species investigated in this study include Fe^{2+}, Al^{3+}, Cu^{2+}, Zn^{2+}, $HAsO_4^{2-}$, and Pb^{2+}, which are common metals present in ARDs. Different commercial sources of these metals were investigated in order to choose the proper substance. Considering that ARDs usually contain sulfate ions in their composition, most of the solutions were prepared by using the sulfate specie: $FeSO_4$, $Al_2(SO_4)_3$, $CuSO_4$, and $ZnSO_4$. However, in case of As, the pentavalent salt ($Na_2HAsO_4 \cdot 7H_2O$) was used, and in case of Pb, the NO_3 specie was used ($PbNO_3$) as it has higher solubility than the sulfate or chloride compound. However, in some cases, $PbCl_2$ was also used.

5.2.3 Single Metal Solutions

Single metal solutions were used for time step batch sorption tests on bentonite, zeolite and ferrihydrite. They were prepared by dissolving $FeSO_4 \cdot 7H_2O$, $Al_2(SO_4)_3 \cdot 8H_2O$, $CuSO_4$, $ZnSO_4 \cdot 7H_2O$, $Na_2HAsO_4 \cdot 7H_2O$, or $PbNO_3/PbCl_2$, in distilled water according to Table 5-1. Six different concentrations ranging from 1 μM to 100 mM (2 μM to 200 mM in case of Al) were prepared: 1 μM, 10 μM, 100 μM, 1mM, 10 mM, and 100 mM (2 μM, 20 μM, 200 μM, 2mM, 20 mM, and 200 mM in case of Al).
The pH of all the solutions was adjusted to either 3 by adding H_2SO_4, or to 8 by adding NaOH. The pH 3 solutions, which simulate the acidic condition observed in most ARD cases, were used in case of

Table 5-1 Solution preparation

Target metal	Metal source	Metal concentration
Fe	$FeSO_4 \cdot 7H_2O$	1 μM, 10 μM, 100 μM, 1 mM, 10 mM, and 100mM
Al	$Al_2(SO_4)_3 \cdot 8H_2O$	2 μM, 20 μM, 200 μM, 2 mM, 20 mM, and 200mM
Cu	$CuSO_4$	1 μM, 10 μM, 100 μM, 1 mM, 10 mM, and 100mM
Zn	$ZnSO_4 \cdot 7H_2O$	1 μM, 10 μM, 100 μM, 1 mM, 10 mM, and 100mM
As	$Na_2HAsO_4 \cdot 7H_2O$	1 μM, 10 μM, 100 μM, 1 mM, 10 mM, and 100mM
Pb	$PbNO_3/PbCl_2$	1 μM, 10 μM, 100 μM, 1 mM, 10 mM, and 100mM

bentonite and zeolite. However, in case of ferrihydrite, all the experiments were conducted at pH 8 due to the stability of this material at high pH.

5.2.4 Bi-metal Solutions

Bi-metal solutions were used for conducting sorption test and swelling test on bentonite. For the bi-metal solutions, 2 mM solution of each metal was prepared separately and, then, the same volume of two of them were combined (50 mL), according to the pair of metals specified and marked with O in Table 5-2.

In order to evaluate the role of a second metal in As retention, sorption tests were conducted with bi-metal solutions; 1 mM solution of As was tested against 0.01, 0.1, 1, 10, and 100 mM of each metal. The total volume of the solution was 50 mL in each case and 0.1 g of bentonite was added and placed on a shaking table at 100 rpm for 24 hours at 20 ^{o}C. After this period, the mixture was centrifuged and filtered through a filter with a 0.45-μm pore size. The concentration of Fe, Cu. Zn, Al, As, Pb, Na, Ca, Mg, and K before and after the sorption tests were analyzed by ICP (ICPS- 800 Shimadzu).

5.2.5 Artificial ARD Solutions

Similar to the description presented in Chapter 4, artificial ARD solutions were prepared by mixing $FeSO_4 \cdot 7H_2O$, $Al_2(SO_4)_3 \cdot 16H_2O$, $CuSO_4 \cdot 5H_2O$, $ZnSO_4 \cdot 7H_2O$, $Na_2HAsO_4 \cdot 7H_2O$, $PbNO_3/PbCl_2$, K_2SO_4, Na_2SO_4, $CaSO_4$, and $MgSO_4$, all GR grade (Guaranteed Reagent) provided by Nacalai Tesque. The pH was adjusted either by using NaOH or H_2SO_4. After mixing the chemicals in the proportion specified in Table 5-3 (target concentration), precipitation was observed and therefore, it was necessary to filter the mixture before conducting experiments. The concentration of each metal in solution was measured by ICP (ICPS – 800 Shimadzu) and reported as real concentration.

Table 5-2 Bi-metal solution combinations

	Cu	Fe	Zn	Al	As	Pb
Cu	×	○	○	○	○	○
Fe	○	×	○	○	○	○
Zn	○	○	×	○	○	○
Al	○	○	○	×	○	○
As	○	○	○	○	×	○
Pb	○	○	○	○	○	×

○: Performed

×: Not performed

Table 5-3 Metal concentration of elements present in the artificial ARD

	ARD 248	ARD 406	ARD 625	ARD 512	ARD 747	ARD 718	ARD 684	ARD 222	ARD 220	ARD 246
Na	9.76	0.00	23.58	14.24	45.54	9.76	140.78	386.61	327.07	35.43
Mg	96.94	0.00	168.15	0.03	230.89	96.94	292.13	87.10	180.67	0.13
Al	0.10	0.01	24.33	123.63	272.42	0.10	12121.44	0.18	0.16	0.47
K	6.04	0.29	4.01	1.07	31.50	6.04	6.07	16.10	11.37	11.50
Ca	79.07	0.00	157.88	0.02	448.01	79.07	321.05	325.11	298.14	807.64
Fe	1304.02	1.87	777.76	1598.44	4591.14	1304.02	94128.81	1.02	0.03	0.00
Cu	12.02	0.95	0.98	0.08	96.33	12.02	9762.40	0.00	0.00	0.00
Zn	133.40	5.00	64.86	70.04	536.37	133.40	4.81	0.11	0.00	0.00
As	0.65	0.15	0.72	9.59	1.85	0.65	1.13	0.30	0.36	0.40
Pb	0.28	0.00	0.26	0.55	2.30	0.28	0.27	0.16	0.14	0.20

Unit: mg/L

5.2.6 Sorption Tests

Sorption test were conducted using single metal, bi-metal, and ARDs, as shown in Table 5-4.

Table 5-4 Summary of the performed sorption tests

Type of solution	Type of test	Sorbent	Preparation	Evaluation purpose
Single metal	Time step batch sorption test	Bentonite Zeolite Ferrihydrite	0.1 g in 50 mL 4 to 80 g bentonite/L	Time to reach equilibrium Sorption capacity of minerals
Bi-metal	24 hour test	Bentonite	0.1 g in 50 mL	Metal competition Role of second metal on As retention
Natural ARD	Time step batch sorption test (5 cases), and 24 hour test (all cases)	Bentonite Zeolite Ferrihydrite	0.1 g in 50 mL	Sorption capacity of minerals against complex metal solutions
Artificial ARDs: ARD 248, 406, 625, 512, 747, 718, 684, 222, 220, and 246	24 hour test	Bentonite	0.2 to 1g in 50 mL	Sorption capacity of bentonite against complex metal system and low pH

In case of single metals, time step batch sorption tests provided information about the time to reach equilibrium, the chemical performance of the mineral materials (bentonite, zeolite, and ferrihyrdite) against different metals and metalloids, as well as the mechanism involved. Twenty four-hour sorption tests using bi-metal combinations gave information about competition between metals as well as the role of a second metal on As sorption. Sorption tests using ARDs were performed to evaluate real cases and evaluate the performance of these minerals when exposed to several conditions of pHs and heavy metal concentrations and judge whether bentonite, zeolite, and ferrihydrite can be used in rock waste containments.

5.2.6.1 Time Step Batch Sorption Test

Time step batch sorption tests were performed for single metals and ARDs. Experiments were performed by mixing 0.1 g of sorbent with 50 mL of single metal solution (the concentration of each solution was described in section 5.2.5) in a 100 mL plastic bottle with cap. Samples were taken after 1, 3, 6, 12, and 24 hours of shaking on an incubator shaker at 100 rpm and 25 ºC. In addition, two blanks were prepared: the first one before the addition of sorbent, which corresponds to 0 hour sorption; and the other one, after 24 hours of shaking but without sorbent, to evaluate if sorption on the plastic bottle occurs. After shaking, each mixture was centrifuged and filtered using a 0.22 μm filter. The concentration of Fe, Cu. Zn, Al, As, Pb, Na, Ca, Mg, and K before and after the sorption tests were analyzed by ICP-MS (Agilent 7500ce). A picture of the experiment procedure is presented in Figure 5-1, where (a) solution preparation, (b) solution pouring into plastic vessels, (c) sorbent addition, (d) shaking, (e) centrifuge, (f) filtration, (g) pH, EC, and ORP measurement, and (h) ICP analysis.

5.2.6.2 Batch Sorption Test with Artificial ARDs

Sorption tests with 10 artificial ARDs were performed for bentonite and one test using the most severe ARD case (ARD 747) was performed for zeolite and ferrihydrite. Two types of sorption tests using the ARDs (Table 5-3) were performed. In one of them, different amount of bentonite was used (from 4 to 80 g bentonite/L solution) and in the other, different dilutions of the ARD (from 2 to 100%) were tested using the same amount of bentonite (20 g bentonite/L solution). The experiments were conducted in 100 mL plastic bottles with cap and the volume of the solution was fixed to 50 mL in all cases. Once the bentonite was added into the solution, the mixture was placed on the shaking table at 100 rpm for 24 hours, at 25ºC. After this period, the mixture was centrifuged and filtered using a 0.45 μm filter. The concentration of metals before and after the sorption tests were analyzed by ICP (ICPS – 800 Shimadzu).

5.2.6.3 Bi-metal Batch Sorption Test

Bi-metal sorption tests were conducted for bentonite. After the addition of 0.1 g of this mineral into 50 mL of the bi-metal solution (contained in a 100 mL plastic bottle with hermetic cap), the sample was placed on the shaking table at 100 rpm for 24 hours. After this period, the mixture was centrifuged and filtered using a 0.45 μm filter. The concentration of Fe, Cu. Zn, Al, As, Pb, Na, Ca, Mg, and K before and after the batch sorption tests were analyzed by ICP (ICPS – 800 Shimadzu).

a Solution preparation

b 50 mL of solution in 100 mL plastic bottle

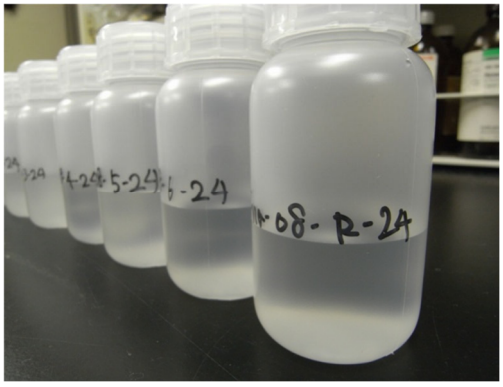

c Mineral addition into the solution

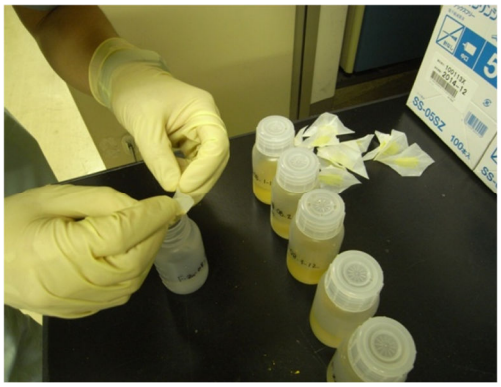

d Shaking at 100 rpm

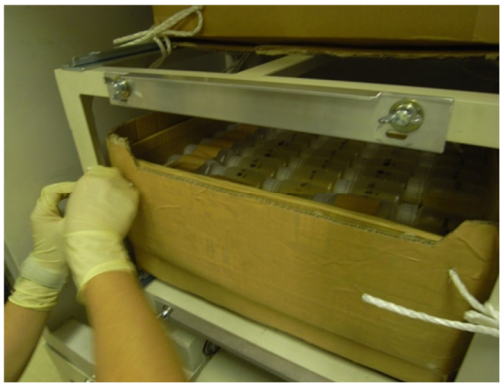

e Centrifuge

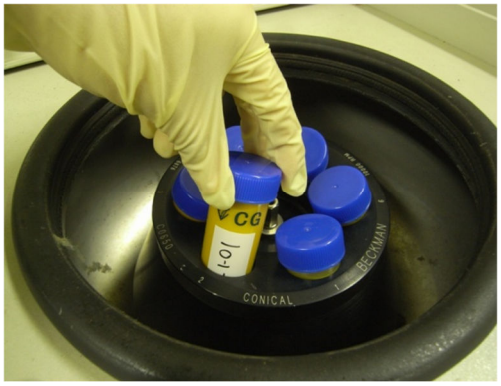

f Filtration

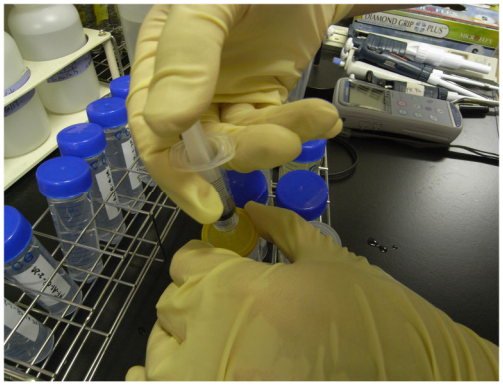

g EC, pH and ORP measurement

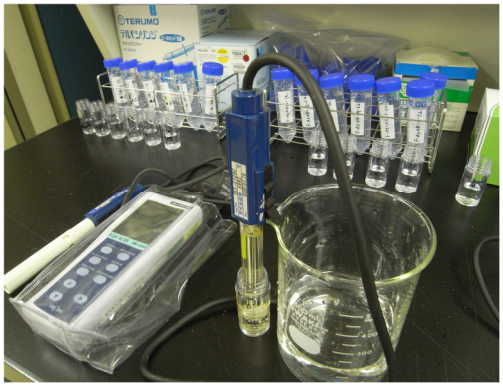

h Metal concentration measurement by ICP

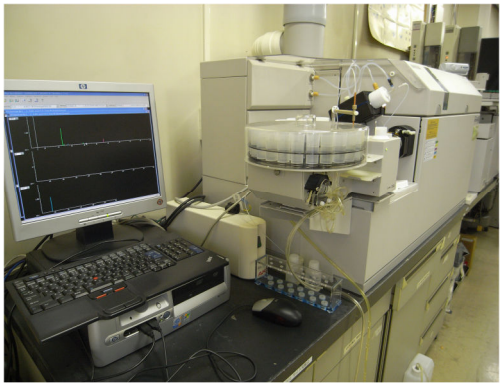

Figure 5-1 Steps for sorption test

5.3 Single Metal Sorption Test Results for Bentonite

The pH, EC, and ORP for each metal, concentration, and time were measured. From the pH versus time graph (Figure 5-2, Left), information about the change in pH was obtained. Before adding the sorbent into the solution (t=0), the pH was 3 (initial pH) but, after some time of being in contact with bentonite, it rose from 1 to 5 units. This suggests that sorption of H^+ may preferably occur, or that the solution turns alkaline because of the release of Na, Ca, Mg, and K from bentonite. In addition, it can be inferred that, due to the change in pH, precipitation of metals may occur in some cases.

From the EC versus time graph (Figure 5-2, Right), information about the amount of species in solution was obtained. In case of ORP, two types of graphs are presented. The first is the change of ORP versus time (Figure 5-3, Left) and the second the change of ORP versus pH (Figure 5-3, Right). From the last graph it is possible to see what specie is present in the solution under given condition. The graphs for Cu are presented in this section only as an example. The rest of the graphs are shown in Appendix B.

Metal sorption capacity of bentonite over time is shown in Figure 5-4 to Figure 5-6. It was observed that at high metal concentrations (100 and 10 mM) only a very small decrease in concentration can be detected and, thus, no important change over time was perceived (Figure 5-4). On the other hand, at very low metal concentration (1, 10, and 100 µM) metal sorption onto bentonite was almost immediate with no further change over time observed. At intermediate metal concentration (1 mM) a gradual decrease in metal concentration was observed over time. From Figure 5-5 (Left) it can be concluded that, in most of

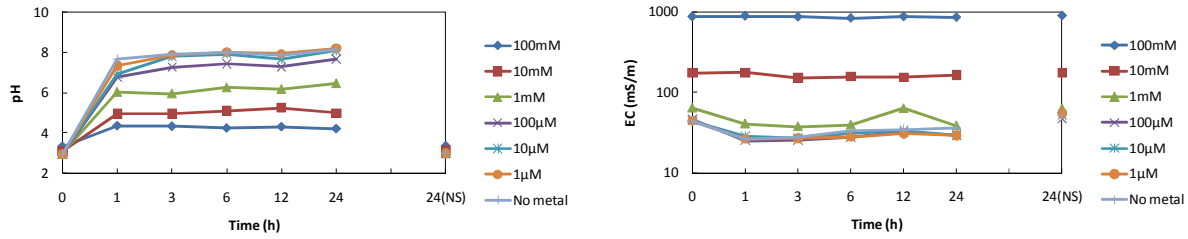

Figure 5-2 Bentonite-Cu system Left: Change of pH versus time; Right: Change of EC over time

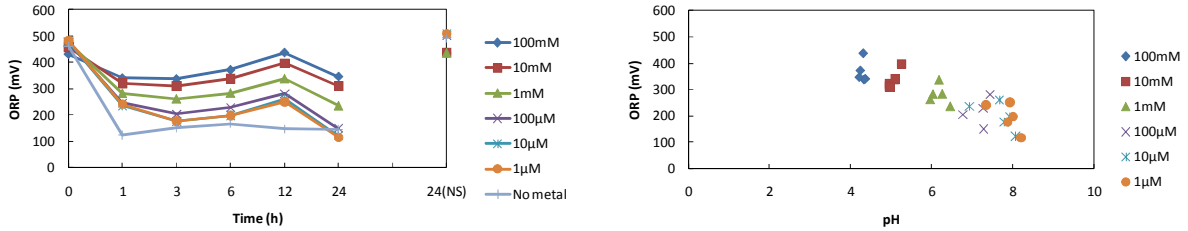

Figure 5-3 Bentonite-Cu system Left: Change of ORP over time; Right: Relationship ORP-pH

the cases, the equilibrium was reached after 1 to 6 hours. In addition, from the same figure it can be inferred that Fe was preferably sorbed onto bentonite (almost 100% sorbed), followed by Cu and Al (around 75% sorbed) and the less sorbed ion was Zn (40% sorbed).

Na, Ca, Mg, and K quantities were also investigated. Six graphs were created for each metal and for each metal concentration. The pattern of most of them was similar to the one presented in Figure 5-7 to Figure 5-9 for bentonite-Zn system. Therefore, the graphs for all sorbent-metal systems are not shown in this section, but in Appendix E.

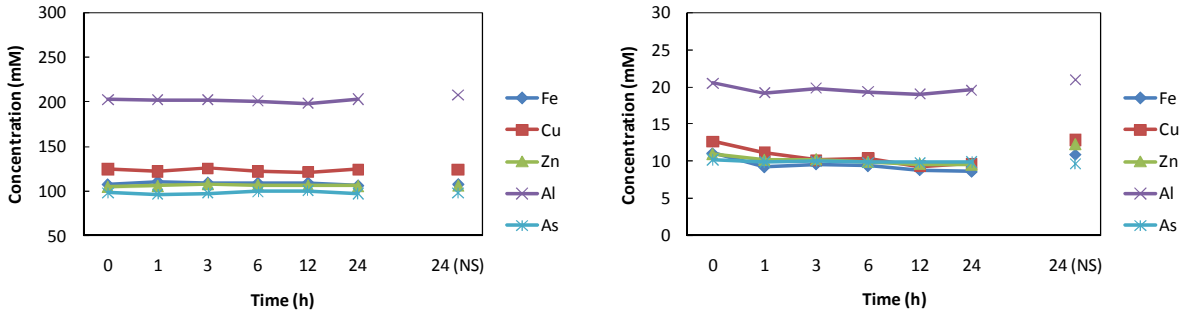

Figure 5-4 Metal sorption on bentonite Left: 100 mM; Right 10 mM

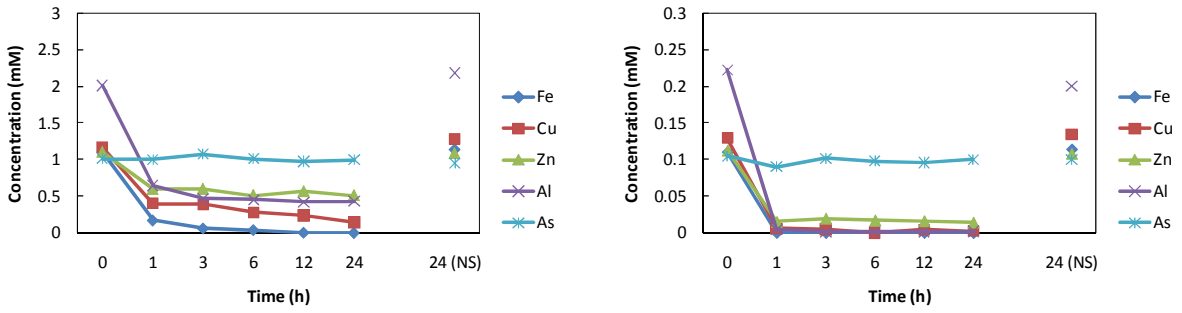

Figure 5-5 Metal sorption on bentonite Left: 1 mM; Right 100 µM

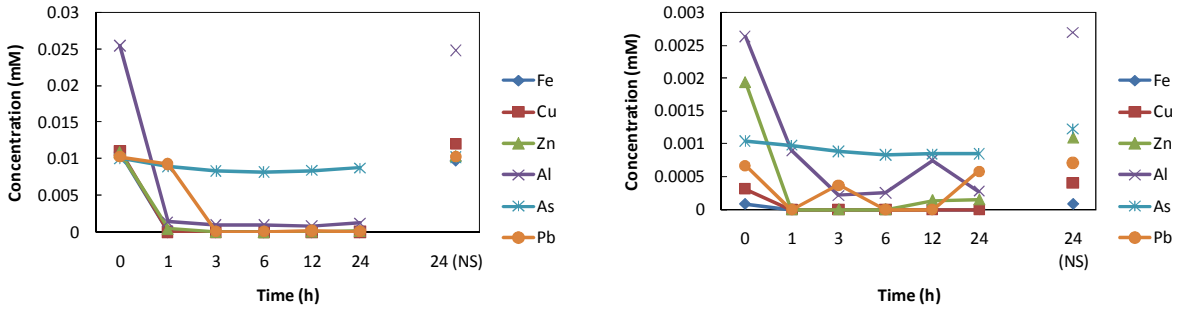

Figure 5-6 Metal sorption on bentonite Left: 10 µM; Right 1 µM

The six graphs presented in Figure 5-7 to Figure 5-9 correspond to each metal concentration (100 mM, 10 mM, 1 mM, 100 µM, 10 µM, and 1 µM) and from all of them, except Figure 5-7 (Left), the release of Na, Ca, Mg, and K over time was observed. This provides important information about the attenuation process of bentonite toward heavy metals and suggests that ion exchange is probably the mechanism that dominates in this case.

From all the measured parameters and collected data, graphs of sorbed amount per gram of bentonite versus equilibrium concentration (isotherm) were created. Figure 5-10 presents a plot of all the data points. However, for the highest concentrations, it was observed that, except in case of Al, the sorption amounts tend to decrease dramatically. Three reasons can be attributed to this phenomenon. The first one is probably due to the lower pH at high metal concentrations (Figure 5-2, Left). At low pH, the sorption amount is also low because of the competitive sorption resulting from the increasing concentration of H^+ (Hui et al. 2005). The second reason is probably because, for analyzing the concentration of this point by ICP (even after sorption), diluting by 1000 times was necessary, which raises the possibility of error. The third reason can be attributed to the ion strength (or initial metal concentration), which also affects the sorption amount. Therefore, in this case it can be said that highest selectivity or metal sorption occurred at certain point and after that, a significant reduction in sorption occurred because of a dramatic increase in the ion strength. The reason why the last point (highest concentration point) decreases dramatically is not well known, so it has been omitted and, thus, 5 points, as shown in Figure 5-11 are considered. According to this graph, the sorption capacity of bentonite towards these metals can be sequenced as follows:

$$Cu = Fe >> Zn > Al > As \tag{5.1}$$

The range of the determined sorption capacity was from 0.2 to 1.5 mmol/g bentonite, which will provide necessary information to the assessment of potential application of bentonite in water treatment.

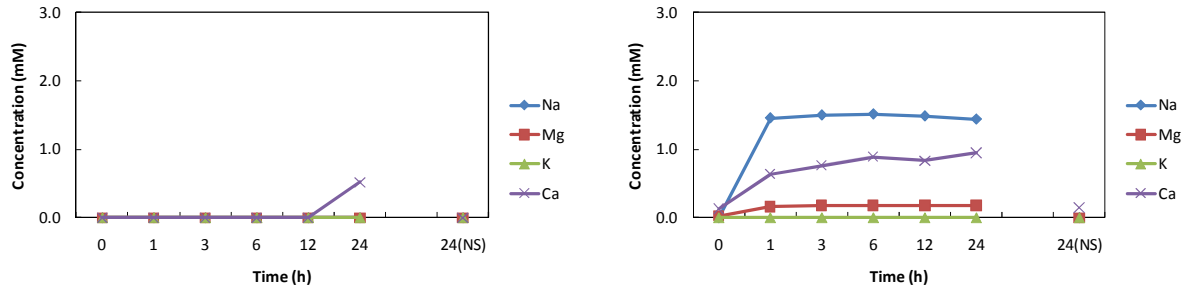

Figure 5-7 Na, Mg, K, and Mg concentration in bentonite-Zn system Left: 100 mM; Right 10 mM

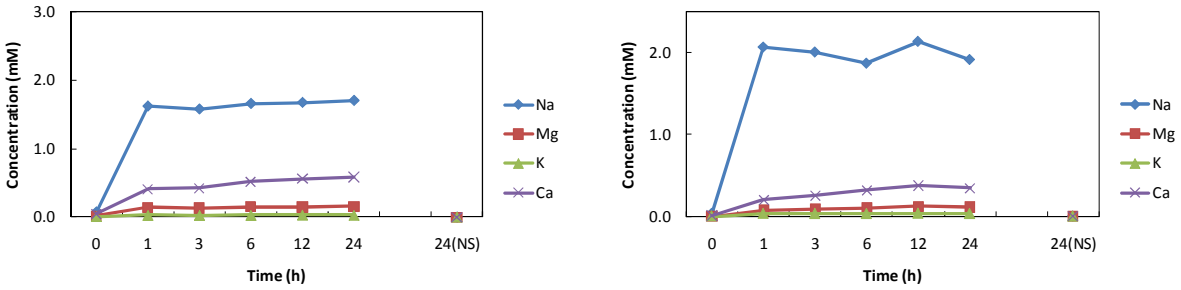

Figure 5-8 Na, Mg, K, and Mg concentration in bentonite-Zn system Left: 1 mM; Right 100 µM

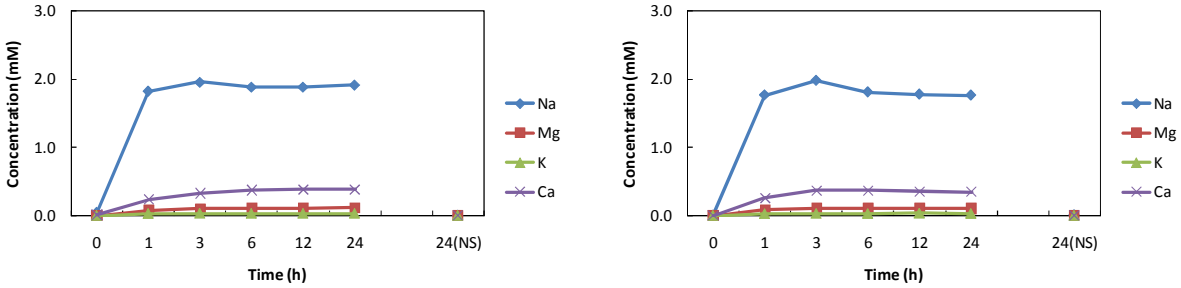

Figure 5-9 Na, Mg, K, and Mg concentration in bentonite-Zn system Left: 10 µM; Right 1 µM

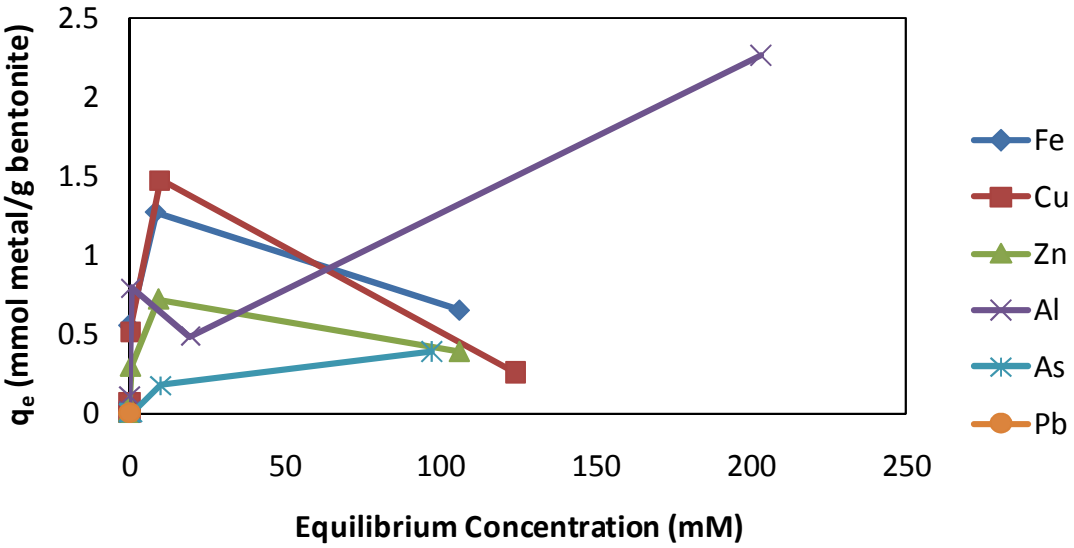

Figure 5-10 Isotherm of heavy metal sorption on bentonite

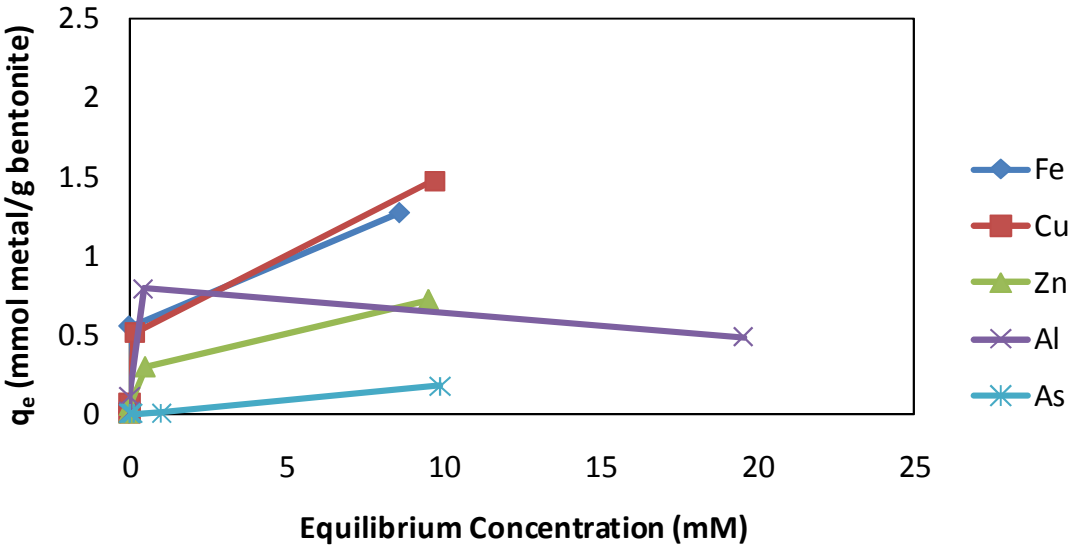

Figure 5-11 Isotherm of heavy metal sorption on bentonite (adjusted)

5.4 ARD Sorption Test Results for Bentonite

The presence of many cations (many with charges +2 or +3), complexing anions, and ligands, in rock leachates or acid rock drainage, often results in activities of metal ions different from what single metal sorption tests would suggest. In cation exchange, or non-specific adsorption, the adsorbent shows preference for certain ions, typically dependent on their valence, size, and degree of hydration. Therefore, it is important to evaluate metal sorption not only in presence of single metals, but when they are in combination such as bi-metal combinations or complex mixtures.

In the previous section, it was concluded that among the three minerals tested, bentonite showed better performance. So, it is worthwhile to conduct a thorough and long term evaluation of this mineral under more extreme conditions than those observed in the previous section.

In this section, the sorption capacity of bentonite contained in the GCL was tested against ten artificial ARDs in order to have better understanding of metal activities when they are in combination and, therefore, better explain which metals are preferably sorbed onto bentonite and what factors have greatest influence. Graphs in the left column indicate the sorbed ratio of Al, Fe, Cu, Zn, As, and Pb, whereas graphs in the right column show the sorbed ratio of Na, Mg, K, and Ca. From the graphs to the left, it can be said that, in general, at low ARD concentrations, 100% of metals are sorbed in bentonite. As the ARD percentage increases, the sorbed ratio of metals decreases. From the graphs to the right, occurrence of ion exchange is indicated by the observation of alkaline metals being released if originally present in the bentonite.

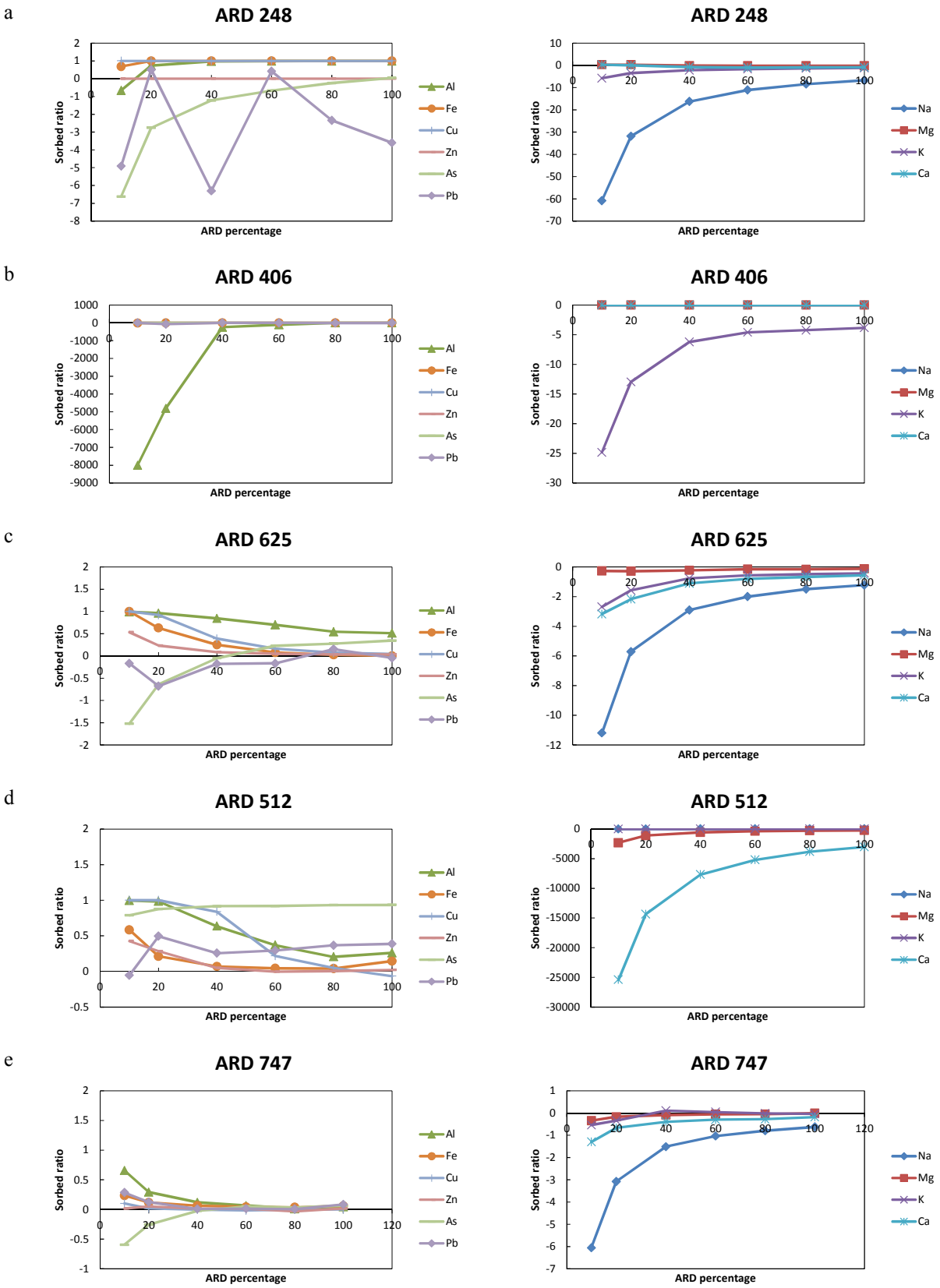

Figure 5-12 Sorption test results of 10 selected artificial ARDs

f

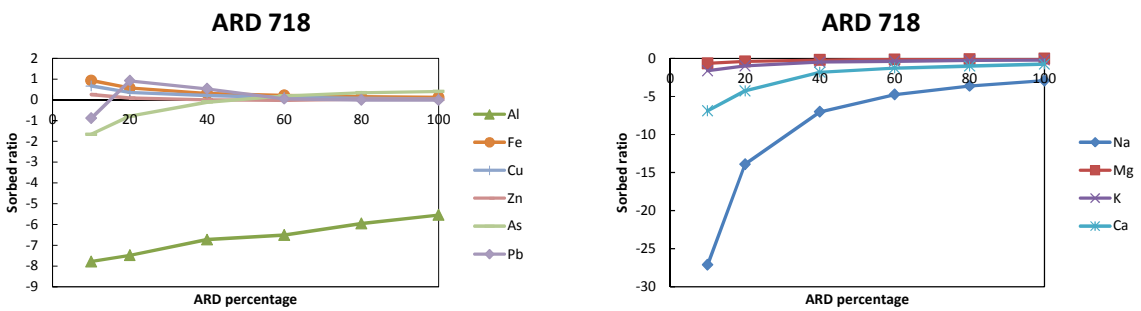

g

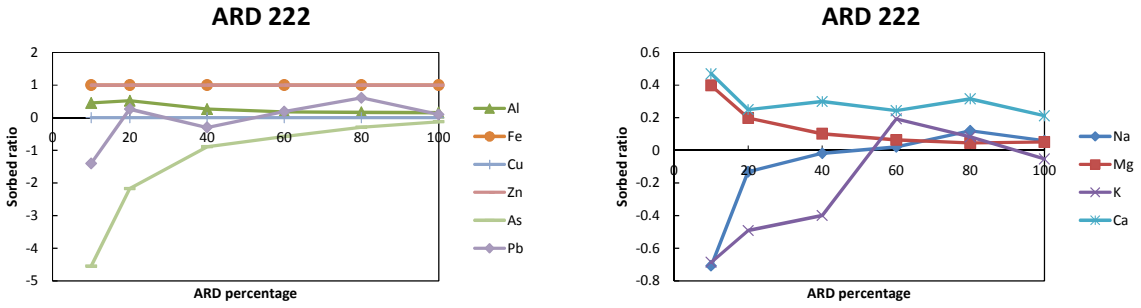

h

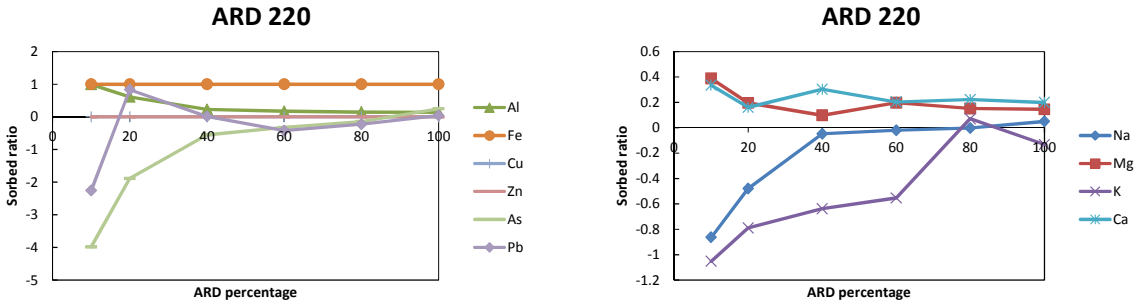

i

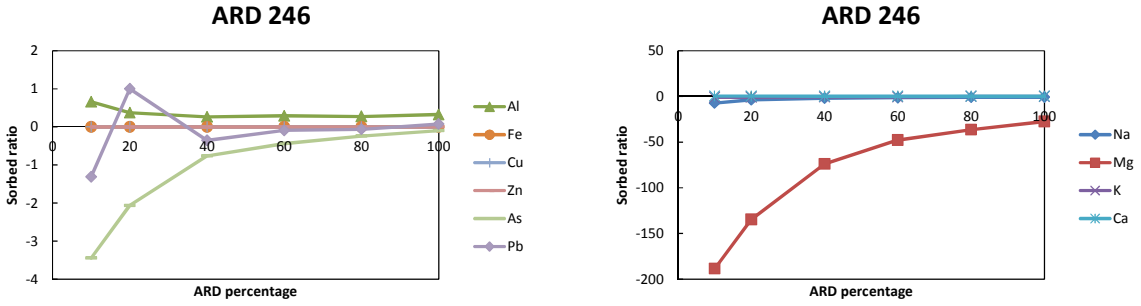

Figure 5 12 Sorption test results of 10 selected artificial ARDs (continued)

5.5 Effluent Analysis of the Hydraulic Conductivity Test for GCL

Figure 5-13 shows the pH, EC (left), and metal release (right) over time. In all ARD cases, except for ARD 747, it was observed that the pH was high (around 9) and the EC was decreasing over time (around 500 mS/m). For ARD 747, it was observed that the pH and EC reached equilibrium (around pH=3, EC=900 mS/m). There was no heavy metal release in all cases, except for ARD 747.

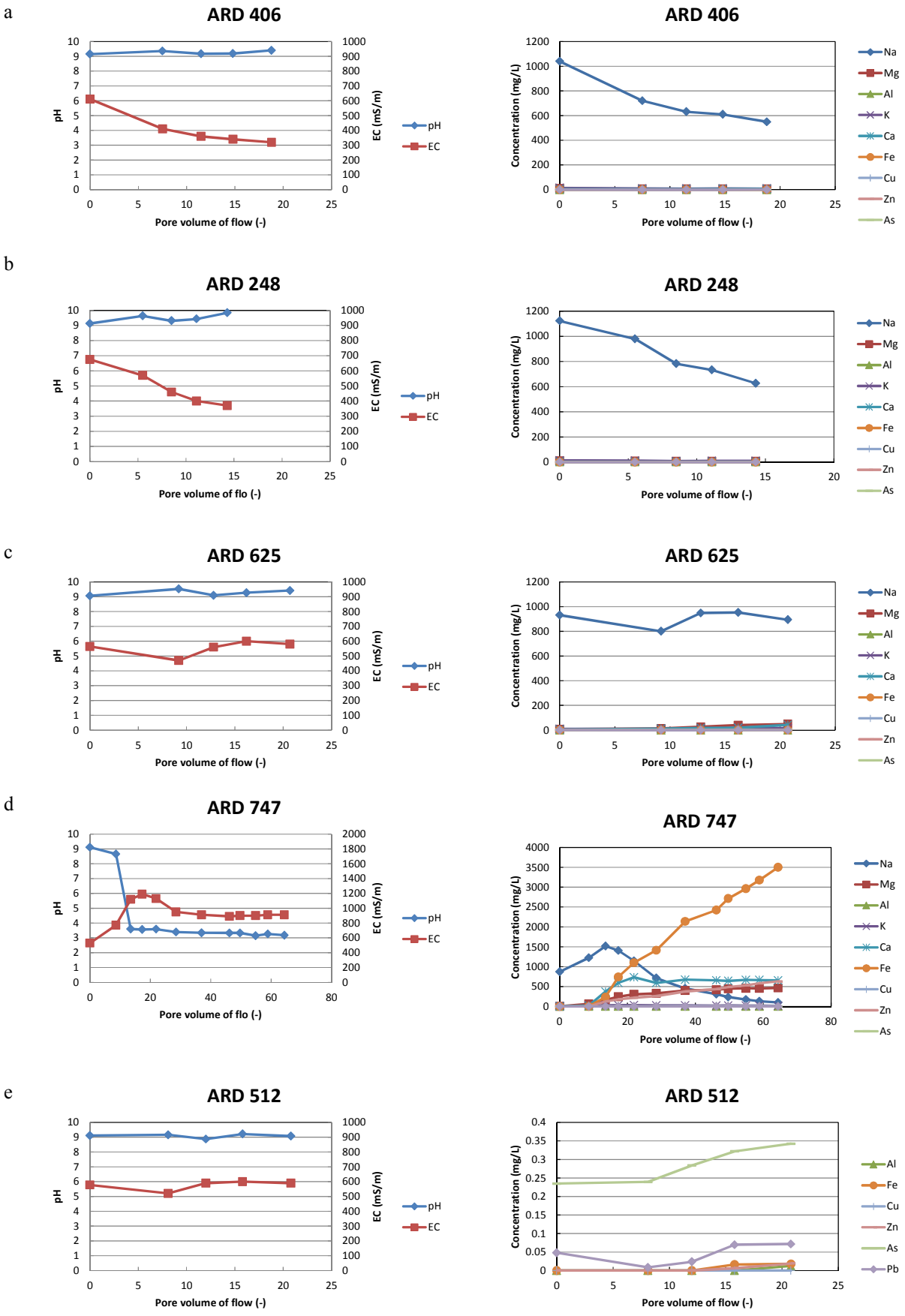

Figure 5-13 Effluent analysis of hydraulic conductivity tests: pH, EC and metal release over time

f

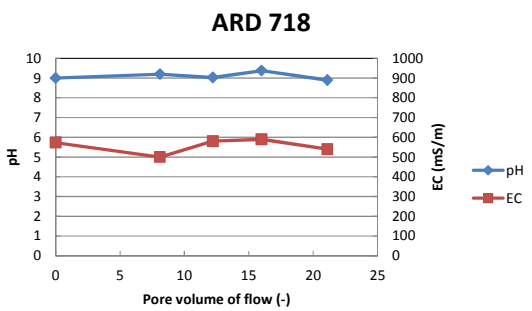

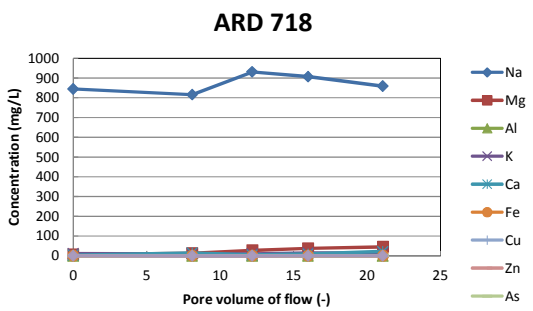

g

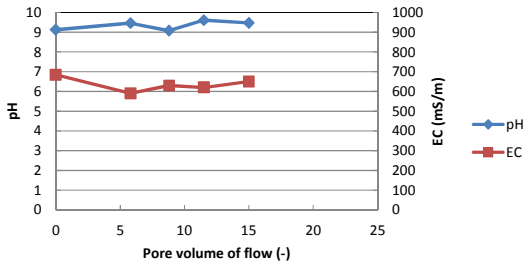

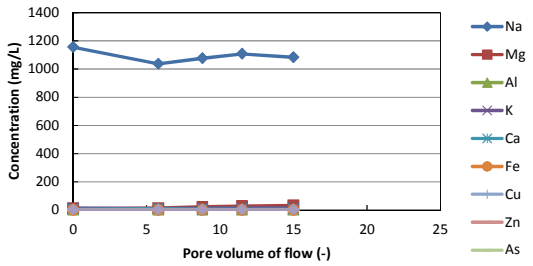

h

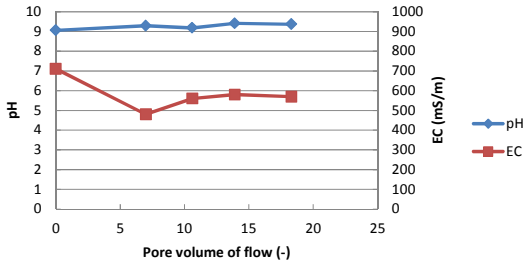

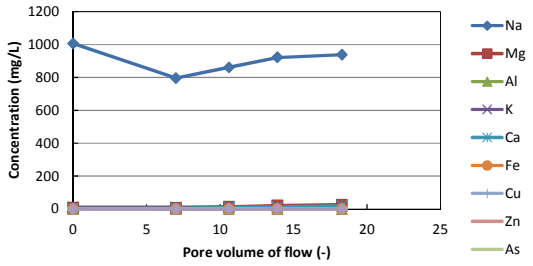

i

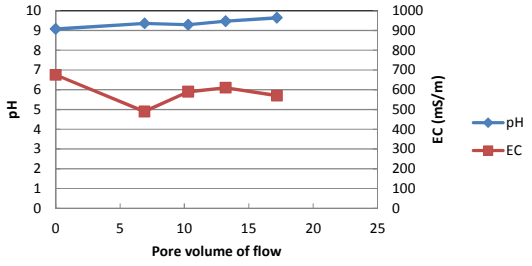

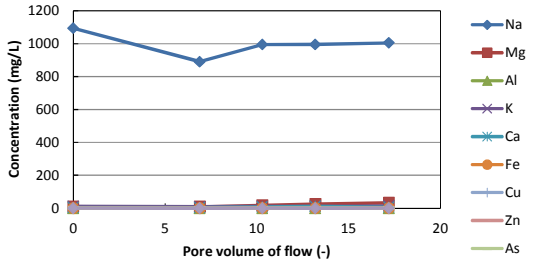

j

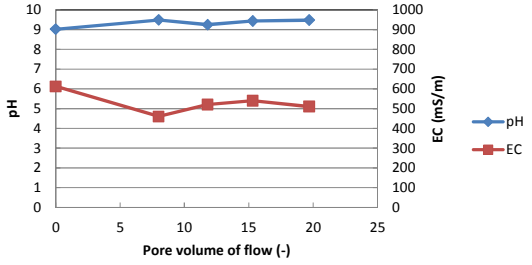

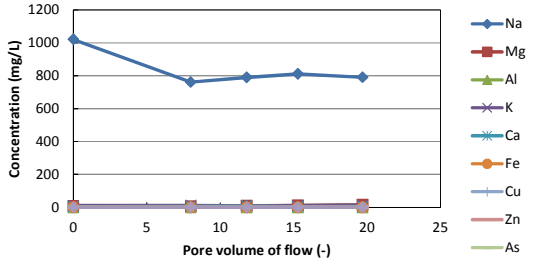

Figure 5-13 Effluent analysis of hydraulic conductivity tests: pH, EC and metal release over time (continued)

5.6 Sorption Test of Bentonite with Bi-metal Solutions

Sorption tests of bi-metal solutions provide information about the competition between metals. The concentration of each metal in the solution was 1 mM. The results of the sorption tests on bi-metal solutions are presented in Figure 5-14 to Figure 5-16 and show that some metals were more preferably sorbed than others and that the presence of a second metal affects the sorption capacity of the bentonite on the metal being studied. It can be inferred that Al is most preferably sorbed onto bentonite, followed by Fe, Pb, Cu, and Zn (Al > Fe > Pb > Cu > Zn). In case of As, an interesting phenomenon was observed. When the As is not in combination with other metals, the sorption onto bentonite is almost zero, but it is favored when a second metal is present. According to the results obtained and presented in Figure 5-16 (Left), Fe has greater influence on the As absorption, followed by Zn, Pb, Al, and Cu. It is probably that these metals favor the precipitation of As or the As is attached to these metals and then to the bentonite.

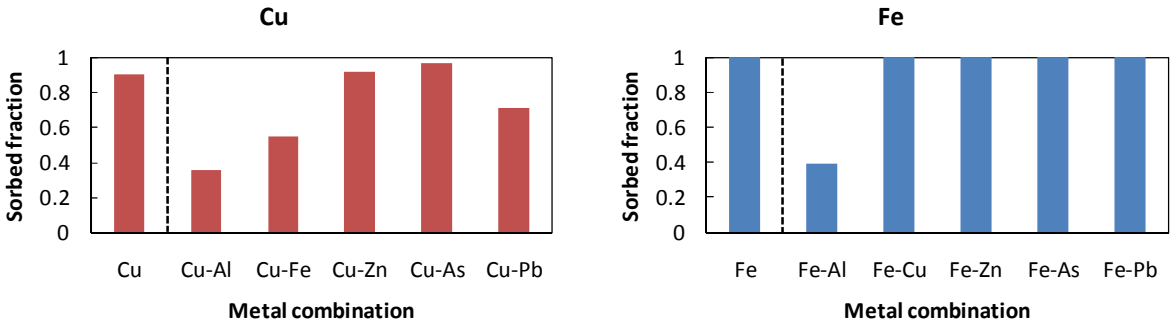

Figure 5-14 Sorption test of bi-metal solution Left: Copper; Right: Iron

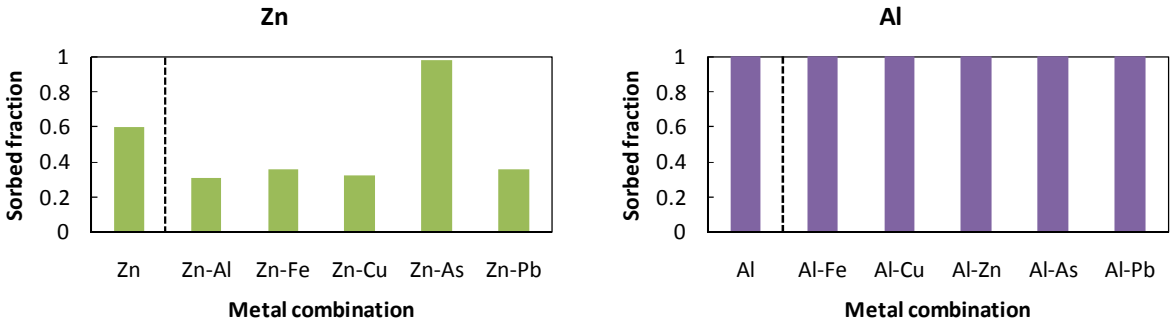

Figure 5-15 Sorption test of bi-metal solution Left: Zinc; Right: Aluminum

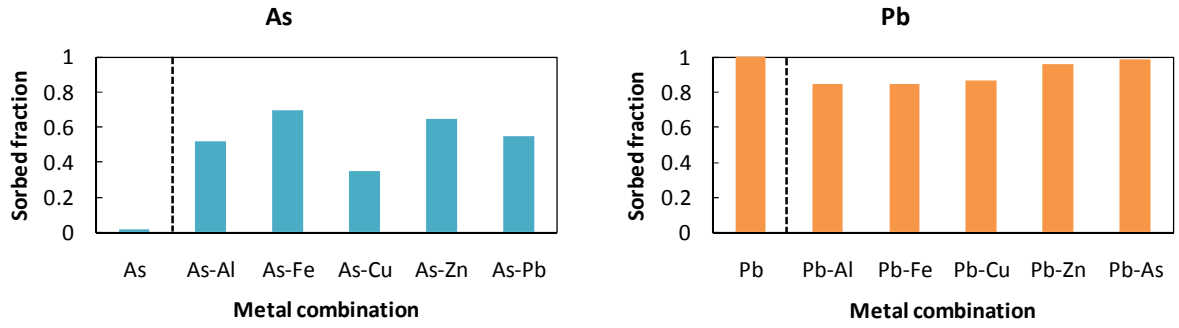

Figure 5-16 Sorption test of bi-metal solution Left: Arsenic; Right: Lead

5.6.1 Arsenic Retention in GCLs

Arsenic is a metalloid that, together with heavy metals, is commonly found in high concentrations in the tailings and sulfidic waters of gold, copper-gold, tin, lead-zinc, and some uranium ore mines (Lottermoser 2007). Mobilization of heavy metals is controlled by pH and Eh and occurs primarily in low pH and oxidizing environments, whereas, due to its significant difference in aqueous chemistry, arsenic is mobile over a wider pH range. Previous studies have shown the role of iron and calcium in arsenic mobilization control (Lange et al. 2010b), but there is no research on the effect of other metals present in ARD. To understand the behavior of As in the presence of other metals, single metal (from 1 μM to 100 mM), bi-metal (metal:As relationship 0.01:1, 0.1:1, 1:1, 10:1, and 100:1) sorption tests and sorption tests using an artificial ARD were conducted.

5.6.2 Role of Fe in As Sorption

In Figure 5-17a it can be seen that as the Fe concentration increases, the As sorption percentage increases which suggests that Fe positively impacts the As sorption. When the Fe is 10 times higher than the As it seems that it is able to sorb 100% of the As. Figure 5-17b shows the As behavior at different ARD 747 percentages and it seems that there is a relationship between Fe and As. In addition, Figure 5-17c shows the Fe and As concentration ratio from the effluent analysis of GCL permeated with ARD 747. It can be seen that the concentration ratio of As was kept at approximately 0.1 throughout the experiments. Although the sorption capacity of bentonite against As is very low or almost zero, the presence of other metals induce results that make it necessary to study the mechanism involved.

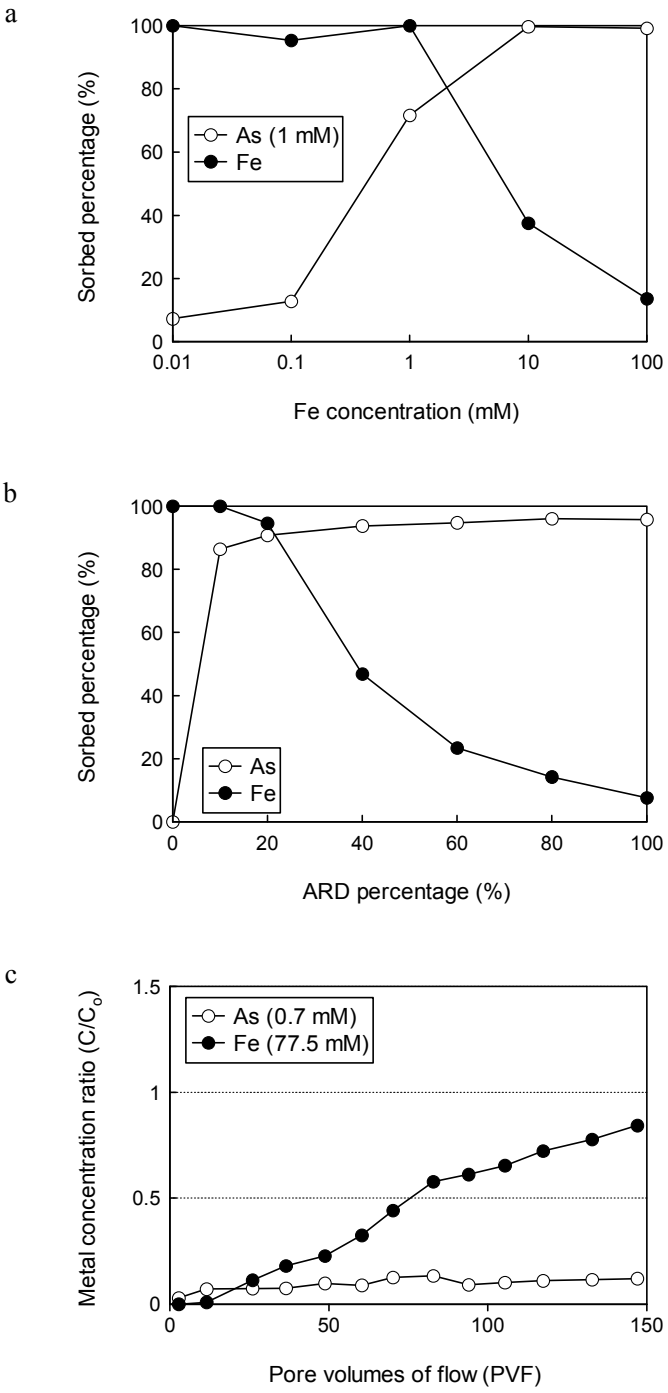

Figure 5-17 Role of Fe in As retention: a) bi-metal sorption, b) ARD sorption, c) effluent analysis

In case of Fe, the precipitation of Fe present in ARD and the subsequent sorption of As onto Fe is probably the main mechanism for As sorption. Considering that the Fe concentration in the artificial ARD 747 is 100 times higher than the concentration of As, it can be said that Fe is responsible for As sorption. Figure 5-18 shows a possible mechanism of the interaction between Fe and As and the role that iron plays in its immobilization.

(1) Iron hydroxide formation:

$$Fe^{2+} + 1/4O_2 + H^+ \rightarrow Fe^{3+} + 1/2H_2O \quad (5.2)$$

$$Fe^{3+} + 3OH^- \rightarrow Fe(OH)_3 \quad (5.3)$$

(2) Anion adsorption onto iron hydroxide:

$$\equiv Fe—wOH + A^{a-} + H^+ \rightarrow \equiv Fe—wA^{(a+1)-} + H_2O \quad (5.4)$$

$$\equiv Fe—wOH + A^{a-} \rightarrow \equiv Fe—wOA^{a-} \quad (5.5)$$

Figure 5-18 shows the possible pathways of As secondary sorption on bentonite, proposed by Davis et al. (1988). This illustrates both monodentate and bidentate bonding using arsente complexes.

5.6.3 Role of Cu in As Sorption

From Figure 5-19a, it can be seen that as Cu concentration increases, the As sorption percentage increases which suggests that Cu positively impacts the As sorption. When the concentration of Cu is 100 times higher than the concentration of As, it seems that it is able to sorb 60% As. Figure 5-19b shows the As behavior at different ARD 747 percentages and it seems that there is a relationship between Cu and As. At lower ARD percentage, the sorption of As is around 85% and it slightly increases as the ARD percentage (or, which is equivalent, metal concentration) increases.

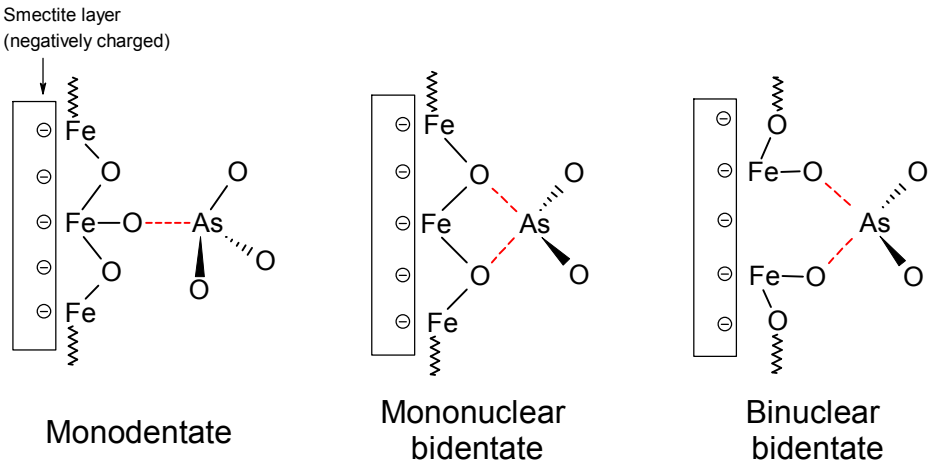

Figure 5-18 Possible pathways of As secondary sorption (sorption on Fe) on bentonite

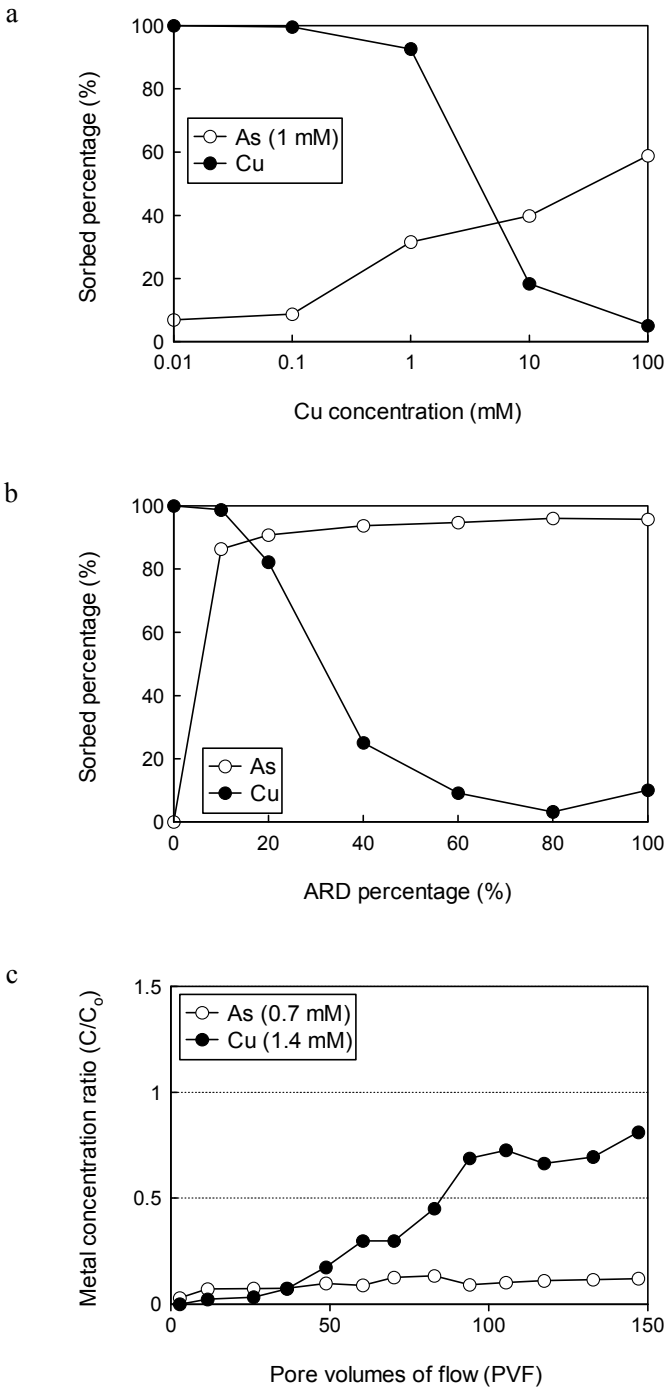

Figure 5-19 Role of Cu in As retention: a) bi-metal sorption, b) ARD sorption, c) effluent analysis

In addition, Figure 5-19c shows the Cu and As concentration ratio from the effluent analysis of GCL permeated with ARD obtained in the author's previous research. It can be seen that the concentration ratio of As was kept at approximately 0.1 throughout the experiment. Considering that the concentration of Cu in the artificial ARD is 2 times higher (Cu = 1.4 mM, As = 0.7 mM) than the concentration of As, it can be inferred that Cu is probably responsible for 40% of As sorption at most.

5.6.4 Role of Al in As Sorption

From Figure 5-20a, at concentrations lower than 10 mM it can be seen that as the Al concentration increases, the As sorption percentage increases which suggests that Al positively impacts As sorption. At 10 mM Al, the percentage of As sorbed becomes 80%. However, when the Al is 100 times higher than the As it is probable that polynuclear complexes of Al form and therefore there is no available binding site for As. Figure 5-20b shows the As behavior at different ARD 747 percentages and it seems that there is probably a relationship between Al and As.

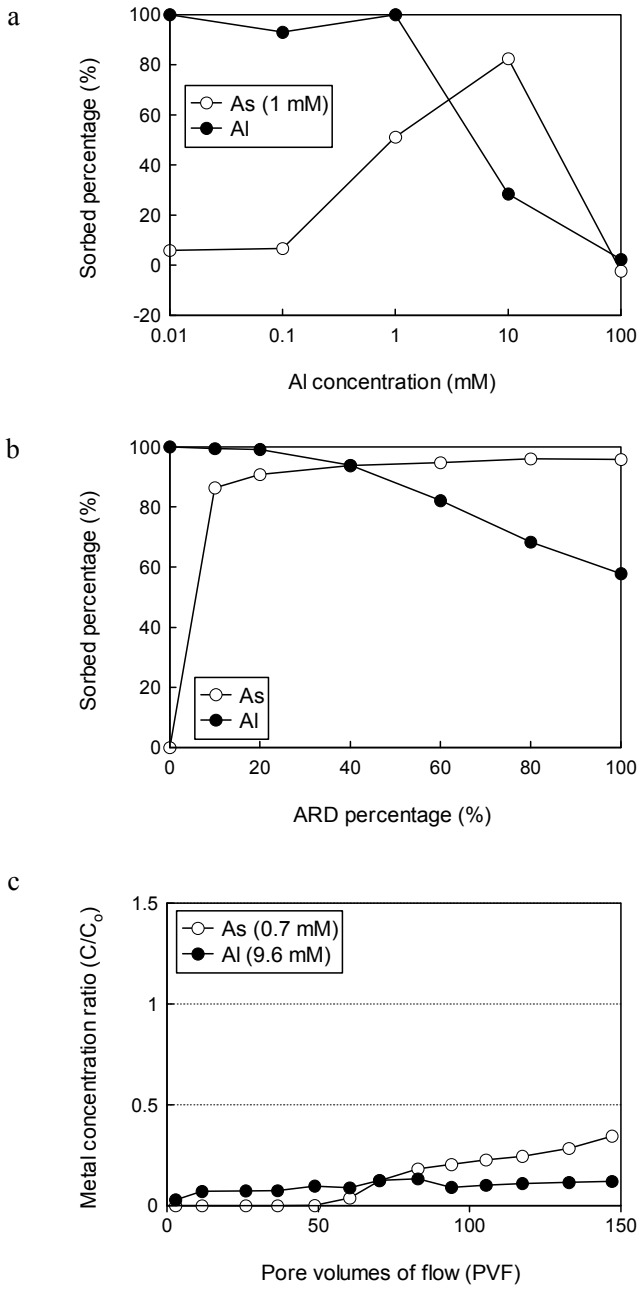

Figure 5-20 Role of Al in As retention: a) bi-metal sorption, b) ARD sorption, c) effluent analysis

In addition, Figure 5-20c shows the Al and As concentration ratio from the effluent analysis of GCL permeated with ARD 747. It can be seen that the concentration ratio of As was kept at approximately 0.1 throughout all the experiment. Considering that the concentration of Al in the artificial ARD is around 10 times higher than the concentration of As, it can be inferred that the As is probably responsible for 80% of As sorption at most.

Younger at al. (2002) report that mine waters with pH less than 4 commonly contain high concentrations of Al (>10 mg/L or 0.4 mM) while waters with pH between 5 and 8 generally have dissolved Al at less than 1 mg/L (or 0.04 mM). At certain pHs, the formation of Al hydroxide will occur, which is probably responsible for As retention. The solid resulting from the following reaction typically forms a white precipitate which is commonly amorphous.

$$Al^{3+} + 3H_2O \rightarrow Al(OH)_3 + 3H^+ \quad (5.6)$$

5.6.5 Role of Zn in As Sorption

From Figure 5-21a, at concentrations lower than 10 mM it can be seen that as the Zn concentration increases, the As sorption percentage increases which suggests that Zn positively impacts on As sorption. At 10 mM Zn, 100% of As is sorbed. Figure 5-21b shows As behavior at different ARD 747 percentages and it seems that there is probably a relationship between Zn and As. In addition, Figure 5-21c shows the Zn and As concentration ratio from the effluent analysis of GCL permeated with ARD 747. It can be seen that the concentration ratio of As was kept at approximately 0.1 throughout the experiment. Considering that the concentration of Zn in the artificial ARD is 10 times higher than the concentration of As, it can be inferred that the Zn is probably responsible for 95% of As sorption at most.

In case of Zn, as reported by Younger et al (2002) the free ion (Zn^{2+}) may react with other solutes to form complexes such as $ZnOH^+$, $Zn(OH)_2$, $ZnCO_3$, etc. which are probably responsible for As retention.

$$Zn^{2+} + H_2O \rightarrow ZnOH^+ + H^+ \quad (5.7)$$

Other possible Zn species are polynuclear complexes such as $Zn_2(OH)_6^{2-}$, which contain more than one metal atom and are probably also able to sorb the As.

$$2Zn^{2+} + 6H_2O \rightarrow Zn_2(OH)_6^+ + 6H^+ \quad (5.8)$$

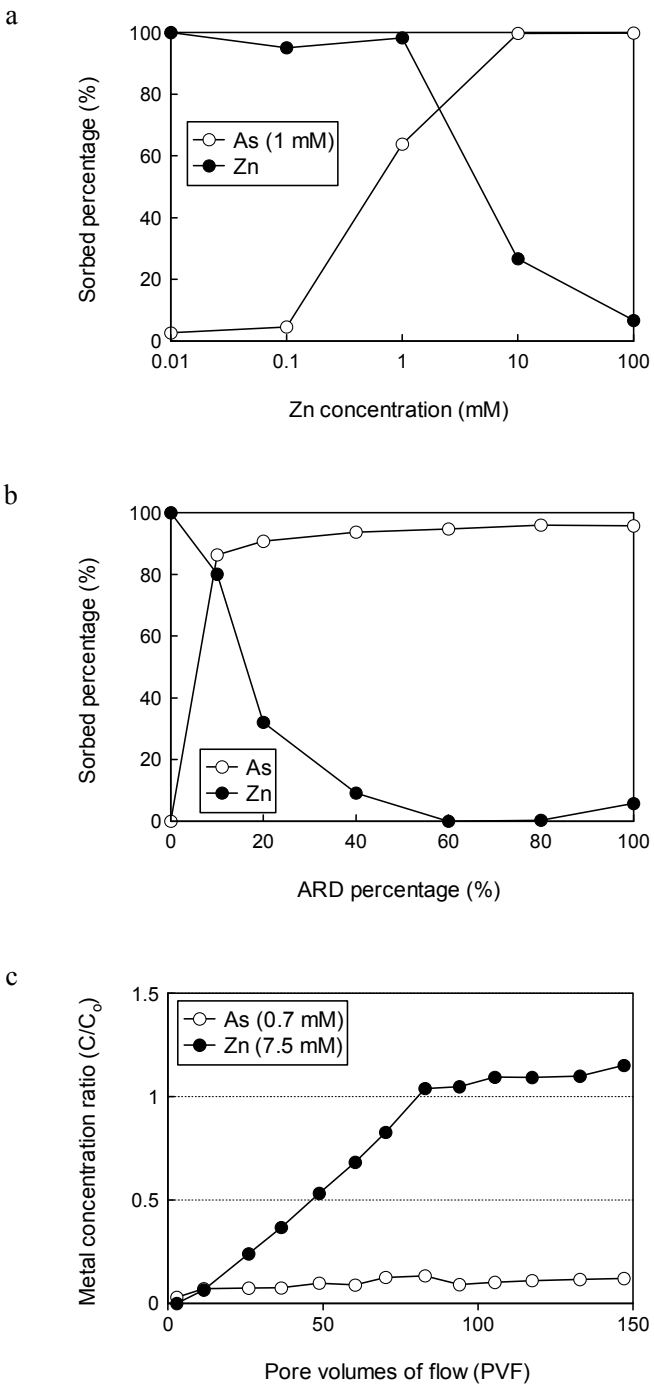

Figure 5-21 Role of Zn in As retention: a) bi-metal sorption, b) ARD sorption, c) effluent analysis

5.6.6 Role of Pb in As Sorption

From Figure 5-22a, at concentrations lower than 10 mM it can be seen that as Pb concentration increases, the As sorption percentage increases which suggests that Pb positively impacts As sorption. At 10 mM Pb, the As sorbed percentage is around 90%. Figure 5-22b shows the As behavior at different ARD 747

percentages. Considering that the Pb is 70 times less than the As concentration (Pb = 0.01 mM, As = 0.7 mM), there is probably no impact on As retention. In addition, Figure 5-22c shows the Pb and As concentration ratio from the effluent analysis of GCL permeated with ARD 747. It can be seen that the concentration ratio of the As was kept at approximately 0.1 throughout the experiment. As mentioned above, the concentration of Pb is much lower than the As concentration, which may suggest that in this case, there is no effect of Pb on As immobilization mechanism.

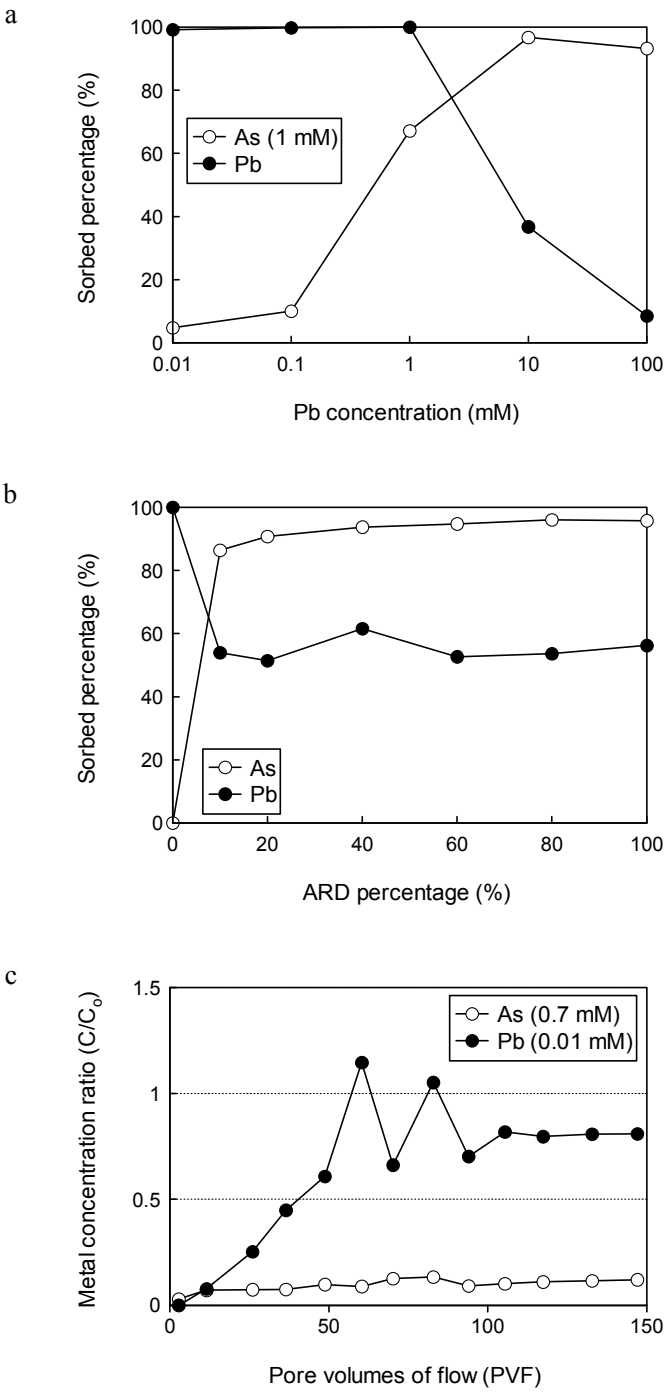

Figure 5-22 Role of Pb in As retention: a) bi-metal sorption, b) ARD sorption, c) effluent analysis

5.6.7 Role of Alkaline Metals in As Sorption

The sorption of As was minimally affected by the presence of Ca, Mg, K, and Na. At 100 mM of these alkaline metals (100 times the concentration of As), an As sorption between 1 to 11% was observed (Figure 5-23). The sorption of 1mM of As in presence of 100 mM of Ca, Mg, K, and Na was 11%, 6%, 1% and 5%, respectively. The highly negative values of Ca, Mg, K, and Na observed are due to the presence of these alkaline metals in the GCL which are also the responsible of the pH rise in the final solution. Figure 5-23 presents the role of Ca (a), K (b), Na (c), and Mg (d) in As retention at bi-metal sorption test (left), sorption test with ARD 747 at different percentages (center), effluent analysis of hydraulic conductivity test on GCL permeated with ARD 747 (right).

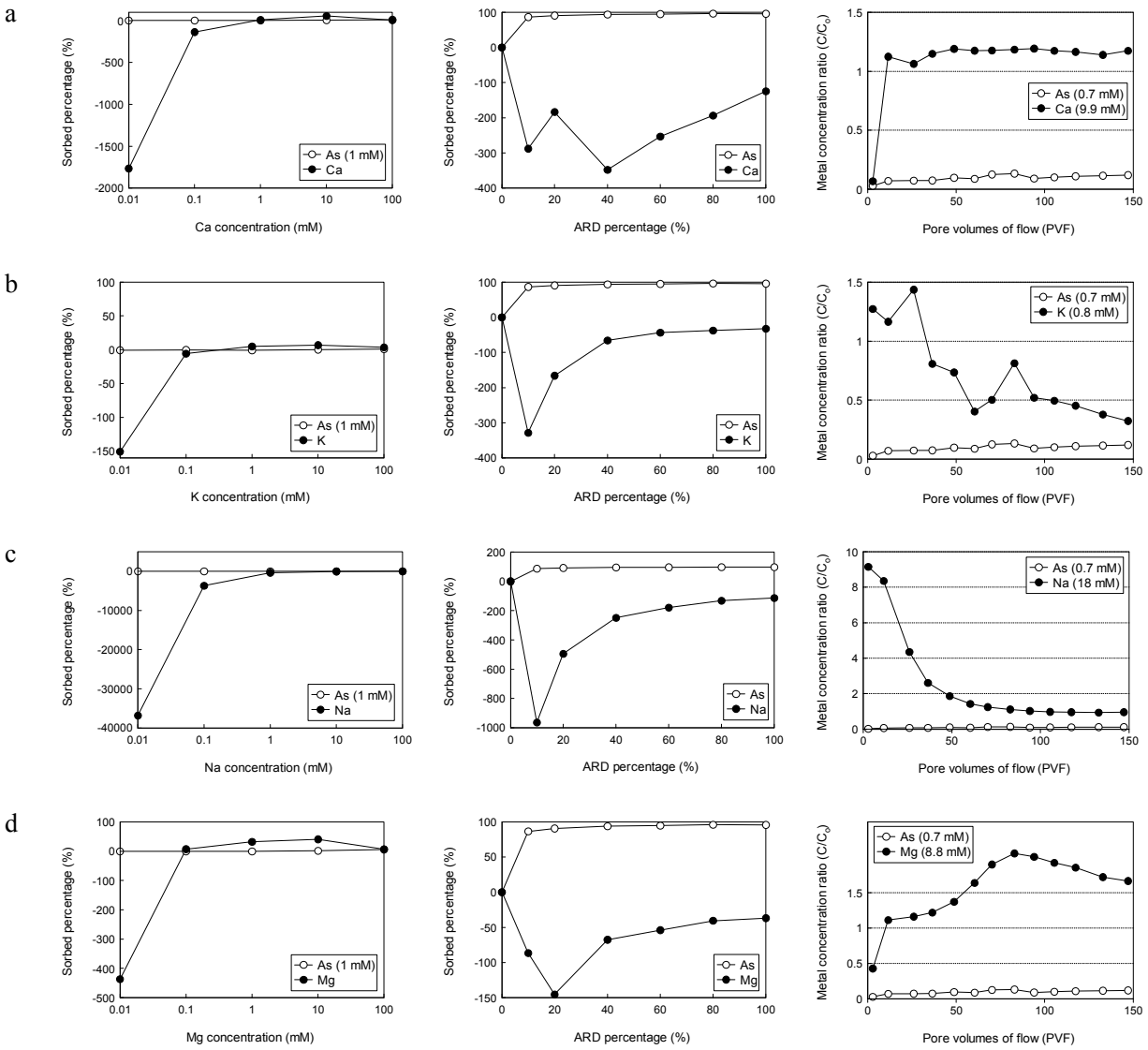

Figure 5-23 Role of a) Ca, b) K, c) Na and d) Mg in As retention

5.6.8 Summary of the Role of Metals in As Sorption

Results presented in Figure 5-24a show that at 1 mM of metal (metal-As relationship 1:1), the sorption of As on bentonite (2 g/L bentonite) increased from 0% to 71, 31, 51, 63, and 67 percent in presence of Fe, Cu, Al, Zn, and Pb, respectively. This indicates that As has affinity for the metals in the following order: Fe > Pb > Zn >Al > Cu.

It is observed that as the concentration of the second metal increases, the amount of As decreases, except when the concentration of Al was 100 times higher than the concentration of As. This can be attributed to the formation of polynuclear complexes of Al which reduces the binding site for As.

The affinity of As towards alkaline metals was very low. At 1 mM (metal-As relationship 1:1), the sorption of As was 3 percent in presence of Ca and 0 percent in presence of Mg, K and Na (Figure 5-24a).

a

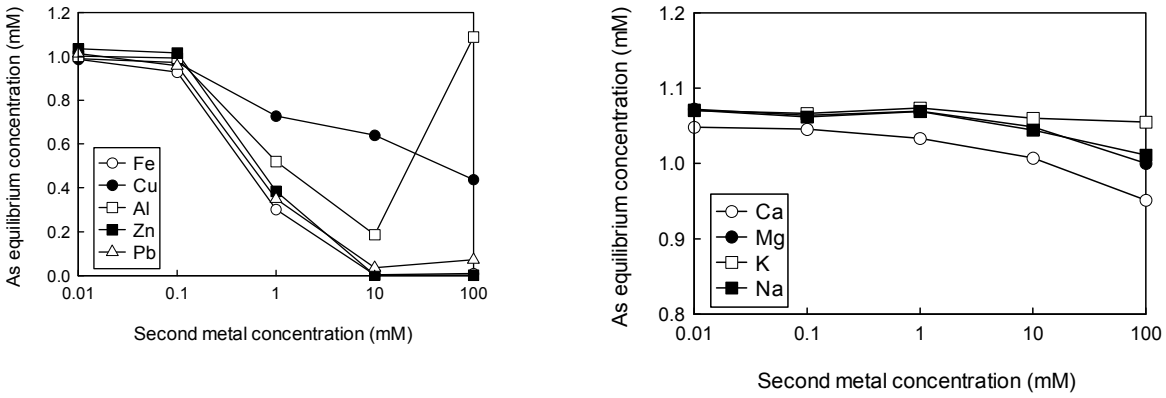

b

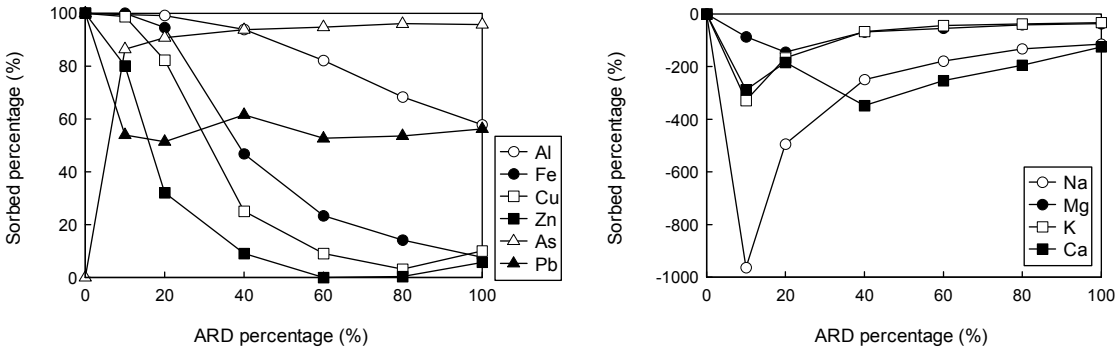

c

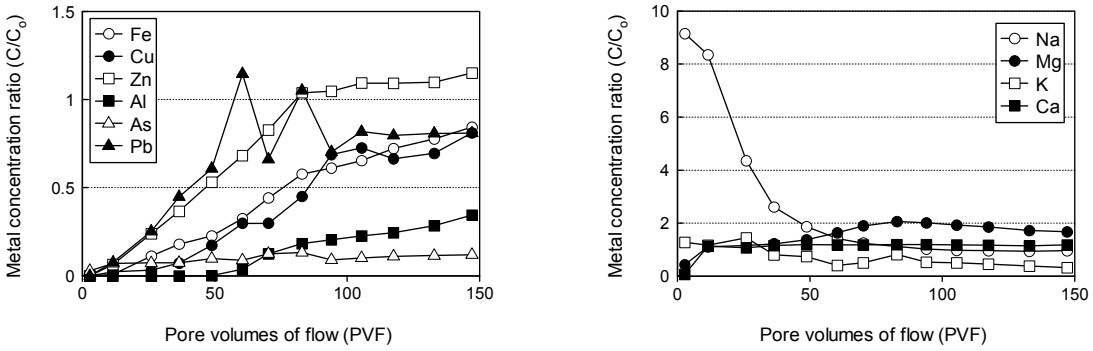

Figure 5-24 Summary of role of metals in As sorption: a) bi metal, b) ARD and c) effluent analysis

From the ARD 747 sorption test on bentonite (Figure 5-24b), the effects of metal concentration in metal sorption on bentonite can be well understood. Figure 5-24b shows the sorbed percentages of the metals present in different ARD dilutions (from 10 to 100% ARD proportion) using 20 g/L of bentonite. When the ARD percentage was 100% ARD, around 8% of Fe, 10% Cu, 6% Zn, 58% Al, 56% Pb, and 95% As were sorbed on bentonite. The sorbed percentage of As exhibits an abnormal behavior because sorption increases with ARD concentration. This phenomenon can be attributed to the additional sorption of As on other metals, especially on Fe because its concentration in the ARD is much higher. Negative values of sorption percentage observed in Figure 5-24b for Na, Mg, K, and Ca can be attributed to the release of these metals from the bentonite during the cation exchange.

From the ARD permeation test (effluent analysis of the hydraulic conductivity test) presented in Figure 5-24c, it was found that the results were consistent with the results obtained in the sorption tests. Low As release was observed which can be attributed to the presence of other metals. Metal concentrations ratio of Ca, Mg, Na, and K were more than one because of the release of these alkaline metals from the GCL (Figure 5-24c).

5.7 Factors affecting Heavy Metal Retention in Bentonite

All ARDs around the world are different in acidity and metal concentrations. They usually represent a threat to groundwater and surface water at mining sites because of their extremely low pH and high metal content. The most common elements found in ARDs from metallic mine wastes are sulfur, iron, copper, zinc, silver, gold, cadmium, arsenic, and uranium (Ripley et al. 1996).

Using GCLs, metals can be immobilized through many adsorption mechanisms which include cation exchange, surface complexation, surface-induced precipitation, surface co-precipitation, surface colloid formation, and diffusion into particle micropores (Xu et al. 2008). The main parameters affecting adsorption are pH, ionic strength, nature, and concentration of competing cations, all of which are discussed in this paper. Although, based on the cation exchange capacity (CEC), bentonite has a limited metal buffering capacity, its low k value make bentonite a suitable material for waste rock containment facilities with potential of ARD generation.

5.7.1 Effect of Buffering Capacity

Bentonite shows permanent negative surface charge due to the isomorphous substitution of cations of charge +4 and +3 with cations of charge +3 and +2, respectively. Either type of substitution creates a -1 charge that is usually compensated by interlayer cations. Cations balancing the layer negative charges are exchangeable with different ones present in solutions through an ion exchange mechanism. However,

bentonite also presents exposed layer edges (OH^-) with variable surface charge depending on the pH. At pH above the point of zero charge, the layer edges will have a negative charge, contributing to cation adsorption (Petrangeli and Majone 2002).

Ion exchange processes in bentonite are equilibrium processes. The occupation of a cation exchanger depends on the kind and concentration of the cations available for the exchange. Furthermore, the size and the charge of the cations are important. It is known that bivalent cations are more easily exchanged against monovalent cations than vice versa (Egloffstein 2001). This illustrates that for ARD solutions there is considerable potential to retain metals, although this potential is limited by the buffering capacity of the bentonite.

5.7.2 Effect of pH

The influence of pH on the adsorption of bivalent and trivalent metal ions (Cd, Cr, Cu, Mn, Ni, and Pb) on Na-montmorillonite was studied by Abollino et al. (2003). They demonstrated that the adsorption of metals decreases with decreasing pH because at low pH (between 2.5 and 3.5), the hydrogen ion competes with the heavy metals towards the superficial sites. Besides, the silanol ($Si–O^-$) and aluminol ($Al–O^-$) groups are less deprotonated and hence they are less available to retain metals. Sorption of metals increases at intermediate pH over a relatively small range called the pH-adsorption edge. At high pH values, the metal ions showed high retention on bentonite (Bradl 2004).

5.7.3 Effect of Metal Ions

Abollino et al. (2003) have reported that at pH < 3.5 metals are adsorbed on Na-montmorillonite in the following order: $Cu^{2+} < Pb^{2+} < Cd^{2+} < Zn^{2+} < Mn^{2+} = Cr^{3+} = Ni^{2+}$. However, a rule of metal selectivity cannot always be predicted, especially in complex metal systems, because it depends on a number of factors such as: the chemical nature of the surface at certain pH; the solid-liquid ratio; the pH at which adsorption is measured; and the ionic strength of the solution. These factors all determine the intensity of competition from other cations for the bonding sites. All these variables may change the metal adsorption isotherms and it is necessary to consider all these factors to study a real bentonite/ARD system and effectively predict the fate of heavy metals in the environment. Preference or affinity is measured by a selectivity or distribution coefficient, K_d, extensively studied by Lange et al. (2007) through diffusion tests. They found significant attenuation of metals in GCLs from the measured diffusion profiles, where concentrations in the receptor reservoir remained very low for the duration of the tests. This helps to confirm that GCLs have potential use as a barrier material for the containment metal-bearing wastes.

5.7.4 Effect of Liquid-Solid Ratio

Figure 5-25 shows the sorption percentage of each metal using different amounts of bentonite (from 4 to 20 g bentonite/L solution) against ARD 747. The sorbed percentage was calculated by dividing the

sorbed amount (initial minus final concentration) by the initial concentration. In the case of Cu (initial concentration, 86.9 mg/L) and Al (initial concentration, 259.2 mg/L), 100% of these metals were sorbed by 80 g/L of bentonite. Around 45% of Zn (initial concentration, 493.1 mg/L) and 75% of Fe (initial concentration, 4330.2 mg/L) were sorbed by 80 g/L of bentonite.

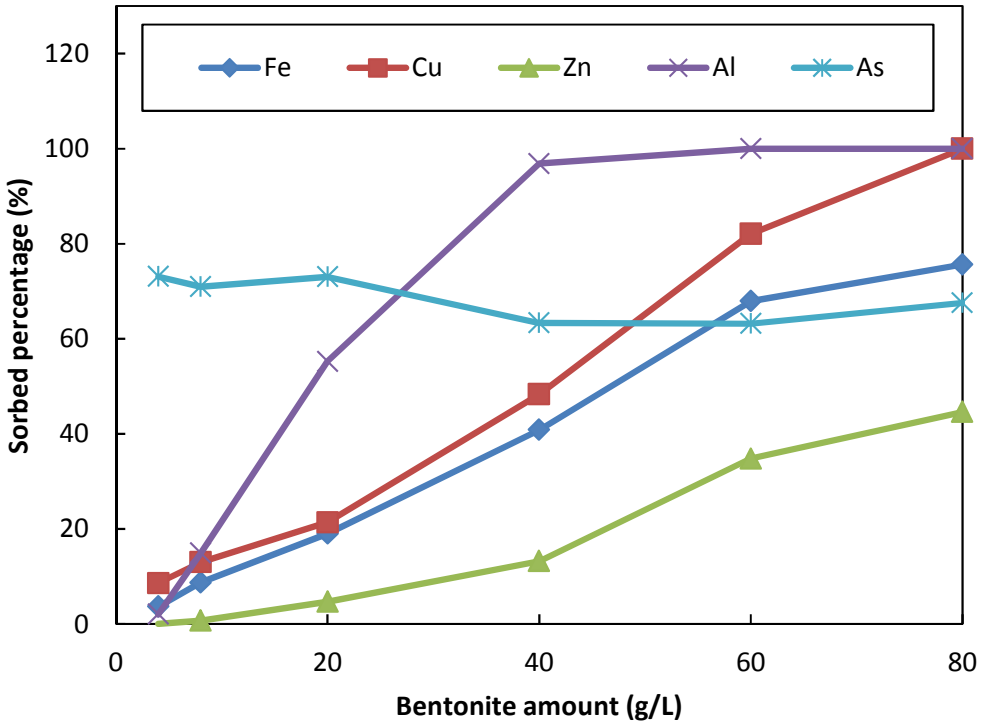

Figure 5-25 Sorbed percentage of metals present in ARD 747 solution

For As, it was observed that the sorbed amount was constant, even at high adsorbent concentration. The sorbed percentage of Pb was not plotted because the initial concentration was very low (2.9 ppm) and the dilution level made for the analysis in the ICP (100 times dilution) did not allow for Pb detection. There was no linear correlation between the sorbed percentage and the amount of bentonite because, as the amount of bentonite increased, there was less adsorbent contact area and therefore, the capacity of bentonite to retain cations decreased.

Figure 5-26 shows the sorbed percentage of Na, K, Ca, and Mg present in ARD solution. These high negative values of sorbed percentage indicate that these elements were released from the bentonite and instead, di and tri-valent cations were sorbed.

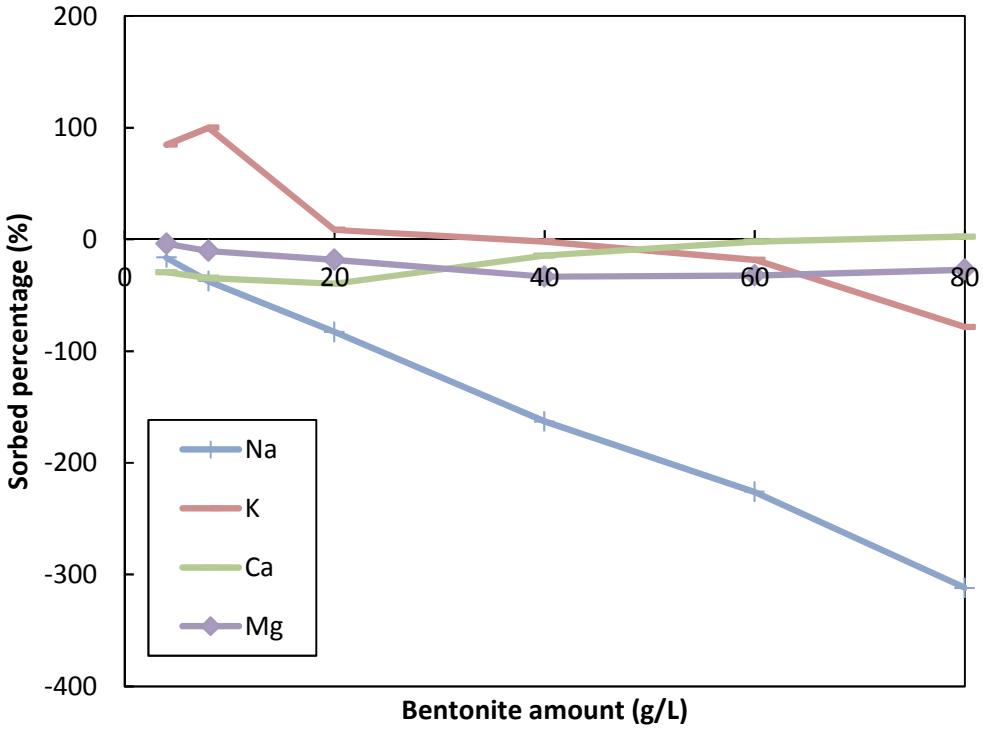

Figure 5-26 Sorbed percentage of Na, K, Ca, and Mg present in ARD solution

5.7.5 Effect of Metal Concentration

Figure 5-27 and Figure 5-28 show the sorbed percentage of metals present in different ARD 747 dilutions (from 2 to 80% ARD), using 20 g/L of bentonite.

When the ARD proportion was around 0.1 (or 10% diluted ARD) all the metals were completely sorbed on bentonite, except in the case of As, in which only 0.2% were sorbed. At 0.8 ARD proportion (or 80% ARD), around 25% of Fe, 33% Cu, 11% Zn, 77% Al, 80% As, and 16% of Pb were sorbed on bentonite. In the case of As, an abnormal behavior was observed, because at high ARD concentration, the sorption was higher. This phenomenon can be attributed to an additional sorption on $Fe(OH)_3$.

Figure 5-29 shows the amount of metal sorbed per gram of bentonite using different ARD proportion. It was divided into three graphs, according to a better range fit. Those figures show that even at high ARD concentration (80% ARD), a high amount of metals were retained by bentonite. However, a saturation point was observed in the cases of Fe, Zn, Cu, and Pb. The maximum amount of Fe sorbed was around 0.85 mmol/g bentonite. For Cu, the limit was around 0.02 mmol/g bentonite, for Zn, around 0.035 mmol/g bentonite, and, for Pb, around 0.00004 mmol/g bentonite. In case of Al, the sorbed amount at 80% ARD was around 0.3 mmol/g bentonite and, in case of As, 0.003 mmol/g bentonite.

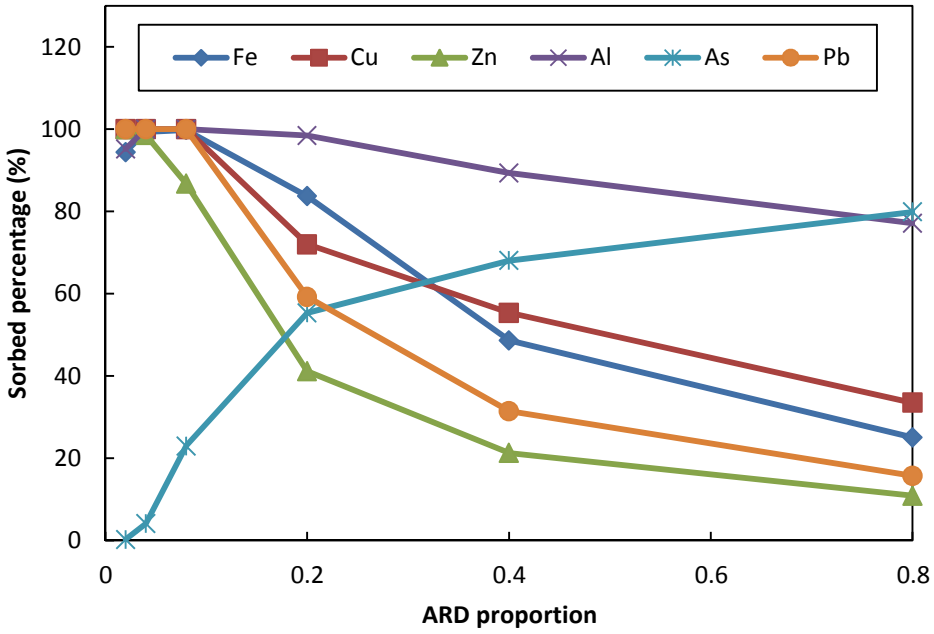

Figure 5-27 Sorbed percentage of Fe, Cu, Zn, Al, As, and Pb at different ARD dilutions

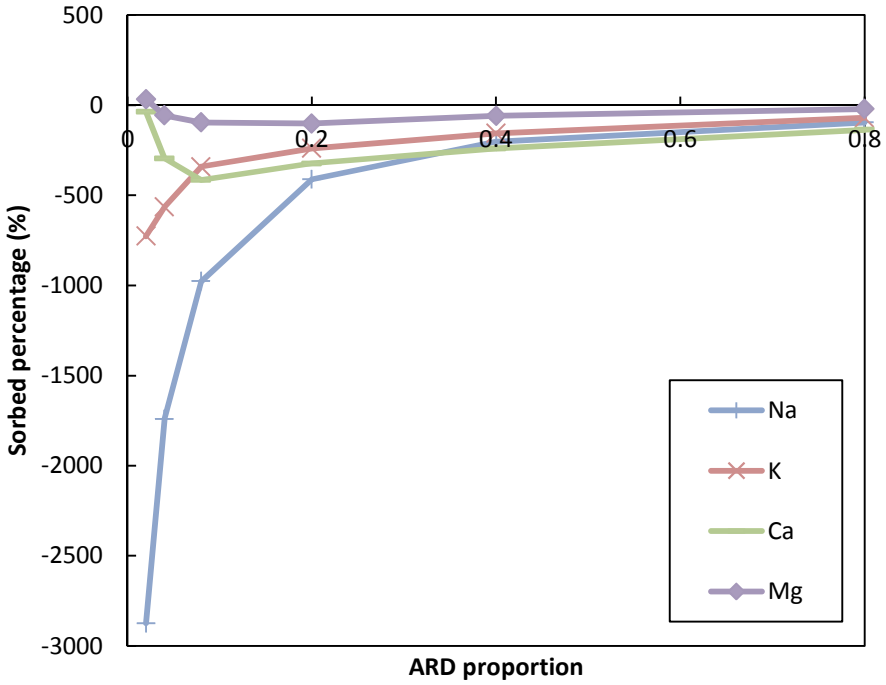

Figure 5-28 Sorbed percentage of Na, K, Ca, and Mg at different ARD dilutions

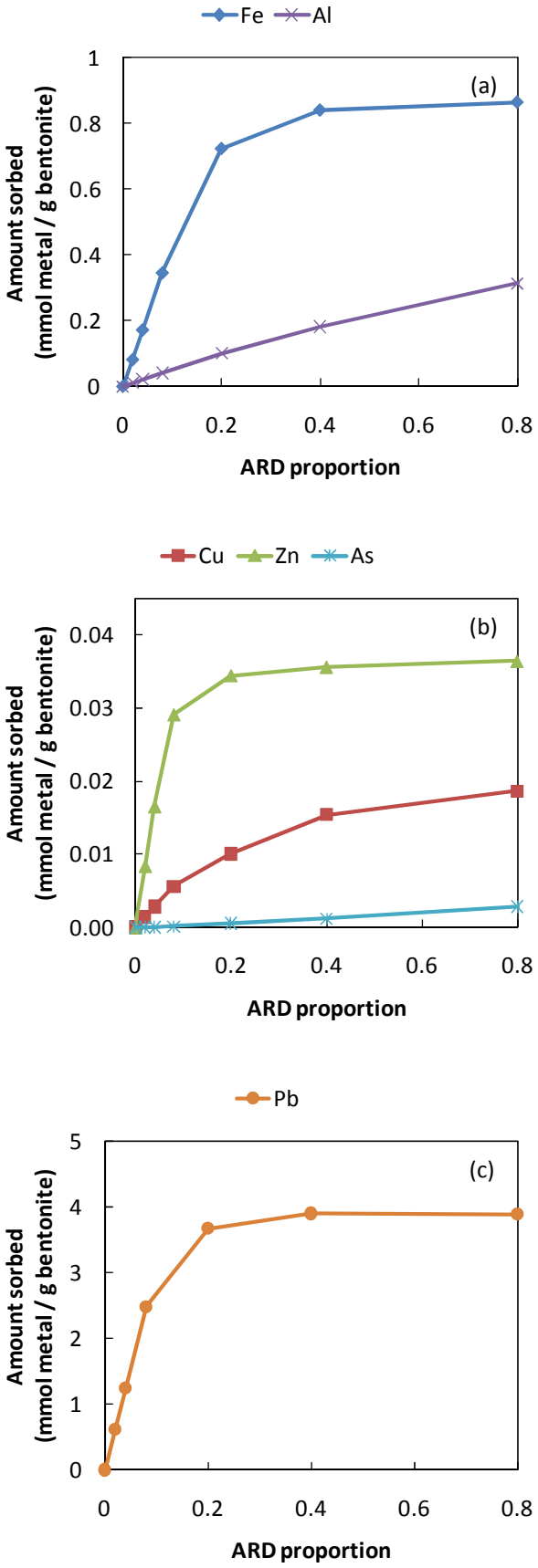

Figure 5-29 Sorbed amount of Fe and Al (a), Cu, Zn, and As (b) and Pb (c) at different ARD dilutions

5.8 Comparison of Bentonite Sorption Capacity with Other Materials

5.8.1 Metal Sorption Capacity of Zeolite

Time step batch sorption tests were conducted for Fe, Cu, Zn, Al, As, and Pb. The pH, EC, and ORP for each metal, concentration and time was measured. From the pH versus time graph (Figure 5-30, Left), information about the change in pH was obtained. Before adding the sorbent into the solution (t=0) the pH was 3 (initial pH) and after mixing them, the pH did not change, as in the case of bentonite.

From the EC versus time graph (Figure 5-30, Right), information about the amount of species in solution was obtained. In case of ORP, two types of graphs were presented. The first one is the change of ORP versus time (Figure 5-31, Left) and the second one, the change of ORP versus pH (Figure 5-31, Right). From the last graph it is possible to see what specie is present in the solution under given condition. The graphs for Cu are presented in this section only as an example. The rest of the graphs are shown in Appendix C.

The metal sorption capacity of zeolite over time is shown in Figure 5-32 to Figure 5-34. It was observed that at high metal concentrations (100 and 10 mM for some metals, and 1 mM for other) only a very small decrease in concentration can be detected and, thus, no important change over time was perceived (Figure 5-32 and Figure 5-33). On the other hand, at very low metal concentration (1 and 10 µM) metal sorption onto bentonite was so fast that no change over time was observed (Figure 5-34). At intermediate metal concentration (1 mM and 100 µM) a gradual decrease in metal concentration was

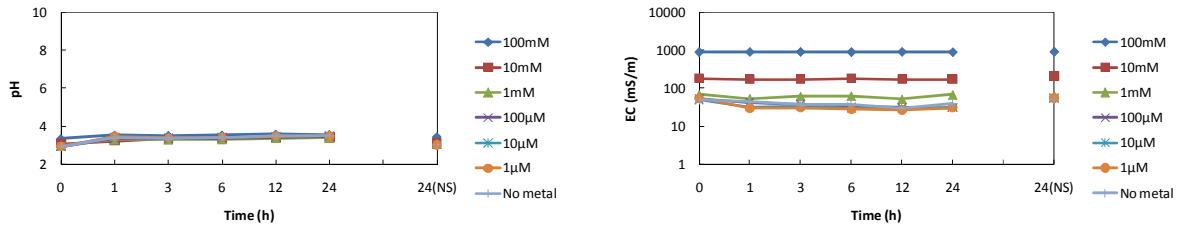

Figure 5-30 Zeolite-Cu system Left: Change of pH versus time; Right: Change of EC over time

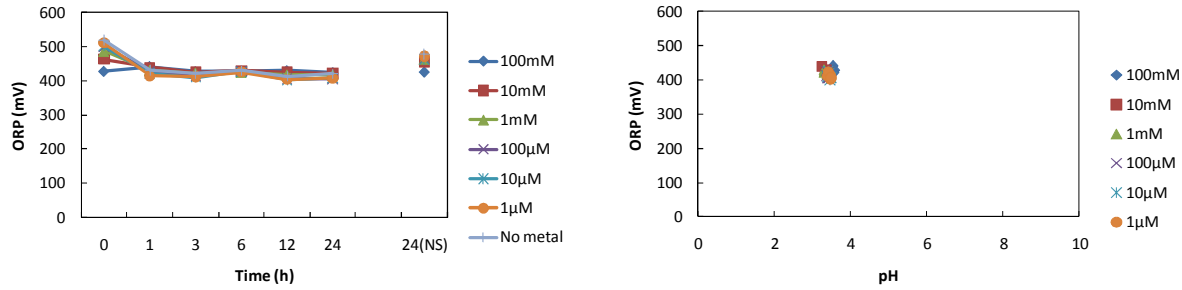

Figure 5-31 Zeolite-Cu system Left: Change of ORP over time; Right: Relationship ORP-pH

observed over time (Figure 5-33). From Figure 5-33 it can be concluded that, in most of the cases, the equilibrium was reached before 24 hours (between 1 to 6 hours). In addition, from the same graph it can be inferred that Fe and Cu were preferably sorbed onto zeolite, followed by Zn, and the less sorbed ion was Al.

Moreover, the amount of Na, Ca, Mg, and K was investigated. Six graphs were created for each metal (for each metal concentration) and each sorbent. The pattern of most of them was similar to the one presented in Figure 5-35 to Figure 5-37 for zeolite-Zn system. Therefore, the graphs for all sorbent-metal systems are not shown in this section, but in Appendix F.

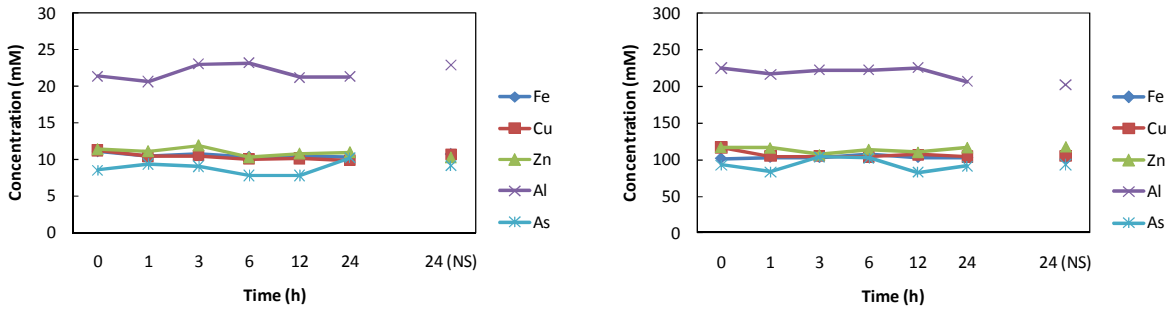

Figure 5-32 Metal sorption on zeolite Left: 100 mM; Right 10 mM

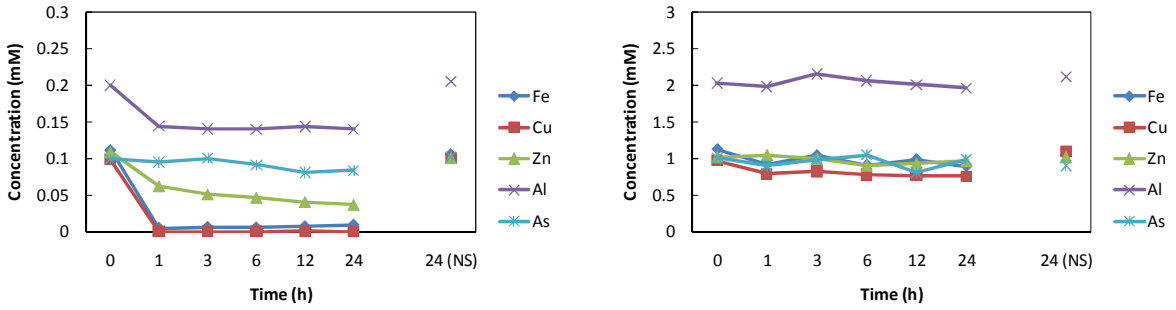

Figure 5-33 Metal sorption on zeolite Left: 1 mM; Right 100 µM

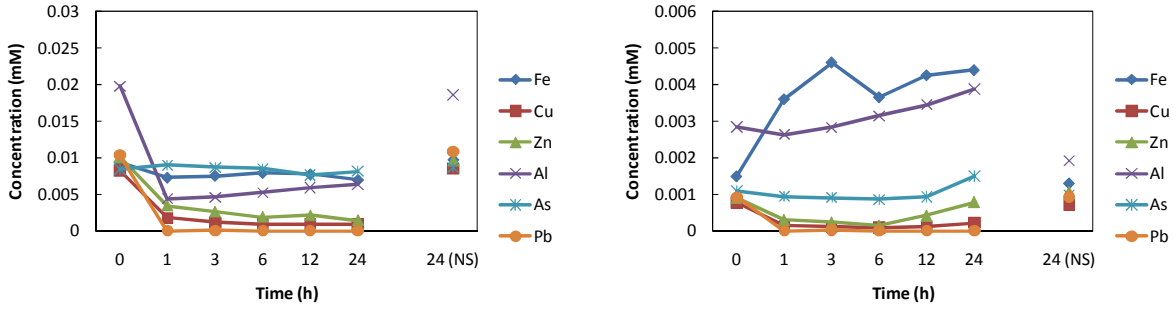

Figure 5-34 Metal sorption on zeolite Left: 10 µM; Right 1 µM

The six graphs presented in Figure 5-35 to Figure 5-37 correspond to each metal concentration (100 mM, 10 mM, 1 mM, 100 µM, 10 µM, and 1 µM) and from all of them, except Figure 5-35 (Left), a release of Na was observed. It provides important information about the attenuation process of zeolite toward heavy metals and suggests that ion exchange is probably the mechanism that dominates in this case.

From the collected data, graphs of sorbed amount per gram of zeolite versus equilibrium concentration (isotherm) were created. In Figure 5-38, all the points were plotted. However, for the Fe highest concentration, a negative value was observed. This can possibly be because the highest

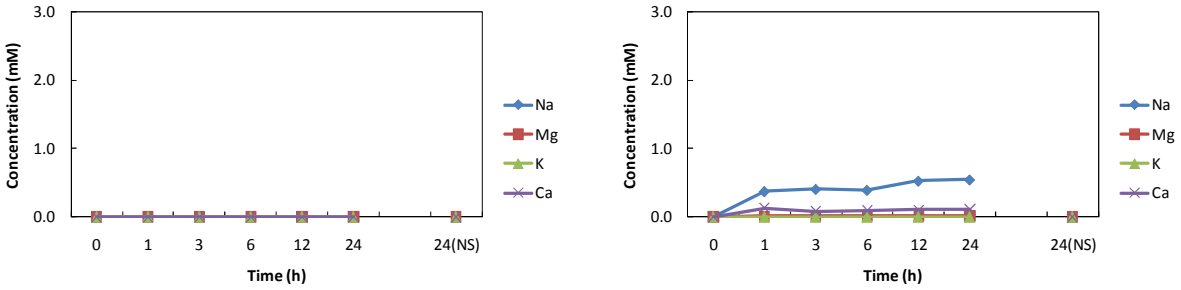

Figure 5-35 Na, Mg, K, and Mg concentration in zeolite-Zn system Left: 100 mM; Right 10 mM

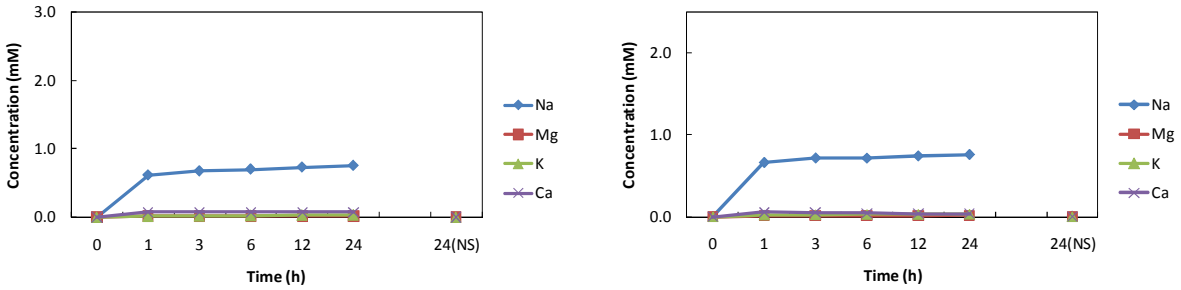

Figure 5-36 Na, Mg, K, and Mg concentration in zeolite-Zn system Left: 1 mM; Right 100 µM

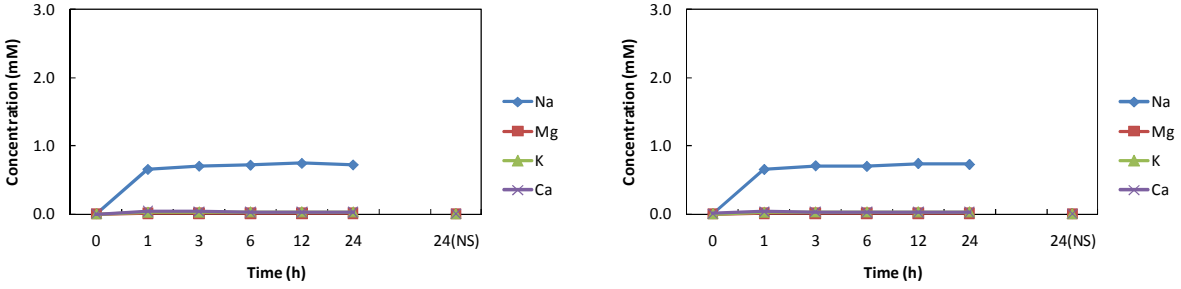

Figure 5-37 Na, Mg, K, and Mg concentration in zeolite-Zn system Left: 10 µM; Right 1 µM

concentration point corresponds to a 1000 times diluted solution, so the possibility of error arises. Therefore, the highest point can be omitted and only 5 points are considered, as shown in Figure 5-39. From this graph it can be said that zeolite has more preference for Cu, followed by Fe, Zn, and Al.

5.8.2 Metal Sorption Capacity of Ferrihydrite

Time step batch sorption tests were conducted for Fe, Cu, Zn, Al, As, and Pb. The pH, EC and ORP for each metal, concentration and time was measured. From the pH versus time graph (Figure 5-40, Left), information about the change in pH was obtained. It was observed that the pH was constant over time.

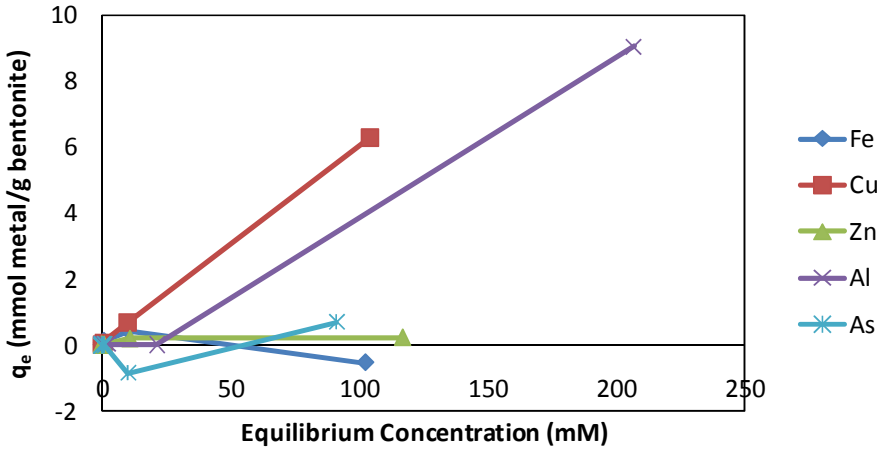

Figure 5-38 Isotherm of heavy metal sorption on zeolite

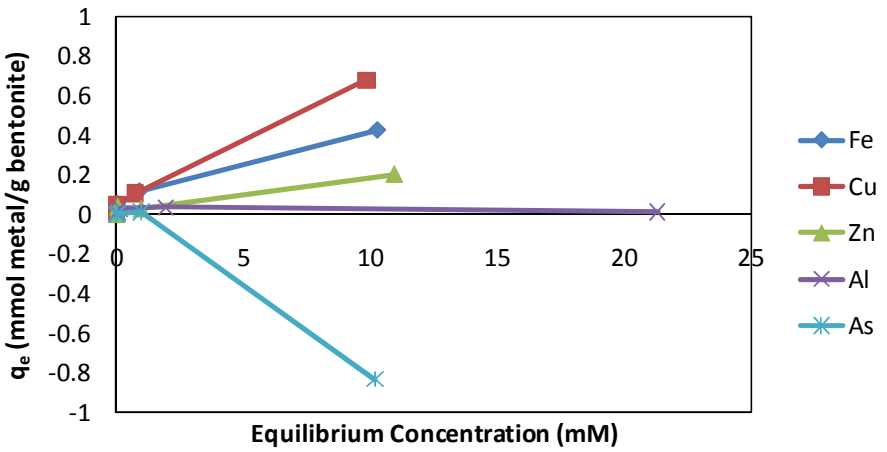

Figure 5-39 Isotherm of heavy metal sorption on zeolite (adjusted)

However the initial pH was not constant in all cases due to the concentration effect. When the metal concentration was high, the pH was lower.

From the EC versus time graph (Figure 5-40, Right), information about the amount of species in solution was obtained. In case of ORP, two types of graphs were presented. The first one is the change of ORP versus time (Figure 5-41, Left) and the second one, the change of ORP versus pH (Figure 5-41, Right). From the last graph it is possible to see what specie is present in the solution under given condition. The graphs for Cu are presented in this section only as an example. The rest of the graphs are shown in Appendix D.

Metal sorption capacity of ferrihydrite over time is shown in Figure 5-42 to Figure 5-44. It was observed that at high metal concentrations (100 and 10 mM for some metals, and 1 mM for others) only a very small decrease in concentration can be detected and, thus, no important change over time was perceived (Figure 5-42 and Figure 5-43). On the other hand, at very low metal concentration (1, and 10 µM) metal sorption onto ferrihydrite was very fast so no change over time was observed (Figure 5-44). At intermediate metal concentration (1 mM and 100 µM) a gradual decrease in metal concentration was observed over time (Figure 5-43). From Figure 5-43 it can be concluded that, in most of the cases, the equilibrium was reached before 24 hours. In addition, it can be inferred that Fe and Cu were preferably sorbed onto zeolite, followed by Zn, and the less sorbed ion was Al.

For metal solutions with lower initial concentration (<100 µM), the adsorption equilibrium can be achieved within 2 hours after the addition of ferrihydrite, which guarantees the strong affinity of ferrrihydrite against these toxicant species, as well as the use of this value for further research.

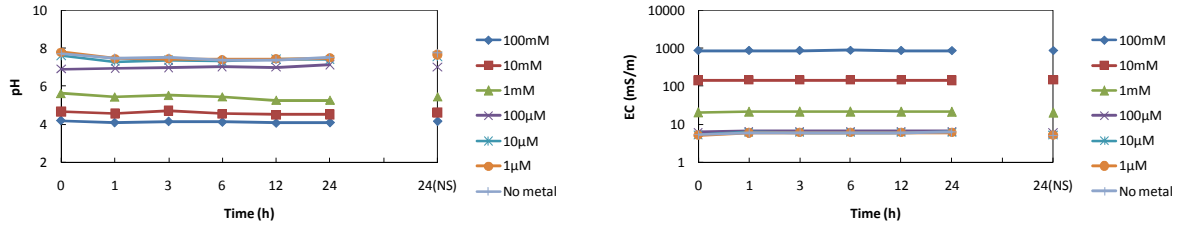

Figure 5-40 Ferrihydrite-Cu system Left: Change of pH versus time; Right: Change of EC over time

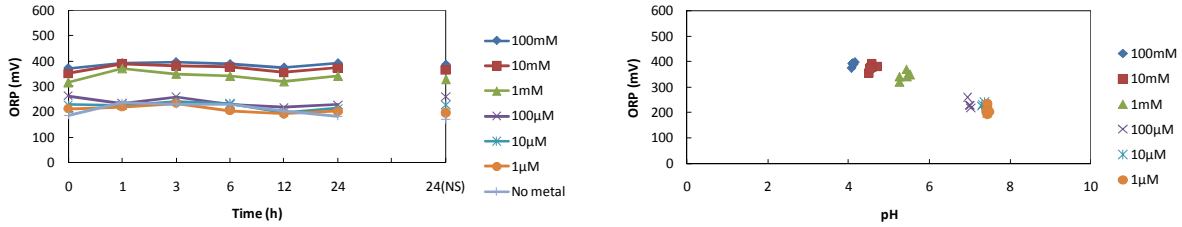

Figure 5-41 Ferrihydrite-Cu system Left: Change of ORP over time; Right: Relationship ORP-pH

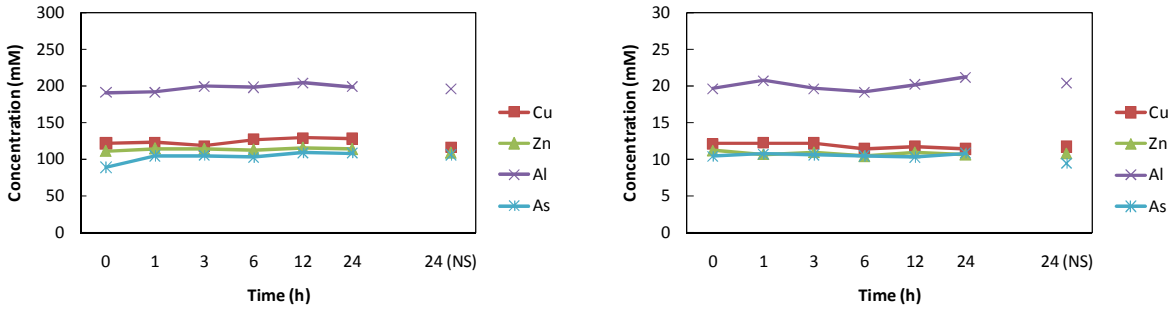

Figure 5-42 Metal sorption on ferrihydrite Left: 100 mM; Right 10 mM

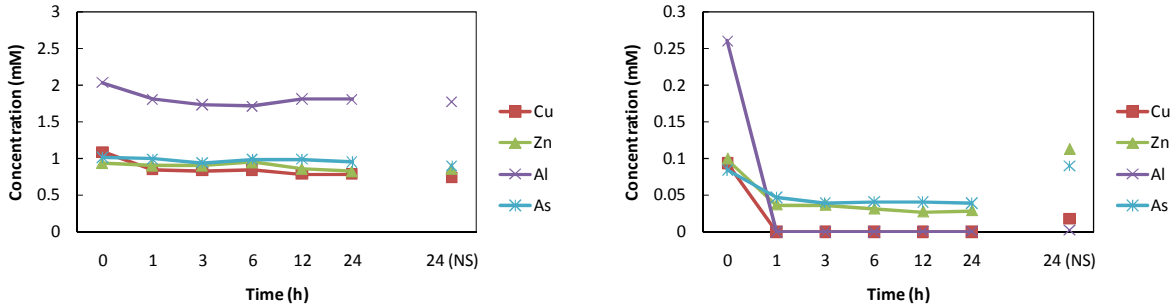

Figure 5-43 Metal sorption on ferrihydrite Left: 1 mM; Right 100 µM

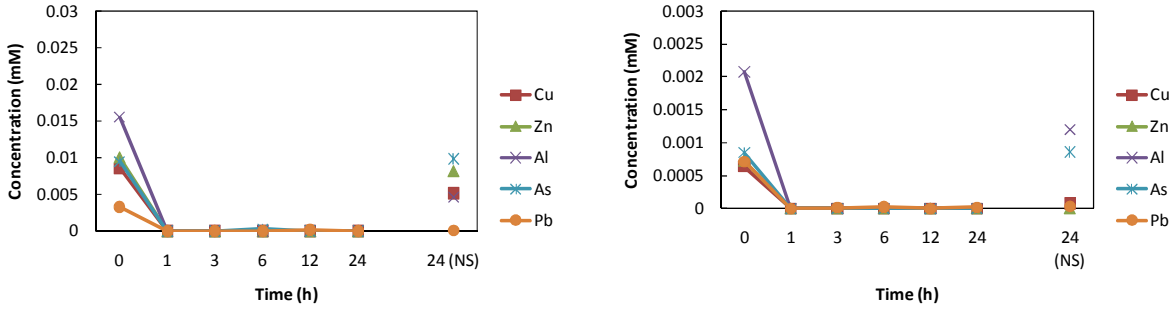

Figure 5-44 Metal sorption on ferrihydrite Left: 10 µM; Right 1 µM

In addition, the amount of Na, Ca, Mg, and K was investigated. Six graphs were created for each metal (for each metal concentration) and each sorbent. The pattern of most of them was similar to the one presented in Figure 5-45 to Figure 5-47 for ferrihydrite-Cu system. Therefore, the graphs for all sorbent-metal systems are not shown in this section, but in the Appendix G.

The six graphs presented in Figure 5-45 to Figure 5-47 correspond to each metal concentration (100 mM, 10 mM, 1 mM, 100 µM, 10 µM, and 1 µM) and from all of them, except Figure 5-45 (Left), it was observed a high Na release amount due to the NaOH used in adjusting the pH. So, it can be inferred that the mechanism in this case is not ion exchange, as was observed in case of bentonite and zeolite.

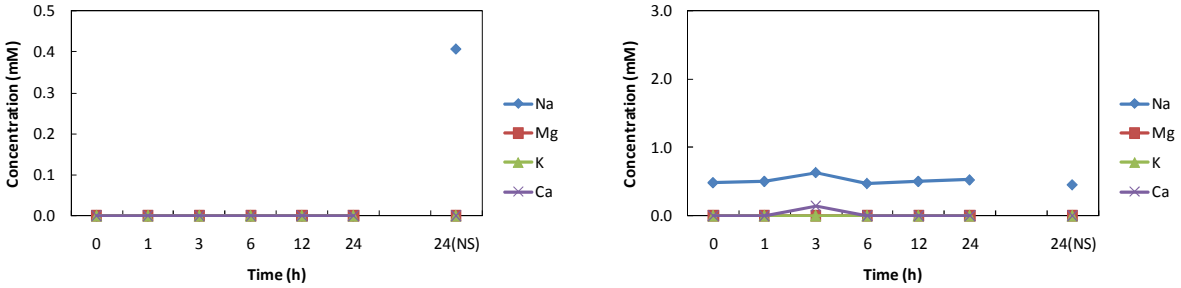

Figure 5-45 Na, Mg, K, and Mg concentration in ferrihydrite-Zn system Left: 100 mM; Right 10 mM

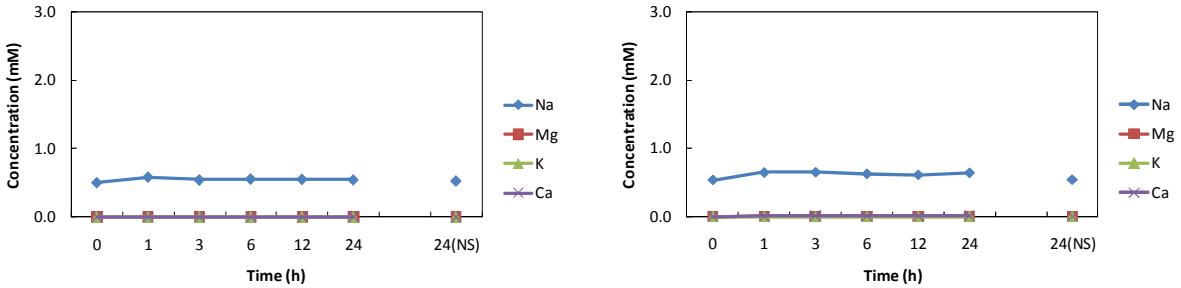

Figure 5-46 Na, Mg, K, and Mg concentration in ferrihydrite-Zn system Left: 1 mM; Right 100 µM

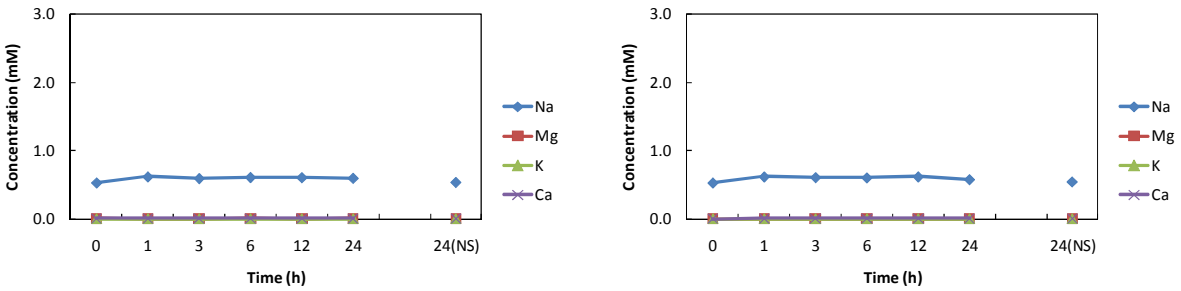

Figure 5-47 Na, Mg, K, and Mg concentration in ferrihydrite-Zn system Left: 10 µM; Right 1 µM

From the collected data, graphs of sorbed amount per gram of ferrihydrite versus equilibrium concentration (isotherm) were created. In Figure 5-48, all the points were plotted. However, for the highest concentration points, a negative value was observed. This is probably because the highest concentration point correspond to a lower pH (lower pH, lower sorption capacity) or because of the 1000 times dilution causing an error. Therefore, the highest point and the second highest point were omitted and only 4 points considered, as shown in Figure 5-49. From this graph it can be said that ferrihydrite has more preference for Cu, followed by Al, Zn, and As.

Correlating to the above mentioned results about time-step sorption test, the following conclusion can

be raised: Although ferrihydrite has faster sorption rates, its sorption capacity appears to be lower than the other two mineral tested in this study. It was observed that the sorption capacity decreased as following: Cu > Al > Zn > As. The sorption capacity ranges from 0.025 to 0.15 mmol/g ferrihydrite.

5.8.3 Comparison of Metal Sorption Capacity among Bentonite, Zeolite, and Ferrihydrite

Isotherms provide information about the sorption capacity of each mineral against certain metals. In case of Cu, Figure 5-51 (Left), it was observed that bentonite had higher capacity to sorb this metal than zeolite and ferrihydrite. Similarly, Fe, Zn, and Al (Figure 5-50 to Figure 5-52) showed more affinity to bentonite than other minerals. However, in case of As, Figure 5-52 (Left) it was found that it was more preferably sorbed on ferrihydrite than bentonite and zeolite. From Pb isotherms, no conclusion can be taken because the amount used for the experiments was very low (10 µM was the highest concentration

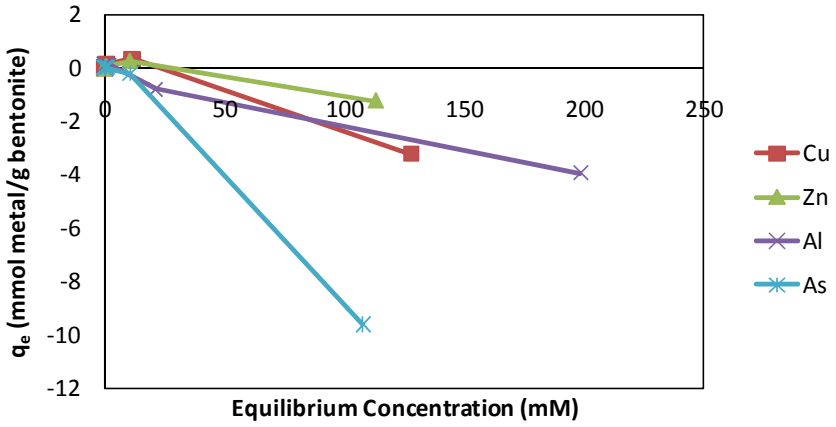

Figure 5-48 Isotherm of heavy metal sorption on ferrihydrite

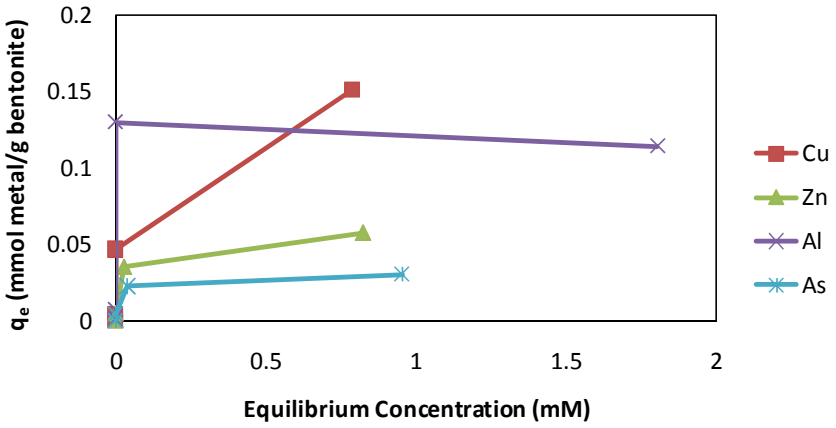

Figure 5-49 Isotherm of heavy metal sorption on ferrihydrite (adjusted)

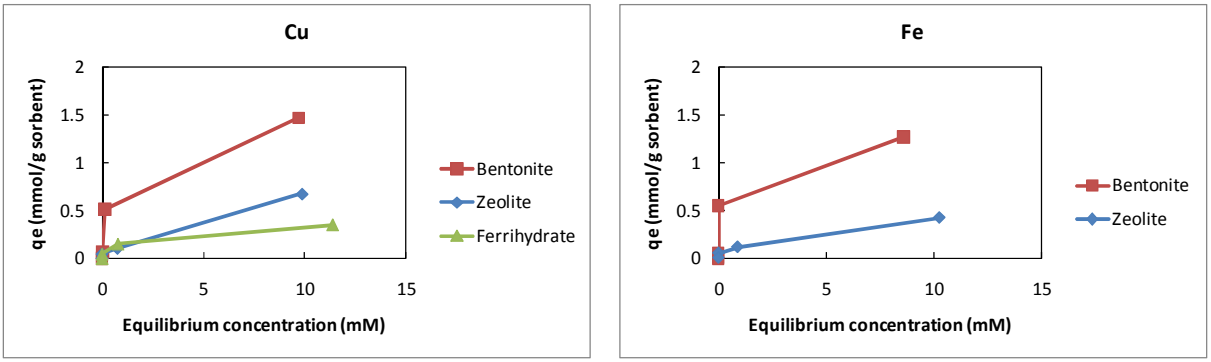

Figure 5-50 Isotherm for sorption on bentonite, zeolite and ferrihydrite Left: Cu; Right: Fe

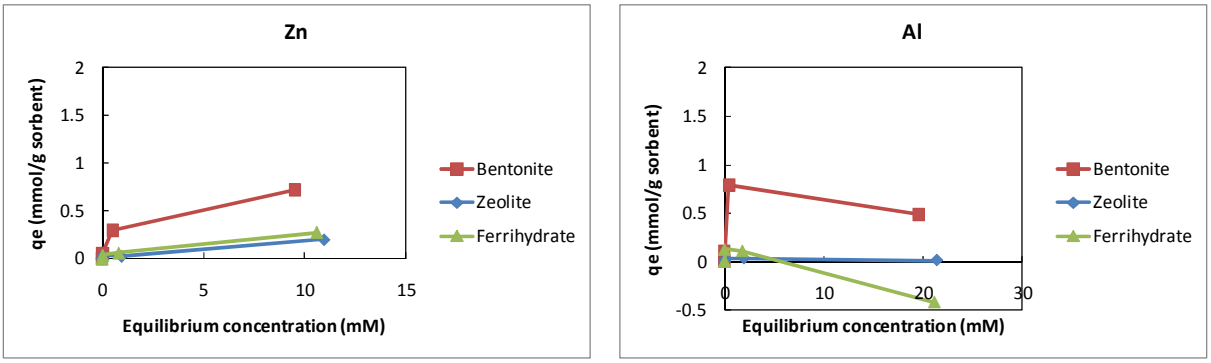

Figure 5-51 Isotherm for sorption on bentonite, zeolite and ferrihydrite Left: Zn; Right: Al

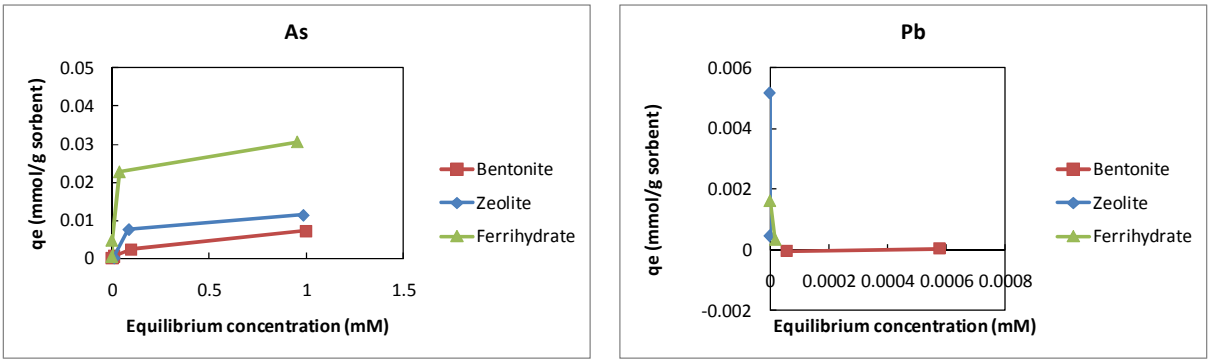

Figure 5-52 Isotherm for sorption on bentonite, zeolite and ferrihydrite Left: As; Right: Pb

because it was not possible to dissolve more $PbCl_2$) and it was immediately sorbed on all minerals. The shape of these isotherms (L or H type) suggests a chemisorption process and indicates that in most of the cases there was a relatively high affinity between the adsorbate and the adsorbent.

The sorption capacity of bentonite, zeolite, and ferrihydrite are shown in Table 5-5. According to these results, metal selectivity of each mineral is as follows:

(a) Bentonite: Cu > Fe > Zn > Al >> As >> Pb (5.9)

(b) Zeolite: Cu > Fe > Zn >> Pb ≈ Al ≈ As (5.10)

(c) Ferrihydrite: Cu > Zn >> Al > As >> Pb (5.11)

These results show that As sorption on bentonite and zeolite is very low (0.6 mg/g bentonite and 0.9 mg/g zeolite), whereas for ferrihydrite is the highest among these three minerals (2.3 mg/g ferrihydrite). It proves the hypothesis that As is also sorbed or co-precipitated by Fe and other metals present in ARD. Bentonite, zeolite, and ferrihydrite show high affinity for Cu (93.7 mg/g bentonite, 43.1 mg/g zeolite, and 22.4 mg/g ferrihydrite), followed by Fe (71 mg/g bentonite and 23.7 mg/g zeolite) and Zn (47.1 mg/g bentonite, 13.1 mg/g zeolite, and 17.7 mg/g ferrihydrite), but lower for Al (13.2 mg/g bentonite, 1 mg/g zeolite, and 3.1 mg/g ferrihydrite), As (0.6 mg/g bentonite, 0.9 mg/g zeolite, and 2.3 mg/g ferrihydrite), and Pb (0.01 mg/g bentonite, 1.1 mg/g zeolite, and 0.3 mg/g ferrihydrite). Bentonite has higher sorption capacity than zeolite and ferrihydrite except in case of As and Pb, in which zeolite and ferrihydrite appear to perform better.

Sorption test results may represent ideal conditions and overestimate the sorption capacity because the surface area of contact between metal and mineral is at the maximum in these experiments. Besides, application of these data to ARD may raise some concern as multiple metal ions in the solution may interact due to the synergetic and antagonistic effect that they exert on each other (Kaoser et al. 2005). In multi-metal solutions, metal sorption tends to increase with the decrease in ion exchange, or less competitive species (Lange et al. 2009). Therefore, to evaluate field application of bentonite, zeolite, and ferrihydrite as adsorption layer in waste rock containments, additional tests, such as hydraulic conductivity, become necessary.

Table 5-5 Metal sorption capacity of bentonite, zeolite, and ferrihydrite

Metal	Bentonite (mg/g bentonite)	Zeolite (mg/g zeolite)	Ferrihydrite (mg/g ferrihydrite)
Al	13.2	1.0	3.1
Fe	71.0	23.7	NA
Cu	93.7	43.1	22.4
Zn	47.1	13.1	17.7
As	0.6	0.9	2.3
Pb	0.01	1.07	0.34

5.8.4 Effluent Analysis of Hydraulic Conductivity Test for Minerals against ARD 747

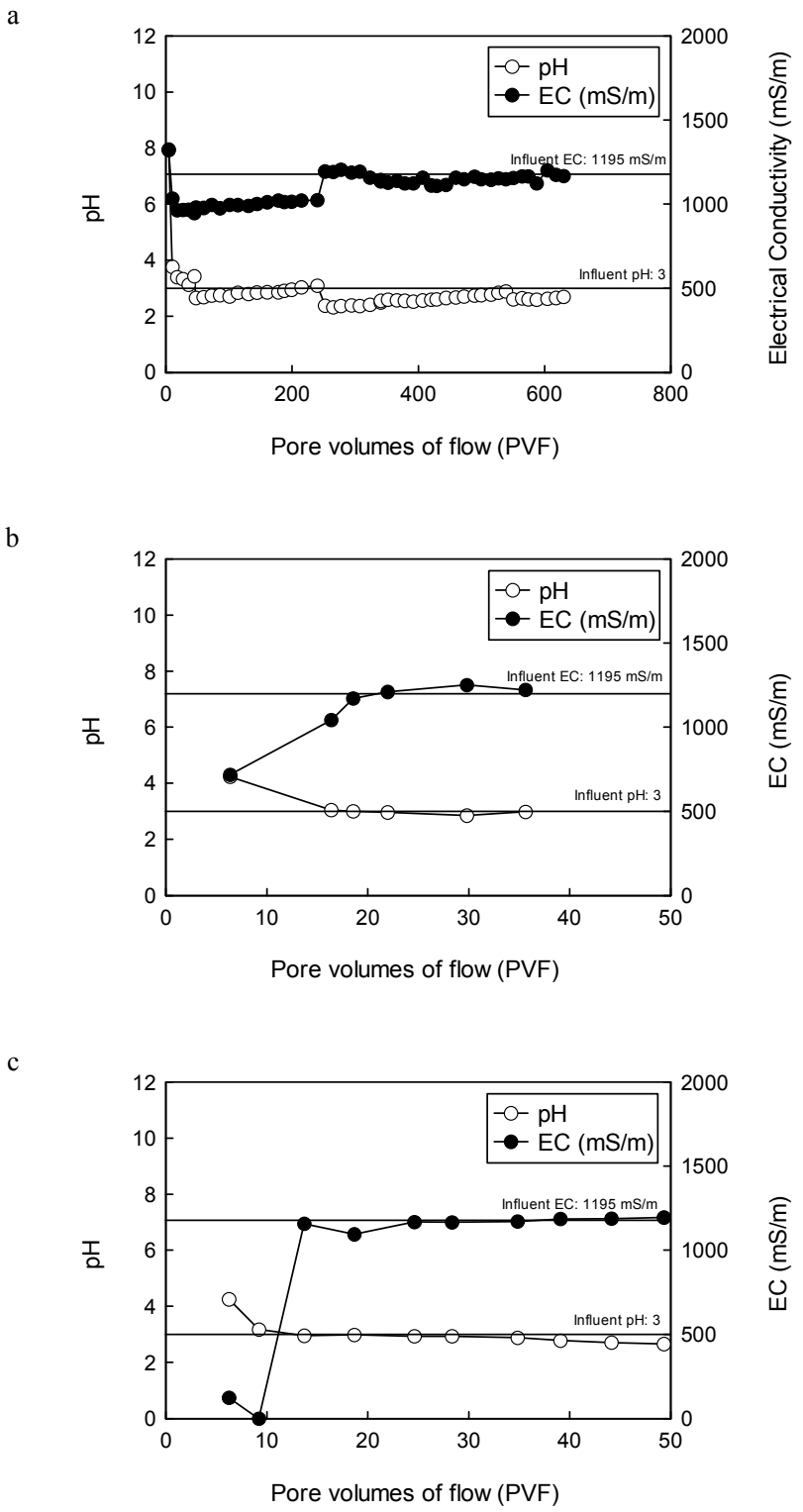

Figure 5-53 pH and EC of effluents after ARD permeation (a) GCL, (b) zeolite, and (c) ferrihydrite

a

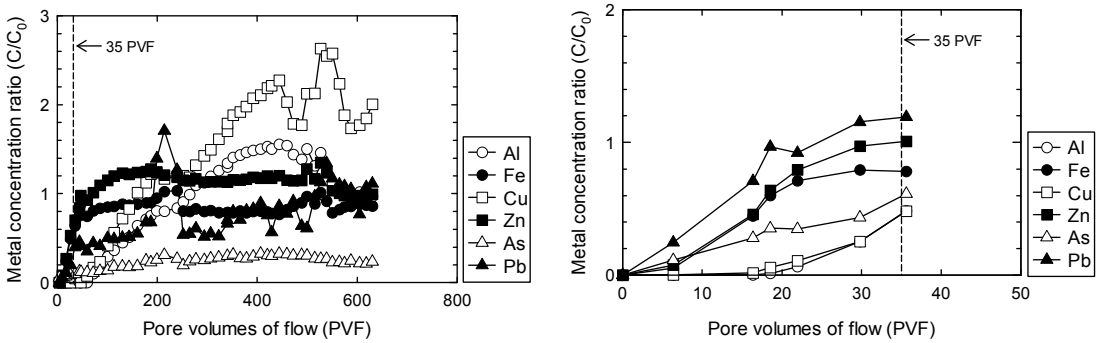

b

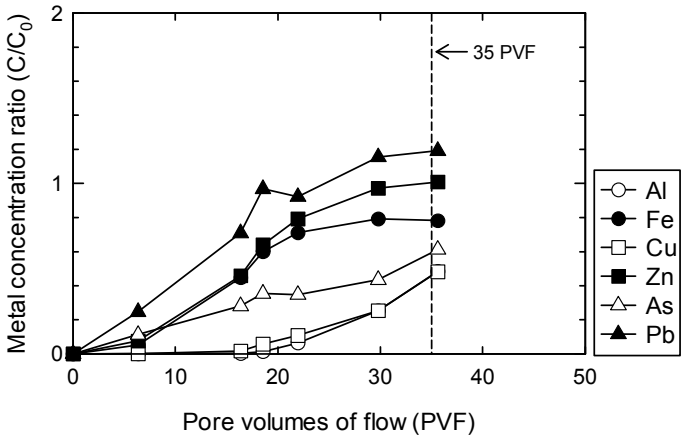

c

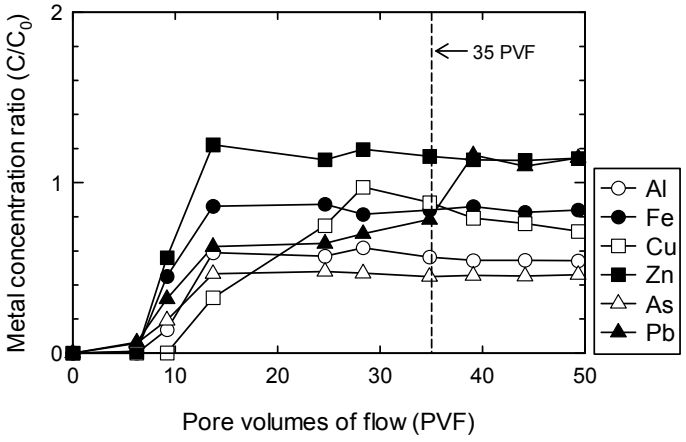

Figure 5-54 Effluent analysis after ARD permeation (a) GCL, (b) zeolite, and (c) ferrihydrite

The removal or sorption of metals in multiple-species occur either through ion exchange (bentonite and zeolite), or specific binding to the surface (ferrihydrite). In the latter, heavy metals are sorbed from the solution without releasing other ion in equivalent proportion as it happens in the ion exchange mechanism. In both mechanisms, the selectivity is determined by the strength of electrostatic forces. Thus, metal

Table 5-6 Metal sorption capacity at 35 PVF from effluent analysis in hydraulic conductivity test

Metal	Bentonite (mg/g bentonite)	Zeolite (mg/g zeolite)	Ferrihydrite (mg/g ferrihydrite)
Al	2.3	1.1	1.0
Fe	26	10.9	13.4
Cu	0.7	0.4	0.3
Zn	2.8	0.9	0.8
As	0.05	0.01	0.02
Pb	0.01	0.001	0.005

sorption is governed by the ion valence of cations, the free energy of hydration of the cations, molecular size, and hydrated radius of cations. In that case, the order would be Al > Fe > Cu > Zn > Pb. However, these results differ slightly from what it was observed in experiments. This is probably due to the competition among metals for binding sites, the difference in metal concentration, and other mechanisms such as precipitation. Table 5-6 shows the amount of metal sorbed on bentonite, zeolite, and ferrihydrite taking into consideration the amount of mineral used in each case. After similar amounts of PVF (35 PVF), more metal retention was observed for bentonite than zeolite and ferrihydrite. However, according to the results presented in Table 5-6, none of them had reached the maximum sorption capacity (Table 5-5), except for the zeolite-Al system. For bentonite, the difference between single metal sorption test results and ARD sorption results are between 0 – 37%, for zeolite it ranges between 0.1 and 46%, whereas for ferrihydrite, it ranges between 1 and 32%, being lower in case of ARD compared to single metals because of metal competition. This may indicate that the values obtained in sorption tests were overestimated or the contact time between minerals and metals were not enough to favor sorption mechanisms. In case of bentonite, for Cu, it was observed that the ratio went up to 2, which can be attributed to the release of Cu that was sorbed into the GCL during the prehydration process with ARD solution.

5.9 Summary and Conclusions for this Chapter

All ARDs around the world are different in acidity and metal concentrations. They usually represent a threat to groundwater and surface water at mining sites because of their extremely low pH and high metal content. This chapter summarizes the metal retention capacity of GCL (bentonite), zeolite, and ferrihydrite in terms of single metal, bi-metal, and ARD sorption tests. The effluent after hydraulic conductivity was also evaluated in this chapter. For GCL, 10 ARDs were tested, whereas for zeolite and ferrihydrite, only

the most severe case of ARD (ARD 747) was tested. Besides, the effect of buffering capacity, pH, metal ions, solid-liquid ratio as well as the effect of metal concentration in sorption capacity of GCL (bentonite) was more deeply studied in this chapter.

From single metal time step batch sorption tests using bentonite, zeolite, and ferrihydrite, information about the time to reach equilibrium (6 hours in majority of the cases), the mechanisms that are involved in metal uptake (ion exchange, surface complexation, and precipitation), and the metal sorption capacity against single and complex mixture of metals were obtained. The sorption capacity of bentonite, zeolite, and ferrihydrite against single metals and complex mixtures differ and depends on the metal competition and metal affinity. For bentonite, the difference between single metal sorption test results and ARD sorption results are between 0 – 37%, for zeolite it ranges between 0.1 and 46%, whereas for ferrihydrite, it ranges between 1 and 32%, being lower in case of ARD compared to single metals because of metal competition.

From studies of the structure of the minerals, presented in Chapter 2, and some evidence from the experimental results (such as the release of Na, K, Ca, and Mg), it can be inferred that the heavy metal uptake on bentonite, zeolite, and ferrihydrite can be attributed to ion exchange processes (for bentonite and zeolite) and surface complexation (for ferrihydrite). However these are not the only mechanisms that occur. Although it was not possible to determine the proportion between sorption and precipitation, the latter mechanism also plays an important role in metal mobilization.

From single metal batch sorption tests, it was observed that bentonite has no sorption capacity towards As. However, in the sorption test with ARD (ARD 747) and in the effluent analysis after hydraulic conductivity against ARD 747, the As concentration was kept below the influent through the duration of the tests. This phenomenon was attributed to a secondary retention mechanism in other metals present in ARD such as Al, Fe, Cu, Zn, Pb. Results of bi-metal sorption of As against different metals show that at 1 mM of metal (metal-As relationship 1:1), the sorption of As on bentonite (2 g/L bentonite) increased from 0% to 71, 31, 51, 63, and 67 percent in presence of Fe, Cu, Al, Zn, and Pb, respectively, which indicates that As has affinity for the metals in the following order: Fe > Pb > Zn >Al > Cu. Moreover, it was found that as the concentration of the second metal increases, the amount of As decreases. On the contrary, the affinity of As towards alkaline metals was very low. At 1 mM (metal-As relationship 1:1), the sorption of As was 3 percent in presence of Ca and 0 percent in presence of Mg, K and Na. The mechanism for As retention from other metals was also proposed in this chapter. Further research on the mechanism such as using sequential extraction may help confirm the proposed mechanisms.

Results presented in this chapter show that bentonite, zeolite, and ferrihydrite can be used effectively for removal of metal cations present in ARD. These materials provide an alternative for barriers against rock leachates with high heavy metal content. However, among all these minerals, it was found that bentonite is a better sorbent for Cu, Fe, Zn, Al, and Pb, with ferrihydrite suitable for As retention. Although, based on the cation exchange capacity (CEC), bentonite has a limited metal buffering capacity, its low hydraulic conductivity value make bentonite a suitable material for waste rock containment facilities with potential of ARD generation.

6 PRACTICAL IMPLICATIONS

A relatively new and cost-effective measure to minimize migration of contaminants in waste containment facilities and embankments is the construction of an adsorption layer using readily or locally available materials. The performance of adsorbent materials should be carefully examined beforehand in order to guarantee effective long term barrier performance. Moreover, the use of certain materials as adsorption layer in the field should be determined not only by chemical compatibility, but also by the availability of the material, the type of contaminants that may leach from rocks, and the price of the materials, including the cost of transportation and installation.

As the construction of an adsorption layer involves the use and transport of a large amount of materials, the choice of the latter has a large impact on the cost. Thus, the possibility of mixing zeolite and ferrihydrite (GCL is already a commercial material) with local soil or material generated in excavation sites in different proportions (such as 5, 10 or even higher percentages) should be evaluated as part of future research.

In this chapter, field applications of the findings from both the database and experimental work of this research are presented. Moreover, predictions of hydraulic conductivity and metal retention are also shown in this chapter, based on total monovalent, divalent, and trivalent cations, as well as metal transport through mineral barriers.

6.1 ARD in the World according to the Type of Mine

Considering that ARDs in the world are highly variable in terms of pH, and cation and anion concentrations, a database that collects several ARD compositions from different parts of the world constitutes a useful tool to estimate the leaching amount of chemicals depending on the type of mine and other factors.

Besides, the relationships between sulfate and EC, sulfate and pH, and sulfate with heavy metals that are usually present in ARDs (reported in Chapter 3) constitute useful tools to predict the composition of ARDs in the field by only measuring EC and pH. These two parameters are easy to measure in-situ by using a portable conductimeter and pH-meter, respectively.

In case that ARD potential generation from rocks samples need to be studied, laboratory tests, such as leaching test is recommended. For the leaching test, there are several methods available. One such method is the Japanese Leaching Test (JLT No 46), established by the Japanese Environmental Agency in 1995 for liquid/solid ratio (L/S) = 10:1. For this method, 6 hours shaking is required, followed by filtration using a 0.45 μm opening membrane filter and finally measurement of certain parameters such as EC, metal and anion concentrations. Hattori et al. (2003) proposed a simplified leaching test. For this method, samples are crushed to grain smaller than 10 mm in size after being dried. Portions of 100 g of the crushed samples are mixed with 500 mL of distilled water and shaken for 3 minutes. The pH, EC, and metal concentration of the leachates are measured after 24 hours, 7 days, 28 days, and 56 days.

Table 6-1 Average pH, sulfate, and metal concentration according to the type of mine

	Arsenic	Coal	Gold	Leachate	Metal	Polymetallic	Phosphate	Sulfide
pH	4.2 ±0.6	4.9 ±0.1	5.5 ±0.2	3.8 ±0.4	4.1 ±0.3	5.1 ±0.1	3.4 ±0.6	3.3 ±0.6
EC (mS/m)	51.8 ±132	147 ±41.1	391 ±52.2	462 ±72.7	372 ±115.8	330 ±27.4		402 ±295.3
Sulfate (mg/L)	190 ±10534	988 ±3362	1748 ±3882	1900 ±20171	2217 ±5823	7448 ±2279	15308 ±11048	11537 ±11646
Al (mg/L)	4.8 ±135	33.9 ±42.7	227 ±83.2	38.7 ±135	153 ±73.6	189 ±29.5	1018 ±141.6	46.5 ±149.3
As (mg/L)	0.06 ±7.6	0.03 ±2.4	2.4 ±2.5	3.1 ±4.9	1.2 ±5.6	3.5 ±1.7	84.2 ±8.0	0.1 ±14.5
Cu (mg/L)	0.02 ±64.1	10.1 ±23.2	2.3 ±18.7	6.0 ±36.4	20.2 ±30.6	43.8 ±11.5		0.2 ±76.6
Fe (mg/L)	2.1 ±1536.3	85.4 ±413.3	146 ±588.4	644 ±930.3	525 ±805.7	951 ±293.7	4305 ±1611.3	1908 ±1611.3
Pb (mg/L)		0.02 ±3.6	0.2 ±0.7	0.36 ±1.3	0.34 ±1.5	2.38 ±0.5	1.62 ±2.3	
Zn (mg/L)		18.5 ±286.4	3.0 ±255.0	185 ±467.7	23.1 ±383.9	814 ±153.4	359 ±849.7	1.3 ±1015.6
Ca (mg/L)	26.1 ±48.2	98.7 ±18.8	198 ±17.2	268 ±29.2	136 ±30.2	146 ±10.6		164 ±65.2
K (mg/L)	1.0 ±10.1	4.0 ±4.4	20.0 ±5.2	12.2 ±6.7	2.9 ±6.4	3.9 ±2.7		7.0 ±13.7
Mg (mg/L)	7.3 ±186.8	38.0 ±71.5	172 ±91.4	117 ±113.1	10 ±117.1	333 ±41.3		55.6 ±252.9
Na (mg/L)	5.6 ±58.0	22.1 ±25.3	198 ±21.2	17.0 ±37.0	18.2 ±36.4	27.3 ±15.6		33.7 ±78.5

Table 6-1 summarizes the average pH, and sulfate and metal concentrations according to the type of mine (arsenic, coal, gold, leachate, metal, polymetallic, phosphate, and sulfide) and also presents the standard deviation of the respective values.

6.2 Hydraulic Conductivity Prediction

From Chapter 4, hydraulic conductivity for different ARD compositions and relationships between swell index and hydraulic conductivity, EC and hydraulic conductivity, and pH and hydraulic conductivity

were presented. In Chapter 5, the influence of metal concentration in the metal retention in mineral barriers as well as metal competition was studied. However, the relationship between metal concentration and hydraulic conductivity was not studied, nor was the effect of the ARD metal composition in the hydraulic conductivity discussed. In this section, an approach to combine these two parameters is discussed in terms of the effect of total monovalent, divalent, and trivalent cations on hydraulic conductivity.

The monovalent ions in this research are Na and K, whereas the divalent cations are Ca, Fe, Pb, Cu, Mg, and Zn. The trivalent metal is Al. All cation concentrations were reported in mM. Table Table 6-2 shows the total monovalent cations (TMC), total divalent cations (TDC), total trivalent cations (TTC), and sum of total divalent and trivalent cations (TDTC) for each ARD used in experiments. From Figure 6-1, it can be assumed that there is not a clear relationship between total monovalent cations and hydraulic conductivity. However, from Figure 6-2, Figure 6-3 and Figure 6-4, it can be observed that as the total divalent, trivalent, and sum of divalent and trivalent increase, the hydraulic conductivity also increases. The direct relationship between total divalent, trivalent, and sum of divalent and trivalent cations against hydraulic conductivity was obtained for each case and is as follows:

- For TDC: $k = 8\times10^{-12}e^{0.021(TDC)}$
- For TTC: $k = 1\times10^{-11}e^{0.1612(TTC)}$
- For TDTC: $k = 8\times10^{-12}e^{0.0192(TDTC)}$

Table 6-2 Total monovalent, divalent and trivalent cations for 10 ARDs

ARD	Total monovalent cations (mM)	Total divalent cations (mM)	Total trivalent cations (mM)	Sum of divalent and trivalent cations (mM)	k (m/s)
248	0.6	31.5	0.0	31.5	1.16×10^{-11}
406	0.0	0.1	0.0	0.1	1.07×10^{-11}
625	1.1	25.8	0.9	26.7	1.17×10^{-11}
747	2.8	112.6	10.1	122.7	9.64×10^{-11}
512	0.6	29.7	4.6	34.3	1.28×10^{-11}
718	0.6	31.5	0.0	31.5	1.26×10^{-11}
684	0.7	20.1	4.4	24.6	9.52×10^{-12}
222	17.2	11.7	0.0	11.7	1.19×10^{-11}
220	14.5	14.9	0.0	14.9	1.12×10^{-11}
246	1.8	20.2	0.0	20.2	1.32×10^{-11}

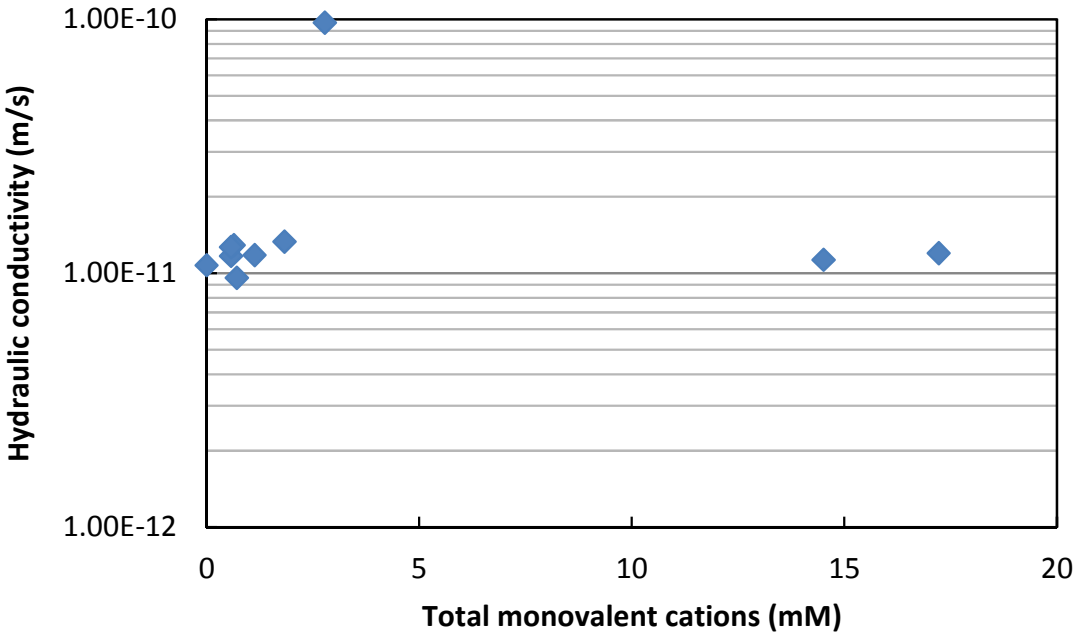

Figure 6-1 Hydraulic conductivity variation at different total monovalent cations

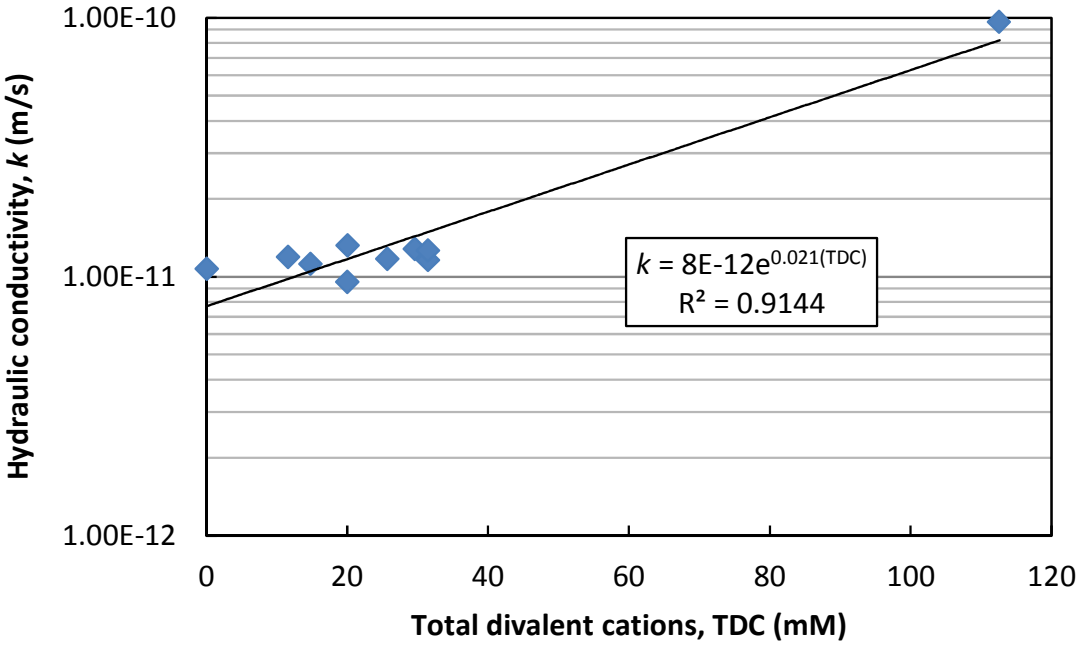

Figure 6-2 Hydraulic conductivity variation at different total divalent cations

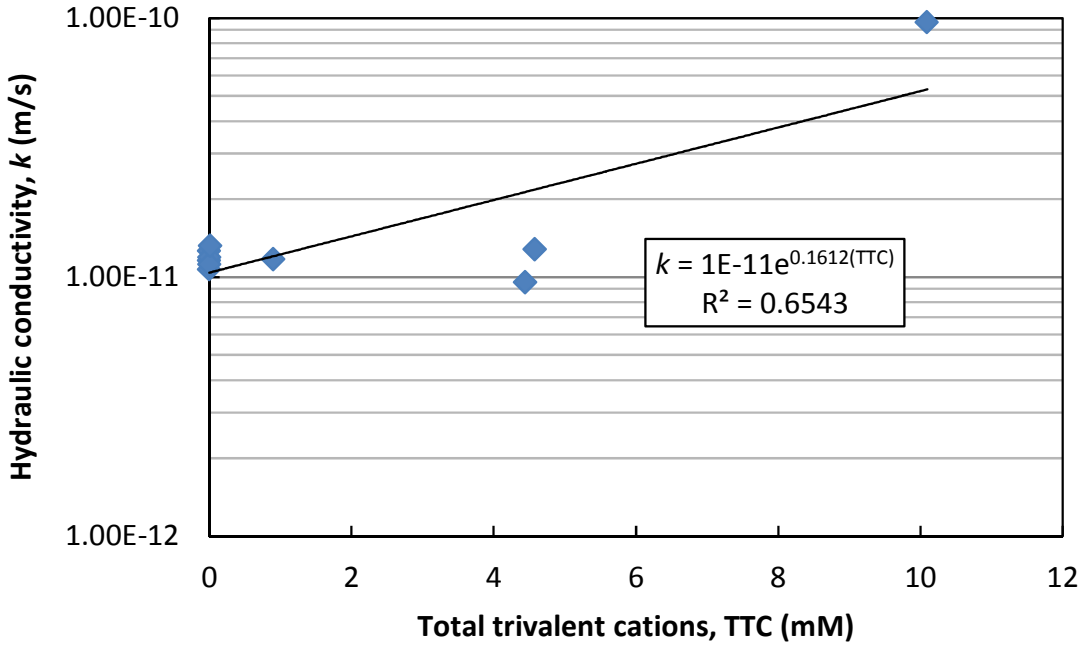

Figure 6-3 Hydraulic conductivity variation at different total trivalent cations

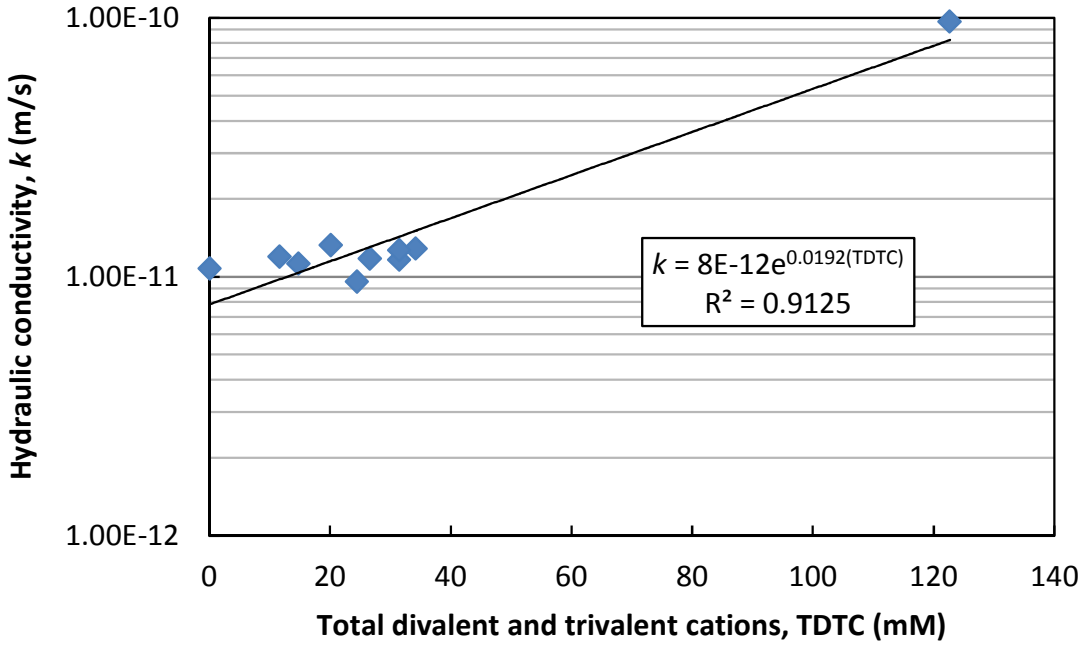

Figure 6-4 Hydraulic conductivity variation at different total divalent and trivalent cations

6.3 Barrier Performance Prediction against Natural Leakage

GCLs show advantages over conventional bottom liners because of cost-effectiveness and ease of installation. GCLs have low hydraulic conductivity and high self-healing capacity. Sodium bentonite, contained inside the GCL, is comprised mainly of montmorillonite, a layered clay mineral with sodium ions located in between. Montmorillonite has the ability to swells up to 15 times its own volume in water, becoming a dense mass with no individual particles. Besides, natural environmental stresses like freeze/thaw and desiccation/rewetting cycles have no effect on sodium bentonite's performance.

Hydraulic conductivity is an important parameter that measures water flow through a soil layer or that of another material. Flow (volume/time) is another essential parameter that calculates the quantity of leakage through a soil or barrier layer. Flux is a very helpful parameter that provides information about the rate of flow per unit area per unit time through a soil or barrier layer, typically expressed in $m^3/m^2/s$ or L/ha/year. Hydraulic conductivity only provides a relative indication of the performance of the mineral barrier or barrier layer. However, this is not a direct measure of leakage and, thus, if the expected performance of a product is to be determined, total leakage is the best parameter to be evaluated. Comparing total leakage between two barrier systems allows determining which one has superior performance. Total leakage may either be measured directly or calculated using Darcy's Law:

$$Q = kiA$$

where, Q = total leakage (m^3/s), k = hydraulic conductivity (m/s), i = hydraulic gradient (m/m or (hydraulic head + barrier thickness) / barrier thickness), A = area through which flow occurs (m^2) as shown in Figure 6-5. Because most GCL applications involve replacing a compacted clay liner (CCL) of specified thickness and permeability, the above equation can be used to quantify the theoretical performance of the CCL such that a design comparison can be made. Also it can be used to compare the performance of GCL over zeolite and ferrihydrite. For simplicity of analysis, we will study an area of one hectare (10,000 m^2), with an ARD hydraulic head of 0.3 m, and zeolite and ferrihydrite layer thickness of 0.5 m. The total leakage can be calculated as shown in Table 6-3.

Table 6-3 Total leakage per year for bentonite, zeolite and ferrihydrite

	Bentonite	Zeolite	Ferrihydrite
k (m/s)	1.40×10^{-11}	3.00×10^{-10}	7.30×10^{-10}
H (m)	0.3	0.3	0.3
L (m)	0.006	0.5	0.5
A (m^2)	10000	10000	10000
Q ($m^3/m^2/s$)	7.14×10^{-6}	4.8×10^{-6}	1.168×10^{-5}
Q (L/ha/year)	225167.0	151372.8	368340.5
Total mass/ha	4670g/m^2 46,7 ton/ha	Assuming 50 cm height Max. dry density: 1.04 g/cm^3 5217 ton/ha	Assuming 50 cm height Max. dry density: 1.08 g/cm^3 5404 ton/ha

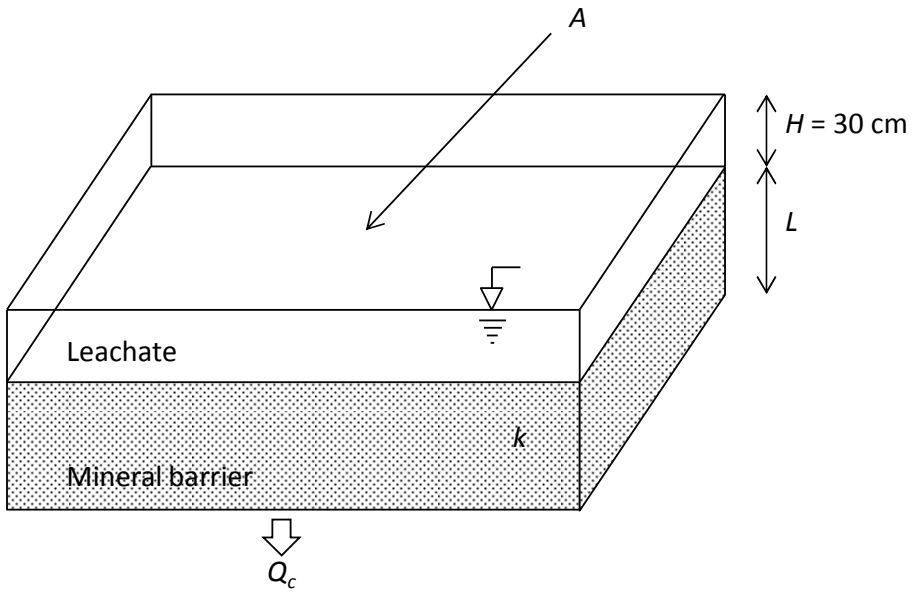

Figure 6-5 Schematic design of a rock containment facility

Considering the composition of the 10 ARDs used in this research as shown in Table 6-4 and the sorption capacity of each mineral summarized in Table 6-5, the expected service life for each material according to the type of mineral and metal can be calculated as shown in Table 6-6, Table 6-7 and Table 6-8. For the most severe case of ARD used in this research (ARD 747) it was calculated that the GCL service life would be 1 year, whereas zeolite and ferrihydrite would be effective for approximately 130 and 170 years, respectively. However, this is a very simplified calculation considering only sorption capacity and advection. Besides, the calculations were strictly done for a period with no leakage from rock containments. In other words, it represents the time in which the sorption capacity of the mineral barrier would be depleted. This calculation does not consider diffusion of contaminants and mass flux. In addition to this, while heavy metals can leach from the containment areas, the underground water flow will dilute the metal released and, thus, the concentration will be reduced and may fulfill the requirements of the Environmental Standards. Therefore, mass flux calculations need to be considered as part of a future research.

Table 6-4 Heavy metal composition of 10 ARDs selected from the database

	ARD 248	ARD 406	ARD 625	ARD 512	ARD 747	ARD 718	ARD 684	ARD 222	ARD 220	ARD 246
Al	0.1	0.01	24.33	123.63	272.42	0.1	120.01	0.18	0.16	0.47
Fe	1304.02	1.87	777.76	1598.44	4591.14	1304.02	931.97	1.02	0.03	0
Cu	12.02	0.95	0.98	0.08	96.33	12.02	96.66	0	0	0
Zn	133.4	5	64.86	70.04	536.37	133.4	4.81	0.11	0	0
As	0.65	0.15	0.72	9.59	1.85	0.65	1.13	0.3	0.36	0.4
Pb	0.28	0	0.26	0.55	2.3	0.28	0.27	0.16	0.14	0.2

Table 6-5 Single, bi-metal, ARD sorption tests and effluent from hydraulic conductivity test

		Bi-metal from 1mM : 1mM								
		Single metal (mg/g)	Al	Fe	Cu	Zn	As	Pb	Sorption ARD 747 (mg/g)	Effluent ARD 747 (mg/g)
Bentonite	Al	13.2	1*	1:0.4	1:0.4	1:0.3	1:0.5	1:0.8	3.3	2.3
	Fe	71.0		1*	1:0.6	1:0.4	1:0.7	1:0.8	111.1	26.0
	Cu	93.7			0.6*	0.9:0.3	1:0.4	0.7:0.9	1.4	0.7
	Zn	47.1				0.9*	1:0.6	0.4:1	5.3	2.8
	As	0.6					0.0*	0.6:1	0.8	0.1
	Pb	0.0						1*	0.1	0.01
Zeolite	Al	1.0							2.3	1.1
	Fe	23.7							102.6	10.9
	Cu	43.1							0.8	0.4
	Zn	13.1							18.6	0.9
	As	0.9							0.4	0.01
	Pb	1.1							0.3	0.001
Ferrihydrite	Al	3.1							0.2	1.0
	Fe	0.0							34.1	13.4
	Cu	22.4							0.0	0.3
	Zn	17.7							0.7	0.8
	As	2.3							0.4	0.0
	Pb	0.3							0.00	0.01

* Corresponds to sorbed percentage of 2 mM solution

Table 6-6 Period in years with no leakage in a 1 ha rock containment with GCL

	ARD 248	ARD 406	ARD 625	ARD 512	ARD 747	ARD 718	ARD 684	ARD 222	ARD 220	ARD 246
Al	27377	273770	113	22	10	27377	23	15209	17111	5825
Fe	11	7875	19	9	3	11	16	14437	490850	
Cu	1617	20456	19830	242919	202	1617	201			
Zn	73	1954	151	139	18	73	2031	88806		
As	191	830	173	13	67	191	110	415	346	311
Pb	7		8	4	1	7	8	13	15	10
ARD*	7	830	8	4	1	7	8	13	15	10

* Duration of GCL in years considering all metals

Table 6-7 Period in years with no leakage in a 1 ha rock containment with zeolite

	ARD 248	ARD 406	ARD 625	ARD 512	ARD 747	ARD 718	ARD 684	ARD 222	ARD 220	ARD 246
Al	344633	3446325	1416	279	127	344633	287	191463	215395	73326
Fe	626	436780	1050	511	178	626	876	800764	27225969	
Cu	123575	1563543	1515680	18567077	15420	123575	15367			
Zn	3384	90294	6961	6446	842	3384	93882	4104260		
As	47718	206780	43079	3234	16766	47718	27432	103390	86158	77542
Pb	209241		225337	106523	25473	209241	214463	366172	418482	292938
ARD*	626	90294	1050	279	127	626	287	103390	86158	73326

* Duration of zeolite in years considering all metals

Table 6-8 Period in years with no leakage in a 1 ha rock containment with ferrihydrite

	ARD 248	ARD 406	ARD 625	ARD 512	ARD 747	ARD 718	ARD 684	ARD 222	ARD 220	ARD 246
Al	454798	4547975	1869	368	167	454798	379	252665	284248	96765
Fe	NA	NA	NA	NA	NA	NA	NA	NA	NA	NA
Cu	27340	345924	335335	4107849	3411	27340	3400			
Zn	1947	51935	4004	3708	484	1947	53999	2360679		
As	51912	224954	46865	3519	18239	51912	29843	112477	93731	84358
Pb	17815		19185	9069	2169	17815	18259	31176	35629	24941
ARD*	1947	51935	1869	368	167	1947	379	31176	35629	24941

* Duration of ferrihydrite in years considering all metals

Another important factor to consider is metal release from the containment and how this will impact on the groundwater. For this purpose, chemical transport of bentonite, zeolite, and ferrihydrite was calculated. Because bentonite, zeolite, and ferrihydrite have relatively low hydraulic conductivity, dispersive and advective transport must be considered. The 1D advection-dispersion equation that accounts for adsorption can be expressed as:

$$\left(1+\frac{\rho_d K_p}{n}\right)\frac{\partial c}{\partial t} = D\frac{\partial^2 c}{\partial x^2} - v_s\frac{\partial c}{\partial x} \tag{5.12}$$

where c is the concentration of the solute, ρ_d the dry density of the clay, n the porosity of the clay, K_P the clay-solute partition coefficient, D the dispersion coefficient for the solute, and v_s the seepage velocity. The

term ($1 + \rho_d K_p/n$) is called retardation factor. Bottom liners placed above the groundwater table are generally unsaturated. However, if seepage is assumed to be steady-state and suction existing at the bottom of the liner is ignored, the transport calculations can be performed easily. If the soil properties are assumed to be homogeneous and time invariant, and no chemical reactions occur, then the concentration of the solute at the bottom liner at time t can be obtained by the following equation (Ogata and Banks 1961; Shackelford 1990; Katsumi et al. 2001):

$$\frac{c(x=L,t)}{c_0} = 0.5\left\{\operatorname{erfc}\left[\frac{1-T_R}{2\sqrt{T_R/P_L}}\right]\right\} + \exp(P_L)\ \operatorname{erfc}\left[\frac{1+T_R}{2\sqrt{T_R/P_L}}\right] \tag{5.13}$$

where L is the thickness of the bottom liner and x the vertical downward coordinate with the origin at the surface of the liner. The parameter T_R is the dimensionless time factor:

$$T_R = \frac{v_S t}{RL} \tag{5.14}$$

and P_L is the Peclet number:

$$P_L = \frac{v_S L}{D} \tag{5.15}$$

The Peclet number represents the relative magnitudes of advective and dispersive transport, with dispersion becoming more important as P_L becomes smaller. The initial and boundary conditions are $c(0, t) = c_0$, $c(x, 0) = 0$ (for $x > 0$), and $\delta c(\infty, t)\delta/x = 0$. The last boundary condition implies that the concentration gradient $\delta c/\delta x$ is negligible for distances far ($x=\infty$) (Katsumi et al. 2001).

Table 6-9 shows the parameters used to calculate the chemical transport of heavy metals through minerals. The hydraulic conductivity was obtained from experiments (reported in Chapter 4), the water head of the ARD leachate above the liner (H) was assumed to be 30 cm and the thickness of the mineral barrier (L) was considered to be 0.6 cm for GCL (provided by the company), and 50 cm for both zeolite and ferrihydrite which are reasonable thickness to be applied in the field. The porosity (n) of each material was obtained from void ratio (e) which was obtained from experiments. The dry density (ρ_d) was determined by using a pycnometer, the dispersion coefficient (D) was obtained from a chemistry and physics handbook (Lide 2001-2002) and the partition coefficient (K_p) was calculated from single metal sorption tests at different metal concentrations (1μ M to 10 mM) and 0.1 g of mineral as presented in Chapter 5. As part of future research, the K_p value should be considered using bi-metal or polymetallic mixtures of metals. In this research, for simplicity, only single metal were considered, neglecting the interactions between metals (e.g. the role of metals in As retention), lower sorption capacity due to the presence of other metals, precipitation mechanisms, etc. Although this method has its limitations, it provides a broad idea about the chemical transport with time.

Table 6-9 Parameters used to calculate chemical transport

		Bentonite	Zeolite	Ferrihydrite
k (cm/h)		5.04×10^{-6} (1.40×10^{-11} m/s)	1.08×10^{-4} (3.00×10^{-10} m/s)	2.63×10^{-3} (7.30×10^{-10} m/s)
H (cm)		30	30	30
L (cm)		0.6	50	50
n		0.357	0.686	0.811
ρ_d (g/cm^3)		2.185	2.33	3.506
D (cm^2/h)	Al	0.0195		
	As	0.0326		
	Cu	0.0257		
	Fe	0.0217		
	Pb	0.034		
	Zn	0.0253		
K_p (mL/g)	Al	1844.6	218.2	63.3
	As	17.7	7.7	32
	Cu	152.7	60.5	192.1
	Fe	148.1	41.9	
	Pb	0.9	88.9	212.6
	Zn	577.5	18.4	25.7

Figure 6-6 shows the result of chemical release at bottom liners for different metals. It can be said that zeolite and ferrihydrite show a better metal retention capacity due to the thickness of the material (50 cm). However, in the field, these materials tend to be expensive if they are placed as pure materials and therefore mixing with soil (amended soil) should be considered as part of future research. For Pb, a rapid release was observed for bentonite that can be attributed to a low K_p value found for bentonite in presence of Pb.

Having this information, it is easy to predict the metal release per year and the concentration in the groundwater. For simplification purposes, the depth of the groundwater was assumed to be constant and equal to 10 m, the porosity equal to 0.4, and the groundwater velocity to 45 m/s (Figure 6-7 and Table 6-10). The results of the final concentrations in the aquifer are presented in Table 6-11, Table 6-12 and Table 6-13 for GCL, zeolite, and ferrihydrite respectively for 1 year of service. Table 6-14, Table 6-15, and Table 6-16 show the results of final concentrations in the aquifer after 10 years of service.

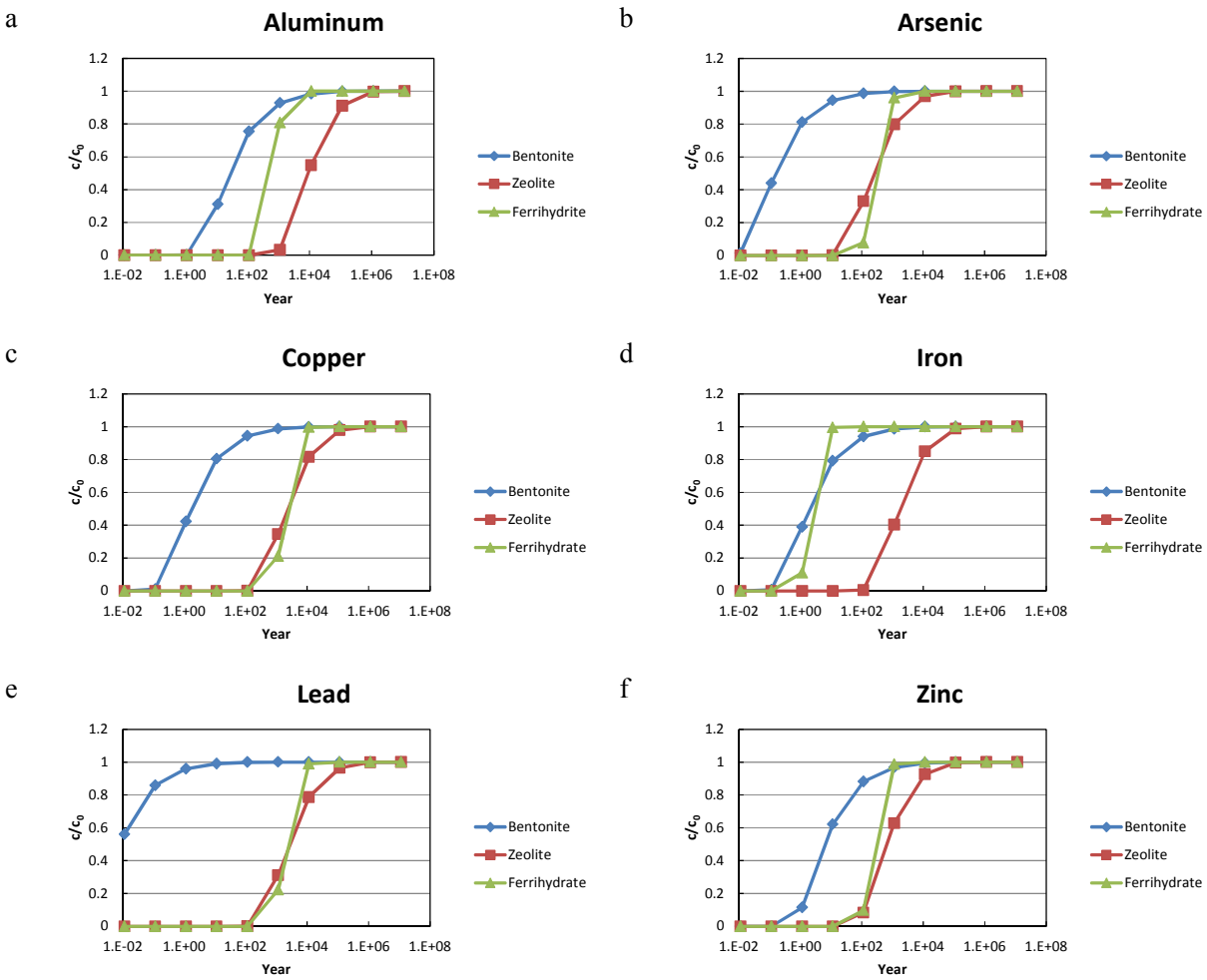

Figure 6-6 Chemical release prediction for bentonite, zeolite and ferrihydrite

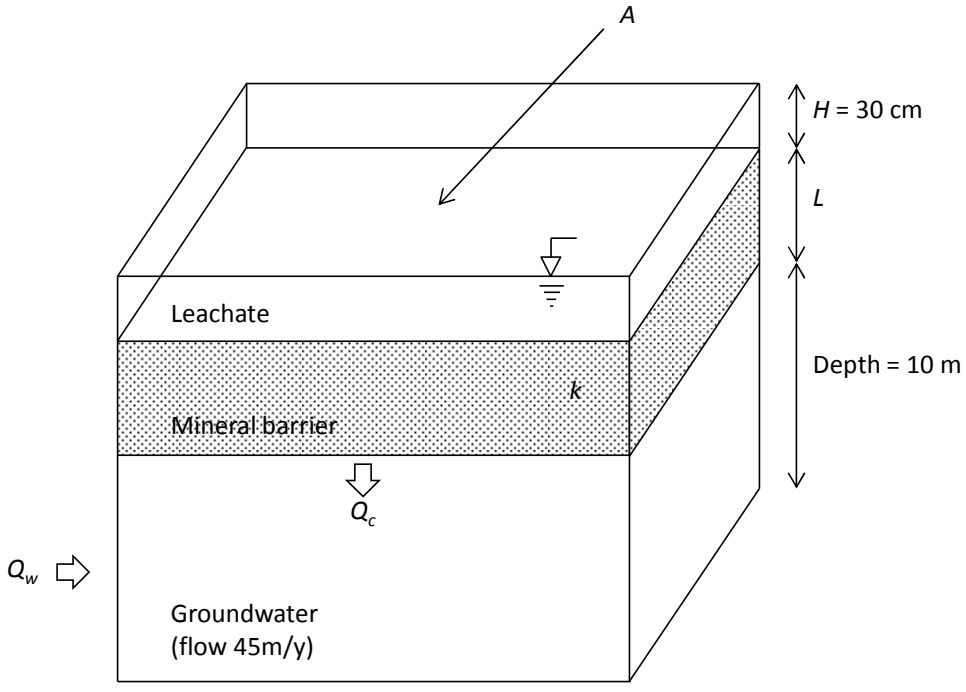

Figure 6-7 Schematic design of a rock containment facility considering groundwater flow

Table 6-10 Parameters used for metal concentration after sorption capacity depletion of mineral

Parameter	Value
Volume below containment (m^3)	100000
Porosity of the soil	0.4
Effective water below (m^3)	40000
Velocity (m/year)	45
Length of containment (m)	100
Years to renew the water	2.2

Table 6-11 Metal concentration in groundwater after 1 year using GCL

	ARD 248	ARD 406	ARD 625	ARD 512	ARD 747	ARD 718	ARD 684	ARD 222	ARD 220	ARD 246
Al	0.0	0.0	0.0	0.0	0.0	0.0	0.0	0.0	0.0	0.0
Fe	6.4	0.0	3.8	7.8	22.4	6.4	4.5	0.0	0.0	0.0
Cu	0.1	0.0	0.0	0.0	0.5	0.1	0.5	0.0	0.0	0.0
Zn	0.2	0.0	0.1	0.1	0.8	0.2	0.0	0.0	0.0	0.0
As	0.007	0.002	0.007	0.097	0.019	0.007	0.011	0.003	0.004	0.004
Pb	0.003	0.000	0.003	0.007	0.028	0.003	0.003	0.002	0.002	0.002

Table 6-12 Metal concentration in groundwater after 1 year using zeolite

	ARD 248	ARD 406	ARD 625	ARD 512	ARD 747	ARD 718	ARD 684	ARD 222	ARD 220	ARD 246
Al	0.0	0.0	0.0	0.0	0.0	0.0	0.0	0.0	0.0	0.0
Fe	0.0	0.0	0.0	0.0	0.0	0.0	0.0	0.0	0.0	0.0
Cu	0.0	0.0	0.0	0.0	0.0	0.0	0.0	0.0	0.0	0.0
Zn	0.0	0.0	0.0	0.0	0.0	0.0	0.0	0.0	0.0	0.0
As	0.000	0.000	0.000	0.000	0.000	0.000	0.000	0.000	0.000	0.000
Pb	0.000	0.000	0.000	0.000	0.000	0.000	0.000	0.000	0.000	0.000

Table 6-13 Metal concentration in groundwater after 1 year using ferrihydrite

	ARD 248	ARD 406	ARD 625	ARD 512	ARD 747	ARD 718	ARD 684	ARD 222	ARD 220	ARD 246
Al	0.0	0.0	0.0	0.0	0.0	0.0	0.0	0.0	0.0	0.0
Fe	0.0	0.0	0.0	0.0	0.0	0.0	0.0	0.0	0.0	0.0
Cu	0.0	0.0	0.0	0.0	0.0	0.0	0.0	0.0	0.0	0.0
Zn	0.0	0.0	0.0	0.0	0.0	0.0	0.0	0.0	0.0	0.0
As	0.000	0.000	0.000	0.000	0.000	0.000	0.000	0.000	0.000	0.000
Pb	0.000	0.000	0.000	0.000	0.000	0.000	0.000	0.000	0.000	0.000

Table 6-14 Metal concentration in groundwater after 10 years using GCL

	ARD 248	ARD 406	ARD 625	ARD 512	ARD 747	ARD 718	ARD 684	ARD 222	ARD 220	ARD 246
Al	0.0	0.0	0.1	0.5	1.1	0.0	0.5	0.0	0.0	0.0
Fe	12.9	0.0	7.7	15.8	45.5	12.9	9.2	0.0	0.0	0.0
Cu	0.1	0.0	0.0	0.0	1.0	0.1	1.0	0.0	0.0	0.0
Zn	1.0	0.0	0.5	0.5	4.2	1.0	0.0	0.0	0.0	0.0
As	0.008	0.002	0.009	0.113	0.022	0.008	0.013	0.004	0.004	0.005
Pb	0.003	0.000	0.003	0.007	0.028	0.003	0.003	0.002	0.002	0.002

Table 6-15 Metal concentration in groundwater after 10 years using zeolite

	ARD 248	ARD 406	ARD 625	ARD 512	ARD 747	ARD 718	ARD 684	ARD 222	ARD 220	ARD 246
Al	0.0	0.0	0.0	0.0	0.0	0.0	0.0	0.0	0.0	0.0
Fe	0.0	0.0	0.0	0.0	0.0	0.0	0.0	0.0	0.0	0.0
Cu	0.0	0.0	0.0	0.0	0.0	0.0	0.0	0.0	0.0	0.0
Zn	0.0	0.0	0.0	0.0	0.0	0.0	0.0	0.0	0.0	0.0
As	0.000	0.000	0.000	0.000	0.000	0.000	0.000	0.000	0.000	0.000
Pb	0.000	0.000	0.000	0.000	0.000	0.000	0.000	0.000	0.000	0.000

Table 6-16 Metal concentration in groundwater after 10 years using ferrihydrite

	ARD 248	ARD 406	ARD 625	ARD 512	ARD 747	ARD 718	ARD 684	ARD 222	ARD 220	ARD 246
Al	0.0	0.0	0.0	0.0	0.0	0.0	0.0	0.0	0.0	0.0
Fe	26.5	0.0	15.8	32.5	93.5	26.5	19.0	0.0	0.0	0.0
Cu	0.0	0.0	0.0	0.0	0.0	0.0	0.0	0.0	0.0	0.0
Zn	0.0	0.0	0.0	0.0	0.0	0.0	0.0	0.0	0.0	0.0
As	0.000	0.000	0.000	0.000	0.000	0.000	0.000	0.000	0.000	0.000
Pb	0.000	0.000	0.000	0.000	0.000	0.000	0.000	0.000	0.000	0.000

Table 6-17 Effluent, groundwater and drinking water standards in Japan

	Groundwater	Effluent	Drinking water
Al	Not specified	Not specified	0.2 mg/L
Fe	Not specified	10 mg/L	0.3 mg/L
Cu	Not specified	3 mg/L	1.0 mg/L
Zn	Not specified	2 mg/L	1.0 mg/L
As	0.01mg/L or less	0.1 mg/L	0.01 mg/L
Pb	0.01mg/L or less	0.1 mg/L	0.01 mg/L
pH	Not specified	Non coastal areas: 5.8 – 8.6 Coastal areas 5.0 – 9.0	5.8 – 8.6

The groundwater, effluent, and drinking water Quality Standards in Japan are presented in Table 6-17. From the results of the concentrations of metal release in the aquifer after one and ten years presented in Table 6-11 to Table 6-16, it can be concluded that the majority of the cases fulfill the groundwater and effluent Quality Standard requirements. However, there are certain cases in which the containment bottom liner does not fulfill the drinking water Quality Standards. The Environmental Quality Standards for Groundwater Pollution regulate 28 hazardous substances and items including heavy metals, volatile organic carbons, and others. However, there is no specification for Al, Fe, Cu, and Zn. The national effluent standards are made up of two categories: the standards for protecting human health (27 items including cadmium and cyanide) and the standards for protecting the living environment (15 items). The effluent standards listed in this table apply to the effluents of factories or commercial facilities which discharge 50m^3 or more of effluent per day on average. The drinking water Quality Standards in Japan are much stricter than for groundwater and effluent standards to ensure the safety of drinking water, and include as many items as possible, even those associated only with regional or personal issues. If the effluent or drinking water standard is followed, it can be said that the Fe concentration for GCL does not fulfill the requirements. However, this will depend on the conditions in the real field such as the groundwater flow rate, the depth of the water table, among others.

6.4 Cost Analysis

The main advantages of GCLs over CCLs or other soil compacted materials are the low hydraulic conductivity, easy and economic transportation, and installation. Table 6-18 shows the cost for material, installation, test pad, quality control, shipping, and the total cost for each mineral.

Table 6-18 Sample calculation cost of using GCL, zeolite, and ferrihydrite

	GCL	Zeolite	Ferrihydrite
MATERIAL COST			
Delivered material (USD/m^2)	4.85		
Material (USD /ton)		50	100
Particle density (g/cm^3)		2.33	3.51
Thickness (m)		0.5	0.5
Compaction factor		1.31	1.31
Area (m^2)	10000	10000	10000
Subtotal 1	48500	763075	2299050
INSTALLATION COST			
Installation (USD /m^2 for GCL, USD /m^3 for others)	1.60	8.00	8.00
Thickness (m)		0.5	0.5
Area (m^2)	10000	10000	10000
Subtotal 2	16146	40000	40000
TEST PAD COST			
Test pad (USD /m^3)	not required	0.35	0.35
Area (m^3)	10000	10000	10000
Subtotal 3	0	3500	3500
QUALITY CONTROL COST			
Quality control (USD /m^2)	0.10	0.23	0.23
Area (m^2)	10000	10000	10000
Subtotal 4	1000	2300	2300
SHIPPING COST			
Shipping cost (USD /metric ton-km)	0	0.17	0.17
Thickness (m)	0.5	0.5	0.5
Distance (km)	20	20	20
Compaction factor		1.31	1.31
Area (m^2)	10000	10000	10000
Subtotal 5	0	28944	28944
TOTAL (USD)	65,646	837,819	2,373,794

The cost calculations were done following the sample calculation available online in the website of Colloid and Environmental Technologies Company (CETCO) for GCLs and CCLs (CCLs were used as models for zeolite and ferrihydrite in this analysis). For the material cost, it was assumed that the delivered GCL unit cost was 4.84 USD per square meter (average commercial price in the United States). Prices for natural zeolites vary with zeolite and content and processing. Prices listed in Industrial Minerals and Rocks for industrial or agricultural applications were 30 to 70 USD per ton for granular products down to 40 mesh and 50 to 120 USD per ton for ground material ranging from 40 mesh to 325 mesh (Virta). For calculation in this research, 50 USD per ton of zeolite was used. The price of the zeolite used for experiments in this research was 35 yen per kilogram without transportation fee. The cost of ferrihydrite was fixed at 100 USD per ton in this sample cost calculation. The price range of iron oxides is very broad, varying from 0.81 to 1.94 USD per kg (Potter 2000) or from 100 to 14,000 USD per ton (Kumar et al. 2009) for arsenic adsorbents or from 100 to 2,500 USD per ton for iron oxides used in a variety of industrial and manufacturing applications (Hedin). The price of the ferrihydrite used in experiments for this research was 3200 yen per 500 g because it was a laboratory scale and high purity product.

In order to make calculations simpler, the area of the containment was assumed to be 10000 m^2, the transportation distance, 20 km, and the compaction factor, 1.31 (according to CETCO). This company mentions that loose clay has a bulk relative density between 0.8 – 1.3 g/cm^3. Compacted clay bulk densities are in the 1.6 – 1.8 g/cm^3 range. For simplicity, they assume bulk densities of 1.3 g/cm^3 for loose clay and 1.7 g/cm^3 for compact clay. The compaction factor is then: 1.7/1.3 = 1.31. In other words, it takes 1.31 m^3 of loose clay to construct 1 m^3 of in-place compacted soil.

From this cost analysis it can be noticed that the total cost for GCL is approximately 66,000 USD, whereas for zeolite and ferrihydrite is 840,000 USD and 2,400,000 USD respectively. The total cost for zeolite and ferrihydrite are 13 to 39 times higher than that of GCL. In the previous section it was found that the metal sorption capacity of 50 cm of material is extremely high, and thus, mixing with local soil will be an option to reduce the cost of these two minerals. In order to calculate the ratio between zeolite or ferrihydrite with soil, further experimental research is required. The hydraulic conductivity of the mixture, as well as the sorption capacity should be calculated before applying this technology in the field.

6.5 Use of GCL, Zeolite, and Ferrihydrite in the Field

As, to the best knowledge of the author, there are no regulations for excavated rock containments, landfill containment will be used to illustrate field applications of GCLs, zeolite, and ferrihydrite.

Lining systems are required to provide short, medium and long-term protection of the environment and therefore must be durable and resistant to puncture and chemical attack. Landfill liner systems consist of a combination of barriers and fluid collection layers, in addition to mineral or synthetic components. There are three main liner systems that are applied in landfills (Figure 6-8):

- A simple liner: This type of liner system is applied when there is low risk to pollution. It consists of a single primary barrier overlain by a leachate collection system with a separation or protection layer.

- A composite liner: This type of liner system is usually applied in medium-sensitivity situations. It consists of two separated barriers called primary and secondary made of different material. Usually, a primary geomembrane is placed above a secondary low permeability mineral barrier. Above the primary barrier, a leachate drain is placed. This is most probably the best system to be used for GCLs installations.
- A double liner: this type of liner system favors monitoring and removal of leachates coming from the primary barrier. The design includes primary and secondary barriers with an intermediate high-permeability drainage layer.

GCLs are delivered to sites in rolls and then unrolled onto a prepared surface. The strips are stitched together by overlapping their edges and applying clay (usually bentonite) in between. GCLs can replace about 600 mm of clay thickness in a conventional compacted clay liner (CCL). Table 6-19 shows the differences between GCL liners and CCLs.

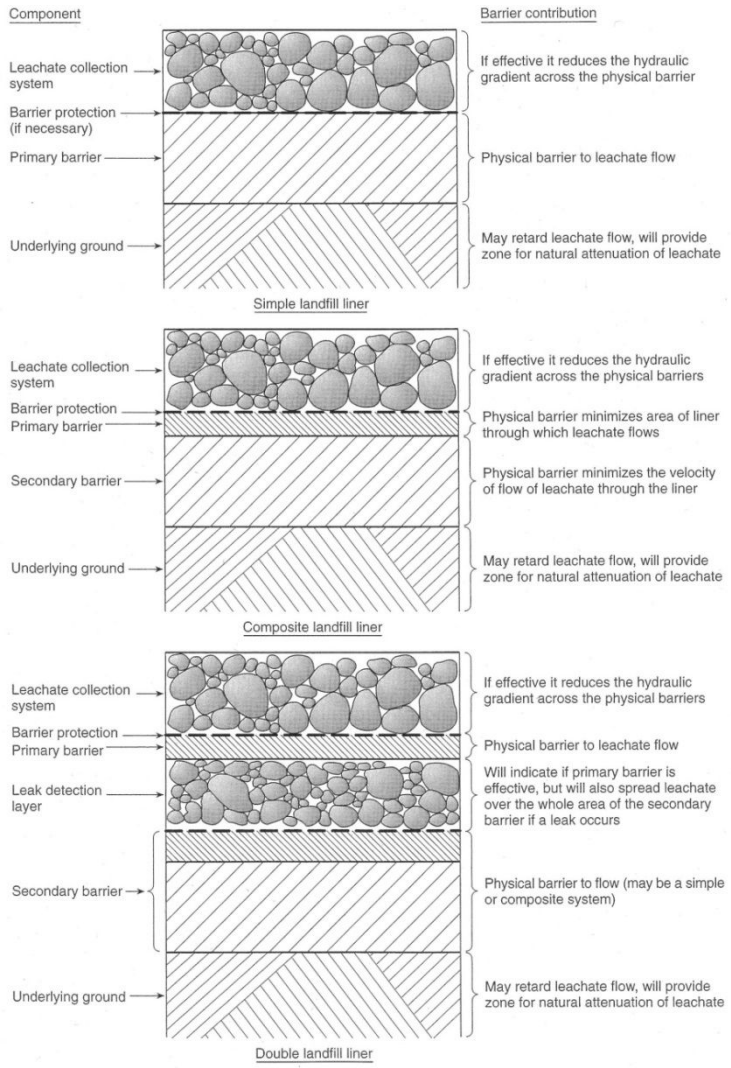

Figure 6-8 Types of liner system (Sarsby 2000)

Table 6-19 Comparison of GCLs and CCLs (Sarsby 2000)

Characteristic	GCL	CCL
Thickness	Typically 12-25 mm, thus uses up very little tipping space within the site	Typically 300 – 1000 mm
Coefficient of permeability	$\leq 5\times10^{-11}$ m/s	$\leq 10^{-9}$ m/s
Construction	Actual installation is a relatively simple process, but significant advance ground preparation is required	Construction is relatively slow because of the quantity of materials to be placed
Potential for damage from puncture	Thin, very vulnerable; protection is required	Thick; cannot be punctured accidentally
Susceptibility to climatic effects	GCLs placed dry cannot suffer desiccation during construction; completeness of subsequent hydration is questionable	Difficult to place in wet weather; can desiccate and crack after construction if not protected; freeze–thaw action is unlikely to be a problem if layers are covered properly
Availability	Materials can be relatively easily transported to site	Suitable materials are not always readily available, and they cannot be transported over large distances because of the large quantity required
Long term stability	May become brittle due to chemical interactions	Essentially inert
Experience of usage	Limited	Has been used for many years and appropriate site techniques have been developed

Zeolite and ferrihydrite are suggested to be applied in the field either as pure materials of 300 to 1000 mm thickness (similar to the case of CCLs) or in combination with local soil. The ratio between mineral and soil constitute part of further research. The installation will be probably relatively slower than in the case of GCLs because of the quantity of materials to be placed and the necessary equipment/machinery to either compact or mix and compact the absorption layer.

6.6 Summary and Conclusions for this Chapter

In Chapter 4 and 5, the chemical and hydraulic performance of GCL (bentonite), zeolite, and ferrihydrite were evaluated. The performance of mineral materials should be carefully examined beforehand in order to guarantee their effective long term barrier performance. Moreover, the availability of the materials, the type of contaminants that may leach from rocks, and the price of the materials, including the cost of transportation and installation should be also considered.

In this chapter, pH, EC, sulfate and metal (Al, As, Cu, Fe, Pb, Zn, Ca, K, Mg and Na) concentrations for every type of mine was summarized in terms of average and standard deviation. Although the ranges are very broad for some parameters, it represents a useful tool for engineering purposes. Also metal relationship for predictions was briefly discussed.

The hydraulic conductivity prediction from monovalent, divalent, trivalent, and sum of divalent and trivalent were discussed in this chapter. No relationship between total monovalent cations and hydraulic conductivity was found, but direct relationships between total divalent cations (TDC), total trivalent cations (TTC), and sum of divalent and trivalent cations (TDTC) against hydraulic conductivity were determined. These relationships can be used for future predictions of k values without conducting hydraulic conductivity tests.

Metal prediction from experimental results was also conducted assuming a rock containment facility of 1 ha, leachate above mineral barrier of 30 cm, groundwater flow and depth of 45 m/year and 10 m, respectively. The period without any leakage was calculated for all 10 ARDs studied in this research. In case of GCL this period ranges between 1 to 800 years approximately depending on the ARD. For a 50 cm zeolite, this period was between 130 to 100,000 years approximately, and for 50 cm ferrihydrite, it was 170 to 50,000 years approximately.

Moreover, the concentration of metals in the groundwater after one and ten years was calculated based on chemical transport calculations presented in this chapter. For the chemical transport, experimental data of hydraulic conductivity, porosity, dry density, and partition coefficient were used. It was found that although metals will be diluted in the groundwater, there are some values of metal release (especially for ARD 747) above the drinking water Quality Standards in Japan.

The cost of materials, installation, and transport was calculated using simple cost analysis, assuming a rock containment facility of 1 ha. For GCL, it was found that the total cost will be approximately 66,000 USD, whereas for zeolite and ferrihydrite was approximately 840,000 and 2,400,000 USD respectively. These values may change according to the price of materials, availability, etc. The prices presented in this research are just for reference and consider the use of zeolite and ferrihydrite as pure materials. A mixture of local soil with zeolite and ferrihydrite should be studied in the future in order to determine the best ratio of mineral and soil and thus, reduce costs.

7 CONCLUSIONS AND FURTHER RESEARCH

7.1 Major Conclusions

This dissertation presents experimental results of the barrier performance of GCL, zeolite, and ferrihydrite when used as bottom liners in rock containment facilities with ARD potential generation. The barrier performance was studied in terms of hydraulic conductivity and metal retention capacity. A compilation of ARD from mining sites was also analyzed using statistical tools in order to characterize ARDs in the world and use representative cases to test the barrier performance of minerals. The overall results indicate that GCL, zeolite, and ferrihydrite can be potentially used to mitigate ARD. The main results and achievements for each chapter are summarized in Sections 7.1.1 to 7.1.6.

In Chapter 1, the overall study background was clarified and the objectives, research overview and contents, as well as the originality of this research were presented. The need to reuse and recycle excavated materials was highlighted, but it was mentioned that, before doing so, the environmental impact of potential metal release from these materials has to be assessed. The use of minerals such as bentonite, zeolite and ferrihydrite as bottom liners in rock containment facilities with ARD potential generation has been proposed to mitigate heavy metal leaching.

In Chapter 2, the sources and origins of heavy metal were presented, as were the characteristics of ARD and ways that it is generated. Besides, heavy metal and available ARD treatment methods were summarized. Moreover, descriptions of GCL, zeolite, and ferrihydrite in terms of chemical structure, heavy metal retention capacity and mechanisms involved in metal uptake were also described.

In Chapter 3, the compilation of ARD from different parts of the world was analyzed. Although ARDs around the world differ in terms of pH and metal composition, ARD database analysis provides an idea on how low and high pH and metal concentration can be depending on the type of mine, location, etc., and also gives information regarding the relationships between the different parameters, such as sulfate concentration and EC. This represents also a valuable scientific tool for the prediction of water chemistry in the future.

The minimum, maximum, media, and average values for the pH, EC, metal concentration of the ARD compositions of the database were calculated. The average pH value was 4.9±2.1, for EC, it was, 302±427 mS/m, for sulfate, it was 4755 mg/L±34896 mg/L; for Al, it was 159 mg/L±471 mg/L, for As, it was 4.0±27.8 mg/L, for Cu, it was 26.9±205 mg/L, for Fe, it was 665±5142 mg/L, for Pb, it was 1.5±7.3mg/L, and for Zn, it was 437±2711 mg/L.

A clear inverse linear relationship was determined for EC-pH, sum of metal-pH, sulfate-pH, Al-pH, Cu-pH, Fe-pH, and Zn-pH systems for the whole range of pH, except for the bicarbonate-pH, in which a direct linear relationship was observed. In general, it can be said that at low pH values, more metals are found in solution. Besides, the oxidation of sulfide minerals is particularly characterized by high sulfate

(>1000 mg/L), high Al and Fe (>100 mg/L), and elevated Cu, Pb and Zn (>10 mg/L). Ca, K, Mg and Na may also occur in strongly elevated concentrations. A direct linear relationship between EC and sulfate was observed, which constitutes a useful tool for ARD indication. This becomes an important finding as EC can be easily measured in the field compared to sulfate concentration. The Pearson correlation between sulfate and EC was calculated for each type of mine. For arsenic mines, the relationship between sulfate and EC in terms of Pearson correlation was 0.994, for coal mines, it was 0.962, for gold mines, it was 0.759, for leachate, it was 0.999, for metal mines it was 0.955, and for polymetallic mines, it was 0.893. Besides, the relationship between sulfate and metal concentration as well as the relationship between EC against pH and metal concentration in terms of Pearson correlation was also established, which indicates that metals can also be predicted indirectly by measuring the EC in the fields.

Considering that ARDs differ in terms of pH, EC, metal concentration, among others, the database provided in this chapter can be used to determine the average values of the main parameters of ARDs in general and according to the type of mine. For this research in particular, this database was used not only to characterize ARDs in the world, but also to strategically choose certain ARD cases (e.g. low pH and high EC, low pH and low EC, high pH and low EC, high pH and high EC, among others) to test the barrier performance of GCL, zeolite, and ferrihydrite.

In Chapter 4, the barrier performance of GCL, zeolite, and ferrihydrite was tested in terms of hydraulic conductivity. For this purpose, hydraulic conductivity tests and swelling tests were done for every ARD selected from the database. Moreover, several factors that affect the hydraulic performance of GCLs against ARD were also evaluated. The effect of prehydration over non-prehydration, the effect of short and long term experimental tests, and the effect of type of bentonite were also studied.

For GCL, the hydraulic conductivity was tested against 10 ARDs and the hydraulic conductivity values range between 9.5×10^{-12} and 5.0×10^{-10} m/s, which represents a 1 order magnitude maximum compared to the water permeation case (1.4×10^{-11} m/s). Moreover, for values lower than or equal to 400 mS/m of EC, almost no change in hydraulic conductivity was observed compared to water permeation, even at different pH values. This is an indicator of the efficiency of the GCL at this range. Even though at EC = 1011 mS/m, an increase of one order of magnitude in the hydraulic conductivity was observed, this values is low enough to be used in rock containments facilities.

The hydraulic conductivity of zeolite permeated with water was 3.0×10^{-10} m/s, while when permeated with ARD 747 (the most severe case of this study), 1.4×10^{-9} m/s. Similar to GCL, a 1 order of magnitude increment in the hydraulic conductivity was observed for the most severe ARD case. Besides, the hydraulic conductivity of ferrihydrite was the highest among the three minerals with a hydraulic conductivity value of 7.3×10^{-9} m/s in the case of permeation with water. This value remained constant after ARD 747 (the most severe case presented in this research) permeation, with a value of 8.6×10^{-9} m/s.

The swell index of bentonite, which is the only material among the three materials that shows swelling capacity, was also studied in this section. The swelling test is a simple test that provides important information about the hydraulic conductivity. If the swell volume is high, the clay layers tend to expand

and, thus, it is more difficult for the liquid to flow through the material. As a result, the hydraulic conductivity is very low. The swell index of the water was around 33 mL/2 g bentonite and this value tends to decrease as the pH decreases or the EC increases. The lowest swell index observed was 8.5 mL/2g bentonite, for ARD 747 (most severe case of ARD).

A possible exponential relationship was obtained between EC and swell index and between EC and hydraulic conductivity. Besides, a relationship between hydraulic conductivity and swell index was observed for GCL. An equation for the relationship between swell index and hydraulic conductivity was first proposed by Katsumi et al (2007) for GCL against alkaline metals. This was adjusted for ARD cases according to the experimental values and the difference between the predicted hydraulic conductivity values and the real ones decreased from 60 – 76% to 0.9 – 19.2%.

Among the three materials tested in this research against ARDs, GCL showed the best barrier performance with a hydraulic conductivity between 9.6×10^{-11} – 5.0×10^{-10} m/s. Besides, considering that GCL is a commercial material that is easy to transport and install, it can be suitable for bottom liners in rock containment facilities. However, zeolite and ferrihydrite also showed a good performance against ARD, with hydraulic values of 1.4×10^{-9} m/s and 8.6×10^{-9} m/s respectively. After establishing a proper thickness for these two materials, they can also be successfully used as absorption layer for rock containment facilities.

In Chapter 5, the barrier performance of GCL, zeolite and ferrihydrite was tested in terms of metal sorption. For this purpose, single metal, bi-metal, and ARD sorption tests were conducted. Also the effluents collected from hydraulic conductivity tests were also analyzed. Besides, the effect of buffering capacity, pH, metal ions, solid-liquid ratio, as well as the effect of metal concentration in sorption capacity of GCL (bentonite) were more deeply studied in this chapter.

From single metal time step batch sorption tests using bentonite, zeolite, and ferrihydrite, information about the time to reach equilibrium (6 hours in majority of the cases), the mechanisms that are involved in metal uptake (ion exchange, surface complexation, and precipitation), and the metal sorption capacity against single and complex mixture of metals were obtained. The sorption capacity of bentonite, zeolite, and ferrihydrite against single metals and complex mixtures differ and depends on the metal competition and metal affinity. For bentonite, the difference between single metal sorption test results and ARD sorption results are between 0 – 37%, for zeolite it ranges between 0.1 and 46%, whereas for ferrihydrite, it ranges between 1 and 32%, being lower in case of ARD compared to single metals because of metal competition.

From studies of the structure of the minerals, presented in the background section, and some evidence from the experimental results (such as the release of Na, K, Ca, and Mg), it can be inferred that the heavy metal uptake on bentonite, zeolite, and ferrihydrite can be attributed to ion exchange processes (for bentonite and zeolite) and surface complexation (for ferrihydrite). However these are not the only mechanisms that occur. Although it was not possible to determine the proportion between sorption and precipitation, the latter mechanism also plays an important role in metal mobilization.

From single metal batch sorption tests, it was observed that bentonite has no sorption capacity

towards As. However, in the sorption test with ARD (ARD 747) and in the effluent analysis after hydraulic conductivity against ARD 747, the As concentration was kept below the influent through the duration of the tests. This phenomenon was attributed to a secondary retention mechanism in other metals present in ARD such as Al, Fe, Cu, Zn, Pb. Results of bi-metal sorption of As against different metals show that at 1 mM of metal (metal-As relationship 1:1), the sorption of As on bentonite (2 g/L bentonite) increased from 0% to 71, 31, 51, 63, and 67 percent in presence of Fe, Cu, Al, Zn, and Pb respectively. The precipitation mechanism of As in other metals, favored by the low hydraulic conductivity of the GCL, was also proposed in this chapter. Further research on the mechanism such as using sequential extraction may help confirm the proposed mechanisms.

Results presented in this chapter show that bentonite, zeolite, and ferrihydrite can be used effectively for removal of metal cations present in ARD. These materials provide an alternative for barriers against rock leachates with high heavy metal content. However, among all these minerals, it was found that bentonite is a better sorbent for Cu, Fe, Zn, Al, and Pb, with ferrihydrite suitable for As retention. Although, based on the cation exchange capacity (CEC), bentonite has a limited metal buffering capacity, its low hydraulic conductivity value make bentonite a suitable material for waste rock containment facilities with potential of ARD generation.

In Chapter 6, the field application of GCL, zeolite and ferrihydrite was evaluated combining the results or Chapter 3, 4, and 5. The pH, EC, sulfate and metal (Al, As, Cu, Fe, Pb, Zn, Ca, K, Mg and Na) concentrations for every type of mine was summarized in terms of average and standard deviation. The hydraulic conductivity prediction in terms of cation concentration and chemical release over time was calculated. The price of applying GCL, zeolite and ferrihydrite in the field was also estimated.

The hydraulic conductivity prediction from monovalent, divalent, trivalent, and sum of divalent and trivalent were discussed. No relationship between total monovalent cations and hydraulic conductivity was found, but direct relationships between total divalent cations (TDC), total trivalent cations (TTC) and the sum of divalent and trivalent cations (TDTC) against hydraulic conductivity were found. These relationships can be used for future predictions of k values without conducting hydraulic conductivity tests.

Metal prediction from experimental results was also conducted assuming a rock containment facility of 1 ha, leachate above mineral barrier of 30 cm, groundwater flow and depth of 45 m/year and 10 m, respectively. The period without any leakage was calculated for all 10 ARDs studied in this research. In case of GCL this period ranges between 1 to 800 years approximately depending on the ARD. For a 50 cm zeolite, this period was between 127 to 100,000 years approximately, and for 50 cm ferrihydrite, it was 167 to 50,000 years approximately.

Moreover, the concentration of metals in the groundwater after one and ten years was calculated based on chemical transport calculations presented in this chapter. For the chemical transport, experimental data of hydraulic conductivity, porosity, dry density, and partition coefficient were used. It was found that although metals will be diluted in the groundwater, there are some values of metal release (especially for ARD 747) above the drinking water Quality Standards in Japan.

The cost of materials, installation, and transport was calculated using simple cost analysis, assuming a rock containment facility of 1 ha. For GCL, it was found that the total cost will be approximately 66,000 USD, whereas for zeolite and ferrihydrite was approximately 840,000 and 2,400,000 USD respectively. These values may change according to the price of materials, availability, etc. The prices presented in this research are just for reference and consider the use of zeolite and ferrihydrite as pure materials.

From the three minerals that were evaluated in this chapter, it can be inferred that the GCL is the most cost-effective proposal for rock containment facilities, considering the easier transportation and installation. Although its buffer capacity is limited by its thinness, GCL can immobilize heavy metals from ARD. For zeolite and ferrihydrite, a mixture of local soil should be studied in the future in order to determine the best ratio of mineral and soil and thus reduce costs.

7.2 Further Research

Short term future research involves the X-Ray Diffraction (XRD) and Scanning Electron Microscopy (SEM) analysis of the bentonite inside the GCL after hydraulic conductivity test. The purpose of these analyses is to study the structure of bentonite after being exposed to ARD and evaluate the changes that occur in its structure. In addition, numerical analysis using PHREEQC or MINTEQ can also be developed in order to predict sorption capacity of minerals when exposed to certain metals at certain concentration and combination.

Long term future research involves evaluation of the sorption capacity of minerals against heavy metals, focused on the identifications of the factors that favor sorption of one metal from another. Another major challenge is to understand the mechanisms (e.g. by doing sequential extraction) and the sequence of interactions that occur within these minerals over time, so that improvements can be proposed in case they are necessary.

Results obtained in this research showed that the chemical composition of solutions greatly affects the order in which metals are retained into minerals. Thus, it was known that a single metal batch sorption test itself cannot provide accurate result if directly extended or applied to ARD, because metal behavior may differ when they are in combination. So, future research may consider studies related to the migration of metals through bentonite, zeolite, and ferrihydrite, as well as the competition among metals and the retention mechanism on these minerals. For this purpose, diffusion tests, chemo-osmosis tests, sorption tests (multiple metal sorption test), and long term hydraulic conductivity tests can be considered to be performed for bentonite, zeolite, and ferrihydrite. Results from all these tests will become important and necessary when projecting the long-term fate of metals within these mineral materials, as many factors such as pH and redox, saturation, among others that influence these mechanisms, may change over time.

After having a better understanding of the factors that affect the performance of the three minerals when applied to ARD cases, different ways to improve their performance can be proposed. Currently, there are several studies related to the improvement of GCLs, such as the application of microbial biofilms (using Pseudomonas putida, Burkholderia cepacia, among others) (Templeton et al. 2001; Toner et al. 2005),

addition of materials that have affinity for some metals (such as zero valent iron, especially for As treatment), addition of complexing agents such as polypropylene carbonate (PC) (Onikata et al. 1999), implementation of a layer of sand or other material above the GCL to retain metals, and the development of chemical resistant bentonites. Katsumi et al. (2008c) evaluated the long-term barrier performance of two modified bentonites, a multiswellable bentonite (MSB) and a dense-prehydrated one (DPH-GCL), against electrolytic chemical solutions. Studies about the applicability of these new materials to ARD cases, as well as diffusion effects and sorption properties are also necessary.

Although bottom liners are the final defense against the leakage of ARD, minerals studied in this research can be also considered for final covers because they can minimize the infiltration of rainfall water into waste layer and thus lower the potential generation of ARD.

REFERENCES

Abollino, O., Aceto, M., Malandrino, M., Sarzanini, C., and Mentasti, E. (2003): Adsorption of heavy metals on Na-montmorillonite. Effect of pH and organic substances, *Water Research,* Vol.37, No.7, pp.1619-1627.

Akcil, A., and Koldas, S. (2006): Acid mine drainage (AMD): causes, treatment and case studies, *Journal of Cleaner Production,* Vol.14, No.12-13, pp.1139-1145.

Appelo, C. A. J., and Postma, D. (2009): Geochemistry, groundwater and pollution, CRC Press Taylor & Francis Group.

Arp, C. D., Cooper, D. J., and Stednick, J. D. (1999): The effects of acid rock drainage onCarex aquatilis leaf litter decomposition in rocky Mountain fens, *Wetlands,* Vol.19, No.3, pp.665-674.

ASTM (2007): D698 Standard test methods for laboratory compaction characteristics of soil using standard effort. ASTM International, West Conshohocken.

ASTM (2009a): D 5084-03 Standard test methods for measurement of hydraulic conductivity of saturated porous materials using a flexible wall permeameter, Vol 04.08, pp.1045-1067.

ASTM (2009b): D 7100-06 Standard test method for hydraulic conductivity compatibility testing of soils with aqueous solutions, Vol 04.09, pp.1213-1229.

ASTM (2009c): D 5890-06 Standard test method for swell Index of clay mineral component of geosynthetic clay liners, Vol 04.13, pp.245-247.

Aykol, A., Budakoglu, M., Kumral, M., Gultekin, A. H., Turhan, M., Esenli, V., Yavuz, F., and Orgun, Y. (2003): Heavy metal pollution and acid drainage from the abandoned Balya Pb-Zn sulfide Mine, NW Anatolia, Turkey, *Environmental geology,* Vol.45, No.2, pp.198-208.

Banks, D., Younger, P. L., Arnesen, R.-T., Iversen, E. R., and Banks, S. B. (1997): Mine-water chemistry: the good, the bad and the ugly, *Environmental Geology,* Vol.32, No.3, pp.157-174.

Barnes, H. L. (2008): Composition and method to control acid rock drainage, US Patent App. 20,080/221,379.

Benson, C. H., Thorstad, P. A., Jo, H.-Y., and Rock, S. A. (2007): Hydraulic performance of geosynthetic clay liners in a landfill final cover, *Journal of Geotechnical and Geoenvironmental Engineering,* Vol.133, No.7, pp.814-827.

Berger, A. C., Bethke, C. M., and Krumhansl, J. L. (2000): A process model of natural attenuation in drainage from a historic mining district, *Applied Geochemistry,* Vol.15, No.5, pp.655-666.

Bird, D. A. (2003): Characterization of anthropogenic and natural sources of acid rock drainage at the Cinnamon Gulch abandoned mine land inventory site, Summit County, Colorado, *Environmental geology,* Vol.44, No.8, pp.919-932.

Black, A., and Craw, D. (2001): Arsenic, copper and zinc occurrence at the Wangaloa coal mine, southeast Otago, New Zealand, *International Journal of Coal Geology,* Vol.45, No.2, pp.181-193.

Blight, G. (2009): Geotechnical engineering for mine waste storage facilities, CRC Press, Taylor & Francis Group.

Boult, S., Collins, D. N., White, K., and Curtis, C. (1994): Metal transport in a stream polluted by acid mine

drainage—the Afon Goch, Anglesey, UK, *Environmental Pollution,* Vol.84, No.3, pp.279-284.

Bradl, H. B. (2004): Adsorption of heavy metal ions on soils and soils constituents, *Journal of Colloid and Interface Science,* Vol.277, No.1, pp.1-18.

Bradl, H. B. (2005): Heavy metals in the environment: origin, interaction and remediation, Elsevier.

Brownlow, A. H. (1996): Geochemistry, Prentice Hall Englewood Cliffs.

Carroll, S. A., O'day, P. A., and Piechowski, M. (1998): Rock-water interactions controlling zinc, cadmium, and lead concentrations in surface waters and sediments, US Tri-State Mining District. 2. Geochemical interpretation, *Environmental Science & Technology,* Vol.32, No.7, pp.956-965.

Casiot, C., Egal, M., Elbaz-Poulichet, F., Bruneel, O., Bancon-Montigny, C., Cordier, M.-A., Gomez, E., and Aliaume, C. (2009): Hydrological and geochemical control of metals and arsenic in a Mediterranean river contaminated by acid mine drainage (the Amous River, France); preliminary assessment of impacts on fish (< i> Leuciscus cephalus</i>), *Applied Geochemistry,* Vol.24, No.5, pp.787-799.

CETCO. "GCL vs CCL Cost/Performance Comparison." Retrieved February 5, 2014, from http://lining.cetco.com/DesktopModules/Bring2mind/DMX/Download.aspx?Command=Core_Download&EntryId=5140&PortalId=12&TabId=1493.

Christensen, B., Laake, M., and Lien, T. (1996): Treatment of acid mine water by sulfate-reducing bacteria; results from a bench scale experiment, *Water Research,* Vol.30, No.7, pp.1617-1624.

Cidu, R., Caboi, R., Fanfani, L., and Frau, F. (1997): Acid drainage from sulfides hosting gold mineralization (Furtei, Sardinia), *Environmental Geology,* Vol.30, No.3-4, pp.231-237.

Daniel, D. E., Bowders, J. J., and Gilbert, R. B. (1997): Laboratory hydraulic conductivity testing of GCLs in flexible-wall permeameters, *Testing and Acceptance Criteria for Geosynthetic Clay Liners*, pp.208-226.

Das, B. M. (2009): Principles of geotechnical engineering, Stamford, Connecticut, CENGAGE Learning.

DeNicola, D. M., and Stapleton, M. G. (2002): Impact of acid mine drainage on benthic communities in streams: the relative roles of substratum vs. aqueous effects, *Environmental Pollution,* Vol.119, No.3, pp.303-315.

Dinelli, E., and Tateo, F. (2002): Different types of fine-grained sediments associated with acid mine drainage in the Libiola Fe–Cu mine area (Ligurian Apennines, Italy), *Applied Geochemistry,* Vol.17, No.8, pp.1081-1092.

Dold, B., Wade, C., and Fontboté, L. (2009): Water management for acid mine drainage control at the polymetallic Zn–Pb–(Ag–Bi–Cu) deposit Cerro de Pasco, Peru, *Journal of Geochemical Exploration,* Vol.100, No.2, pp.133-141.

Drever, J. I. (1997): The geochemistry of natural waters: surface and groundwater environments.

Egloffstein, T. A. (2001): Natural bentonites-influence of the ion exchange and partial desiccation on permeability and self-healing capacity of bentonites used in GCLs, *Geotextiles and Geomembranes,* Vol.19, No.7, pp.427-444.

Erdem, E., Karapinar, N., and Donat, R. (2004): The removal of heavy metal cations by natural zeolites, *Journal of Colloid and Interface Science,* Vol.280, No.2, pp.309-314.

Feng, D., Aldrich, C., and Tan, H. (2000): Treatment of acid mine water by use of heavy metal precipitation and ion exchange, *Minerals Engineering,* Vol.13, No.6, pp.623-642.

Ficklin, W., and Mosier, E. (1999): Field methods for sampling and analysis of environmental samples for unstable and selected stable constituents, *The environmental geochemistry of mineral deposits. Society of Economic Geologists. Part A*, pp.249-264.

Fukushi, K., Sasaki, M., Sato, T., Yanase, N., Amano, H., and Ikeda, H. (2003): A natural attenuation of arsenic in drainage from an abandoned arsenic mine dump, *Applied Geochemistry,* Vol.18, No.8, pp.1267-1278.

Gammons, C. H., Nimick, D. A., Parker, S. R., Snyder, D. M., McCleskey, R. B., Amils, R., and Poulson, S. R. (2008): Photoreduction fuels biogeochemical cycling of iron in Spain's acid rivers, *Chemical Geology,* Vol.252, No.3, pp.202-213.

Gammons, C. H., Duaime, T. E., Parker, S. R., Poulson, S. R., and Kennelly, P. (2010): Geochemistry and stable isotope investigation of acid mine drainage associated with abandoned coal mines in central Montana, USA, *Chemical Geology,* Vol.269, No.1, pp.100-112.

Gates, W. P., Bouazza, A., and Churchman, G. J. (2009): Bentonite clay keeps pollutants at bay, *Elements,* Vol.5, No.2, pp.105.

Gault, A. G., Cooke, D. R., Townsend, A. T., Charnock, J. M., and Polya, D. A. (2005): Mechanisms of arsenic attenuation in acid mine drainage from Mount Bischoff, western Tasmania, *Science of the Total Environment,* Vol.345, No.1, pp.219-228.

Gazea, B., Adam, K., and Kontopoulos, A. (1996): A review of passive systems for the treatment of acid mine drainage, *Minerals Engineering,* Vol.9, No.1, pp.23-42.

Gerhardt, A., Janssens de Bisthoven, L., and Soares, A. (2004): Macroinvertebrate response to acid mine drainage: community metrics and on-line behavioural toxicity bioassay, *Environmental Pollution,* Vol.130, No.2, pp.263-274.

Grande, J., Beltrán, R., Sáinz, A., Santos, J., De la Torre, M., and Borrego, J. (2005): Acid mine drainage and acid rock drainage processes in the environment of Herrerías Mine (Iberian Pyrite Belt, Huelva-Spain) and impact on the Andevalo Dam, *Environmental Geology,* Vol.47, No.2, pp.185-196.

Gray, N. (1996): Field assessment of acid mine drainage contamination in surface and ground water, *Environmental Geology,* Vol.27, No.4, pp.358-361.

Gray, N. (1998): Acid mine drainage composition and the implications for its impact on lotic systems, *Water Research,* Vol.32, No.7, pp.2122-2134.

Gulec, S., Benson, C., and Edil, T. (2005): Effect of acidic mine drainage on the mechanical and hydraulic properties of three geosynthetics, *Journal of Geotechnical and Geoenvironmental Engineering,* Vol.131, No.8, pp.937-950.

Guyonnet, D., Touze-Foltz, N., Norotte, V., Pothier, C., Didier, G., Gailhanou, H., Blanc, P., and Warmont, F. (2009): Performance-based indicators for controlling geosynthetic clay liners in landfill applications, *Geotextiles and Geomembranes,* Vol.27, No.5, pp.321-331.

Hamilton, Q., Lamb, H., Hallett, C., and Proctor, J. (1999): Passive treatment systems for the remediation of

acid mine drainage at Wheal Jane, Cornwall, *Water and Environment Journal,* Vol.13, No.2, pp.93-103.

Hammarstrom, J., Seal II, R., Meier, A., and Kornfeld, J. (2005): Secondary sulfate minerals associated with acid drainage in the eastern US: recycling of metals and acidity in surficial environments, *Chemical Geology,* Vol.215, No.1, pp.407-431.

Hattori, S., Ohta, T., and Kiya, H. (2003): Geology study on exhudation of acid water from rock mucks - evaluation methods of rocks at the Hakkoda Tunnel near mine area, *Journal of the Japan Society of Engineering Geology,* Vol.46, No.3, pp.359-371.

He, M., Wang, Z., and Tang, H. (1997): Spatial and temporal patterns of acidity and heavy metals in predicting the potential for ecological impact on the Le An river polluted by acid mine drainage, *Science of the Total Environment,* Vol.206, No.1, pp.67-77.

Hedin, R. "Recovery of a Marketable Iron Product from Coal Mine Drainage." Retrieved February 6, 2014, from http://wvmdtaskforce.com/proceedings/98/98HED/98HED.HTM.

Herrera, P., Uchiyama, H., Igarashi, T., Asakura, K., Ochi, Y., Iyatomi, N., and Nagae, S. (2007): Treatment of acid mine drainage through a ferrite formation process in central Hokkaido, Japan: Evaluation of dissolved silica and aluminium interference in ferrite formation, *Minerals Engineering,* Vol.20, No.13, pp.1255-1260.

Herrera S, P., Uchiyama, H., Igarashi, T., Asakura, K., Ochi, Y., Ishizuka, F., and Kawada, S. (2007): Acid mine drainage treatment through a two-step neutralization ferrite-formation process in northern Japan: Physical and chemical characterization of the sludge, *Minerals Engineering,* Vol.20, No.14, pp.1309-1314.

Hewlett, L., Craw, D., and Black, A. (2005): Comparison of arsenic and trace metal contents of discharges from adjacent coal and gold mines, Reefton, New Zealand, *Marine and Freshwater Research,* Vol.56, No.7, pp.983-995.

Hochella, M. F., Moore, J. N., Golla, U., and Putnis, A. (1999): A TEM study of samples from acid mine drainage systems: Metal-mineral association with implications for transport, *Geochimica et Cosmochimica Acta,* Vol.63, No.19, pp.3395-3406.

Hornsey, W. P., Scheirs, J., Gates, W. P., and Bouazza, A. (2010): The impact of mining solutions/liquors on geosynthetics, *Geotextiles and Geomembranes,* Vol.28, No.2, pp.191-198.

Igarashi, T., Sasaki, R., and Tabelin, C. B. (2013): Chemical Forms of Arsenic and Selenium Leached from Mudstones, *Procedia Earth and Planetary Science,* Vol.6, pp.105-113.

Jasmund, K., and Lagaly, G. (1993): Tonminerale und Tone, Darmstadt, Steinkopff Verlag.

Jo, H. Y., Katsumi, T., Benson, C. H., and Edil, T. B. (2001): Hydraulic conductivity and swelling of nonprehydrated GCLs permeated with single-species salt solutions, *Journal of Geotechnical and Geoenvironmental Engineering,* Vol.127, No.7, pp.557-567.

Jo, H. Y., Benson, C. H., and Edil, T. B. (2004): Hydraulic conductivity and cation exchange in non-prehydrated and prehydrated bentonite permeated with weak inorganic salt solutions, *Clays and Clay Minerals,* Vol.52, No.6, pp.661.

Johnson, C. A., and Thornton, I. (1987): Hydrological and chemical factors controlling the concentrations of Fe,

Cu, Zn and As in a river system contaminated by acid mine drainage, *Water Research,* Vol.21, No.3, pp.359-365.

Johnson, D. B. (2003): Chemical and microbiological characteristics of mineral spoils and drainage waters at abandoned coal and metal mines, *Water, Air and Soil Pollution: Focus,* Vol.3, No.1, pp.47-66.

Johnson, D. B., and Hallberg, K. B. (2003): The microbiology of acidic mine waters, *Research in Microbiology,* Vol.154, No.7, pp.466-473.

Kaoser, S., Barrington, S., Elektorowicz, M., and Wang, L. (2005): Effect of Pb and Cd on Cu adsorption by sand-bentonite liners, *Canadian Journal of Civil Engineering,* Vol.32, No.1, pp.241-249.

Kashir, M., and Yanful, E. K. (2001): Hydraulic conductivity of bentonite permeated with acid mine drainage, *Canadian Geotechnical Journal,* Vol.38, No.5, pp.1034-1048.

Katayama, M., Hirota, M., Inui, T., Takeshi, K., and Takai, A. (2011): Long-term leaching of heavy metals from excavated soils and rocks with natural contamination. *Geo-Environmental Engineering*, Takamatsu, Japan, pp.41-46.

Katsumi, T., Benson, C., Foose, G., and Kamon, M. (2001): Performance-based design of landfill liners, *Engineering Geology,* Vol.60, No.1, pp.139-148.

Katsumi, T., Ishimori, H., Ogawa, A., Yoshikawa, K., Hanamoto, K., and Fukagawa, R. (2007): Hydraulic conductivity of nonprehydrated geosynthetic clay liners permeated with inorganic solutions and waste leachates, *Soils and Foundations,* Vol.47, No.1, pp.79-96.

Katsumi, T., Inui, T., and Kamon, M. (2008a): Wastes and by-products used in geotechnical applications in Japan. *Geo-Environmental Engineering 2008 -Proceedings of the Eighth Japan-Korea-France Joint Seminar on Geoenvironmental Engineering*, pp.275-282.

Katsumi, T., Ishimori, H., Ogawa, A., Maruyama, S., and Fukagawa, R. (2008b): Effects of water content distribution on hydraulic conductivity of prehydrated CGLs against calcium chloride solutions, *Soils and Foundations,* Vol.48, No.3, pp.407-417.

Katsumi, T., Ishimori, H., Onikata, M., and Fukagawa, R. (2008c): Long-term barrier performance of modified bentonite materials against sodium and calcium permeant solutions, *Geotextiles and Geomembranes,* Vol.26, No.1, pp.14-30.

Katsumi, T. (2010): Hydraulic conductivity of geosynthetic clay liners, *Geosynthetic Clay Liners for Waste Containment Facilities*, A. a. J. J. B. e. Bouazza. London, CRC Press/Balkema**:** 55-83.

Katsumi, T., Inui, T., and Kamon, M. (2010): Sustainable geotechnics for reuse of by-products. *Environmental Geotechnics for Sustainable Development - Proceedings of the 6th International Congress on Environmental Geotechnics*, New Delhi, India, pp.302-317.

Kielland, J. (1937): Individual activity coefficients of ions in aqueous solutions, *Journal of the American Chemical Society,* Vol.59, No.9, pp.1675-1678.

Kim, J.-Y., and Chon, H.-T. (2001): Pollution of a water course impacted by acid mine drainage in the Imgok creek of the Gangreung coal field, Korea, *Applied Geochemistry,* Vol.16, No.11, pp.1387-1396.

Kimball, B. A., Callender, E., and Axtmann, E. V. (1995): Effects of colloids on metal transport in a river receiving acid mine drainage, upper Arkansas River, Colorado, USA, *Applied Geochemistry,* Vol.10,

No.3, pp.285-306.

Koerner, R. M., and Koerner, G. R. (2010): Background and overview of geosynthetic clay liners, *Geosynthetic Clay Liners for Waste Containment Facilities*, A. a. J. J. B. e. Bouazza. London, CRC Press/Balkema**:** 1-16.

Kolstad, D. C., Benson, C. H., and Edil, T. B. (2004): Hydraulic conductivity and swell of nonprehydrated geosynthetic clay liners permeated with multispecies inorganic solutions, *Journal of Geotechnical and Geoenvironmental Engineering,* Vol.130, pp.1236.

Krause, E., and Ettel, V. (1988): Solubility and stability of scorodite, FeAsO4• 2H2O: new data and further discussion, *The American mineralogist,* Vol.73, No.7-8, pp.850-854.

Kumar, A., Bucciarelli-Tieger, R. H., and Gurian, P. L. (2009): Cost-effectiveness of arsenic adsorbents.

Lange, K., Rowe, R. K., and Jamieson, H. (2005): Attenuation of heavy metals by geosynthetic clay liners, *GRI-18 Geosynthetics Research and Development in Progress*, pp.1-8.

Lange, K., Rowe, R. K., and Jamieson, H. (2007): Metal retention in geosynthetic clay liners following permeation by different mining solutions, *Geosynthetics International,* Vol.14, No.3, pp.178-187.

Lange, K., Rowe, R. K., and Jamieson, H. (2009): Diffusion of metals in geosynthetic clay liners, *Geosynthetics International,* Vol.16, No.1, pp.11-27.

Lange, K., Rowe, R. K., and Jamieson, H. (2010a): The potential role of geosynthetic clay liners in mine water treatment systems, *Geotextiles and Geomembranes,* Vol.28, No.2, pp.199-205.

Lange, K., Rowe, R. K., Jamieson, H., Flemming, R. L., and Lanzirotti, A. (2010b): Characterization of geosynthetic clay liner bentonite using micro-analytical methods, *Applied Geochemistry,* Vol.25, pp.1056-1069.

Lee, G., Bigham, J. M., and Faure, G. (2002): Removal of trace metals by coprecipitation with Fe, Al and Mn from natural waters contaminated with acid mine drainage in the Ducktown Mining District, Tennessee, *Applied Geochemistry,* Vol.17, No.5, pp.569-581.

Lee, J., and Chon, H. (2006): Hydrogeochemical characteristics of acid mine drainage in the vicinity of an abandoned mine, Daduk Creek, Korea, *Journal of Geochemical Exploration,* Vol.88, No.1, pp.37-40.

Lide, D. (2001-2002): CRC Handbook of Chemistry and Physics, CRC Press.

Lottermoser, B. G. (2007): Mine Wastes: characterization, treatment and environmental impacts, Berlin, Springer.

Ludwig, R. D., Smyth, D. J., Blowes, D. W., Spink, L. E., Wilkin, R. T., Jewett, D. G., and Weisener, C. J. (2009): Treatment of arsenic, heavy metals, and acidity using a mixed ZVI-compost PRB, *Environmental Science & Technology,* Vol.43, No.6, pp.1970-1976.

Magombedze, C. (2010): Geochemical controls and environmental impacts of acid mine drainage: a case study of geochemical processes controlling AMD in semi arid conditions, VDM Verlag Dr. Muller Aktiengesellschaft & Co. KG.

Matlock, M. M., Howerton, B. S., and Atwood, D. A. (2002): Chemical precipitation of heavy metals from acid mine drainage, *Water Research,* Vol.36, No.19, pp.4757-4764.

McCauley, C. A., O'Sullivan, A. D., Milke, M. W., Weber, P. A., and Trumm, D. A. (2009): Sulfate and metal

removal in bioreactors treating acid mine drainage dominated with iron and aluminum, *Water Research,* Vol.43, No.4, pp.961-970.

Milu, V., Leroy, J., and Peiffert, C. (2002): Water contamination downstream from a copper mine in the Apuseni Mountains, Romania, *Environmental Geology,* Vol.42, No.7, pp.773-782.

Morin, K. A., Hutt, N. M., and McArthur, R. (1995): Statistical assessment of past water chemistry to predict future chemistry at Noranda Minerals' Bell Mine. *Proceedings of the Conference on Mining and the Environment*, Sudbury, Ontario, Canada, pp.925-934.

Morin, K. A., and Hutt, N. M. (1997): Environmental geochemistry of minesite drainage: practical theory and case studies, MDAG Pub.

Munro, L. D., Clark, M. W., and McConchie, D. (2004): A Bauxsol™-based permeable reactive barrier for the treatment of acid rock drainage, *Mine Water and the Environment,* Vol.23, No.4, pp.183-194.

Naicker, K., Cukrowska, E., and McCarthy, T. (2003): Acid mine drainage arising from gold mining activity in Johannesburg, South Africa and environs, *Environmental Pollution,* Vol.122, No.1, pp.29-40.

Naka, A., Katsumi, T., Inui, T., Flores, G., and Ohta, T. (2011): Na-bentonite as rock containment barrier against heavy metals and acid leachates, GEOMAT2011, Japan, Vol 1, pp.333-336.

Nieto, J. M., Sarmiento, A. M., Olías, M., Canovas, C. R., Riba, I., Kalman, J., and Delvalls, T. A. (2007): Acid mine drainage pollution in the Tinto and Odiel rivers (Iberian Pyrite Belt, SW Spain) and bioavailability of the transported metals to the Huelva Estuary, *Environment International,* Vol.33, No.4, pp.445-455.

Nordstrom, D. K., and Alpers, C. (1999): Geochemistry of acid mine waters, *The environmental Geochemistry of Mineral Deposits,* Vol.6, pp.133-160.

Nordstrom, D. K., Alpers, C. N., Ptacek, C. J., and Blowes, D. W. (2000): Negative pH and extremely acidic mine waters from Iron Mountain, California, *Environmental Science & Technology,* Vol.34, No.2, pp.254-258.

Nordstrom, D. K. (2004): Negative pH, Efflorescent Mineralogy, and the Challence of Environmental Restoration at the Iron Mountain Superfund site or why not plug a mine, *Wissenschaftliche Mitteilungen,* Vol.25, pp.125-131.

Norrish, K., and Quirk, J. P. (1954): Crystalline swelling of montmorillonite, *Nature,* Vol.173, pp.255-257.

Ogata, A., and Banks, R. B. (1961): A solution of the differential equation of longitudinal dispersion in porous media, US Government Printing Office Washington, DC.

Ohta, T., Hattori, S., and Kiya, H. (2005): Elution characteristics of fresh mudstone from the underground opening. *Proceedings of the First Kyoto International Sympossium on Underground Environment*, pp.127-132.

Ohta, T., Enomoto, H., and Tokunaga, T. (2006): Evaluation and prediction of pollution caused by acid water exuded from mud sediment in urban ground, *IAEG 2006*, No.265, pp.1-9.

Ohta, T., Enomoto, H., Kawagoe, T., and Hasegawa, A. (2008): Evaluation of environmental pollution caused by heavy metal elements in natural ground, *Quarterly Report of RTRI,* Vol.49, No.3, pp.139-144.

Ohta, T., Hattori, S., and Kikuchi, Y. (2010): Water-rock interaction and heavy metal drainage at rock muck

disposal sites. *Proceedings of the 11th Congress of the IAEG*, pp.547-556.

Olıas, M., Nieto, J., Sarmiento, A., Cerón, J., and Cánovas, C. (2004): Seasonal water quality variations in a river affected by acid mine drainage: the Odiel River (South West Spain), *Science of the Total Environment,* Vol.333, No.1, pp.267-281.

Onikata, M., Kondo, M., Hayashi, N., and Yamanaka, S. (1999): Complex formation of cation-exchanged montmorillonites with propylene carbonate: Osmotic swelling in aqueous electrolyte solutions, *Clays and Clay Minerals,* Vol.47, No.5, pp.672-677.

Petrangeli, M., and Majone, M. (2002): Modeling of heavy metal adsorption at clay surfaces, Encyclopedia of Surface and Colloid Science, CRC, pp.3483-3497.

Petrov, R. J., and Rowe, R. K. (1997): Geosynthetic clay liner (GCL)-chemical compatibility by hydraulic conductivity testing and factors impacting its performance, *Canadian Geotechnical Journal,* Vol.34, No.6, pp.863-885.

Plumlee, G. S., Smith, K. S., Ficklin, W. H., and Briggs, P. H. (1992): Geological and geochemical controls on the composition of mine drainages and natural drainages in mineralized areas, *Water-Rock Interaction,* Vol.1, pp.419-422.

Potter, M., 2000. "Iron Oxide Pigments." Retrieved February 6, 2014, from http://minerals.usgs.gov/minerals/pubs/commodity/iron_oxide/750400.pdf.

Razo, I., Carrizales, L., Castro, J., Diaz-Barriga, F., and Monroy, M. (2004): Arsenic and heavy metal pollution of soil, water and sediments in a semi-arid climate mining area in Mexico, *Water, Air, and Soil Pollution,* Vol.152, No.1-4, pp.129-152.

Ripley, E. A., Redmann, R. E., and Crowder, A. A. (1996): Environmental effects of mining, St. Lucie Press Delray Beach, FL.

Romero, F. M., Prol-Ledesma, R. M., Canet, C., Alvares, L. N., and Pérez-Vázquez, R. (2010): Acid drainage at the inactive Santa Lucia mine, western Cuba: Natural attenuation of arsenic, barium and lead, and geochemical behavior of rare earth elements, *Applied Geochemistry,* Vol.25, No.5, pp.716-727.

Rowe, R. K., Quigley, R. M., Brachman, R. W., Booker, J. R., and Brachman, R. (2004): Barrier systems for waste disposal facilities, Spon Press.

Rowe, R. K. (2006): Some factors affecting geosynthetics used for geoenvironmental applications. *5th International Conference on Environmental Geotechnics*, London, pp.43-69.

Ruhl, J. L., and Daniel, D. E. (1997): Geosynthetic clay liners permeated with chemical solutions and leachates, *Journal of Geotechnical and Geoenvironmental Engineering,* Vol.123, pp.369.

Sánchez España, J., López Pamo, E., Santofimia, E., Aduvire, O., Reyes, J., and Barettino, D. (2005): Acid mine drainage in the Iberian Pyrite Belt (Odiel river watershed, Huelva, SW Spain): geochemistry, mineralogy and environmental implications, *Applied Geochemistry,* Vol.20, No.7, pp.1320-1356.

Saria, L., Shimaoka, T., and Miyawaki, K. (2006): Leaching of heavy metals in acid mine drainage, *Waste Management & Research,* Vol.24, No.2, pp.134-140.

Sarmiento, A. M., Oliveira, V., Gómez-Ariza, J. L., Nieto, J. M., and Sánchez-Rodas, D. (2007): Diel cycles of arsenic speciation due to photooxidation in acid mine drainage from the Iberian Pyrite Belt (Sw Spain),

Chemosphere, Vol.66, No.4, pp.677-683.

Sarsby, R. W. (2000): Environmental geotechnics, Thomas Telford.

Shackelford, C. D. (1990): Transit-time design of earthen barriers, *Engineering Geology,* Vol.29, No.1, pp.79-94.

Shackelford, C. D., Malusis, M. A., Majeski, M. J., and Stern, R. T. (1999): Electrical conductivity breakthrough curves, *Journal of Geotechnical and Geoenvironmental Engineering,* Vol.125, pp.260.

Shackelford, C. D., Sevick, G. W., and Eykholt, G. R. (2010): Hydraulic conductivity of geosynthetic clay liners to tailings impoundment solutions, *Geotextiles and Geomembranes,* Vol.28, No.2, pp.149-162.

Shan, H. Y., and Lai, Y. J. (2002): Effect of hydrating liquid on the hydraulic properties of geosynthetic clay liners, *Geotextiles and Geomembranes,* Vol.20, No.1, pp.19-38.

Shannon, R. (1976): Revised effective ionic radii and systematic studies of interatomic distances in halides and chalcogenides, *Acta Crystallographica Section A: Crystal Physics, Diffraction, Theoretical and General Crystallography,* Vol.32, No.5, pp.751-767.

Shokes, T. E., and Möller, G. (1999): Removal of dissolved heavy metals from acid rock drainage using iron metal, *Environmental Science & Technology,* Vol.33, No.2, pp.282-287.

Smuda, J., Dold, B., Friese, K., Morgenstern, P., and Glaesser, W. (2007): Mineralogical and geochemical study of element mobility at the sulfide-rich Excelsior waste rock dump from the polymetallic Zn–Pb–(Ag–Bi–Cu) deposit, Cerro de Pasco, Peru, *Journal of Geochemical Exploration,* Vol.92, No.2, pp.97-110.

Strömberg, B., and Banwart, S. (1994): Kinetic modeling of geochemical processes at the Aitik mining waste rock site in northern Sweden, *Applied Geochemistry,* Vol.9, No.5, pp.583-595.

Stumm, W., and Morgan, J. J. (1996): Aquatic Chemistry: Chemical Equilibria and Rates in Natural Wate.

Tabak, H. H., and Govind, R. (2003): Advances in biotreatment of acid mine drainage and biorecovery of metals: 2. Membrane bioreactor system for sulfate reduction, *Biodegradation,* Vol.14, No.6, pp.437-452.

Tabelin, C., and Igarashi, T. (2009): Mechanisms of arsenic and lead release from hydrothermally altered rock, *Journal of hazardous materials,* Vol.169, No.1, pp.980-990.

Tabelin, C. B., Igarashi, T., and Tamoto, S. (2010): Factors affecting arsenic mobility from hydrothermally altered rock in impoundment-type in situ experiments, *Minerals engineering,* Vol.23, No.3, pp.238-248.

Tabelin, C. B., Igarashi, T., and Takahashi, R. (2012a): Mobilization and speciation of arsenic from hydrothermally altered rock in laboratory column experiments under ambient conditions, *Applied Geochemistry,* Vol.27, No.1, pp.326-342.

Tabelin, C. B., Igarashi, T., Tamoto, S., and Takahashi, R. (2012b): The roles of pyrite and calcite in the mobilization of arsenic and lead from hydrothermally altered rocks excavated in Hokkaido, Japan, *Journal of Geochemical Exploration,* Vol.119, pp.17-31.

Tatsuhara, T., Arima, T., Igarashi, T., and Tabelin, C. B. (2012): Combined neutralization–adsorption system for the disposal of hydrothermally altered excavated rock producing acidic leachate with hazardous elements, *Engineering Geology,* Vol.139, pp.76-84.

Templeton, A. S., Trainor, T. P., Traina, S. J., Spormann, A. M., and Brown, G. E. (2001): Pb (II) distributions at biofilm ├ etal oxide interfaces, *Proceedings of the National Academy of Sciences of the United States of America,* Vol.98, No.21, pp.11897.

Todd, A. S., McKnight, D. M., Jaros, C. L., and Marchitto, T. M. (2007): Effects of acid rock drainage on stocked rainbow trout (Oncorhynchus mykiss): An in-situ, caged fish experiment, *Environmental Monitoring and Assessment,* Vol.130, No.1-3, pp.111-127.

Toner, B., Manceau, A., Marcus, M. A., Millet, D. B., and Sposito, G. (2005): Zinc sorption by a bacterial biofilm, *Environ. Sci. Technol,* Vol.39, No.21, pp.8288-8294.

Touze-Foltz, N., Duquennoi, C., and Gaget, E. (2006): Hydraulic and mechanical behavior of GCLs in contact with leachate as part of a composite liner, *Geotextiles and Geomembranes,* Vol.24, No.3, pp.188-197.

Tsukamoto, T., Killion, H., and Miller, G. (2004): Column experiments for microbiological treatment of acid mine drainage: low-temperature, low-pH and matrix investigations, *Water Research,* Vol.38, No.6, pp.1405-1418.

Valente, T. M., and Leal Gomes, C. (2009): Occurrence, properties and pollution potential of environmental minerals in acid mine drainage, *Science of the Total Environment,* Vol.407, No.3, pp.1135-1152.

Van Hille, R. P., Boshoff, G., Rose, P., and Duncan, J. (1999): A continuous process for the biological treatment of heavy metal contaminated acid mine water, *Resources, Conservation and Recycling,* Vol.27, No.1, pp.157-167.

Vangpaisal, T., and Bouazza, A. (2003): Gas permeability of partially hydrated geosynthetic clay liners, *Journal of Geotechnical and Geoenvironmental Engineering,* Vol.130, No.1, pp.93-102.

Virta, R. "Zeolites." Retrieved February 6, 2014, from http://minerals.usgs.gov/minerals/pubs/commodity/zeolites/zeomyb97.pdf.

Wibkirchen, C., Dold, B., Friese, K., and Glaber, W. (2005): Hydrogeochemistry and sediment mineralogy of Lake Yanamate - an extremely acidic lake caused by discharge of acid mine drainage from the Pb-Zn-(Cu) deposit, Cerro de Pasco (Peru), *Securing the Future*, pp.1013-1022.

Williams, M. (2001): Arsenic in mine waters: an international study, *Environmental geology,* Vol.40, No.3, pp.267-278.

Winterbourn, M., McDiffett, W., and Eppley, S. (2000): Aluminium and iron burdens of aquatic biota in New Zealand streams contaminated by acid mine drainage: effects of trophic level, *Science of the Total Environment,* Vol.254, No.1, pp.45-54.

Wolkersdorfer, C. (2008): Water management at abandoned flooded underground mines, Springer.

Wu, P., Tang, C., Liu, C., Zhu, L., Pei, T., and Feng, L. (2009): Geochemical distribution and removal of As, Fe, Mn and Al in a surface water system affected by acid mine drainage at a coalfield in Southwestern China, *Environmental Geology,* Vol.57, No.7, pp.1457-1467.

Xu, D., Tan, X. L., Chen, C. L., and Wang, X. K. (2008): Adsorption of Pb (II) from aqueous solution to MX-80 bentonite: effect of pH, ionic strength, foreign ions and temperature, *Applied Clay Science,* Vol.41, No.1-2, pp.37-46.

Younger, P. L., Banwart, S. A., and Hedin, R. S. (2002): Mine water: hydrology, pollution, remediation,

Springer.

Zanker, H., Moll, H., Richter, W., Brendler, V., Hennig, C., Reich, T., Kluge, A., and Hüttig, G. (2002): The colloid chemistry of acid rock drainage solution from an abandoned Zn–Pb–Ag mine, *Applied Geochemistry,* Vol.17, No.5, pp.633-648.

Appendix A. ARD Database

ARD	Type	Place	EC	pH	ORP	Al	As	Ca	Cu	Fe	K	Mg	Na	Pb	SO_4	Zn	Reference
1	G	R	na	6.2	na	na	na	5.8	0	0.5	na	1.05	1.65	0	na	0.05	Arp et al. (1999)
2	G	R	na	6.7	na	na	na	9.6	0	0.7	na	1.35	1.7	0	na	0.05	Ditto
3	G	R	na	3.8	na	na	na	13.3	0.1	0.1	na	3.3	2.5	0.05	na	2.15	Ditto
4	G	R	na	3.9	na	na	na	45.8	0.8	2.4	na	14.75	4.4	0.25	na	11.95	Ditto
5	P	R	36.7	9.2	na	na	0.017	na	0.0013	na	na	na	na	na	na	na	Aykol et al. (2003)
6	P	R	37.7	8.98	na	na	0.02	na	0.0018	0.014	na	na	na	na	na	0.0007	Ditto
7	P	R	37.5	8.74	na	na	0.013	na	0.0013	0.046	na	na	na	na	na	0.001	Ditto
8	P	R	67.4	7.26	na	na	0.015	na	0.0005	0.069	na	na	na	na	na	na	Ditto
9	P	R	60.5	7.85	na	na	0.015	na	0.0006	0.029	na	na	na	na	na	na	Ditto
10	P	R	63.1	7.65	na	na	0.015	na	0.0006	na	na	na	na	na	na	na	Ditto
11	P	R	65.6	7.72	na	na	0.019	na	0.0005	na	na	na	na	na	na	na	Ditto
12	P	R	57.2	7.93	na	na	0.008	na	0.0014	0.027	na	na	na	na	na	na	Ditto
13	P	R	57.8	7.84	na	na	0.011	na	0.0006	0.021	na	na	na	na	na	na	Ditto
14	P	R	54.3	7.85	na	na	0.003	na	0.0227	na	na	na	na	na	na	4.3658	Ditto
15	P	R	54.6	7.75	na	na	0.01	na	0.0009	0.082	na	na	na	na	na	0.0645	Ditto
16	P	R	49.8	7.45	na	na	0.01	na	0.0007	0.025	na	na	na	na	na	0.0075	Ditto
17	P	R	48.8	7.92	na	na	0.01	na	0.0006	0.014	na	na	na	na	na	0.0193	Ditto
18	P	R	49.4	7.75	na	na	0.011	na	0.0016	0.051	na	na	na	na	na	0.0048	Ditto
19	P	R	49.9	7.55	na	na	0.01	na	0.0005	0.026	na	na	na	na	na	0.0019	Ditto
20	P	R	104.9	7.22	na	na	0.031	na	0.0004	0.028	na	na	na	na	na	0.0009	Ditto
21	P	R	47.3	7.55	na	na	0.013	na	0.0007	0.017	na	na	na	na	na	0.0064	Ditto
22	P	R	45.9	7.75	na	na	0.012	na	0.0019	0.023	na	na	na	na	na	0.0046	Ditto
23	P	R	46.5	7.65	na	na	0.012	na	0.0009	0.015	na	na	na	na	na	0.0072	Ditto
24	P	R	43.9	8.02	na	na	0.014	na	0.0008	0.018	na	na	na	na	na	0.0045	Ditto
25	P	R	47.9	7.82	na	na	0.005	na	0.0119	na	na	na	na	na	na	3.6047	Ditto
26	P	R	49.3	7.55	na	na	0.01	na	0.0008	0.029	na	na	na	na	na	0.0776	Ditto
27	P	R	51.1	7.53	na	na	0.006	na	0.0005	0.054	na	na	na	0.002	na	0.1312	Ditto
28	P	R	41.2	7.41	na	na	0.006	na	0.0006	na	na	na	na	na	na	0.0198	Ditto
29	P	R	40.6	7.91	na	na	0.017	na	0.0004	0.049	na	na	na	na	na	0.0034	Ditto
30	P	R	37.4	7.66	na	na	0.005	na	0.0008	0.023	na	na	na	na	na	na	Ditto
31	P	R	190	6.93	na	na	na	na	0.0007	0.079	na	na	na	na	na	2.8411	Ditto
32	P	R	210	7.12	na	na	na	na	0.0004	na	na	na	na	na	na	5.9832	Ditto
33	P	R	290	7.02	na	na	na	na	0.0004	na	na	na	na	na	na	20.0668	Ditto

ARD	Type	Place	EC	pH	ORP	Al	As	Ca	Cu	Fe	K	Mg	Na	Pb	SO_4	Zn	Reference
34	P	R	270	7.04	na	na	na	na	0.001	na	na	na	na	na	na	2.3841	Ditto
35	P	R	280	7.09	na	na	na	na	0.0003	0.159	na	na	na	na	na	1.2786	Ditto
36	P	R	220	7.4	na	na	0.002	na	0.0005	na	na	na	na	na	na	1.1538	Ditto
37	P	R	120	7.55	na	na	0.107	na	0.0016	0.357	na	na	na	na	na	0.0172	Ditto
38	P	R	107.1	6.54	na	na	0.013	na	0.0157	0.152	na	na	na	na	na	3.6863	Ditto
39	P	R	184.5	3.72	na	na	na	na	5.2603	0.893	na	na	na	4.885	na	330.8636	Ditto
40	P	R	356	2.57	na	na	1.174	na	5.4641	87.474	na	na	na	2.348	na	203.5177	Ditto
41	P	R	114	6.2	na	na	0.008	na	0.0248	0.743	na	na	na	0.016	na	11.021	Ditto
42	P	R	457	2.22	na	na	7.186	na	3.1644	464.974	na	na	na	0.056	na	61.4967	Ditto
43	P	R	64	5.71	na	na	0.03	na	0.0428	2.282	na	na	na	0.219	na	5.3901	Ditto
44	P	R	78	5.99	na	na	0.015	na	0.0278	0.53	na	na	na	0.139	na	6.2763	Ditto
45	P	R	77	6.1	na	na	0.016	na	0.0314	0.348	na	na	na	0.125	na	6.4556	Ditto
46	P	R	25	6.7	na	na	0.036	na	0.0061	2.546	na	na	na	0.005	na	0.02	Ditto
47	P	R	23	6.8	na	na	0.03	na	0.0078	2.372	na	na	na	0.01	na	0.0235	Ditto
48	P	R	25	6.74	na	na	0.029	na	0.0133	3.078	na	na	na	0.013	na	0.0361	Ditto
49	P	R	209	6.48	na	na	na	na	0.0083	0.311	na	na	na	0.004	na	16.7213	Ditto
50	P	R	173	6.61	na	na	0.002	na	0.0103	0.295	na	na	na	0.024	na	6.9041	Ditto
51	P	R	206	6.53	na	na	na	na	0.0104	0.117	na	na	na	na	na	17.9721	Ditto
52	C	MD	na	7.1	na	na	na	na	na	0.63	na	na	na	na	690	0.056	Banks et al. (1997)
53	C	MD	na	7.1	na	na	na	na	na	5.8	na	na	na	na	1170	0.034	Ditto
54	C	MD	na	7.3	na	na	na	na	na	5	na	na	na	na	380	0.03	Ditto
55	C	MD	na	7.7	na	na	na	na	na	25	na	na	na	na	404	na	Ditto
56	C	MD	na	7.4	na	na	na	na	na	3.55	na	na	na	na	na	na	Ditto
57	C	MD	na	8.2	na	0.02	na	na	0.005	0.01	na	na	na	na	7.4	0.055	Ditto
58	C	MD	na	6.3	na	na	na	na	na	2.2	na	na	na	na	148	na	Ditto
59	C	MD	na	6.3	na	0.045	na	na	0.007	10.6	na	na	na	na	210	0.007	Ditto
60	C	MD	na	3.6	na	17.3	na	na	0.007	101.3	na	na	na	na	1044	0.221	Ditto
61	C	MD	na	6.3	na	0.078	na	na	0.005	4.9	na	na	na	na	83	0.048	Ditto
62	C	MD	na	4.2	na	0.5	na	na	na	180	na	na	na	na	1554	0.061	Ditto
63	C	MD	na	7.9	na	0.01	na	na	0.0007	0.097	na	na	na	na	176	0.005	Ditto
64	C	MD	na	3.5	na	na	na	na	na	70	na	na	na	na	810	na	Ditto
65	C	MD	na	4.1	na	na	na	na	na	15	na	na	na	na	1358	na	Ditto
66	C	MD	na	5.5	na	0.97	na	na	0.007	287	na	na	na	na	146	0.05	Ditto
67	C	MD	na	6.8	na	0.045	na	na	na	18.6	na	na	na	na	1327	0.007	Ditto
68	C	MD	na	3.7	na	1.8	na	na	0.014	1.6	na	na	na	na	77	0.49	Ditto

ARD	Type	Place	EC	pH	ORP	Al	As	Ca	Cu	Fe	K	Mg	Na	Pb	SO_4	Zn	Reference
69	C	MD	na	2.7	na	27.5	na	na	0.168	179	na	na	na	na	1077	1.3	Ditto
70	S	MD	na	2.5	na	84.21	na	na	0.16	1460	na	na	na	na	5110	0.94	Ditto
71	P	MD	na	2.9	na	17	na	na	0.049	na	na	na	na	na	643.5	55	Ditto
72	C	MD	na	6.5	na	0.132	na	na	na	14.9	na	na	na	na	124	0.029	Ditto
73	P	MD	na	2.65	na	116	na	na	5.275	na	na	na	na	na	791	777.5	Ditto
74	P	MD	45.7	7.22	na	na	0.192	na	0.0059	na	na	na	na	na	93	na	Ditto
75	P	MD	215.8	2.72	na	na	na	na	25.5	248	na	na	na	na	1564	1.08	Ditto
76	P	MD	na	2.3	na	na	na	na	530	1529	na	na	na	na	na	870	Ditto
77	P	MD	na	2.71	na	20.1	na	na	35.6	210	na	na	na	na	1671	131	Ditto
78	P	MD	44.5	6.28	na	na	na	na	0.2	5.06	na	na	na	na	na	3.3	Ditto
79	P	MD	592.2	2.36	na	na	na	na	129.4	2284	na	na	na	na	7291	256.5	Ditto
80	P	MD	26.7	3.68	na	2.58	na	na	0.776	na	na	na	na	na	68	0.151	Ditto
81	P	MD	na	2.7	na	885	0.28	na	544	3680	na	na	na	na	26500	5640	Ditto
82	P	MD	na	4.1	na	105.8	na	441	22.41	0.82	na	538	na	0.41	8120	2211	Berger et al. (2000)
83	P	MD	na	4.7	na	20.45	na	356	10.65	0.87	na	281	na	0.21	4250	1048	Ditto
84	P	MD	na	4.8	na	16.56	na	267	10.88	2	na	296	na	0.24	4240	897	Ditto
85	P	MD	na	5.3	na	4.59	na	151	5.28	1.46	na	138	na	0.06	2110	568	Ditto
86	P	MD	na	5.5	na	1.02	na	270	1.44	1.17	na	185	na	0.01	2480	681	Ditto
87	P	MD	na	4.7	na	4.59	na	151	5.28	1.46	na	138	na	0.06	5110	568	Ditto
88	P	MD	na	4.7	na	48.55	na	382	13.75	1.05	na	363	na	0.34	5210	1435	Ditto
89	P	MD	na	4.7	na	36.73	na	354	11.13	0.93	na	322	na	0.4	4550	1210	Ditto
90	P	MD	na	4.7	na	33.78	na	355	10.66	0.91	na	318	na	0.38	4540	1239	Ditto
91	P	MD	na	4.7	na	33.78	na	355	10.66	0.91	na	318	na	0.38	4750	1269	Ditto
92	P	MD	na	4.2	na	93.79	na	509	18.83	1.35	na	448	na	0.2	6260	1752	Ditto
93	P	MD	na	4.5	na	44.64	na	388	13.01	1.94	na	308	na	0.1	4320	1232	Ditto
94	P	MD	na	5.8	na	0.1	na	298	0.23	0.23	na	117	na	0	2120	476	Ditto
95	P	MD	na	5.6	na	1.54	na	296	1.73	2.63	na	169	na	0.05	1990	411	Ditto
96	P	MD	na	5.3	na	4.85	na	313	4.45	2.3	na	195	na	0.18	na	581	Ditto
97	P	MD	na	4.5	na	33.35	na	363	10.67	2.24	na	283	na	0.49	4280	1138	Ditto
98	P	MD	na	4.8	na	18	na	322	9.52	3.13	na	254	na	0.44	3510	929	Ditto
99	P	MD	na	4.9	na	16	na	314	9.98	3.05	na	252	na	0.46	3380	893	Ditto
100	P	MD	na	5.8	na	1.49	na	224	3.06	3.68	na	141	na	0.03	2140	448	Ditto
101	P	MD	na	5.9	na	1.48	na	238	2.94	2.85	na	141	na	0.05	2020	516	Ditto
102	P	MD	na	6	na	0.74	na	221	1.98	1.95	na	129	na	0.02	1710	447	Ditto
103	P	MD	na	7.2	na	0.13	na	127	0.39	0.04	na	59	na	0.01	603	135	Ditto
104	P	MD	na	7.2	na	0	na	41	0.01	7.38	na	26	na	0	119	3	Ditto

ARD	Type	Place	EC	pH	ORP	Al	As	Ca	Cu	Fe	K	Mg	Na	Pb	SO_4	Zn	Reference
105	P	MD	48.5	3.11	na	8.5	0.005	6	0.53	23	1.2	4.1	1.7	0.37	160	4.9	Bird (2003)
106	P	MD	50.3	3.16	na	3.7	0.001	15	0.028	15	1.2	7.2	2.8	0.52	160	5	Ditto
107	P	MD	31.8	4.47	na	2.2	0.001	28	0.15	0.036	1.2	7	2.3	0.001	110	0.84	Ditto
108	P	MD	61.1	3.3	na	14	0.001	14	0.21	40	5	15	3.7	0.028	280	7.1	Ditto
109	P	MD	28.7	3.58	na	8.6	0.001	7	0.13	5.9	1	7	2.1	0.021	130	2.3	Ditto
110	P	MD	54.9	3.25	na	16	0.001	12	2	9.9	5	13	4	0.25	250	6.1	Ditto
111	P	MD	8.4	3.95	na	1.7	0.001	2	0.14	0.028	1	1.2	1.3	0.01	26	0.32	Ditto
112	P	MD	3.9	4.38	na	0.058	0.001	3	0.004	0.01	1	0.9	0.9	0.001	13	0.019	Ditto
113	P	MD	21.9	4.03	na	2	0.001	16	0.11	3.6	1.1	5	2.4	0.56	93	1.2	Ditto
114	P	MD	62.9	3.62	na	2	0.003	76	0.28	14	1	16	3.6	0.14	300	8.4	Ditto
115	P	MD	10.4	4.67	na	0.063	0.001	12	0.004	0.044	1	2.5	2.6	0.001	39	0.48	Ditto
116	P	MD	7.5	4.39	na	0.12	0.001	7	0.004	0.076	1	1.3	1.4	0.002	29	0.25	Ditto
117	P	MD	16.5	3.84	na	2.7	0.001	11	0.13	0.21	1	3.4	1.7	0.049	71	1	Ditto
118	P	MD	19.5	4.01	na	3.1	0.001	12	0.15	0.15	1	3.9	1.8	0.01	79	1.2	Ditto
119	P	MD	13.5	4.35	na	1.3	0.001	12	0.17	0.12	1	3.6	1.3	0.004	54	1.3	Ditto
120	P	MD	14.3	4.22	na	1.9	0.001	12	0.19	0.16	1	3.7	1.4	0.00001	58	1.4	Ditto
121	P	MD	28	3.42	na	7.8	0.004	7	0.43	22	1.1	5.1	2.3	0.27	160	5	Ditto
122	P	MD	46.4	2.91	na	4.7	0.001	17	0.012	21	1.4	9	3.5	0.42	190	5.4	Ditto
123	P	MD	28.8	4.41	na	1.4	0.001	37	0.032	0.01	1.4	8.5	2.7	0.001	150	0.97	Ditto
124	P	MD	59.3	3.14	na	14	0.001	14	0.22	39	1.6	15	3.4	0.023	280	7.3	Ditto
125	P	MD	47	3.21	na	14	0.001	12	0.2	12	1.4	12	3.3	0.027	220	4.7	Ditto
126	P	MD	30.3	3.39	na	11	0.001	7	0.78	0.43	1.2	7.8	3.1	0.08	150	3.2	Ditto
127	P	MD	49.6	3.08	na	10	0.001	12	1.1	14	1.6	11	3.9	0.18	220	5	Ditto
128	P	MD	10.6	3.72	na	3.2	0.001	3	0.13	0.01	0.7	2.5	2.1	0.005	49	0.8	Ditto
129	P	MD	25.8	3.35	na	9.7	0.001	8	0.45	0.7	1	5.8	2.5	0.025	130	2.6	Ditto
130	P	MD	17.7	4.92	na	1.6	0.001	17	0.084	3.2	1.1	5.2	2.9	0.35	89	1	Ditto
131	P	MD	55	4.9	na	0.74	0.001	76	0.088	14	1.1	16	3.5	0.004	300	4.4	Ditto
132	P	MD	9.4	5.42	na	0.058	0.001	11	0.003	0.024	0.8	2.5	2.6	0.001	40	0.44	Ditto
133	P	MD	24.9	4.1	na	6	0.001	16	0.25	0.37	1	5.8	2.6	0.013	120	1.8	Ditto
134	P	MD	13	4.15	na	0.47	0.001	13	0.003	0.05	0.7	2.5	2	0.005	60	0.78	Ditto
135	P	MD	21.2	3.73	na	5.2	0.001	15	0.19	0.25	0.9	5.3	2.5	0.049	110	1.6	Ditto
136	P	MD	22.7	3.7	na	5.9	0.001	16	0.23	0.19	0.9	5.9	2.5	0.012	120	2.1	Ditto
137	P	MD	15.3	4.36	na	1.8	0.001	17	0.23	0.1	0.7	5.1	1.5	0.003	78	1.7	Ditto
138	P	MD	16.8	3.85	na	2.4	0.001	17	0.25	0.15	0.7	5.2	1.7	0.009	na	1.9	Ditto
139	C	R	na	7.86	na	na	0.003	na	0.02	na	na	na	na	na	na	na	Black and Craw (2001)
140	C	R	na	7.12	na	na	na	na	na	na	na	na	na	na	na	na	Ditto

ARD	Type	Place	EC	pH	ORP	Al	As	Ca	Cu	Fe	K	Mg	Na	Pb	SO_4	Zn	Reference
141	C	R	na	6.9	na	na	na	na	na	na	na	na	na	na	na	na	Ditto
142	C	R	na	7.2	na	na	0.003	na	0.02	na	na	na	na	na	na	na	Ditto
143	C	R	na	6.8	na	na	0.001	na	0.03	na	na	na	na	na	na	na	Ditto
144	C	R	na	7.43	na	na	0.005	na	0.02	na	na	na	na	na	na	na	Ditto
145	C	LK	na	7.23	na	na	na	na	na	na	na	na	na	na	na	na	Ditto
146	C	MD	na	na	na	na	na	na	na	na	na	na	na	na	na	na	Ditto
147	C	MD	na	na	na	na	na	na	na	na	na	na	na	na	na	na	Ditto
148	C	MD	na	na	na	na	na	na	na	na	na	na	na	na	na	na	Ditto
149	C	MD	na	3.73	na	na	0.002	na	0.02	na	na	na	na	na	na	0.005	Ditto
150	C	MD	na	4.28	na	na	0.001	na	0.02	na	na	na	na	na	na	0.022	Ditto
151	C	MD	na	4.68	na	na	0.003	na	0.02	na	na	na	na	na	na	0.005	Ditto
152	C	MD	na	4.45	na	na	0.002	na	0.02	na	na	na	na	na	na	0.005	Ditto
153	C	MD	na	4.6	na	na	na	na	na	na	na	na	na	na	na	na	Ditto
154	C	MD	na	4.83	na	na	0.046	na	0.17	na	na	na	na	na	na	0.005	Ditto
155	C	MD	na	5.29	na	na	na	na	na	na	na	na	na	na	na	na	Ditto
156	C	MD	na	4.78	na	na	0.001	na	0.02	na	na	na	na	na	na	0.005	Ditto
157	C	MD	na	4.06	na	na	na	na	na	na	na	na	na	na	na	na	Ditto
158	C	MD	na	4.85	na	na	0.002	na	0.03	na	na	na	na	na	na	0.005	Ditto
159	C	MD	na	4.02	na	na	0.006	na	0.01	na	na	na	na	na	na	0.029	Ditto
160	C	MD	na	5.28	na	na	0.001	na	0.03	na	na	na	na	na	na	0.012	Ditto
161	C	MD	na	5.02	na	na	0.005	na	0.02	na	na	na	na	na	na	0.005	Ditto
162	C	MD	na	4.68	na	na	na	na	na	na	na	na	na	na	na	na	Ditto
163	C	MD	na	3.95	na	na	0.006	na	0.01	na	na	na	na	na	na	0.029	Ditto
164	C	MD	na	na	na	na	0.31	na	0.07	na	na	na	na	na	na	0.6	Ditto
165	C	MD	na	na	na	na	0.7	na	0.02	na	na	na	na	na	na	0.57	Ditto
166	C	MD	na	na	na	na	0.41	na	0.1	na	na	na	na	na	na	1.08	Ditto
167	C	MD	na	4.24	na	na	0.002	na	0.02	na	na	na	na	na	na	0.005	Ditto
168	C	MD	na	4.19	na	na	0.001	na	0.02	na	na	na	na	na	na	0.745	Ditto
169	C	MD	na	4.64	na	na	0.001	na	0.02	na	na	na	na	na	na	0.13	Ditto
170	C	MD	na	3.88	na	na	0.001	na	0.02	na	na	na	na	na	na	0.01	Ditto
171	C	MD	na	4.57	na	na	0.003	na	0.02	na	na	na	na	na	na	0.067	Ditto
172	C	MD	na	3.79	na	na	0.002	na	0.02	na	na	na	na	na	na	0.201	Ditto
173	C	MD	na	4.23	na	na	0.002	na	0.03	na	na	na	na	na	na	0.171	Ditto
174	C	MD	na	5.3	na	na	0.002	na	0.02	na	na	na	na	na	na	0.201	Ditto
175	C	MD	na	3.88	na	na	0.001	na	0.02	na	na	na	na	na	na	0.13	Ditto
176	C	MD	na	3.63	na	na	0.001	na	0.02	na	na	na	na	na	na	0.273	Ditto

ARD	Type	Place	EC	pH	ORP	Al	As	Ca	Cu	Fe	K	Mg	Na	Pb	SO_4	Zn	Reference
177	C	MD	na	4.63	na	na	0.001	na	0.02	na	na	na	na	na	na	0.011	Ditto
178	C	MD	na	4.46	na	na	0.001	na	0.03	na	na	na	na	na	na	0.015	Ditto
179	C	MD	na	4.19	na	na	0.001	na	0.02	na	na	na	na	na	na	0.005	Ditto
180	C	MD	na	4.51	na	na	0.001	na	0.02	na	na	na	na	na	na	0.005	Ditto
181	C	MD	na	4.49	na	na	0.001	na	0.02	na	na	na	na	na	na	0.051	Ditto
182	C	MD	na	3.92	na	na	na	na	na	na	na	na	na	na	na	na	Ditto
183	C	MD	na	1.59	na	na	0.002	na	0.03	na	na	na	na	na	na	0.005	Ditto
184	C	MD	na	5.91	na	na	0.046	na	0.17	na	na	na	na	na	na	0.466	Ditto
185	C	MD	na	4.28	na	na	0.006	na	0.01	na	na	na	na	na	na	0.005	Ditto
186	C	MD	na	5.83	na	na	na	na	na	na	na	na	na	na	na	na	Ditto
187	C	MD	na	5.91	na	na	na	na	na	na	na	na	na	na	na	na	Ditto
188	C	MD	na	3.92	na	na	na	na	na	na	na	na	na	na	na	na	Ditto
189	C	MD	na	4.44	na	na	0.003	na	0.02	na	na	na	na	na	na	0.005	Ditto
190	C	MD	na	2.36	na	na	0.001	na	0.02	na	na	na	na	na	na	0.022	Ditto
191	C	MD	na	6.16	na	na	na	na	na	na	na	na	na	na	na	na	Ditto
192	C	MD	na	6.8	na	na	na	na	na	na	na	na	na	na	na	na	Ditto
193	C	MD	na	3.47	na	na	0.001	na	0.03	na	na	na	na	na	na	0.012	Ditto
194	C	MD	na	4.66	na	na	0.001	na	0.03	na	na	na	na	na	na	0.017	Ditto
195	C	MD	na	4.14	na	na	0.008	na	0.04	na	na	na	na	na	na	0.054	Ditto
196	C	MD	na	4.66	na	na	0.001	na	0.02	na	na	na	na	na	na	0.201	Ditto
197	C	MD	na	5.4	na	na	0.001	na	0.02	na	na	na	na	na	na	0.097	Ditto
198	C	MD	na	5.32	na	na	0.002	na	0.02	na	na	na	na	na	na	0.012	Ditto
199	C	MD	na	6.24	na	na	0.001	na	0.02	na	na	na	na	na	na	0.005	Ditto
200	C	MD	na	4.52	na	na	0.001	na	0.03	na	na	na	na	na	na	0.005	Ditto
201	C	MD	na	5.32	na	na	0.051	na	0.15	na	na	na	na	na	na	0.897	Ditto
202	C	MD	na	5.24	na	na	0.002	na	0.02	na	na	na	na	na	na	0.169	Ditto
203	C	MD	na	7.06	na	na	0.002	na	0.02	na	na	na	na	na	na	0.005	Ditto
204	M	R	na	2.4	na	55.56	na	na	19.23	193.24	na	na	na	na	na	30.03	Boult et al. (1994)
205	M	R	na	5.99	na	1.14	na	na	1.42	1.36	na	na	na	na	na	1.99	Ditto
206	M	R	na	6.49	na	0.12	na	na	0.67	0.15	na	na	na	na	na	0.23	Ditto
207	P	R	na	7	na	na	na	185.5	na	0	1.1	4.47	5.86	0	403.5	2.09	Carroll et al. (1998)
208	P	R	na	6.7	na	na	0	210	na	0	2.9	21	8.15	0	492	7.7	Ditto
209	P	R	na	5	na	14	1	na	0.13	23	na	na	na	0.63	840	9	Casiot et al. (2009)
210	P	R	na	8	na	0.007	0.002	na	0.0005	0.006	na	na	na	0.0004	17	0.032	Ditto
211	P	R	na	7.9	na	0.07	0.03	na	0.0013	0.054	na	na	na	0.002	76	0.11	Ditto

ARD	Type	Place	EC	pH	ORP	Al	As	Ca	Cu	Fe	K	Mg	Na	Pb	SO_4	Zn	Reference
212	P	MD	na	5.52	na	1.38	na	500	1.45	139	na	350	na	na	2940	33.5	Christensen et al. (1996)
213	P	MD	na	2.4	na	263	na	382	99.2	1160	na	212	na	na	6600	89.2	Ditto
214	G	R	238	6.6	385	0.9	0.0008	603	0.018	0.13	8	259	440	0.0023	2465	0.42	Cidu et al. (1997)
215	G	R	211	7.7	431	0.05	0.0008	592	0.037	0.03	4.3	249	309	0.0035	2582	0.42	Ditto
216	G	MD	1382	2.4	729	2060	0.427	380	28.695	1755	5.5	1146	33	0.025	19447	10.67	Ditto
217	G	MD	1348	2.3	740	1840	0.36	381	28.328	1750	4.9	1145	32	0.052	19565	10.61	Ditto
218	G	MD	1402	2.3	817	2080	0.257	394	29.331	1733	5.5	1157	32	0.046	20201	10.82	Ditto
219	G	G	32	6.9	421	0.02	0.0008	27	0.0003	0.06	1.6	12	18	0.001	25	0.02	Ditto
220	G	R	1120	7.9	353	0.02	0.0008	740	0.0013	0.04	12.1	476	1368	0.0014	2785	0.003	Ditto
221	G	G	307	6.6	443	0.2	0.0008	205	0.0003	0.06	4.9	91	352	0.005	857	0.01	Ditto
222	G	MD	695	5.7	290	1.03	0.382	470	0.023	37.4	16.6	134	920	0.0045	2084	0.39	Ditto
223	G	R	33	7	347	0.08	0.0008	24	0.0027	0.08	2.1	11	22	0.0013	36	0.005	Ditto
224	G	R	145	7.5	414	0.35	0.0008	105	0.0027	0.3	9	45	134	0.0021	192	0.01	Ditto
225	G	R	682	7.7	397	0.02	0.0008	588	0.004	0.03	9.8	310	656	0.0015	2587	0.04	Ditto
226	G	R	828	4.1	580	61	0.0008	481	0.211	1.46	11.8	315	744	0.0077	2490	5.3	Ditto
227	G	R	965	5.6	480	5.3	0.0008	635	0.017	0.96	16	382	1010	0.0035	2782	2.97	Ditto
228	G	R	1010	7.1	413	0.09	0.0008	669	0.013	0.06	16.4	473	1280	0.0015	2825	0.03	Ditto
229	G	G	119	7.2	351	0.03	0.0008	36	0.0003	0.1	4.7	34	158	0.0002	173	0.01	Ditto
230	G	G	149	7.4	429	0.07	0.0008	131	0.0019	0.04	3.8	42	129	0.0009	202	0.01	Ditto
231	G	G	107	7.3	424	0.01	0.0008	82	0.0003	0.02	15.8	23	99	0.0007	57	0.003	Ditto
232	G	G	164	7.1	271	0.02	0.0008	170	0.0003	0.05	4.1	27	133	0.0008	194	0.07	Ditto
233	G	G	178	7.4	391	0.01	0.0008	45	0.0003	0.04	1.9	34	273	0.0008	159	0.005	Ditto
234	G	G	684	7.2	436	0.02	0.0008	399	0.006	0.1	9.3	268	835	0.0011	2049	0.01	Ditto
235	G	G	569	6.4	154	0.01	0.0008	233	0.008	1.7	11.9	43	1066	0.001	1420	0.02	Ditto
236	G	G	549	6.2	256	4.9	0.0008	449	0.014	13	16.7	181	644	0.001	1524	0.83	Ditto
237	C	R	na	6.3	na	0.1	na	na	na	0.4	na	na	na	na	255	0.07	DeNicola and Stapleton (2002)
238	M	R	177.5	3.8	455	42	na	289	32	9.8	5	159	22.1	na	1500	5.7	Dinelli and Tateo (2002)
239	M	R	520	2.7	610	99	na	252	46	225	0.5	484	42	na	3500	21	Ditto
240	M	R	51	5.9	290	na	na	63	na	0.1	0.1	49	6.4	na	190	0.5	Ditto
241	M	R	795	2.8	590	210	na	333	154	775	0.2	801	41.3	na	6000	26	Ditto
242	M	R	94	5.2	170	na	na	101	5.9	0.6	2.6	72	12.1	na	650	1.5	Ditto
243	M	R	189	7.3	275	na	na	302	na	0.1	1	251	15.6	na	1600	2.3	Ditto
244	M	R	22	8.3	280	na	na	17	na	na	na	26	4.1	na	20	na	Ditto
245	P	MD	na	2.3	na	56.7	6.54	900	26.9	1691	63	4032	111	0.63	44424	578	Dold et al. (2009)
246	P	MD	na	10	na	0.16	0.1	974	0.03	3.63	15.5	na	50.8	0.52	1642	1.09	Ditto
247	G	MD	na	1.65	na	249	na	300	1.8	942	558	359	345	0.349	6305	10.1	Feng et al. (2000)

ARD	Type	Place	EC	pH	ORP	Al	As	Ca	Cu	Fe	K	Mg	Na	Pb	SO_4	Zn	Reference
248	A	MD	94.7	3.08	491	10.5	0.0863	38.6	0.0279	13.5	0.82	12.2	5.85	na	374	na	Fukushi et al. (2003)
249	A	MD	26.3	6.91	33	0.01	0.0336	26.2	na	1.43	1.12	5.43	5.66	na	86.5	na	Ditto
250	A	MD	na	6	265	0.01	0.255	29.3	0.0009	0.05	1.7	7.35	6.11	na	135	na	Ditto
251	A	MD	56.1	3.35	538	5.68	0.0747	25.2	0.0222	2.07	0.84	7.17	5.21	na	209	na	Ditto
252	A	MD	54.1	3.37	547	5.47	0.0665	24	0.02	1.61	0.79	6.86	5.16	na	211	na	Ditto
253	A	MD	54.9	3.36	543	5.78	0.0573	25.4	0.0217	1.72	0.99	7.3	5.62	na	206	na	Ditto
254	A	MD	55.4	3.3	549	6.33	0.0435	27.2	0.0213	1.9	1.01	8.06	6.28	na	208	na	Ditto
255	A	MD	52.7	3.33	503	6.37	0.0125	27.3	0.0243	0.46	0.95	7.61	5.86	na	209	na	Ditto
256	A	MD	51.1	3.33	528	6.2	0.0084	26.4	0.0274	0.42	0.94	7.52	5.68	na	203	na	Ditto
257	A	MD	57.8	3.33	521	6.03	0.0075	26	0.0273	0.38	0.92	7.45	5.69	na	199	na	Ditto
258	A	R	14.8	6.87	268	0.01	0.0005	11.8	0.002	0.01	0.86	3.64	4.52	na	54	na	Ditto
259	P	R	719	2.27	778	455.98	1.288	135.06	128.99	1262.09	2.345	427.76	49.198	0.151	2.834	134.74	Gammons et al. (2008)
260	P	R	1450	2.39	768	1330.18	0.1213	361.10	158.22	586.37	0.547	1769.40	34.714	0.058	6317.00	338.16	Ditto
261	P	R	99	3.04	710	12.41	0.0009	48.09	3.495	1.228	2.072	31.11	19.771	0.0766	130.82	8.503	Ditto
262	P	R	757	2.51	765	582.80	0.065	181.95	67.358	232.31	1.915	751.02	25.518	0.0683	2648.65	147.82	Ditto
263	C	G	50	7.4	na	na	0.001	44	na	0.02	2	50	7.1	na	19	0.006	Gammons et al. (2010)
264	C	G	56	7.2	na	na	0.008	56	na	0.45	5.1	47	18	na	29	0.02	Ditto
265	C	G	61	7.1	na	na	0.001	53	na	0.4	1.7	45	9	na	32	0.006	Ditto
266	C	G	49	7.5	na	na	0.001	45	na	0.01	1.3	45	6.9	na	15	0.038	Ditto
267	C	G	950	1.9	na	na	na	na	na	na	na	na	na	na	na	na	Ditto
268	C	G	70	6.7	na	na	0.001	87	na	34.5	3.5	37	9.6	na	301	0.053	Ditto
269	C	G	75	7	na	na	0.004	128	na	0.1	6.7	40	17	na	184	0.023	Ditto
270	C	G	57	7.6	na	na	0.002	54	na	0.26	1.7	40	7.8	na	29	0.016	Ditto
271	C	G	54	7	na	na	0.001	73	na	0.17	3.3	26	9.3	na	92	0.036	Ditto
272	C	G	64	6.9	na	na	0.001	57	na	0.02	1.6	27	5.6	na	48	0.022	Ditto
273	C	G	53	7.4	na	na	0.001	93	na	0.01	1.4	26	4.2	na	188	0.022	Ditto
274	C	G	107	7.4	na	na	0.001	197	na	0.22	2.1	70	5.5	na	586	0.075	Ditto
275	C	G	88	7.3	na	na	0.002	91	na	0.08	2.3	38	38	na	325	0.011	Ditto
276	C	MD	238	2.9	na	na	na	na	na	na	na	na	na	na	na	na	Ditto
277	C	MD	238	2.9	na	na	na	na	na	na	na	na	na	na	na	na	Ditto
278	C	MD	116	4.9	na	na	na	na	na	na	na	na	na	na	na	na	Ditto
279	C	MD	283	4.2	na	na	na	na	na	na	na	na	na	na	na	na	Ditto
280	C	MD	579	2.6	na	na	na	na	na	na	na	na	na	na	na	na	Ditto
281	C	MD	892	2.5	na	na	na	na	na	na	na	na	na	na	na	na	Ditto
282	C	MD	731	2.6	na	na	na	na	na	na	na	na	na	na	na	na	Ditto
283	C	MD	329	3.1	na	na	na	na	na	na	na	na	na	na	na	na	Ditto

ARD	Type	Place	EC	pH	ORP	Al	As	Ca	Cu	Fe	K	Mg	Na	Pb	SO_4	Zn	Reference
284	C	MD	780	2.6	na	na	na	na	na	na	na	na	na	na	na	na	Ditto
285	C	MD	162	2.9	na	na	na	na	na	na	na	na	na	na	na	na	Ditto
286	M	MD	na	2.3	na	na	2.5	na	2.7	810	na	na	na	1	na	12	Gault et al. (2005)
287	M	MD	na	2.4	na	na	2.4	na	2.7	790	na	na	na	1	na	12	Ditto
288	M	MD	na	2.5	na	na	2.4	na	2.7	790	na	na	na	0.9	na	12	Ditto
289	M	MD	na	2.5	na	na	1.4	na	1.8	550	na	na	na	0.6	na	8	Ditto
290	M	MD	na	2.5	na	na	0.8	na	1.3	310	na	na	na	0.5	na	5.6	Ditto
291	C	MD	na	6.4	na	na	na	na	na	34	na	na	na	na	na	na	Gazea et al. (1996)
292	C	MD	na	6.3	na	na	na	na	na	92	na	na	na	na	na	na	Ditto
293	C	MD	na	6.3	na	na	na	na	na	37	na	na	na	na	na	na	Ditto
294	C	MD	na	6.2	na	na	na	na	na	52	na	na	na	na	na	na	Ditto
295	C	MD	na	6	na	na	na	na	na	2	na	na	na	na	na	na	Ditto
296	C	MD	na	6.3	na	na	na	na	na	151	na	na	na	na	na	na	Ditto
297	C	MD	na	4.7	na	na	na	na	na	89	na	na	na	na	na	na	Ditto
298	C	MD	na	4.4	na	na	na	na	na	162	na	na	na	na	na	na	Ditto
299	C	MD	na	3.5	na	na	na	na	na	125	na	na	na	na	na	na	Ditto
300	C	MD	na	3.5	na	na	na	na	na	246	na	na	na	na	na	na	Ditto
301	C	MD	na	3.1	na	na	na	na	na	149	na	na	na	na	na	na	Ditto
302	C	MD	na	2.7	na	na	na	na	na	284	na	na	na	na	na	na	Ditto
303	C	MD	na	5.5	na	na	na	na	na	31	na	na	na	na	na	na	Ditto
304	C	MD	na	6.4	na	na	na	na	na	100	na	na	na	na	na	na	Ditto
305	S	MD	na	4.7	na	48	0.4	na	na	310	na	na	na	na	na	na	Ditto
306	G	MD	na	7	na	na	0.12	na	1.8	0.05	na	na	na	na	na	1	Ditto
307	G	MD	na	3.2	na	na	2.7	na	7.4	216	na	na	na	na	na	1.8	Ditto
308	G	MD	na	2.3	na	113	na	na	76	735	na	na	na	na	na	na	Ditto
309	G	MD	na	2.35	na	31	na	na	16	202.5	na	na	na	na	na	na	Ditto
310	M	MD	na	6.8	na	na	na	na	na	5	na	na	na	na	na	40	Ditto
311	M	MD	na	7.9	na	na	na	na	na	0	na	na	na	0.4	na	0.18	Ditto
312	P	R	na	na	na	na	0.0015	21.9	0.0062	0.0214	2.2	25.1	50.3	0.0026	na	0.0261	Gerhardt et al. (2004)
313	P	LK	na	na	na	na	0.0316	21.3	0.0239	0.0425	3.8	10.3	23.4	0.0141	na	0.1251	Ditto
314	P	R	na	5	na	na	0.0126	126.8	0.6481	0.8127	6	66.4	52.1	0.0755	na	2.4315	Ditto
315	P	R	na	3	na	na	0.0167	226.6	1.7552	2.9755	6.4	109	72.2	0.178	na	9.725	Ditto
316	P	R	28.8	7.168	na	na	na	na	na	0.286	na	na	na	na	42.994	na	Grande et al. (2005)
317	P	R	327.1	2.953	na	na	na	na	9.099	219.095	na	na	na	na	1583.14	10.32	Ditto
318	C	MD	801	2.7	na	na	na	na	243	1031	na	na	na	na	10579	362	Gray (1996)
319	C	MD	401.9	2.6	na	na	na	na	48	1050	na	na	na	na	5290	93	Ditto

ARD	Type	Place	EC	pH	ORP	Al	As	Ca	Cu	Fe	K	Mg	Na	Pb	SO_4	Zn	Reference
320	C	MD	249	3.6	na	na	na	na	9	177	na	na	na	na	2015	66	Ditto
321	C	R	7.8	6.8	na	na	na	na	0.01	0.11	na	na	na	na	6	0.05	Ditto
322	C	R	11.3	6.1	na	na	na	na	0.03	0.61	na	na	na	na	28	0.58	Ditto
323	C	R	73.5	4.9	na	na	na	na	2.1	13.9	na	na	na	na	507	5.5	Ditto
324	C	MD	194.6	3.6	na	122	0.007	na	4.9	116	na	na	na	na	1584	71	Gray (1998)
325	C	MD	260.5	3.81	na	76	0.02	na	1.8	165	na	na	na	na	1850	33	Ditto
326	C	MD	687.4	2.67	na	774	0.223	na	185	996	na	na	na	na	10203	229	Ditto
327	C	MD	319.9	2.7	na	165	0.373	na	38	635	na	na	na	na	3256	53	Ditto
328	C	MD	267.8	3.5	na	168	0.036	na	10.8	191	na	na	na	na	2069	71	Ditto
329	P	MD	na	3.8	na	50	2.5	na	0.4	136	na	na	na	0.3	1756	77	Hamilton et al. (1999)
330	M	MD	na	4	na	1.2	na	0.05	0.001	na	0.025	0.45	0.27	0.0002	5.9	0.008	Hammarstrom et al. (2005)
331	M	MD	na	4.6	na	0.63	na	0.4	0.0006	na	0.43	0.74	0.71	0	8	0.021	Ditto
332	M	MD	na	3.74	na	2.2	na	60	0.85	na	4.8	12	1.7	0.0004	240	0.35	Ditto
333	M	MD	na	2.4	na	69	na	59	57	na	0.4	36	7.7	0.18	1900	11	Ditto
334	M	MD	na	2.09	na	180	na	97	110	na	0.28	90	9.9	0.00051	4900	25	Ditto
335	P	MD	na	1.1	na	800	na	83	59	na	0.25	900	4	2.1	53600	2300	Ditto
336	M	MD	na	2.95	na	22	na	14	4.6	na	0.009	13	0.02	0.00069	480	0.45	Ditto
337	M	MD	na	3.65	na	0.018	na	0.1	0.35	na	0.33	0.14	0.22	0.00077	15	0.02	Ditto
338	M	MD	na	3.58	na	3.6	na	170	0.13	na	0.009	2.1	0.41	0.0002	410	0.1	Ditto
339	M	MD	na	2.7	na	16	na	0.79	0.43	na	0.009	11	0.01	1.5	760	5.4	Ditto
340	P	R	8.6	7.05	na	na	na	na	na	na	na	na	na	na	na	na	He et al. (1997)
341	P	R	13.1	na	na	na	na	na	na	na	na	na	na	na	na	na	Ditto
342	P	R	39	5.18	na	na	na	na	na	na	na	na	na	na	na	na	Ditto
343	P	R	16.4	6.74	na	na	na	na	na	na	na	na	na	na	na	na	Ditto
344	P	R	15.1	7.08	na	na	na	na	na	na	na	na	na	na	na	na	Ditto
345	P	R	19.6	6.86	na	na	na	na	na	na	na	na	na	na	na	na	Ditto
346	P	R	13.3	7.01	na	na	na	na	na	na	na	na	na	na	na	na	Ditto
347	P	R	na	7.06	na	na	na	na	na	na	na	na	na	na	na	na	Ditto
348	P	R	na	7.08	na	na	na	na	na	na	na	na	na	na	na	na	Ditto
349	P	R	na	6.95	na	na	na	na	na	na	na	na	na	na	na	na	Ditto
350	P	R	12.1	7.09	na	na	na	na	na	na	na	na	na	na	na	na	Ditto
351	P	R	10.7	na	na	na	na	na	na	na	na	na	na	na	na	na	Ditto
352	P	MD	na	2.1	na	45.1	0.862	96.6	13.1	715	na	27.8	na	na	2818	15	Herrera S et al. (2007)
353	G	MD	na	3.2	115	122	na	126	na	211	na	91.1	na	na	1820	3.68	Herrera et al. (2007)
354	G	G	na	7	na	na	0.003	124	0.001	na	4	26	10	0.0002	166	na	Hewlett et al. (2005)
355	G	G	na	6.7	na	na	0.011	39	0.0005	na	1	10	4	0.005	80	0.08	Ditto

ARD	Type	Place	EC	pH	ORP	Al	As	Ca	Cu	Fe	K	Mg	Na	Pb	SO_4	Zn		Reference
356	G	G	na	8.1	na	na	0.003	30	0.007	na	2	11	13	0.101	56	na	Ditto	
357	G	G	na	7.5	na	na	0.007	63	0.0005	na	1	30	15	0.0002	21	0.03	Ditto	
358	G	G	na	7.8	na	na	0.005	23	0.017	na	2	12	61	0.277	43	0.04	Ditto	
359	G	G	na	6.2	na	na	0.003	7	0.004	na	1	3	13	0.038	24	0.24	Ditto	
360	G	R	na	7.1	na	na	0.013	3	0.0006	na	1	3	na	0.0003	8	0.004	Ditto	
361	G	R	na	6.8	na	na	0.01	1	0.002	na	1	1	3	0.001	1	0.01	Ditto	
362	G	G	na	7.3	na	na	23.4	60	0.0028	na	11	81	107	0.0014	511	0.06	Ditto	
363	G	G	na	8.4	na	na	0.024	41	0.0005	na	4	32	76	0.008	166	na	Ditto	
364	G	G	na	7	na	na	0.037	14	0.003	na	1	8	6	0.002	2	0.05	Ditto	
365	G	G	na	6.7	na	na	50.6	137	0.003	na	14	130	213	0.001	1233	na	Ditto	
366	G	G	na	6.8	na	na	1	14	0.002	na	1	24	3	0.001	53	na	Ditto	
367	G	R	na	7.5	na	na	0.45	13	0.0007	na	1	12	na	0.0004	65	0.004	Ditto	
368	G	R	na	7.5	na	na	0.18	5	0.0006	na	1	5	na	0.0002	20	0.002	Ditto	
369	G	MD	na	na	na	na	0.01	na	0.005	na	na	na	na	0.001	na	0.01	Ditto	
370	G	MD	na	na	na	na	0.01	na	0.005	na	na	na	na	0.001	na	0.04	Ditto	
371	G	MD	na	na	na	na	0.02	na	0.286	na	na	na	na	0.786	na	1.36	Ditto	
372	G	R	na	na	na	na	0.01	na	0.005	na	na	na	na	0.001	na	0.02	Ditto	
373	G	MD	na	na	na	na	0.01	na	0.02	na	na	na	na	0.0005	na	0.43	Ditto	
374	G	R	na	na	na	na	0.003	na	0.003	na	na	na	na	0.001	na	0.11	Ditto	
375	G	MD	na	na	na	na	0.01	na	0.005	na	na	na	na	0.001	na	0.3	Ditto	
376	G	MD	na	na	na	na	0.01	na	0.005	na	na	na	na	0.001	na	0.22	Ditto	
377	G	MD	na	na	na	na	0.01	na	0.005	na	na	na	na	0.002	na	0.36	Ditto	
378	G	MD	na	na	na	na	0.01	na	0.005	na	na	na	na	0.001	na	0.05	Ditto	
379	G	MD	na	na	na	na	0.01	na	0.005	na	na	na	na	0.002	na	0.36	Ditto	
380	G	R	na	na	na	na	0.14	na	0.0006	na	na	na	na	0.0002	na	0.0019	Ditto	
381	G	MD	na	na	na	na	0.109	na	na	na	na	na	na	na	na	na	Ditto	
382	G	MD	na	na	na	na	0.108	na	na	na	na	na	na	na	na	na	Ditto	
383	G	MD	na	na	na	na	0.108	na	na	na	na	na	na	na	na	na	Ditto	
384	G	MD	na	na	na	na	0.109	na	na	na	na	na	na	na	na	na	Ditto	
385	G	MD	na	na	na	na	0.123	na	0.002	na	na	na	na	0.001	na	0.01	Ditto	
386	G	R	na	na	na	na	0.029	na	0.0009	na	na	na	na	0.0003	na	0.001	Ditto	
387	G	R	na	na	na	na	0.001	na	0.013	na	na	na	na	0.0003	na	0.0038	Ditto	
388	G	R	na	na	na	na	3.32	na	0.003	na	na	na	na	0.002	na	0.05	Ditto	
389	G	MD	na	na	na	na	58.9	na	0.005	na	na	na	na	0.001	na	0.01	Ditto	
390	G	MD	na	na	na	na	51.1	na	0.002	na	na	na	na	0.001	na	0.01	Ditto	
391	G	MD	na	na	na	na	1.25	na	0.002	na	na	na	na	0.001	na	0.003	Ditto	

ARD	Type	Place	EC	pH	ORP	Al	As	Ca	Cu	Fe	K	Mg	Na	Pb	SO_4	Zn	Reference
392	G	MD	na	na	na	na	12.2	na	0.121	na	na	na	na	0.058	na	0.83	Ditto
393	G	R	na	na	na	na	0.45	na	0.0007	na	na	na	na	0.0004	na	0.0044	Ditto
394	G	MD	na	na	na	na	0.078	na	0.021	na	na	na	na	0.006	na	0.09	Ditto
395	G	MD	na	na	na	na	6.09	na	0.005	na	na	na	na	0.002	na	0.03	Ditto
396	G	MD	na	na	na	na	16.3	na	0.011	na	na	na	na	0.004	na	0.02	Ditto
397	G	MD	na	na	na	na	0.03	na	0.022	na	na	na	na	0.001	na	0.14	Ditto
398	G	R	na	na	na	na	0.001	na	0.002	na	na	na	na	0.001	na	0.013	Ditto
399	G	R	na	na	na	na	0.01	na	0.005	na	na	na	na	0.001	na	0.01	Ditto
400	G	MD	na	na	na	na	0.88	na	0.005	na	na	na	na	0.001	na	0.01	Ditto
401	G	MD	na	na	na	na	0.27	na	0.005	na	na	na	na	0.001	na	0.01	Ditto
402	G	MD	na	na	na	na	0.13	na	0.005	na	na	na	na	0.001	na	0.01	Ditto
403	P	MD	na	6.4	na	na	na	310	na	49	na	207	na	na	1550	57	Hochella et al. (1999)
404	P	MD	na	5.7	na	na	na	12	na	5	na	6	na	na	50	1	Ditto
405	P	R	na	6.6	na	na	0.046	na	0.018	0.02	na	na	na	na	na	0.56	Johnson and Thornton (1987)
406	P	R	na	4.1	na	na	0.021	na	0.9	1.74	na	na	na	na	na	4.6	Ditto
407	P	R	na	4	na	na	0.014	na	0.91	0.47	na	na	na	na	na	3.11	Ditto
408	P	R	na	3.4	na	na	0.15	na	1.2	50.5	na	na	na	na	na	11.9	Ditto
409	P	R	na	6.3	na	na	0.027	na	0.065	0.02	na	na	na	na	na	0.62	Ditto
410	P	R	na	3.9	na	na	0.14	na	0.68	57.4	na	na	na	na	na	35.4	Ditto
411	P	R	na	3.8	na	na	0.046	na	0.6	16.3	na	na	na	na	na	10.3	Ditto
412	C	MD	na	5.9	na	1.2	na	na	1	61	na	na	na	na	na	1	Johnson (2003)
413	C	MD	na	6.2	na	20	na	na	na	160	na	na	na	na	460	na	Ditto
414	C	MD	na	5.5	na	0.97	na	na	0.007	287	na	na	na	na	146	0.05	Ditto
415	C	MD	na	2.7	na	27.5	na	na	0.168	179	na	na	na	na	1077	1.3	Ditto
416	M	MD	na	2.5	na	70	na	na	60	650	na	na	na	na	3100	40	Ditto
417	M	MD	na	3.7	na	4.3	na	na	11	6.7	na	na	na	na	na	3.76	Ditto
418	M	MD	na	3.6	na	50	na	na	2	130	na	na	na	na	350	130	Ditto
419	P	MD	na	2.65	na	116	na	na	5.275	na	na	na	na	na	250	777.5	Ditto
420	S	MD	na	2.4	na	100	na	na	na	2260	na	na	na	na	6590	na	Ditto
421	S	MD	na	2.2	na	na	na	na	na	8100	na	na	na	na	74500	na	Ditto
422	M	MD	na	2.1	na	330	na	na	145	2070	na	na	na	na	na	68	Ditto
423	M	MD	na	2.9	na	19	na	na	10	12	na	na	na	na	na	23	Ditto
424	P	MD	na	1.5	na	na	na	na	293	2670	na	na	na	na	14000	58	Ditto
425	P	MD	na	-2.5	na	na	na	na	4760	124000	na	na	na	na	760000	23500	Ditto
426	M	MD	na	6.5	na	0.03	na	na	0.06	1.6	na	na	na	na	151	2.13	Johnson and Hallberg (2003)

ARD	Type	Place	EC	pH	ORP	Al	As	Ca	Cu	Fe	K	Mg	Na	Pb	SO_4	Zn	Reference
427	C	MD	na	6.2	214	na	na	na	na	160	na	na	na	na	464	na	Ditto
428	C	MD	na	5.9	257	1.2	na	na	na	61	na	na	na	na	na	na	Ditto
429	M	MD	na	3.4	462	27	na	na	1.2	290	na	na	na	na	400	132	Ditto
430	P	MD	na	2.77	na	38.3	na	na	5.65	265	na	na	na	na	1219	61.1	Ditto
431	M	MD	na	2.75	na	22.5	na	na	15.8	172	na	na	na	na	668	25.4	Ditto
432	M	MD	na	2.5	685	70	na	na	40	650	na	na	na	na	1550	60	Ditto
433	P	MD	na	2.2	450	na	na	na	109	2300	na	na	na	na	10000	225	Ditto
434	P	MD	na	0.75	na	4050	na	na	385	16000	na	na	na	na	64000	1650	Ditto
435	P	MD	na	2.5	na	285	na	460	8	198	18.8	1040	412	0.4	10000	1650	Kashir and Yanful (2001)
436	L	I	61.5	10.417	108	147.47	0.61	8.5	0.02	42.53	91.04	23.21	130.08	0.09	na	0.08	Katayama et al. (2011)
437	L	I	49	10.191	106	46.78	0.66	4.14	1.89	977.37	9.86	12.01	0.11	0.16	na	1.35	Ditto
438	C	MD	na	3.49	183	103.1	na	289	na	1033	na	262	na	na	3938.5	na	Kim and Chon (2001)
439	C	MD	na	2.51	587	76.3	na	41.6	na	216.6	na	82	na	na	1612.5	na	Ditto
440	C	MD	na	2.73	554	103	na	0.5	na	71.8	na	9.8	na	na	1108.7	na	Ditto
441	C	MD	na	2.73	517	na	na	2.4	na	11.3	na	14.2	na	na	533.4	na	Ditto
442	C	MD	na	3.66	370	0.3	na	38.1	na	0.6	na	16.1	na	na	300.6	na	Ditto
443	C	MD	na	3.28	305	63	na	14	na	169.4	na	28.7	na	na	1167.9	na	Ditto
444	C	MD	na	2.6	580	337.6	na	23.7	na	311.1	na	27.7	na	na	5046.9	na	Ditto
445	C	MD	na	2.75	517	189.8	na	30.5	na	147.3	na	24	na	na	2276.9	na	Ditto
446	C	MD	na	4.22	230	83.9	na	233.5	na	322.3	na	111.3	na	na	2851.4	na	Ditto
447	C	MD	na	2.43	585	148.5	na	108.2	na	239.4	na	62.3	na	na	3539	na	Ditto
448	C	MD	na	3.13	517	42.6	na	15.5	na	24.6	na	7.5	na	na	670	na	Ditto
449	C	MD	na	2.82	453	13.3	na	6.3	na	17.5	na	4	na	na	334.5	na	Ditto
450	C	MD	na	4.07	351	9.5	na	66.1	na	0.5	na	17.7	na	na	278.7	na	Ditto
451	C	MD	na	3.45	480	17.1	na	38.1	na	3	na	11.2	na	na	337.6	na	Ditto
452	C	MD	na	3.88	261	53.4	na	63.2	na	144.1	na	32.5	na	na	1046	na	Ditto
453	P	R	18.2	8.06	na	10	na	24	1	30	na	9.6	na	1	12	20	Kimball et al. (1995)
454	P	R	28.5	8.08	na	10	na	39	1	8	na	16	na	20	72	490	Ditto
455	P	R	23.8	8.3	na	10	na	33	2.4	3	na	13	na	1	52	274	Ditto
456	P	R	29.1	7.78	na	10	na	33	5.8	3	na	14	na	1	68	976	Ditto
457	P	R	21.8	8.2	na	10	na	27	5	3	na	10	na	9	44	340	Ditto
458	P	R	20.2	7.88	na	10	na	23	1	13	na	8.2	na	1.2	33	356	Ditto
459	P	R	18.2	7.79	na	10	na	21	1	3	na	6.3	na	2.2	2.7	133	Ditto
460	P	R	21.3	8.43	na	10	na	26	1	5	na	7.3	na	1.9	26	60	Ditto
461	P	R	26.3	8.38	na	10	na	35	1	4	na	8.5	na	1.5	15	47	Ditto
462	P	R	26.8	8.41	na	10	na	36	1	5	na	8.8	na	1	23	67	Ditto

ARD	Type	Place	EC	pH	ORP	Al	As	Ca	Cu	Fe	K	Mg	Na	Pb	SO_4	Zn	Reference
463	P	R	20.5	8.52	na	10	na	41	1	6	na	11	na	1	35	22	Ditto
464	P	R	33	8.36	na	10	na	40	1	10	na	11	na	1.3	39	25	Ditto
465	P	R	33.4	8.6	na	10	na	39	1	4	na	11	na	1	23	43	Ditto
466	P	R	52.5	8.54	na	10	na	63	1.5	3	na	20	na	1	28	31	Ditto
467	P	R	73.9	7.13	na	10	na	100	2	80	na	43	na	30	300	3400	Ditto
468	P	R	8.8	7.43	na	10	na	9.6	1	100	na	3.3	na	5	8	50	Ditto
469	P	R	85.4	6.83	na	10	na	96	85.6	3	na	50	na	1	490	27300	Ditto
470	P	R	na	8.14	na	10	na	9.7	1	100	na	3.1	na	10	13	10	Ditto
471	P	R	7.7	7.52	na	10	na	10	1	13	na	1.4	na	16	12	127	Ditto
472	P	R	12	8.25	na	10	na	17	1	24	na	2.7	na	73	na	18	Ditto
473	P	R	20	7.99	na	10	na	22	1.2	5	na	2.3	na	1	17	50	Ditto
474	P	R	45	8.76	na	10	na	50	0.7	3	na	16	na	1	12	27	Ditto
475	P	R	91	9.18	na	10	na	58	1	3	na	20	na	1	79	18	Ditto
476	P	R	28.3	8.69	na	10	na	46	0.8	6	na	10	na	1	7.7	20	Ditto
477	P	R	63.3	8.84	na	10	na	50	1	47	na	26	na	1	69	9	Ditto
478	P	R	60.8	8.22	na	10	na	80	1.3	3	na	23	na	1	190	16	Ditto
479	P	R	160.2	7.85	na	10	na	252	1	8	na	54	na	1	780	29	Ditto
480	P	R	13.8	7.57	na	10	na	14	1	26	na	5.6	na	1	13	37	Ditto
481	P	R	16	7.37	na	10	na	18	1	17	na	7	na	13	25	145	Ditto
482	P	R	8.8	7.47	na	10	na	9.4	1	37	na	3.5	na	1	13	159	Ditto
483	P	R	11.1	7.06	na	10	na	9.9	3	30	na	3.7	na	23	13	163	Ditto
484	P	R	13.9	7.31	na	10	na	14	9	30	na	6.5	na	1	32	1290	Ditto
485	P	R	na	7.57	na	10	na	11	1	30	na	3.9	na	60	15	284	Ditto
486	P	R	10.1	7.14	na	10	na	12	1	30	na	4.4	na	60	20	284	Ditto
487	P	R	na	na	na	10	na	na	14	34	na	na	na	1	na	299	Ditto
488	P	R	na	6.98	na	10	na	13	9	10	na	2.8	na	1	15	35	Ditto
489	P	R	15.1	8.05	na	10	na	21	6	7	na	5.4	na	1	20	16	Ditto
490	P	R	22.1	8.54	na	10	na	28	30	8	na	8.6	na	49	47	19	Ditto
491	P	R	103.8	6.78	na	10	na	120	11	67	na	53	na	63	423	9720	Ditto
492	P	R	4.6	6.67	na	10	na	3.6	1	63	na	1.2	na	19	5.8	177	Ditto
493	P	R	102.3	6.58	na	10	na	98	164	8	na	52	na	1	485	28400	Ditto
494	P	R	7.2	7.27	na	10	na	5.8	1	32	na	1.8	na	1	9.4	348	Ditto
495	P	R	7.6	7.29	na	10	na	11	1	24	na	1	na	6	11	109	Ditto
496	P	R	118.2	7.44	na	10	na	134	1	15	na	45	na	1	490	40	Ditto
497	G	MD	na	6.8	100	4	4.5	116	na	1.2	11	92	650	na	na	na	Lange et al. (2007)
498	na	MD	na	3.3	250	91	2.5	4.5	18	218	667	1	785	na	na	102	Ditto

ARD	Type	Place	EC	pH	ORP	Al	As	Ca	Cu	Fe	K	Mg	Na	Pb	SO_4	Zn	Reference
499	G	MD	na	6.8	198	4	4.5	116	0.1	10	8	92	665	na	1890	na	Ditto
500	na	MD	na	2.6	348	90	2.53	4.61	14	218	400	1	789	na	3102	128	Ditto
501	P	LK	na	2.2	na	42.3	na	86	13	677	2.2	49.2	21	0.008	2040	17400	Lee et al. (2002)
502	P	MD	na	3.4	na	97.4	na	96.4	0.27	6.42	25	50.2	13.2	0.03	1400	37700	Ditto
503	P	R	na	3.1	na	3.39	na	44.9	0.98	6.26	7.8	35	11.2	0.007	605	21200	Ditto
504	P	R	na	3.3	na	18	1	na	na	45	na	na	na	na	1940	38	Lee and Chon (2006)
505	PH	MD	na	2.95	na	67	0.127	na	na	73.4	na	na	na	0.032	1610	2.55	Ludwig et al. (2009)
506	PH	MD	na	3.04	na	167	0.625	na	na	159	na	na	na	0.24	2650	3.43	Ditto
507	PH	MD	na	3.52	na	467	29	na	na	1640	na	na	na	2.475	8180	67.45	Ditto
508	PH	MD	na	3.42	na	2200	197	na	na	9190	na	na	na	3.61	15000	765	Ditto
509	PH	MD	na	3.12	na	2860	207	na	na	10900	na	na	na	4.08	54600	935	Ditto
510	PH	MD	na	3.16	na	69.1	0.261	na	na	83.4	na	na	na	0.032	1800	2.64	Ditto
511	PH	MD	na	3.66	na	124.5	1.865	na	na	233.5	na	na	na	0.524	2623	7.505	Ditto
512	PH	MD	na	4.24	na	142	42.1	na	na	1770	na	na	na	1.23	6720	76.2	Ditto
513	PH	MD	na	3.79	na	1370	158	na	na	8500	na	na	na	1.98	10400	673	Ditto
514	PH	MD	na	3.4	na	2710	206	na	na	10500	na	na	na	2.02	49500	1060	Ditto
515	M	MD	na	0.95	na	na	1	na	0.56	4480.17	na	na	na	0.87	28700	4.88	Magombedze (2010)
516	M	MD	na	3.56	na	na	1	na	0.62	58.74	na	na	na	0.33	1560	0.65	Ditto
517	S	MD	na	2.34	na	161.43	na	2.13	0.34	6172.45	14.32	96.87	67.24	na	11754.22	3.43	Ditto
518	S	MD	na	7.32	na	0.05	na	28.06	0.02	0.87	5.03	29.04	12.66	na	139.45	0.61	Ditto
519	S	MD	na	2.3	na	3.56	na	243.12	0.31	401.22	5.76	24.64	35.21	na	2007.74	1.45	Ditto
520	S	MD	na	2.47	na	9.11	na	320.43	0.04	3.78	5.12	78.9	26.86	na	1242.32	0.54	Ditto
521	M	MD	130.414	7.97	282.08	0	0.001	79.03	0.04	0.86	2.97	153.02	53.04	na	527.29	0.02	Ditto
522	M	MD	126.597	8.06	302	0	0	58.41	0.06	1.52	2.59	105.15	37.59	na	301.05	0.05	Ditto
523	M	MD	211.692	7.88	293.75	0	0.28	296.96	0.04	3.04	22.26	107.88	87.28	na	1189.4	0.33	Ditto
524	M	MD	1940.336	2.4	49.25	133.73	0	1.65	0.31	5542.72	12.01	215.64	44.34	na	10685.66	2.68	Ditto
525	S	R	127.921	3.86	222.17	10.91	0.001	156.32	0.07	2.79	5.46	77.06	33.92	na	749.35	1.01	Ditto
526	S	G	676.456	2.86	235.48	1.57	0.001	236.97	0.41	368.67	6.33	27.3	26.22	na	1737.06	1.4	Ditto
527	C	MD	na	4.5	na	0.483	0.017	na	0.012	194	na	57.4	na	0.02	na	na	Matlock et al. (2002)
528	C	MD	na	na	na	0.515	0.012	na	0.009	28.4	na	57.1	na	0.02	na	na	Ditto
529	C	MD	na	na	na	0.452	0.012	na	0.009	24.2	na	49.4	na	0.02	na	na	Ditto
530	C	MD	na	2.61	na	47.9	na	na	0.201	71	na	na	na	0.0155	655	1.28	McCauley et al. (2009)
531	M	MD	na	4.5	na	0.5	0.0022	222	0.01464	10.34	4.45	8.98	19.56	0.00085	11.8	0.12655	Milu et al. (2002)
532	M	MD	na	3.8	na	185	0.00227	266	na	49.96	6.3	77.9	22.07	0.01515	3.4	5.0303	Ditto
533	M	MD	na	6	na	0.48	0.00038	226	0.00867	0.64	3.25	46	16.4	0.00183	553.2	0.03743	Ditto
534	M	MD	na	4.5	na	3.51	0.00734	213	0.3859	12.17	1.86	12.34	19.85	0.00358	621.2	0.20404	Ditto

ARD	Type	Place	EC	pH	ORP	Al	As	Ca	Cu	Fe	K	Mg	Na	Pb	SO_4	Zn	Reference
535	M	MD	na	4.4	na	8.45	0.00678	198.6	1.0126	11.37	2.08	17.31	20.57	0.00466	615.6	0.36344	Ditto
536	M	R	na	5	na	5.27	0.00415	217	0.5668	6.64	2.51	15.3	16.47	0.00417	436.8	0.2051	Ditto
537	P	R	na	3.6	na	4.38	na	11.37	0.0206	0.124	1.23	6.21	2.74	0.00271	49.2	0.614	Ditto
538	P	R	na	5.9	na	na	na	13.09	0.0084	na	0.69	3.26	1.78	0.00037	31.1	0.186	Ditto
539	P	R	na	6.3	na	na	na	13.15	0.0052	na	0.54	2.78	1.62	0.00061	32.8	0.136	Ditto
540	P	R	na	5.2	na	2.04	na	12.55	0.0243	0.238	0.85	4.59	2.24	0.00213	10.7	0.487	Ditto
541	P	R	na	5.2	na	2.03	na	12.6	0.0191	0.272	0.79	4.49	2.25	0.00143	42.1	0.426	Ditto
542	P	R	na	5.3	na	4.69	na	12.51	0.0222	0.514	0.79	4.53	2.22	0.00222	46.8	0.467	Ditto
543	P	R	na	5.2	na	1.13	na	12.5	0.0163	0.13	0.83	4.52	2.28	0.0011	29.4	0.429	Ditto
544	P	MD	212	3.72	na	28.073	na	na	17.318	2.109	na	na	na	0.038	na	20.157	Munro et al. (2004)
545	G	R	37	7.01	277	na	na	84.6	0.1	2.38	na	na	10.24	0	250	0.1	Naicker et al. (2003)
546	G	G	81	7.04	157	na	na	125.2	0.2	9.78	na	na	19.07	0.1	300	5	Ditto
547	G	R	150	6.17	269	na	na	125.8	0.1	26.61	na	na	49.26	0.1	500	1.5	Ditto
548	G	R	50	7.9	277	na	na	69.4	0.1	0.62	na	na	18.06	0.1	360	0	Ditto
549	G	G	571	3.08	600	na	na	133.1	6	384.3	na	na	25.64	0.4	2080	8	Ditto
550	G	R	131	5.78	316	na	na	121	0.1	19.19	na	na	38.99	0.1	680	1	Ditto
551	G	R	137	5.49	375	na	na	141.6	0.1	23.82	na	na	24.36	0.1	570	1.1	Ditto
552	G	R	138	5.25	400	na	na	145.2	0.2	24.84	na	na	46.81	0.1	530	1.2	Ditto
553	G	G	545	3.76	432	na	na	125.7	6	453.4	na	na	22.6	0.7	1750	8	Ditto
554	G	G	477	3.78	431	na	na	116.4	5	379	na	na	23.28	0.3	1400	7	Ditto
555	G	R	94	7.14	158	na	na	127.3	0.1	12.09	na	na	36.05	0.1	430	0.1	Ditto
556	G	G	133	4.56	408	na	na	204.1	0.4	3.69	na	na	29.09	0.2	570	1.4	Ditto
557	G	R	85	6.73	201	na	na	117.3	0.2	10.09	na	na	44.95	0.2	370	0.3	Ditto
558	G	G	570	3.96	394	na	na	na	na	na	na	na	na	na	na	na	Ditto
559	G	R	114	4.49	442	na	na	100.9	0.3	77.6	na	na	29.31	0.2	530	1.5	Ditto
560	G	R	120	6.36	236	na	na	122.9	0.2	17.38	na	na	44.55	0.2	500	0.5	Ditto
561	G	R	104	6.14	291	na	na	127.1	0.1	14.7	na	na	35.4	0.2	430	0.4	Ditto
562	G	R	101	6.53	234	na	na	115.3	0.2	13.06	na	na	40.55	0.2	490	0.4	Ditto
563	G	R	145	4.55	418	na	0.00894	111.24	1.62	5.03	na	na	12.46	1.11	348.86	20.98	Ditto
564	G	R	37	6.26	300	na	0.0089	34.94	0.03	2.99	na	na	5.95	0.14	424.92	0.76	Ditto
565	G	R	60	5.22	386	na	0.00328	73.28	0.1	12	na	na	12	0.63	500	1.24	Ditto
566	G	R	132	5.78	316	na	0.00057	121	0.1	19.19	na	na	38.99	0.1	680	1	Ditto
567	G	G	510	3.1	712	na	0.0269	415.88	3.89	7.75	na	na	39.71	2.74	1398.34	23.7	Ditto
568	G	G	664	3.2	551	na	0.01404	518	1.84	18.36	na	na	6.23	0.1	1989.74	2.91	Ditto
569	G	G	439	3.21	567	na	0.00702	455.46	1.26	2.47	na	na	12.08	0.83	2108.33	11.12	Ditto
570	G	G	571	3.08	600	na	0.00286	133.1	6	384.3	na	na	25.64	0.4	2080	8	Ditto

ARD	Type	Place	EC	pH	ORP	Al	As	Ca	Cu	Fe	K	Mg	Na	Pb	SO_4	Zn	Reference
572	G	G	433	3.4	500	na	0.01104	619	2.94	20.3	na	na	8.65	0.09	2048.08	3.04	Ditto
573	G	G	417	3.44	439	na	0.00703	359.44	1.49	135.33	na	na	19.02	0.59	2000	12.38	Ditto
574	G	G	545	3.76	432	na	0.00296	125.7	6	453.4	na	na	22.6	0.7	1750	8	Ditto
575	G	R	153	4.42	437	na	0.00777	85.05	1.57	6.31	na	na	19.71	1.08	439.29	20.6	Ditto
576	G	R	58	4.61	441	na	0.01001	47.3	0.07	8.8	na	na	5.94	0.15	419.08	0.96	Ditto
577	G	R	70	4.78	431	na	0.00132	70.73	0.13	16.13	na	na	16.03	0.56	553	1.42	Ditto
578	G	R	139	5.25	400	na	0.00065	145.2	0.2	24.84	na	na	46.81	0.1	530	1.2	Ditto
579	G	G	681	3.16	610	na	0.02925	196.64	4.81	5.64	na	na	2400	3.15	1620.79	19.12	Ditto
580	G	G	462	3.14	540	na	0.01714	329.2	2.4	22.52	na	na	9.03	0.09	1634.58	3.06	Ditto
581	G	G	417	3.16	554	na	0.0031	324.3	2.26	1.65	na	na	11.37	0.73	1975	10.8	Ditto
582	G	G	617	3.46	493	na	0.00325	328.4	5.03	43.8	na	na	28.29	1.03	1400.42	21.24	Ditto
583	G	G	369	3.76	490	na	0.01378	489.9	0.95	14.85	na	na	10.13	0.16	1672.12	2.85	Ditto
584	G	G	380	3.6	413	na	0.00512	339.41	0.6	179.82	na	na	17.09	0.66	2150	13.22	Ditto
585	G	G	477	3.78	431	na	0.006	116.4	5	379	na	na	23.28	0.3	1400	7	Ditto
586	P	R	226	2.89	na	66.5	0.147	73.9	15.7	123	3.6	64.1	38.2	0.121	1221	24.1	Nieto et al. (2007)
587	P	R	100	3.76	na	32.8	0.004	45.7	5.4	4.9	2.4	70.5	17.3	0.045	643	11.5	Ditto
588	P	R	194	3.07	na	na	0.068	112.6	7.6	23.47	3.2	94	26.6	0.207	1204	24.23	Olıas et al. (2004)
589	P	LK	na	9.4	na	na	0.236	na	na	na	na	na	na	na	na	na	Razo et al. (2004)
590	P	MD	na	7.9	na	na	0.42	na	na	na	na	na	na	na	na	na	Ditto
591	P	MD	na	8	na	na	0.286	na	na	na	na	na	na	na	na	na	Ditto
592	P	MD	na	8	na	na	0.406	na	na	na	na	na	na	na	na	na	Ditto
593	P	LK	na	7.8	na	na	0.108	na	na	na	na	na	na	na	na	na	Ditto
594	P	LK	na	9.4	na	na	0.237	na	na	na	na	na	na	na	na	na	Ditto
595	P	LK	na	9.3	na	na	0.265	na	na	na	na	na	na	na	na	na	Ditto
596	P	LK	na	9.6	na	na	0.059	na	na	na	na	na	na	na	na	na	Ditto
597	P	LK	na	8.6	na	na	0.262	na	na	na	na	na	na	na	na	na	Ditto
598	P	LK	na	9.5	na	na	0.199	na	na	na	na	na	na	na	na	na	Ditto
599	P	G	na	7.1	na	na	6.176	na	na	na	na	na	na	na	na	na	Ditto
600	P	G	na	7.4	na	na	6.765	na	na	na	na	na	na	na	na	na	Ditto
601	P	G	na	7.7	na	na	7.165	na	na	na	na	na	na	na	na	na	Ditto
602	P	G	na	7.7	na	na	6.482	na	na	na	na	na	na	na	na	na	Ditto
603	P	G	na	8.2	na	na	6.318	na	na	na	na	na	na	na	na	na	Ditto
604	P	G	na	8.4	na	na	6.106	na	na	na	na	na	na	na	na	na	Ditto
605	P	LK	na	8.2	na	na	5.894	na	na	na	na	na	na	na	na	na	Ditto

ARD	Type	Place	EC	pH	ORP	Al	As	Ca	Cu	Fe	K	Mg	Na	Pb	SO_4	Zn	Reference
606	P	MD	1360	2.6	na	174	0.293	420	0.15	4620	3	780	43.6	0.637	6754	2090	Romero et al. (2010)
607	P	MD	1290	2.7	na	151	0.191	374	0.095	4330	1.33	708	30.9	0.328	6399	1890	Ditto
608	P	MD	440	2.5	na	140	0.005	113	1.79	264	0.59	92.2	27.5	0.662	2149	585	Ditto
609	P	R	530	2.6	na	4.82	0.006	557	0.028	253	9.82	416	31.5	0.911	2589	165	Ditto
610	P	R	170	2.8	na	15.4	0.024	69	0.223	9	12.9	22.4	74.6	1.18	784	30	Ditto
611	P	R	240	2.5	na	43.6	0.005	23	0.202	37	12.2	20.6	27	4.27	1144	30.9	Ditto
612	P	R	20	6.4	na	0.03	0.004	7	0.019	11	4.09	4.57	13.6	0.017	34	0.3	Ditto
613	L	I	9.52	7.7	156	11.2	0	19	0	0	5.7	0.4	4.5	0	na	0	Naka et al. (2011)
614	L	I	57.2	5.16	262	0.7	0	36.3	0	0	39.6	7.7	1	3.2	na	47.4	Ditto
615	L	I	182.1	6.25	205	0	0	123.1	0	0	30.4	52.2	118.9	0	na	0.1	Ditto
616	L	I	51.6	8.09	140	0.2	0	101.9	0	0	10.6	3.6	28.8	0	na	0	Ditto
617	L	I	213	3.33	354	46.2	0	205.3	0	206.9	23.9	35.2	15.5	0	na	1.8	Ditto
618	L	I	297	2.37	10	25.1	0.3	239.8	2.4	228.4	1.5	40.4	49.2	0.3	na	18.4	Ditto
619	L	I	1227	1.23	81	41.2	1.8	13.1	26.8	0	6	4.9	5.1	1	na	8.5	Ditto
620	L	I	208	2.55	48	36	0	61.5	0.4	225.2	1.9	48.6	7.7	0.1	na	6.3	Ditto
621	L	I	620	1.8	69	71.2	0.7	20.7	11.2	0	6	31.1	13.7	0.2	na	17	Ditto
622	P	MD	195	3.1	604	34	0.108	89	8	162	1.1	87	24	0.183	1370	51	Sánchez España et al. (2005)
623	P	MD	na	na	na	47	0.283	54	16	199	0.8	62	14	0.166	330	60	Ditto
624	P	MD	na	na	na	57	0.003	27	21	127	1.4	100	11	0.029	5350	6	Ditto
625	P	MD	372	3.4	495	26	11.375	182	1	908	3.8	196	30	0.023	2980	65	Ditto
626	P	MD	397	2.6	589	54	10.222	123	10	771	3	88	27	0.219	2780	52	Ditto
627	P	MD	101	2.5	616	177	na	69	66	1280	2	68	18	na		97	Ditto
628	P	MD	305	2.5	733	207	0.203	92	31	1241	0.8	257	15	0.05	2650	122	Ditto
629	P	MD	456	2.3	703	154	0.029	73	8	270	0.4	62	22	0.02	2210	138	Ditto
630	P	MD	na	na	na	231	0.211	35	17	592	0.4	67	19	0.011	30	12	Ditto
631	P	MD	570	2	733	273	0.221	14	1	1115	0.2	110	9	0.002	5230	0	Ditto
632	P	MD	na	na	na	47	0.032	9	0	164	1.8	22	8	0.002	900	0	Ditto
633	P	MD	976	2.4	762	652	0.866	174	109	1967	0.3	1034	36	0.022	13700	224	Ditto
634	P	MD	1237	2.2	799	736	4.48	455	115	1667	0.2	410	46	na	17740	736	Ditto
635	P	MD	na	na	na	1760	0.044	285	161	1257	0.2	2340	15	0.003	21800	440	Ditto
636	P	MD	na	na	na	1810	0.646	325	183	1290	0.1	1800	11	0.018	23300	463	Ditto
637	P	MD	1533	2.8	544	2081	0.405	224	180	1844	0.3	2894	14	0.01	24400	557	Ditto
638	P	MD	na	na	na	2566	0.05	446	158	1890	0.2	621	20	0.01	28680	578	Ditto
639	P	MD	1800	na	na	388	0.07	171	53	211	0.5	591	20	0.031	9940	148	Ditto
640	P	MD	1420	2.7	620	1324	0.065	102	440	961	0	1576	22	0.017	19750	339	Ditto
641	P	MD	830	1.7	656	892	0.108	151	166	1170	0	1146	10	0.025	15260	381	Ditto

ARD	Type	Place	EC	pH	ORP	Al	As	Ca	Cu	Fe	K	Mg	Na	Pb	SO_4	Zn		Reference
642	P	MD	940	2.6	748	73	4.59	439	0	1007	20	500	236	0.299	6080	59	Ditto	
643	P	MD	700	4.2	396	58	4.595	428	2	855	18	436	218	0.076	5370	46	Ditto	
644	P	MD	730	2.7	621	317	0.015	320	18	550	1.7	767	206	0.019	7790	58	Ditto	
645	P	MD	124	4.6	478	30	0.004	382	18	4	9.6	87	94	0.324	1670	12	Ditto	
646	P	MD	379	3.2	548	125	na	288	3	511	1.8	181	22	na		125	Ditto	
647	P	MD	419	3.3	565	126	0.37	172	14	688	1.2	153	20	na	3570	436	Ditto	
648	P	MD	205	4.2	360	30	1.189	99	8	363	5	58	22	0.009	1390	17	Ditto	
649	P	MD	274	3.9	438	58	10.74	68	11	770	7.8	38	22	0.009	2150	21	Ditto	
650	P	MD	466	2.6	641	124	0.008	118	9	683	0.2	284	16	0.009	3890	33	Ditto	
651	P	MD	298	2.8	663	70	0.063	75	5	300	1.3	100	13	0.012	2030	15	Ditto	
652	P	MD	180	2.5	661	33	0.031	31	5	147	1.7	30	19	0.089	800	8	Ditto	
653	P	MD	358	2.8	551	110	0.272	128	17	735	4.9	161	23	0.002	2720	14	Ditto	
654	P	MD	447	2.7	599	152	0.497	103	39	838	4.5	100	25	0.012	3710	24	Ditto	
655	P	MD	197	2.8	673	46	0.081	90	77	183	2.1	47	26	0.004	1310	3	Ditto	
656	P	MD	na	na	na	401	17.361	53	302	2849	36.4	105	20	0.002	10400	149	Ditto	
657	P	MD	1008	1.4	595	325	4.54	72	203	2135	15.5	113	20	0.239	8000	122	Ditto	
658	P	MD	282	3.5	615	57	0.019	266	2	37	2.5	247	32	0.02	2160	4	Ditto	
659	P	MD	247	3.6	610	61	0.047	239	3	13	2.6	163	27	0.011	1850	8	Ditto	
660	P	MD	600	3	571	101	0.448	474	7	689	0.2	623	67	0.725	5650	24	Ditto	
661	P	MD	488	2.7	612	57	0.087	529	1	408	11.6	483	74	0.59	4240	16	Ditto	
662	P	MD	775	2.9	491	288	2.389	215	24	2634	5	430	31	0.024	8060	59	Ditto	
663	P	MD	745	2.9	486	317	1.874	177	27	2369	4.5	145	39	0.048	9130	46	Ditto	
664	P	MD	850	1.8	641	296	1.726	38	21	2187	0.2	183	10	0.034	1300	4	Ditto	
665	P	MD	1320	1.5	646	474	5.933	100	27	5532	0.3	130	29	0.071	18180	474	Ditto	
666	P	MD	600	2.3	613	265	0.829	112	21	1426	0.1	251	11	0.027	5890	13	Ditto	
667	P	MD	597	2.2	552	270	0.075	152	6	1799	0.1	156	13	0.034	6310	270	Ditto	
668	P	MD	575	2.7	558	247	1.096	237	30	1986	3.2	113	33	0.013	5810	247	Ditto	
669	P	MD	603	2.5	599	247	1.182	108	69	1523	2.7	85	25	0.027	5850	227	Ditto	
670	P	MD	na	na	na	35	0.012	99	1	95	4.1	94	24	0.005	1100	35	Ditto	
671	P	MD	169	3	699	19	0.017	50	1	9	3.2	70	18	0.016	660	11	Ditto	
672	P	MD	1327	2.3	619	969	0.049	256	147	1918	0.2	2100	22	0.01	18500	363	Ditto	
673	P	MD	1381	2.5	636	1192	0.159	215	132	2004	0.3	567	31	0.009	21380	342	Ditto	
674	P	MD	985	2.2	604	499	0.019	203	140	1883	0.1	950	18	0.004	11100	294	Ditto	
675	P	MD	1065	2.4	607	747	0.04	192	155	2287	0.3	306	22	0.007	13650	398	Ditto	
676	P	MD	428	2.5	779	120	0.012	180	21	125	2.4	455	17	0.052	3700	83	Ditto	
677	P	MD	405	2.9	750	123	0.053	158	22	632	2.1	237	16	0.023	3440	76	Ditto	

ARD	Type	Place	EC	pH	ORP	Al	As	Ca	Cu	Fe	K	Mg	Na	Pb	SO_4	Zn	Reference
678	P	MD	315	3	630	72	0.005	131	9	70	2.2	374	14	0.033	2530	55	Ditto
679	P	MD	348	3.2	629	101	0.012	128	13	39	1.9	232	14	0.014	2840	60	Ditto
680	P	MD	na	na	na	243	0.209	185	52	511	1.7	636	16	0.066	5640	128	Ditto
681	P	MD	494	2.9	616	318	0.113	71	35	524	2.7	163	18	na	4550	62	Ditto
682	P	MD	2390	2.3	658	2580	2.854	384	435	5848	0.1	568	11	0.119	43850	1370	Ditto
683	P	MD	1667	2.3	636	1705	8.071	84	253	4382	0.2	328	9	0.087	27720	772	Ditto
684	P	MD	403	2.6	609	162	1.866	31	124	1231	4.4	30	23	0.003	3360	6	Ditto
685	P	MD	601	2	615	177	2.219	14	121	1123	2.6	24	12	0.034	4110	4	Ditto
686	P	MD	1533	2.7	609	605	4.51	272	77	1999	0	2545	27	na	19200	327	Ditto
687	P	MD	2270	2.2	614	477	39.7	144	204	4122	1	366	124	na	16500	1437	Ditto
688	P	MD	370	2.9	728	243	0.694	73	14	154	0	256	3	na	3140	19	Ditto
689	P	MD	na	na	na	169	0.876	41	29	286	0.7	211	23	0.052	2770	64	Ditto
690	P	MD	na	na	na	490	8.435	179	71	1509	1.9	965	39	0.078	9840	237	Ditto
691	P	MD	287	2.4	800	90	0.067	115	7	363	2.8	129	17	0.107	2500	20	Ditto
692	P	MD	556	2.2	663	426	0.108	123	75	490	0	367	19	0.013	6010	47	Ditto
693	P	MD	830	2.5	434	822	0.048	32	130	736	0.1	702	16	0.026	9650	97	Ditto
694	P	MD	na	na	na	59	3.24	179	23	797	2.2	152	30	0.002	3260	94	Ditto
695	P	MD	350	3.3	560	80	2.268	166	25	773	2.2	145	27	0.001	3070	85	Ditto
696	P	MD	175	3.3	604	25	0.017	126	36	157	1.7	81	22	0.002	1140	19	Ditto
697	P	MD	183	3.3	599	25	0.026	104	30	418	1.4	56	20	0.003	990	14	Ditto
698	P	MD	53.9	5.7	428	0.2	0.001	61	0.5	0	1.4	23	16	0	250	2	Ditto
699	P	MD	68.5	5.5	447	2	0.032	66	2	0.2	1.1	24	13	0.001	280	3	Ditto
700	P	MD	na	na	na	27	0.094	237	4	142	1.8	228	52	0.008	2050	5	Ditto
701	P	MD	114.2	3.2	692	22	0.258	48	5	16	1.1	36	16	0.017	450	3	Ditto
702	L	I	210	6	390	na	na	na	0.03	na	na	na	na	0.01	700	0.04	Saria et al. (2006)
703	L	I	300	2.5	620	na	na	na	0.36	na	na	na	na	0.04	1000	1.58	Ditto
704	L	I	900	2	700	na	na	na	0.97	na	na	na	na	0.15	4000	2.89	Ditto
705	P	MD	452.5	3.4	408	na	0.418	na	1.65	427	na	na	na	na	na	408	Sarmiento et al. (2007)
706	P	MD	452.5	3.4	408	na	0.382	na	1.67	400	na	na	na	na	na	399	Ditto
707	P	MD	452.5	3.4	408	na	0.352	na	1.66	365	na	na	na	na	na	410	Ditto
708	P	MD	452.5	3.4	408	na	0.381	na	1.56	399	na	na	na	na	na	390	Ditto
709	P	MD	452.5	3.4	408	na	0.404	na	1.55	415	na	na	na	na	na	387	Ditto
710	P	MD	452.5	3.4	408	na	0.362	na	1.58	397	na	na	na	na	na	391	Ditto
711	P	MD	452.5	3.4	408	na	0.312	na	1.61	383	na	na	na	na	na	386	Ditto
712	P	MD	452.5	3.4	408	na	0.338	na	1.57	409	na	na	na	na	na	386	Ditto
713	P	MD	na	2.5	na	30	1	300	65	450	na	1500	na	1.2	12000	2400	Shackelford et al. (2010)

ARD	Type	Place	EC	pH	ORP	Al	As	Ca	Cu	Fe	K	Mg	Na	Pb	SO_4	Zn	Reference
714	M	MD	na	2.3	760	286.003	2.1802	na	137.89	191.54	na	na	na	0.866	na	404.22	Shokes and Möller (1999)
715	L	I	400	2.43	na	na	0.92	105	0.5	452	2.64	70	7.24	0.06	na	167	Smuda et al. (2007)
716	L	I	540	1.2	na	na	3.3	60	0	677	4.86	69	6.9	1.85	na	103	Ditto
717	L	I	460	2.56	na	na	0.74	539	4.8	541	4.49	91	8.15	0.03	na	152	Ditto
718	L	I	520	2.32	na	na	14.81	66	10.92	1225	4.14	88	6.98	0.02	na	127	Ditto
719	L	I	350	2.33	na	na	0.02	83	0	157	6.6	74	8.61	0.05	na	86	Ditto
720	L	I	500	2.17	na	na	4.63	259	22.45	872	7.57	6	6.28	0.16	na	130	Ditto
721	L	I	400	2.74	na	na	0.08	501	0	49	7.64	104	7.8	0.11	na	146	Ditto
722	L	I	630	2.32	na	na	11.99	219	0	1968	7.32	7	11.58	0.28	na	116	Ditto
723	L	I	1450	2.33	na	na	33.27	360	35.76	7400	7.38	145	5.43	0.08	na	1389	Ditto
724	L	I	700	2.32	na	na	7.07	164	13.86	1720	6.76	116	8.36	0.03	na	290	Ditto
725	L	I	360	4.02	na	na	0.08	567	15.55	76	0.4	95	1.2	2.27	na	447	Ditto
726	L	I	240	5.6	na	na	na	635	na	0.8	2.1	29	0.8	0.35	na	107	Ditto
727	L	I	870	3.79	na	na	na	517	1.51	251	na	657	0.9	0.07	na	708	Ditto
728	L	I	520	2.82	na	na	0.1	566	4.67	263	na	52	na	0.14	na	322	Ditto
729	L	I	320	5.47	na	na	na	564	na	0.1	3.6	263	3.1	na	na	68	Ditto
730	L	I	970	2.88	na	na	na	504	3.53	141	na	987	0.5	0.06	na	491	Ditto
731	L	I	300	2.91	na	na	0.14	523	16.67	1452	na	178	na	0.22	na	611	Ditto
732	L	I	830	2.77	na	na	0.12	608	0.71	44.9	13	31	0.8	0.06	na	18	Ditto
733	L	I	510	3.2	na	na	0.26	382	11.78	350	na	194	na	na	na	521	Ditto
734	P	MD	2120	4.86	359	na	2.81	411	1.08	3685	19.2	3158	73.8	1.17	na	1845	Ditto
735	P	MD	1900	4.94	336	na	2.09	559	1.13	3152	25	3549	121	0.55	na	1218	Ditto
736	P	MD	2330	5.1	319	na	1.98	694	1.28	5640	27.7	4716	8.2	1.28	na	2302	Ditto
737	P	MD	2600	2.78	684	na	7.99	614	161.1	1632	3.1	7792	na	0.14	na	3000	Ditto
738	C	MD	na	na	na	293	0.512	na	223	514	na	na	213	na	2400	630	Tabak and Govind (2003)
739	P	R	na	6.8	na	0.031	na	na	0.0078	0.021	na	na	na	na	na	0.569	Todd et al. (2007)
740	P	R	na	7.7	na	0.014	na	na	na	0.074	na	na	na	na	na	0.006	Ditto
741	P	R	na	7.3	na	0.037	na	na	0.0041	0.012	na	na	na	na	na	0.325	Ditto
742	P	MD	na	4.78	na	41	0.41	na	na	310	na	na	na	na	1690	na	Tsukamoto et al. (2004)
743	P	MD	na	4.7	na	48	0.28	na	na	380	na	na	na	na	2070	na	Ditto
744	M	MD	497	2.53	730	3735	9.61	257	17.4	2143	1.32	43.2	2.85	na	5880	8.71	Valente and Leal Gomes (2009)
745	M	R	86.6	3.1	737	17.4	0.032	28.8	0.061	48.6	1.29	4.82	5.74	na	327	0.22	Ditto
746	P	MD	na	1.88	na	na	na	na	3.49	98.95	na	na	na	2.35	4415.51	7.16	Van Hille et al. (1999)
747	P	MD	2410	1	653	259	49	397	86.8	4330.2	31.4	214	18	2.9	na	493	Wibkirchen et al. (2005)
748	C	R	2.8	5.7	na	0.18	na	na	na	0.45	na	na	na	na	na	na	Winterbourn et al. (2000)
749	C	R	1.6	4.9	na	0.41	na	na	na	1.24	na	na	na	na	na	na	Ditto

ARD	Type	Place	EC	pH	ORP	Al	As	Ca	Cu	Fe	K	Mg	Na	Pb	SO_4	Zn		Reference
750	C	R	7.7	6.2	na	0.01	na	na	na	0.2	na	na	na	na	na	na	Ditto	
751	C	R	80	2.7	na	6.78	na	na	na	32.6	na	na	na	na	na	na	Ditto	
752	C	R	17.7	4.1	na	1.11	na	na	na	1.7	na	na	na	na	na	na	Ditto	
753	C	R	35.6	3.7	na	8	na	na	na	12.8	na	na	na	na	na	na	Ditto	
754	C	R	61.5	3.1	na	5.7	na	na	na	1.95	na	na	na	na	na	na	Ditto	
755	C	R	21.1	3.4	na	1.51	na	na	na	0.72	na	na	na	na	na	na	Ditto	
756	C	R	6.2	5.8	na	0.27	na	na	na	1.19	na	na	na	na	na	na	Ditto	
757	C	R	25.3	3.5	na	2.97	na	na	na	3.57	na	na	na	na	na	na	Ditto	
758	C	R	4.5	4.8	na	0.04	na	na	na	0.6	na	na	na	na	na	na	Ditto	
759	C	R	15.5	4.2	na	1.6	na	na	na	2.39	na	na	na	na	na	na	Ditto	
760	C	R	23.3	3.2	na	2.8	na	na	na	3.26	na	na	na	na	na	na	Ditto	
761	C	R	69.2	2.9	na	16	na	na	na	5.7	na	na	na	na	na	na	Ditto	
762	C	R	16.9	5.7	na	0.13	na	na	na	0.77	na	na	na	na	na	na	Ditto	
763	C	R	81.5	2.7	na	28.6	na	na	na	11.25	na	na	na	na	na	na	Ditto	
764	C	R	94.2	2.6	na	35.5	na	na	na	7.1	na	na	na	na	na	na	Ditto	
765	C	R	94.4	2.9	na	16.5	na	na	na	5.2	na	na	na	na	na	na	Ditto	
766	C	R	12.6	3.7	na	0.75	na	na	na	3.47	na	na	na	na	na	na	Ditto	
767	C	R	10	4.3	na	0.65	na	na	na	1.68	na	na	na	na	na	na	Ditto	
768	C	R	7.3	6.2	na	0.1	na	na	na	0.45	na	na	na	na	na	na	Ditto	
769	C	R	4.4	4.3	na	0.16	na	na	na	0.83	na	na	na	na	na	na	Ditto	
770	C	R	7.7	4.1	na	0.41	na	na	na	0.68	na	na	na	na	na	na	Ditto	
771	C	R	4.7	4.6	na	0.17	na	na	na	0.48	na	na	na	na	na	na	Ditto	
772	C	R	312	3.02	na	104.27	0.000833	361.8	na	108.5	2.52	115.66	4.33	na	2275.18	na	Wu et al. (2009)	
773	C	R	401	2.69	na	180.43	0.21	326.48	na	742.05	2.31	75.35	2.82	na	3483.43	na	Ditto	
774	C	R	178.3	3.12	na	5.86	0.000587	187.77	na	101.66	4.26	67.14	22.92	na	985.07	na	Ditto	
775	C	R	234	2.84	na	14.7	0.000573	210.19	na	139.19	4.9	68.34	36.84	na	1275.47	na	Ditto	
776	C	R	213	2.81	na	25.26	0.000559	198.53	na	91.64	4.92	69.8	26.52	na	1191.56	na	Ditto	
777	C	R	71	6.04	na	0.02	0.000092	73.21	na	0.03	30.03	26.71	28.61	na	300.78	na	Ditto	
778	C	R	175.2	3.05	na	19.63	0.000465	183.53	na	36.34	8.07	58.25	60.31	na	926.08	na	Ditto	
779	C	R	158.4	3.28	na	12.66	0.000485	193.76	na	9.54	5.22	57.34	53.24	na	984.32	na	Ditto	
780	C	R	146.8	3.35	na	9.39	0.000423	182.05	na	3.39	4.68	51.88	42.96	na	770.59	na	Ditto	
781	C	R	199.7	3.52	na	31.5	0.000621	171.26	na	2.51	6.69	47.75	50.16	na	1012.6	na	Ditto	
782	C	R	167.4	2.95	na	47.36	0.000537	112.44	na	22.93	4.98	33.34	15.6	na	866.07	na	Ditto	
783	C	R	112.6	3.2	na	20.97	0.000425	76.97	na	32.65	5.1	27.01	32.81	na	526.75	na	Ditto	
784	C	R	100.8	3.7	na	8.33	0.000447	104.89	na	4.3	4.6	31.56	11.34	na	534.2	na	Ditto	
785	C	R	84.2	5.86	na	0.18	0.000386	100.01	na	0.22	3.29	29.74	11.54	na	452.75	na	Ditto	

ARD	Type	Place	EC	pH	ORP	Al	As	Ca	Cu	Fe	K	Mg	Na	Pb	SO_4	Zn		Reference
786	C	R	44.2	7.51	na	0.05	0.000326	67.85	na	0.03	0.88	20.99	1.21	na	18.12	na	Ditto	
787	C	R	74	7.09	na	0.01	0.000542	93.18	na	0.01	8.6	23.77	15.15	na	126.26	na	Ditto	
788	C	R	37.3	7.19	na	0.05	0.000132	58.71	na	0.02	1.89	16.93	5.76	na	31.05	na	Ditto	
789	C	R	50.8	8.44	na	0.04	0.000263	71.82	na	0.04	2.46	20.28	8.09	na	207.12	na	Ditto	
790	C	R	78.3	5.06	na	2.88	0.000356	89.9	na	13.11	3.33	22.73	26.67	na	385.08	na	Ditto	
791	C	R	62.9	5.08	na	2.75	0.001258	78.05	na	1.94	3.65	22.99	15.61	na	307.87	na	Ditto	
792	C	R	128	3.43	na	19.36	0.000475	100.55	na	5.78	2.36	33.75	24.57	na	440.4	na	Ditto	
793	C	R	223	3.1	na	4.7	0.000611	141.78	na	6.55	5.04	7.05	57.71	na	777.19	na	Ditto	
794	C	R	163.2	3.3	na	0.03	0.000855	131.17	na	0.1	4.65	41.14	85.72	na	529.32	na	Ditto	
795	C	R	139.1	3.33	na	23.66	0.000511	100.03	na	131.81	2.64	31.8	25.34	na	998	na	Ditto	
796	C	R	103.9	5.22	na	18.98	0.000354	118.52	na	15.36	2.94	38.44	26.26	na	633.16	na	Ditto	
797	C	R	129.5	3.3	na	1.29	0.000495	102.05	na	4.77	3	31.9	26.42	na	620.85	na	Ditto	
798	C	R	80.8	5.4	na	18.24	0.001413	101.14	na	12.07	3.37	24.5	17.25	na	597.25	na	Ditto	
799	C	R	98.3	3.56	na	0.55	0.000424	96.6	na	2.85	2.87	26.28	18.42	na	503.06	na	Ditto	
800	C	R	113.8	3.28	na	9.46	0.0004	87.67	na	7.32	2.76	27.04	17.04	na	569.45	na	Ditto	
801	C	R	83.1	6.54	na	0.02	0.00032	102.35	na	1	3.13	24.63	23.17	na	448.63	na	Ditto	
802	C	R	66.7	7.44	na	0.05	0.000749	82.58	na	0.02	2.82	26.91	10.98	na	289.06	na	Ditto	
803	C	R	95.2	3.31	na	12.59	0.000545	93.72	na	27.02	2.79	26.1	7.42	na	472.68	na	Ditto	
804	C	R	45.4	7.15	na	0.04	0.000244	62.24	na	0.02	1.96	14.68	5.22	na	221.68	na	Ditto	
805	C	R	121.6	2.97	na	3.83	0.000465	93.69	na	2.65	2.74	24.59	5.64	na	533.52	na	Ditto	
806	C	R	82.9	4.36	na	6.73	0.001152	96.06	na	8.3	2.71	27.61	5.68	na	466.01	na	Ditto	
807	C	R	46.3	8.16	na	0.01	0.00007	62.51	na	0.02	1.64	18.27	5.22	na	130.12	na	Ditto	
808	C	R	61.3	7.88	na	0.02	0.000115	80.48	na	0.02	2.72	19.98	10.59	na	106.24	na	Ditto	
809	C	R	76.2	7.74	na	0.04	0.000522	79.87	na	0.02	11.87	24.89	29.32	na	170.52	na	Ditto	
810	C	R	48.3	7.6	na	0.03	0.000067	67.97	na	0.01	1.62	15.63	4.36	na	141.4	na	Ditto	
811	C	R	54	7.94	na	0.02	0.00025	70.36	na	0.02	3.56	17.84	9.57	na	148.24	na	Ditto	
812	C	R	53	7.9	na	0.02	0.000255	70.02	na	0.01	3.61	18.25	9.37	na	149.65	na	Ditto	
813	C	R	52.6	7.9	na	0.02	0.000674	68.91	na	0.01	3.3	18.62	8.32	na	138.92	na	Ditto	
814	C	R	52.5	7.99	na	0.02	0.000346	68.32	na	0.01	3.19	18.94	7.84	na	143.34	na	Ditto	
815	C	R	49.6	8.34	na	0.02	0.000957	63.87	na	0.01	3.1	19.13	7.34	na	148.35	na	Ditto	
816	C	R	50.7	8.18	na	0.06	0.000337	69.68	na	0.07	3.47	19.91	7.85	na	157.26	na	Ditto	
817	P	MD	1420	2.7	670	1343.67	471.256	498.169	96.58	4590.45	na	2092.66	na	22.79	13114.99	4912.21	Zanker et al. (2002)	

Type G: gold mine, P: polymetallic mine, M: metal mining, S: sulfur mine, C: coal mine, L: leachate, A: arsenic, PH: phosphate

Place R: river, MD: mine drainage / discharge water /mine water, G: groundwater well, LK: lake and I: induced.

Units: EC (mS/m), ORP (mV), Al, As, Ca, Cu, Fe, K, Mg, Na, Pb, SO_4, and Zn concentration (mg/L))

Appendix B. pH, EC and ORP for Bentonite

Bentonite-Cu system: pH, EC, and ORP

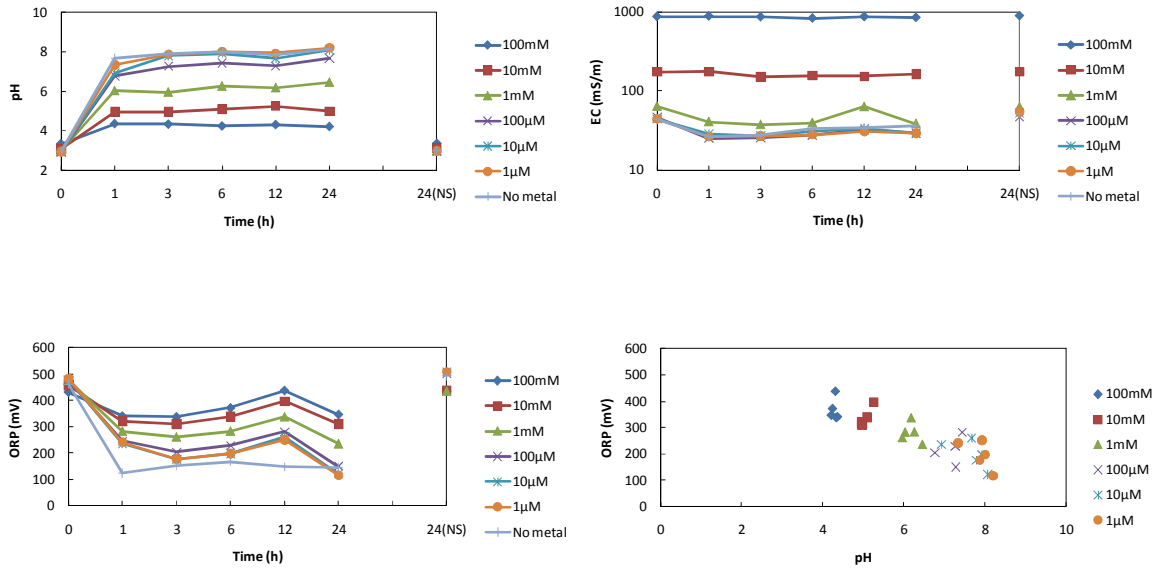

Bentonite-Fe system: pH, EC, and ORP

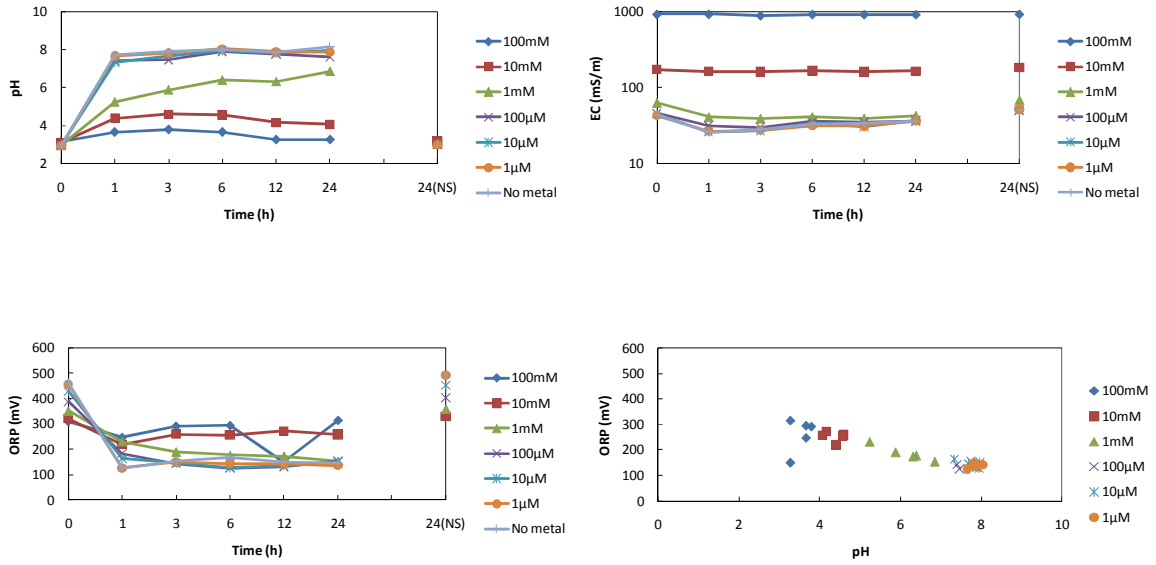

Bentonite-Zn system: pH, EC, and ORP

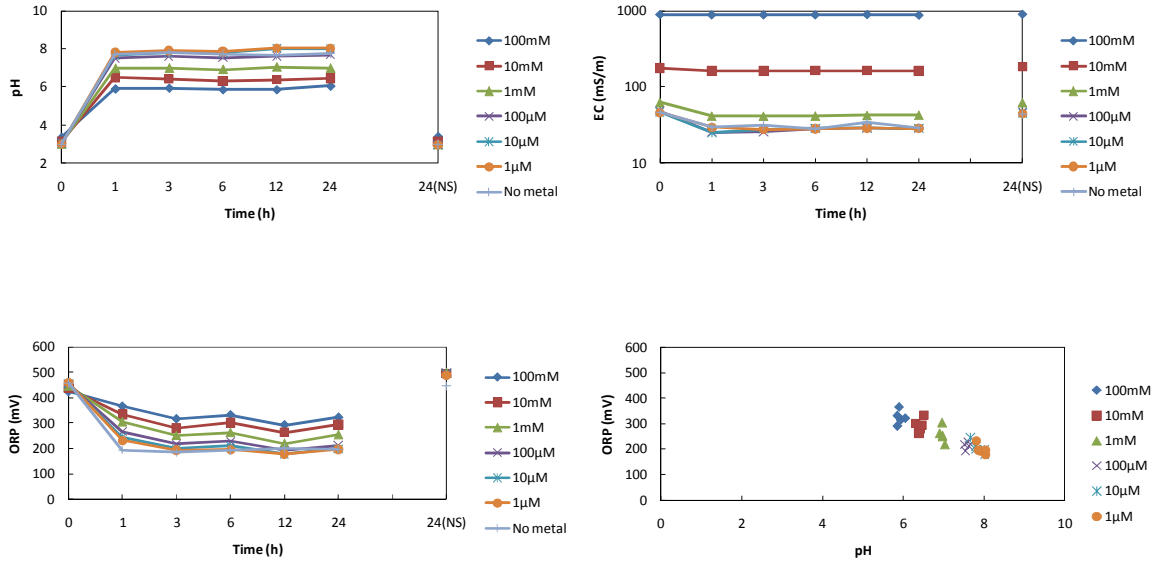

Bentonite-Al system: pH, EC, and ORP

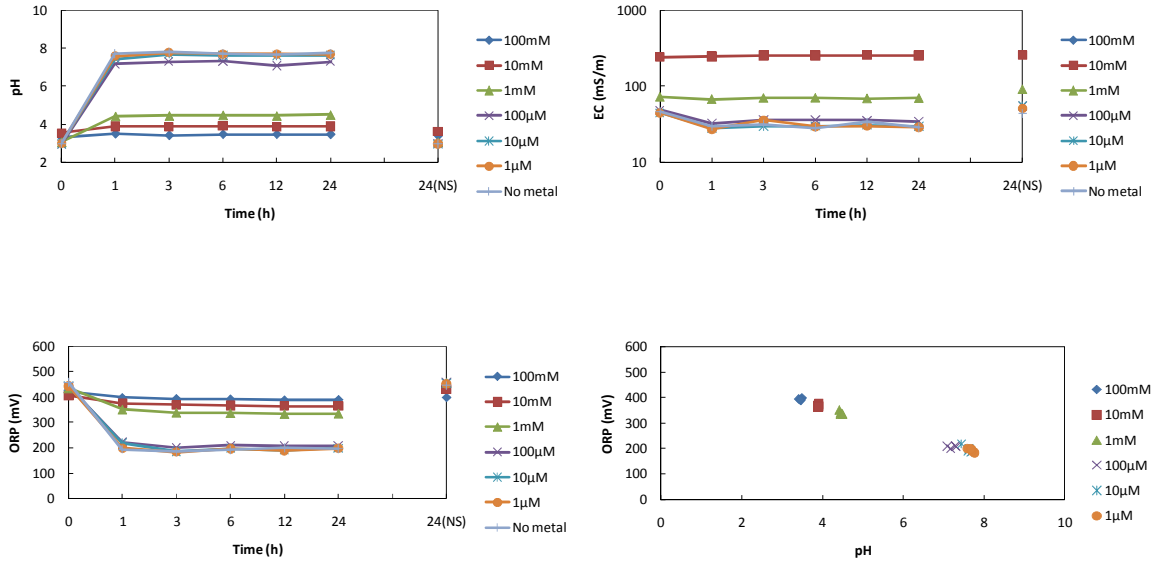

Bentonite-As system: pH, EC, and ORP

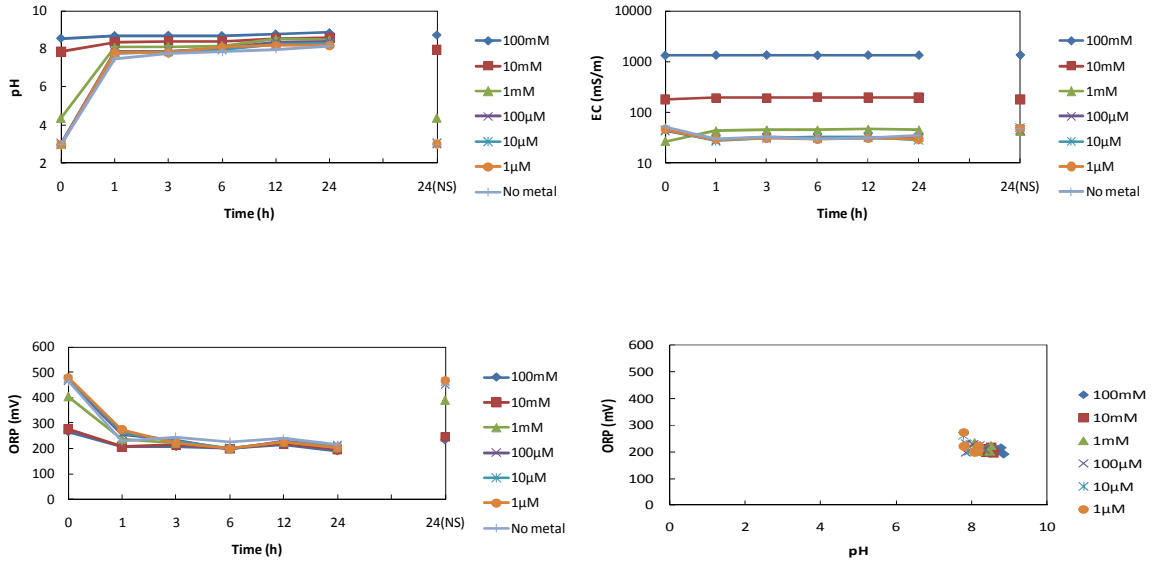

Bentonite-Pb system: pH, EC, and ORP

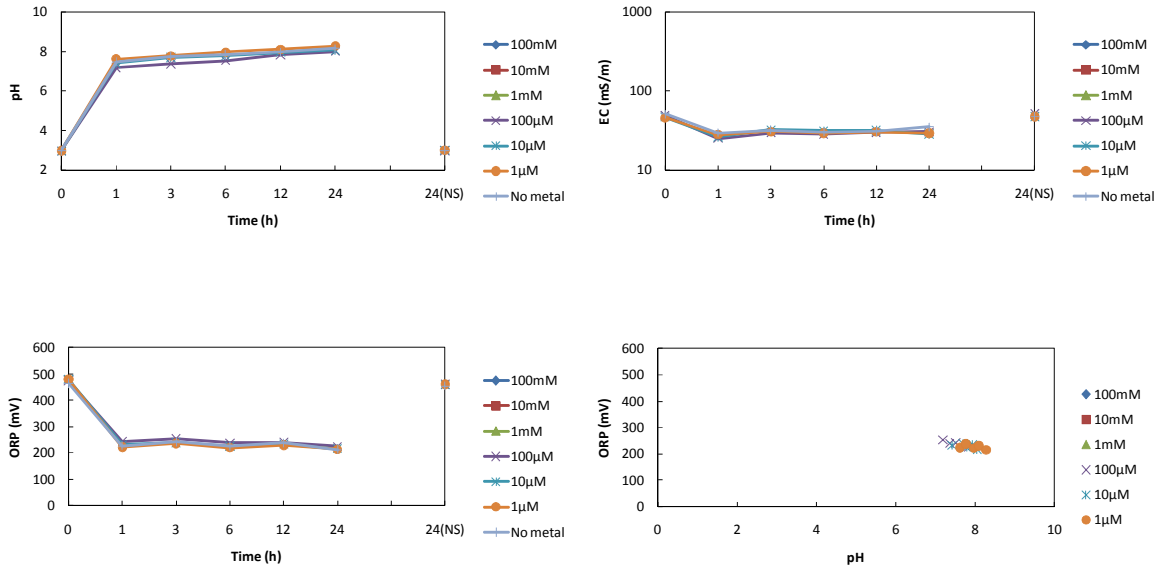

Appendix C. pH, EC and ORP for Zeolite

Zeolite-Cu system: pH, EC, and ORP

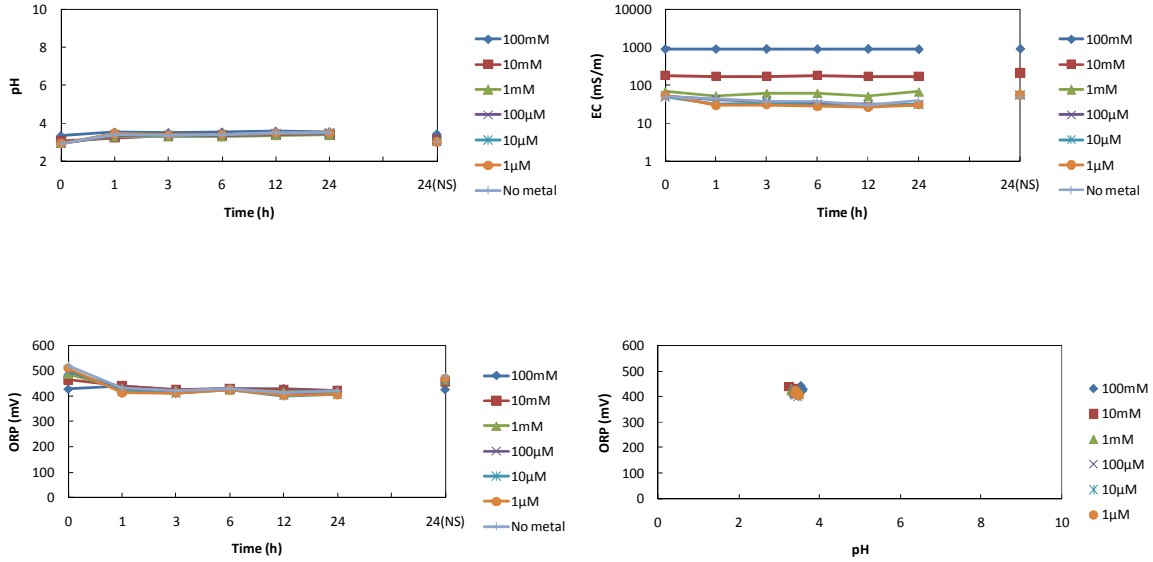

Zeolite-Fe system: pH, EC, and ORP

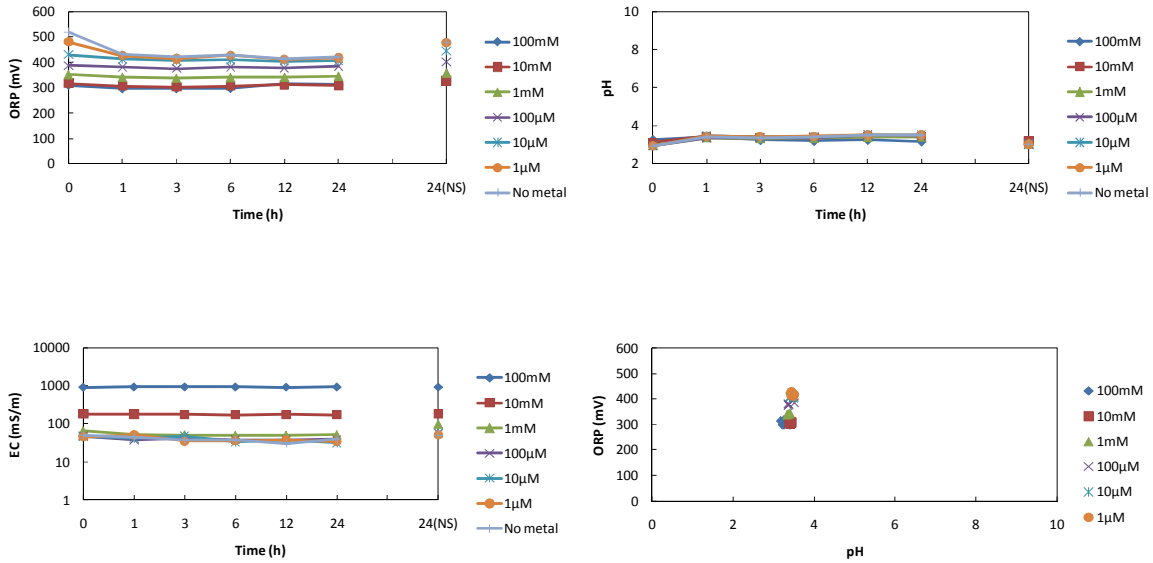

Zeolite-Zn system: pH, EC, and ORP

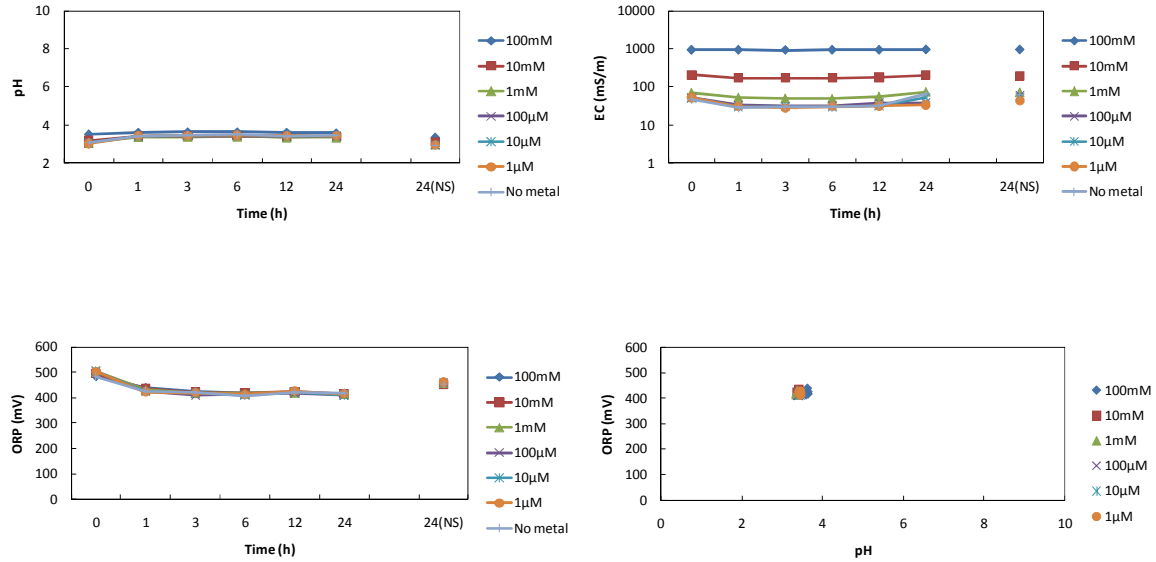

Zeolite-Al system: pH, EC, and ORP

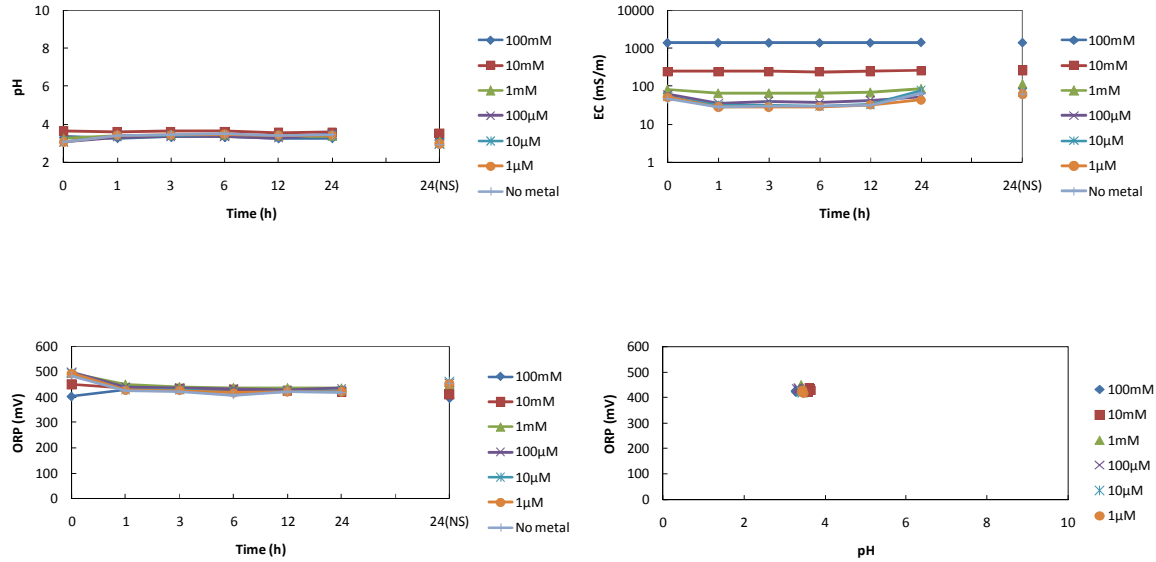

Zeolite-As system: pH, EC, and ORP

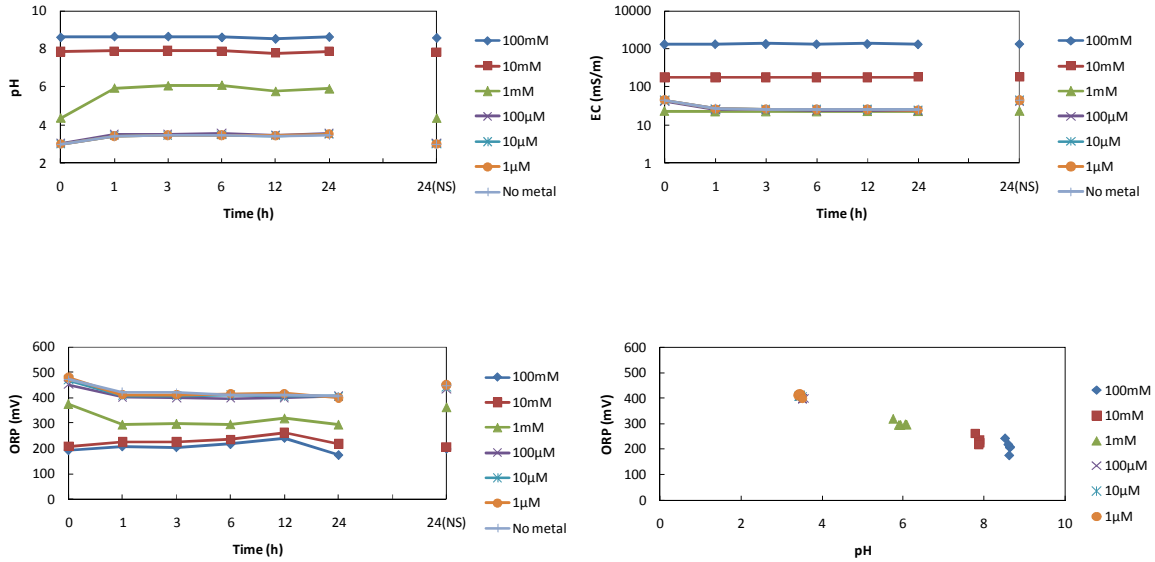

Zeolite-Pb system: pH, EC, and ORP

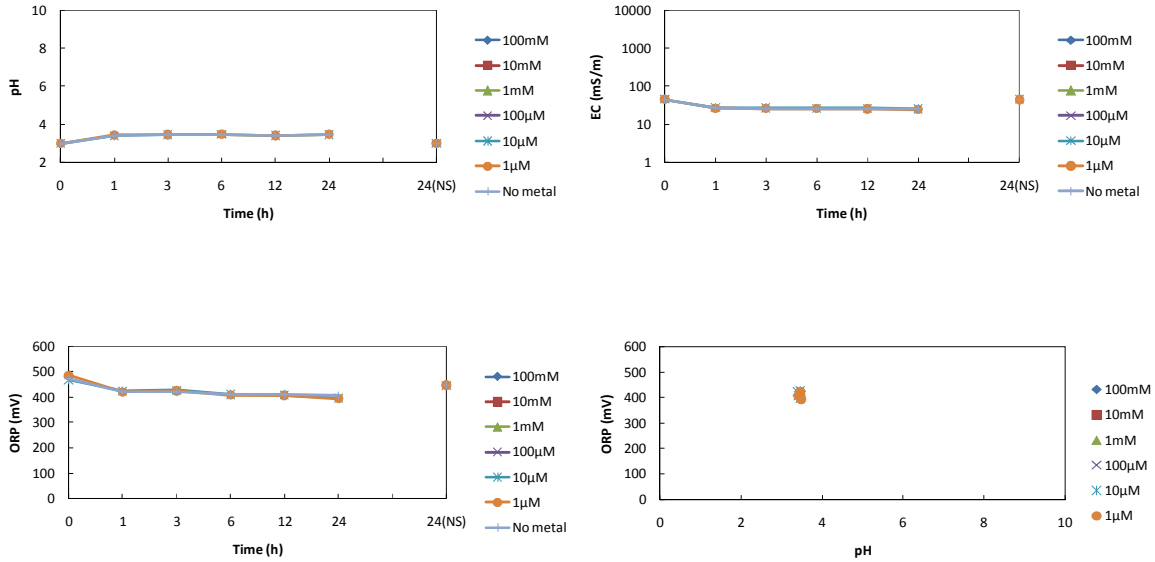

Appendix D. pH, EC and ORP for Ferrihydrite

Ferrihydrite-Cu system: pH, EC, and ORP

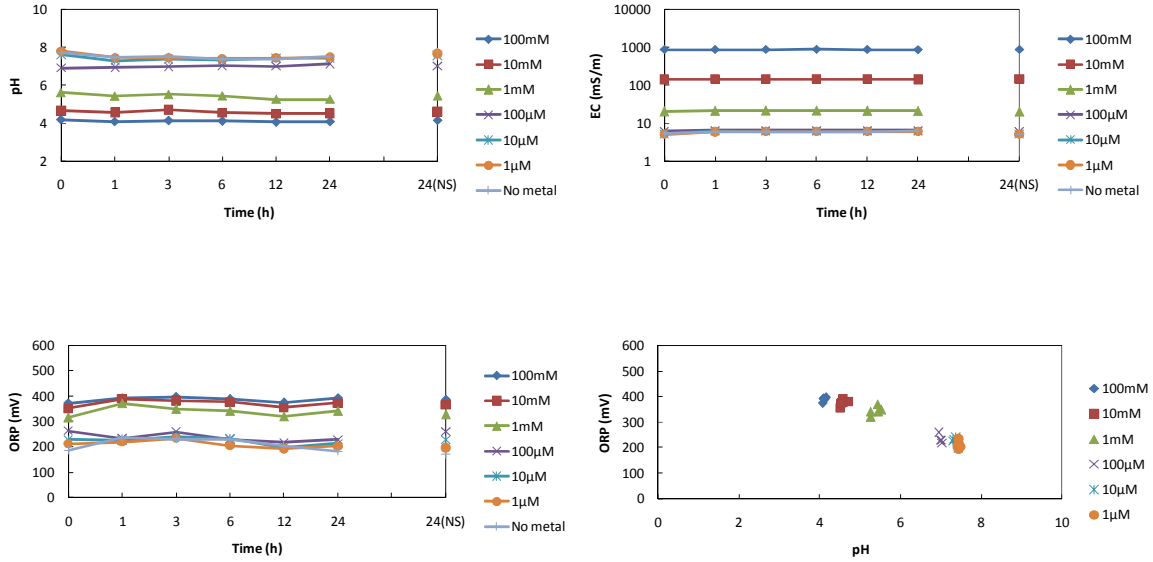

Ferrihydrite-Zn system: pH, EC, and ORP

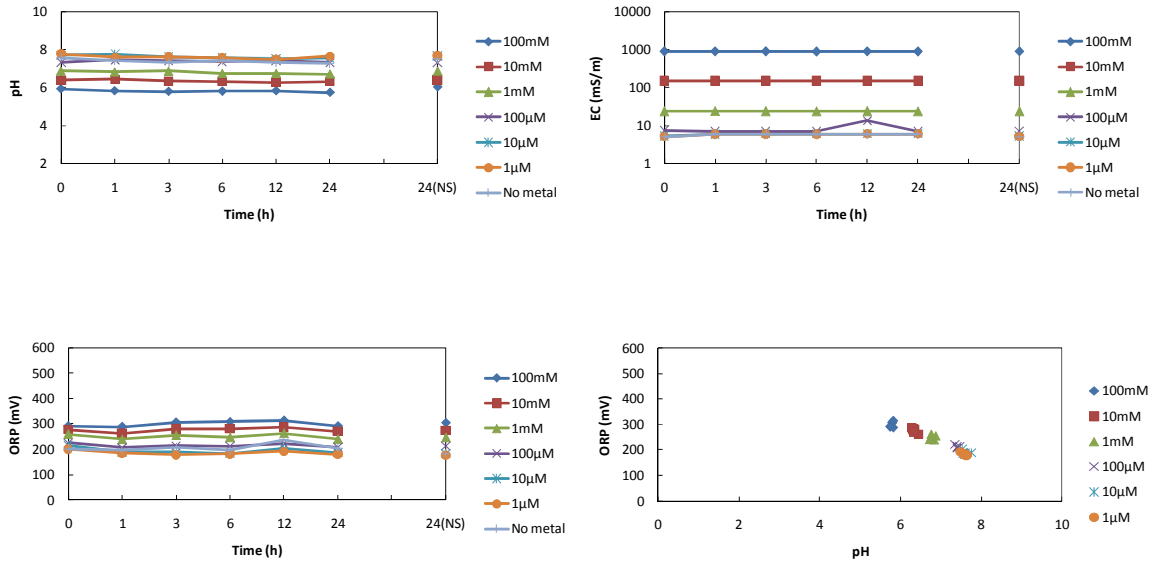

Ferrihydrite-Al system: pH, EC, and ORP

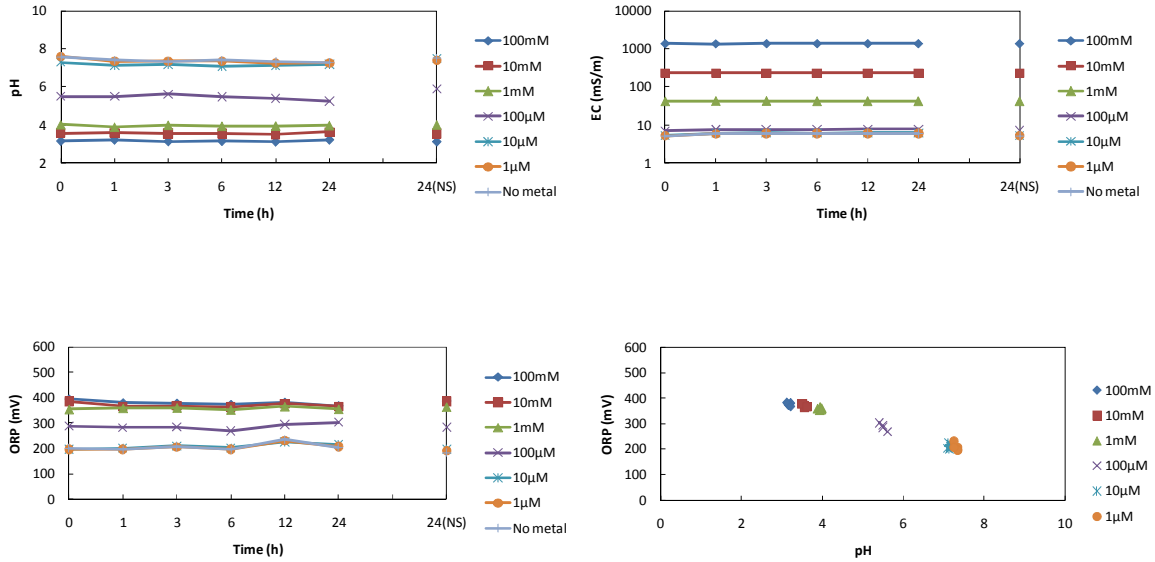

Ferrihydrite-As system: pH, EC, and ORP

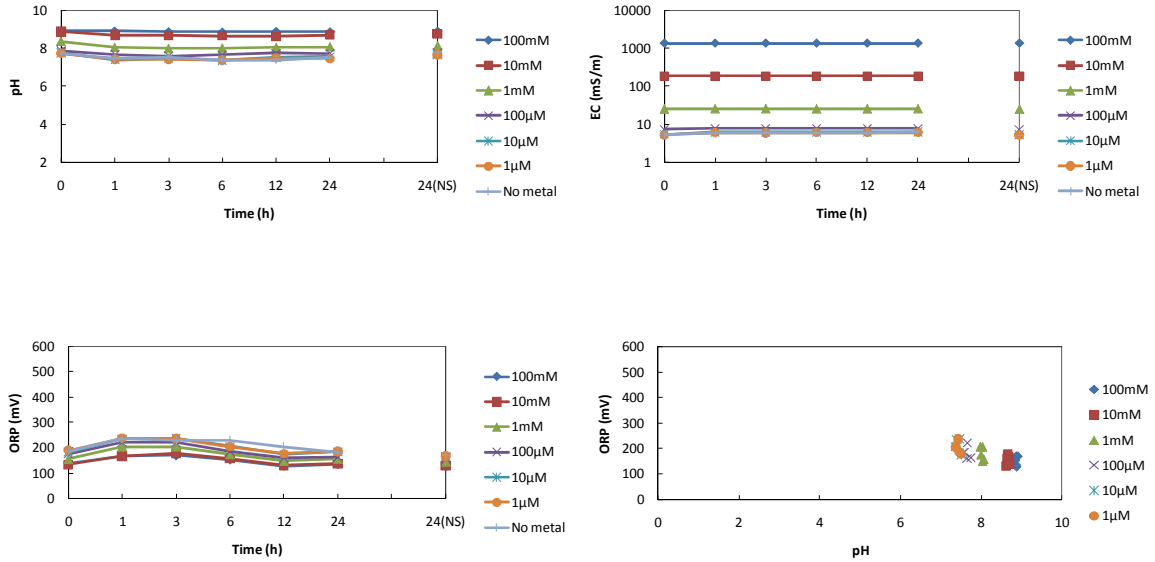

Ferrihydrite-Pb system: pH, EC, and ORP

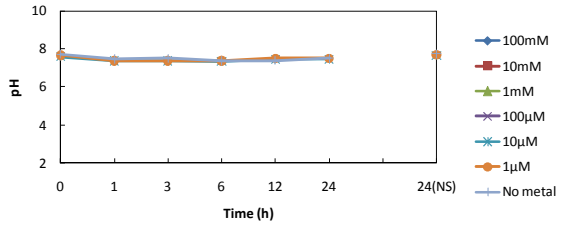

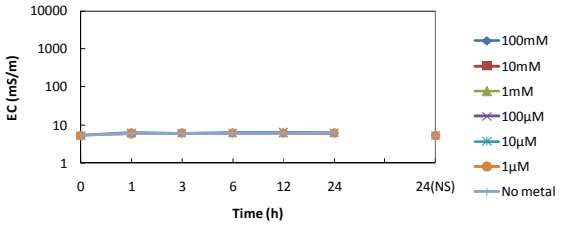

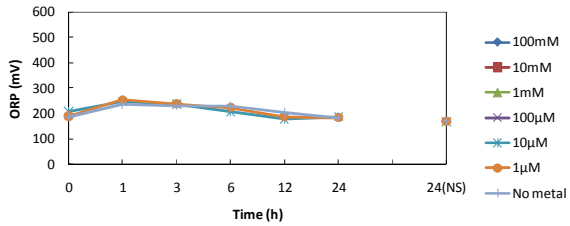

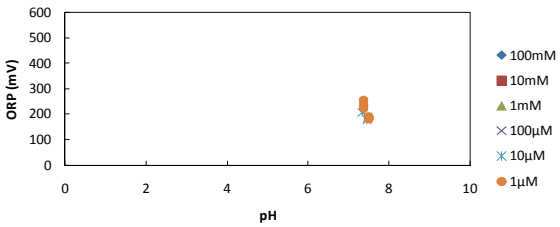

Appendix E. Na, Mg, K and Ca Concentration for Bentonite

Bentonite-Cu system: Na, Mg, K, and Ca concentration

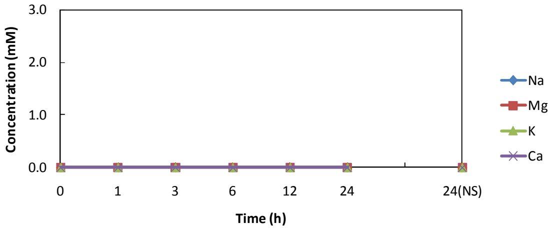

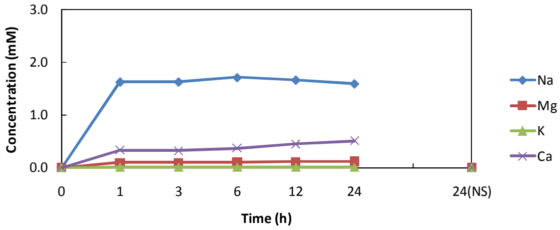

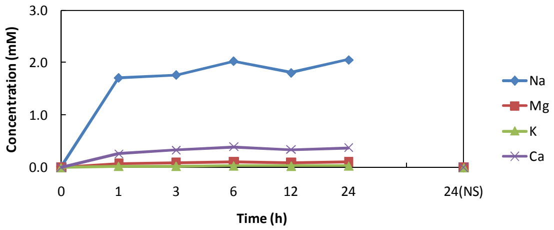

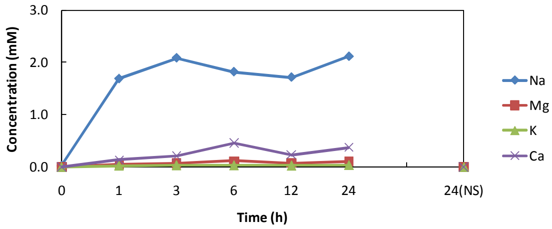

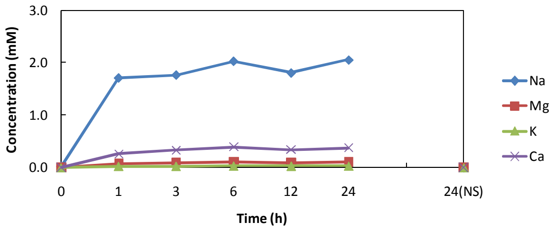

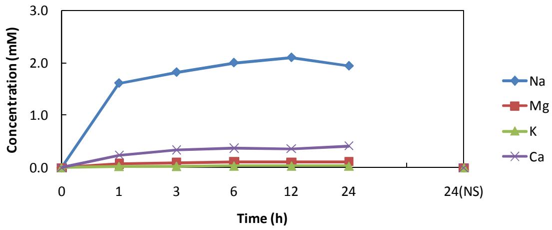

Bentonite-Fe system: Na, Mg, K, and Ca concentration

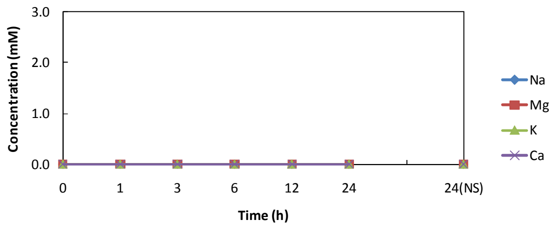

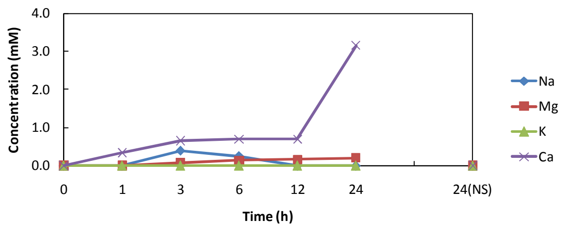

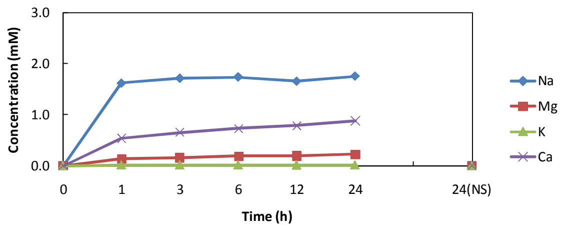

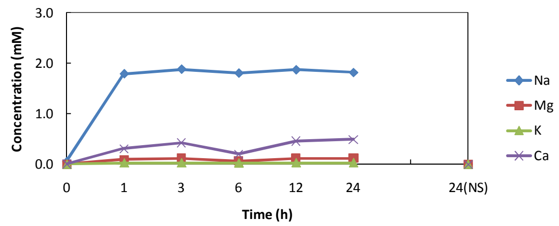

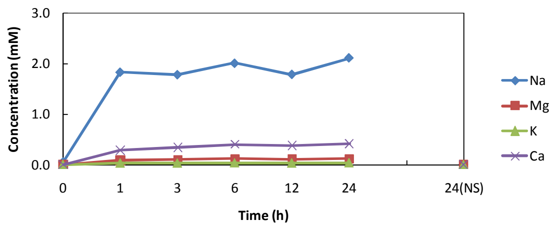

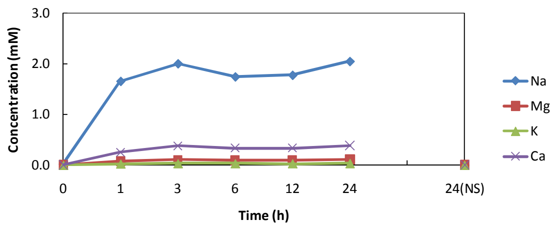

Bentonite-Zn system: Na, Mg, K, and Ca concentration

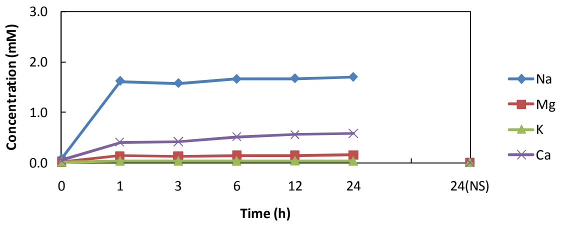

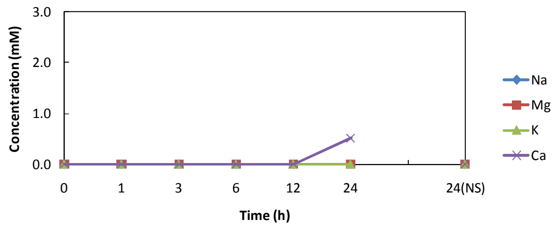

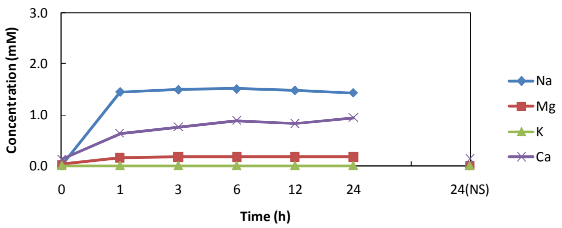

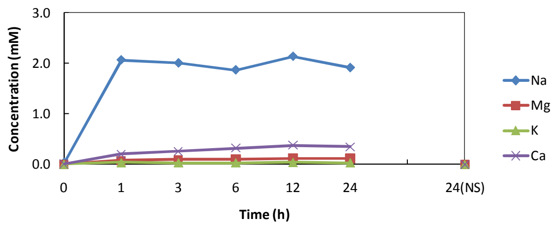

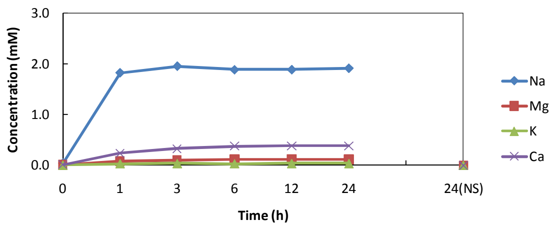

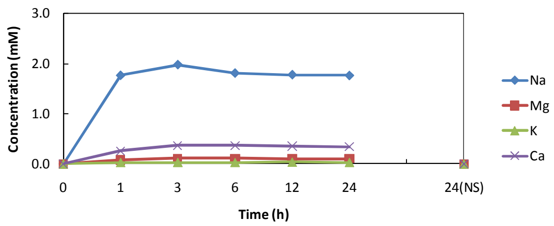

Bentonite-Al system: Na, Mg, K, and Ca concentration

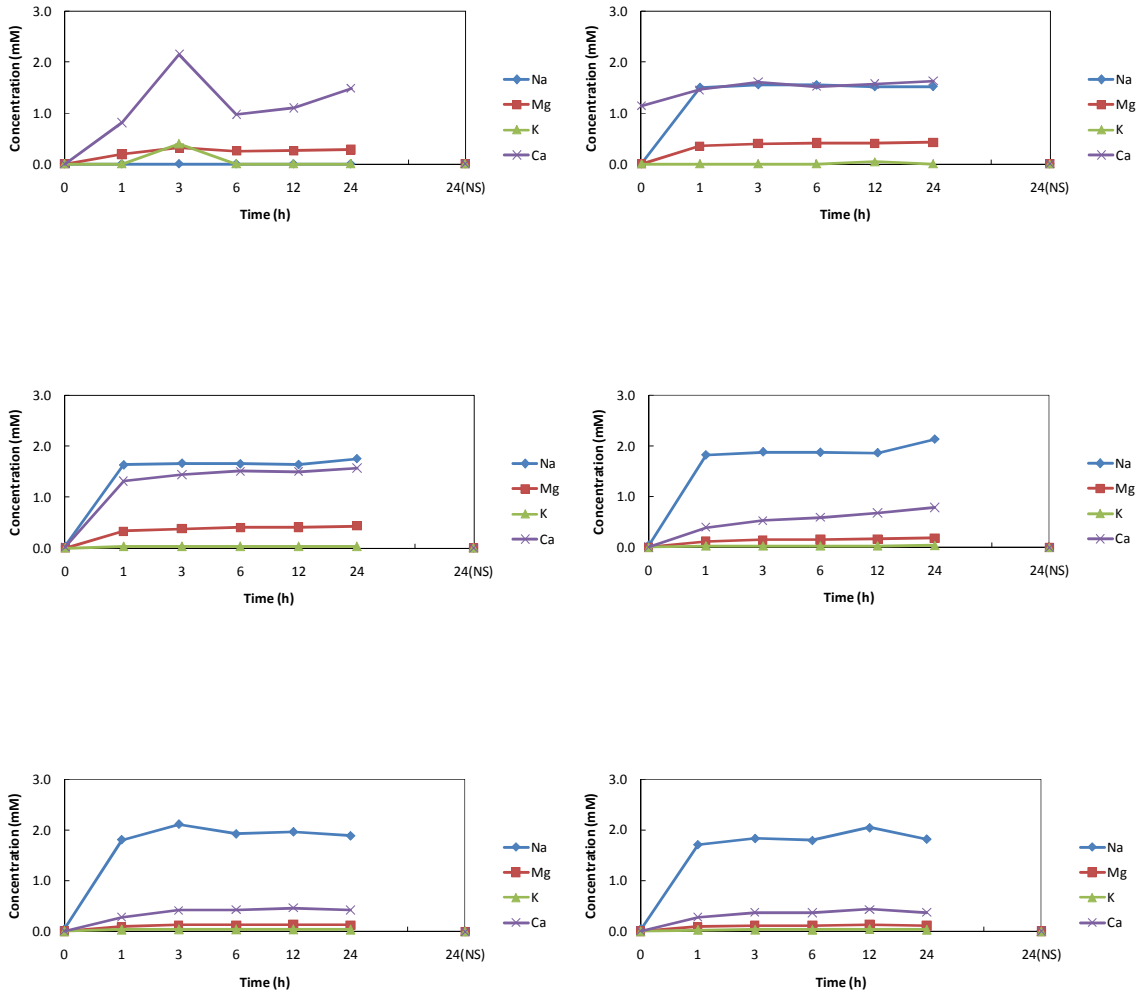

Bentonite-As system: Na, Mg, K, and Ca concentration

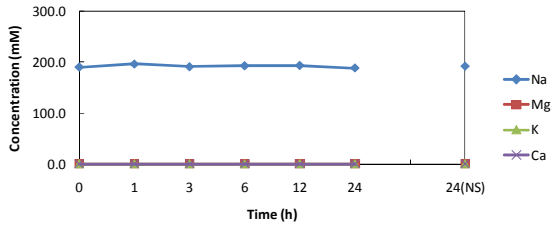

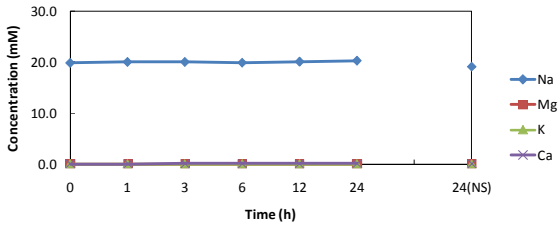

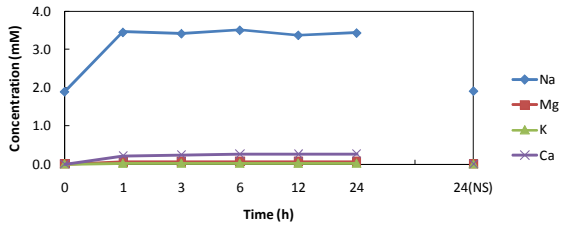

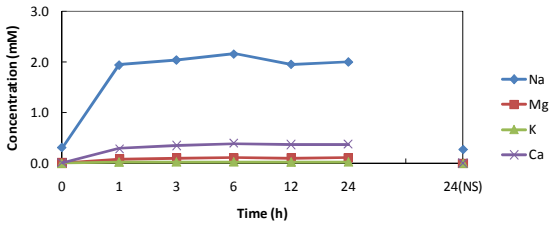

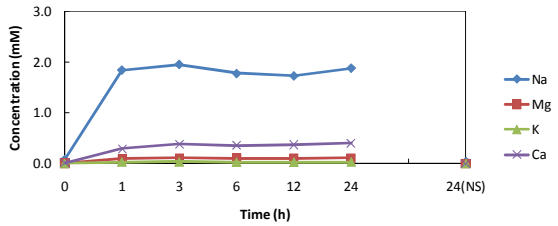

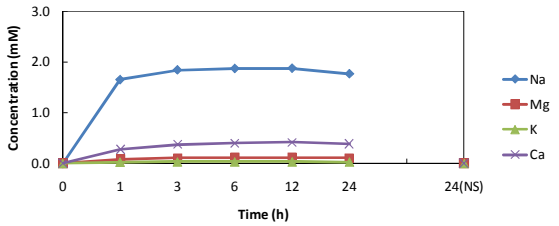

Bentonite-Pb system: Na, Mg, K, and Ca concentration

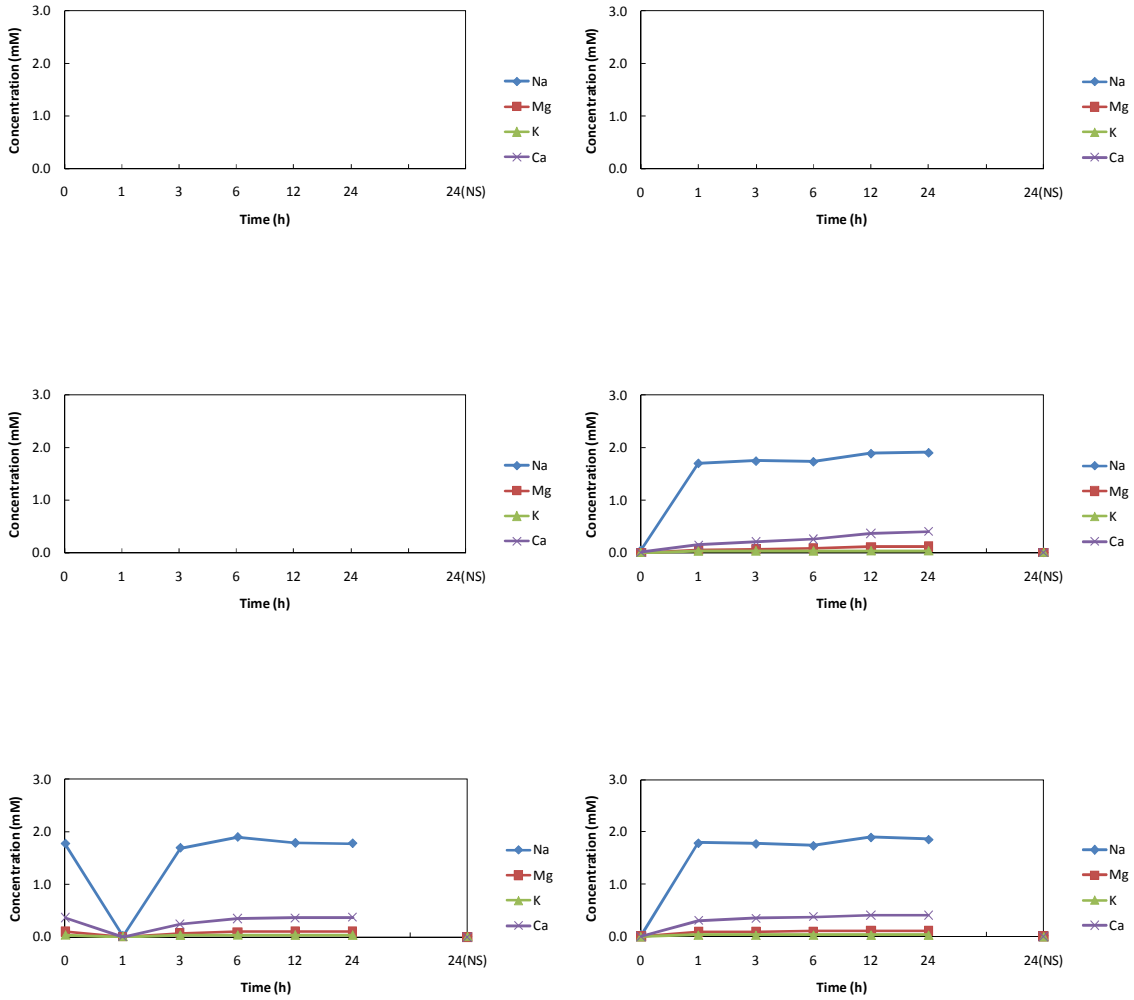

Appendix F. Na, Mg, K and Ca Concentration for Zeolite

Zeolite-Cu system: Na, Mg, K, and Ca concentration

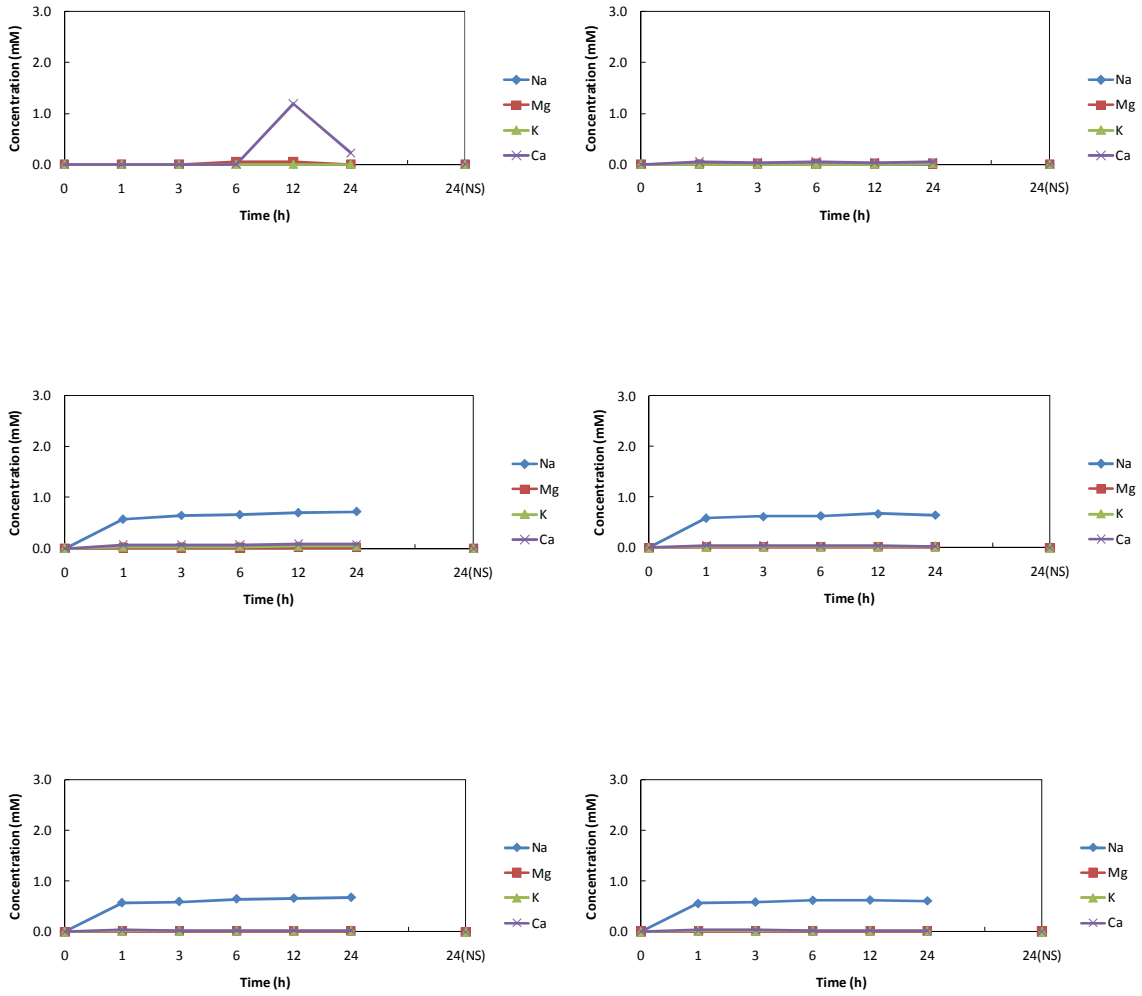

Zeolite-Fe system: Na, Mg, K, and Ca concentration

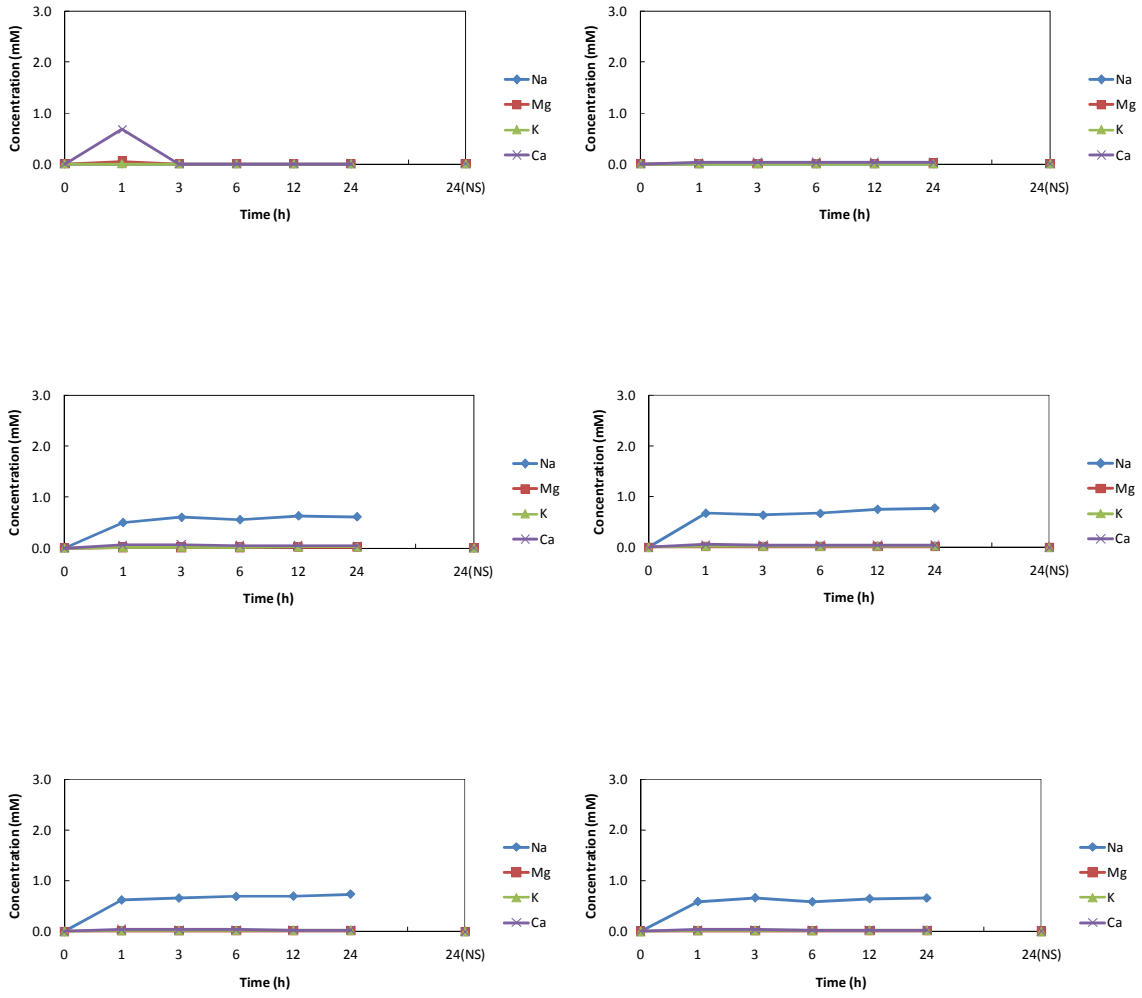

Zeolite-Zn system: Na, Mg, K, and Ca concentration

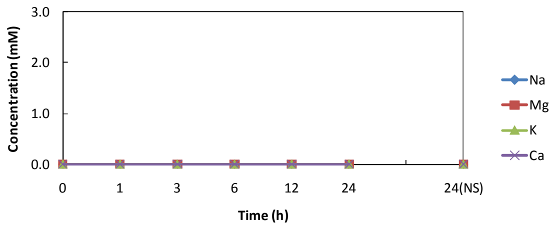

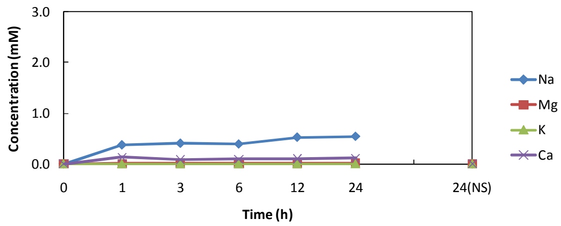

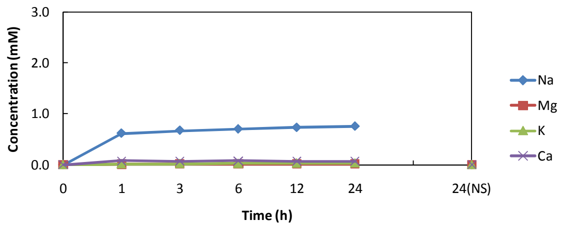

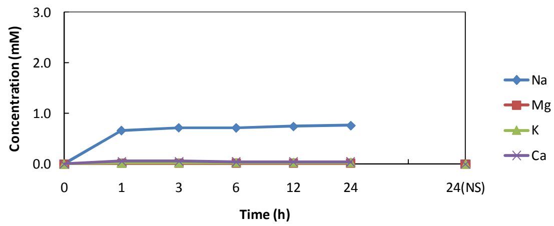

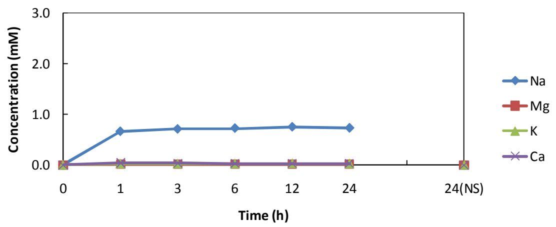

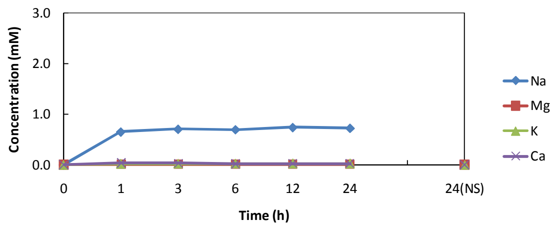

Zeolite-Al system: Na, Mg, K, and Ca concentration

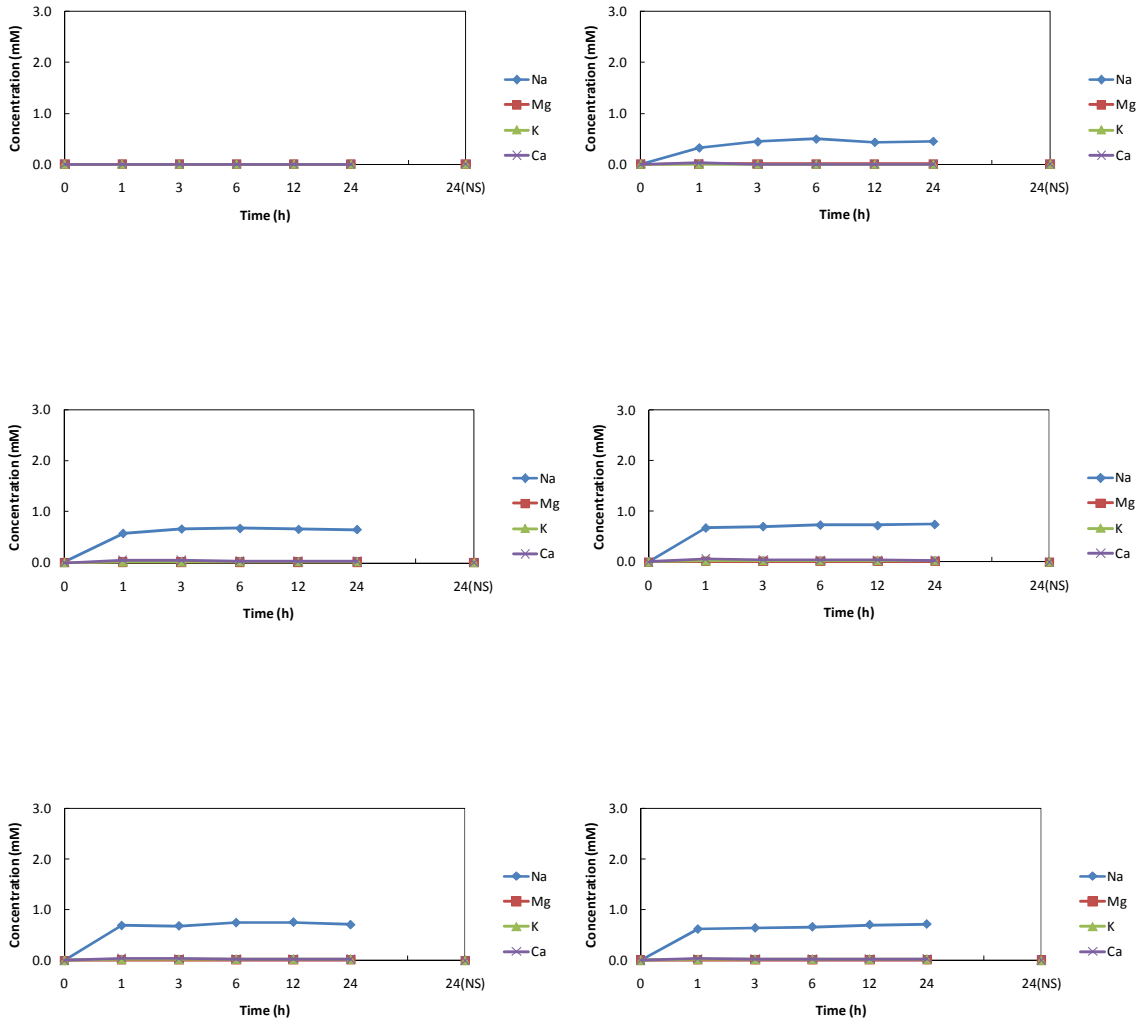

Zeolite-As system: Na, Mg, K, and Ca concentration

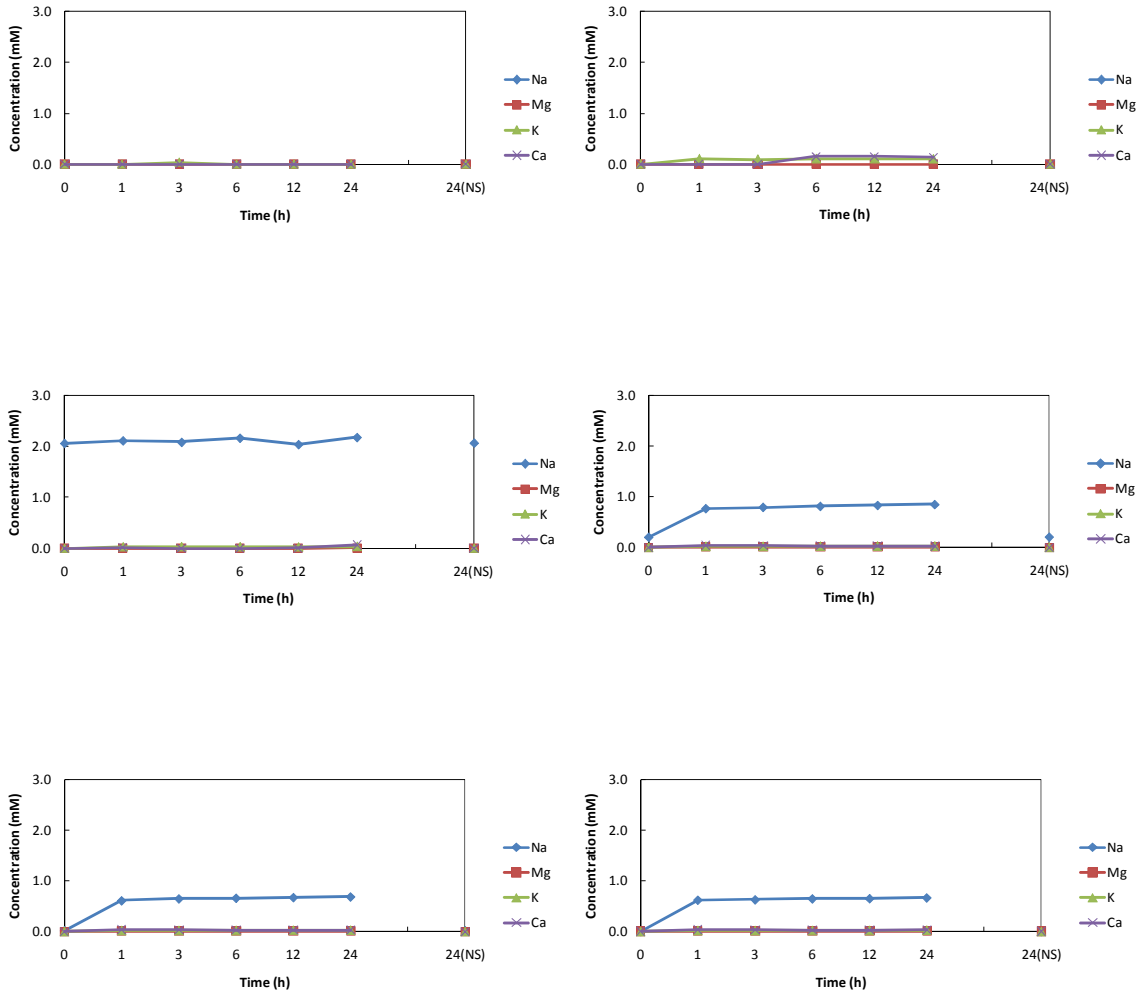

Zeolite-Pb system: Na, Mg, K, and Ca concentration

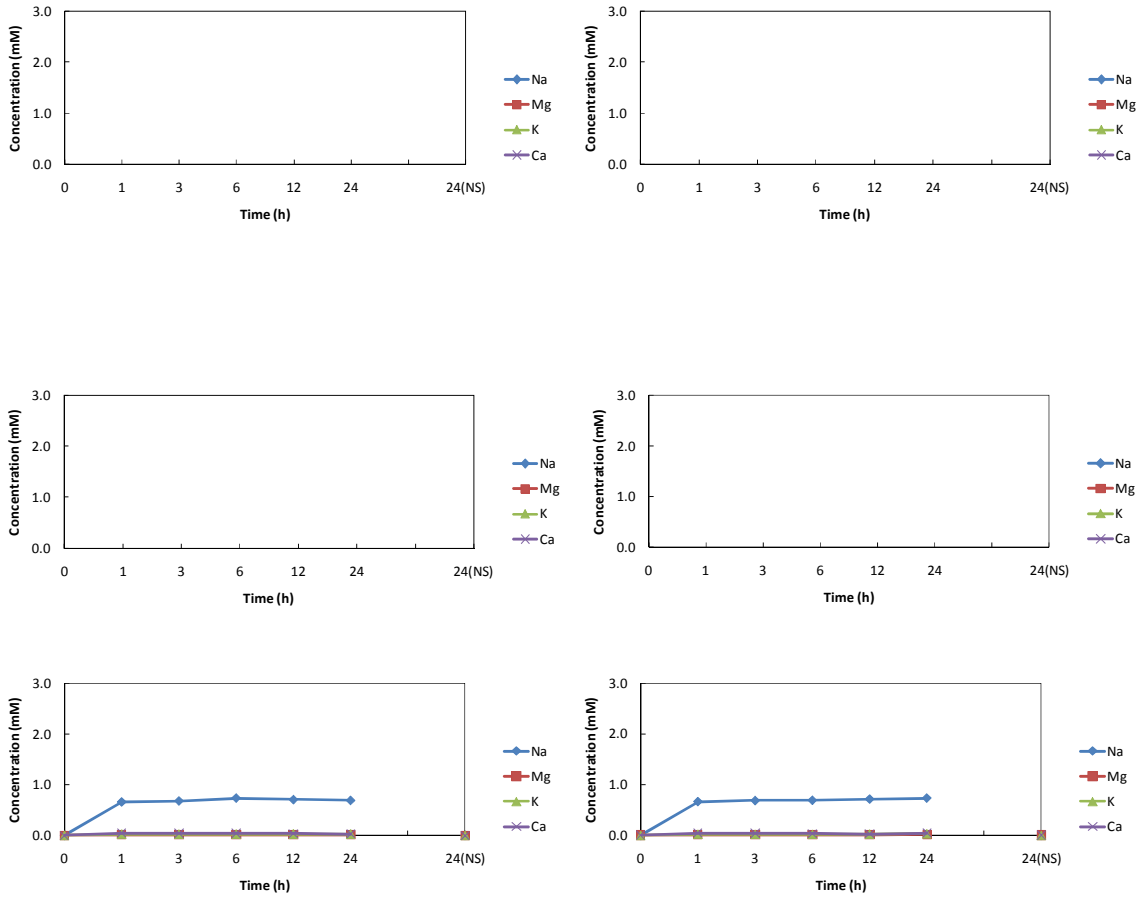

Appendix G. Na, Mg, K and Ca Concentration for Ferrihydrite

Ferrihydrite-Cu system: Na, Mg, K, and Ca concentration

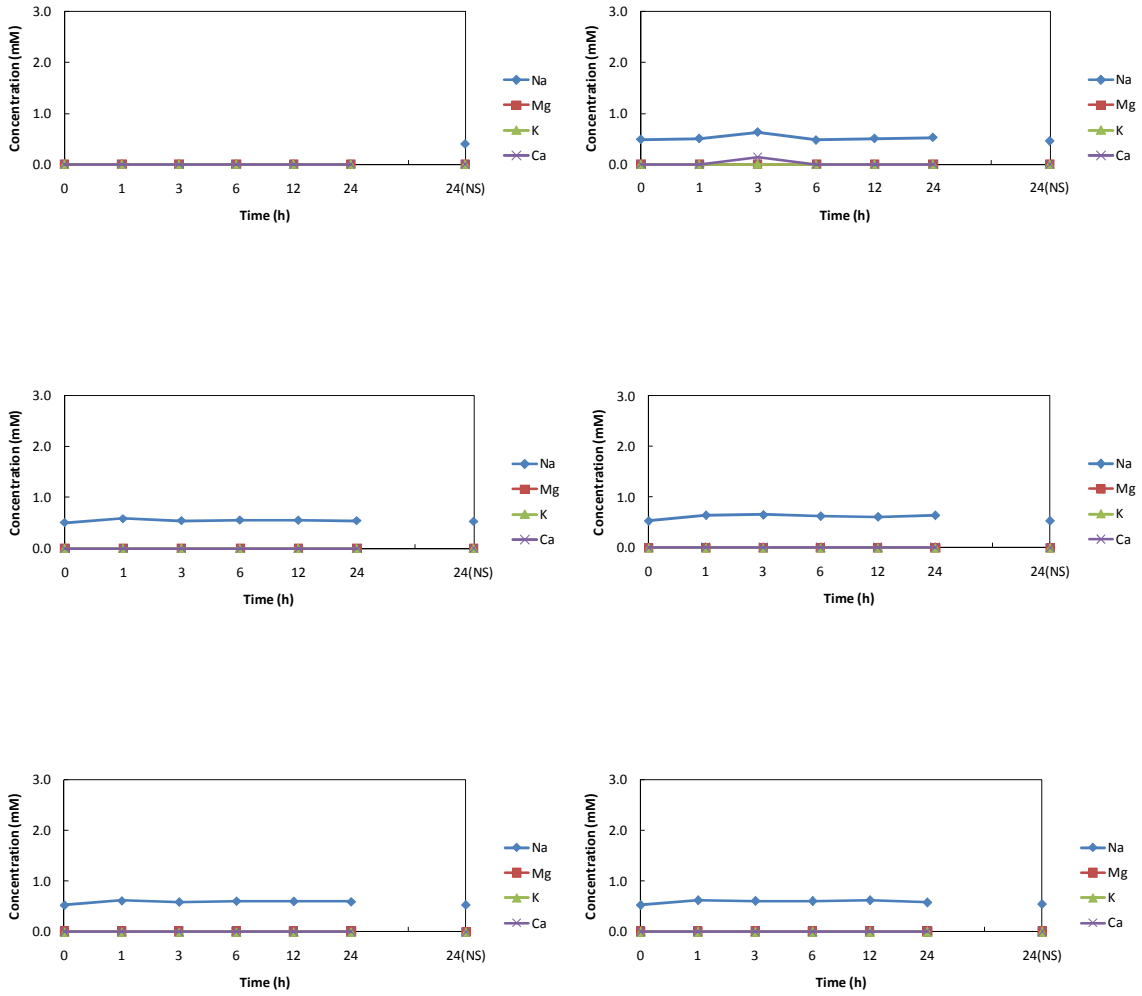

Ferrihydrite-Zn system: Na, Mg, K, and Ca concentration

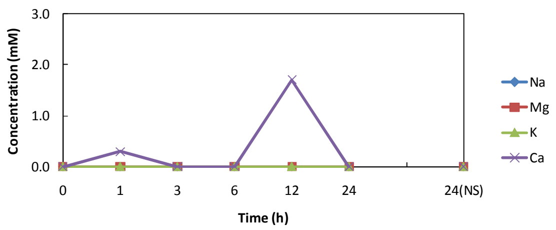

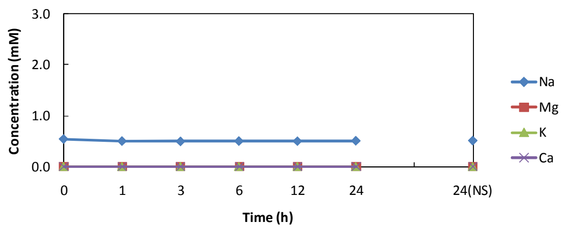

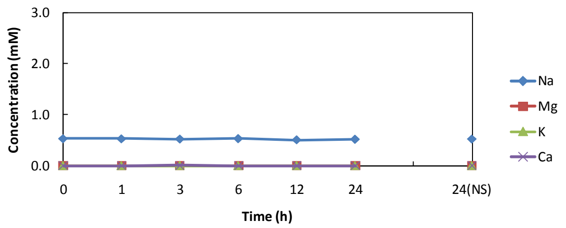

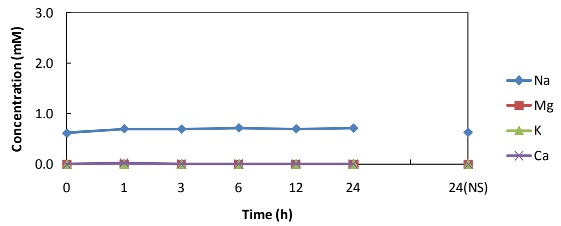

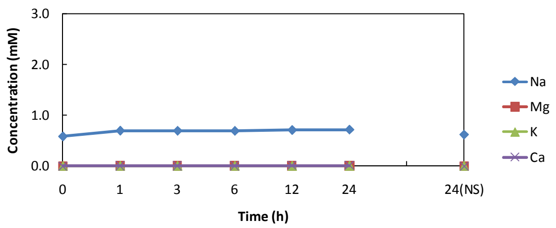

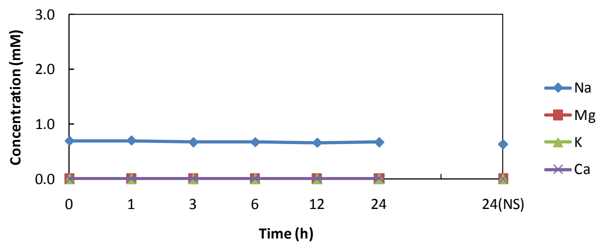

Ferrihydrite-Al system: Na, Mg, K, and Ca concentration

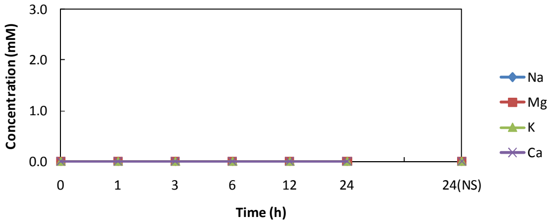

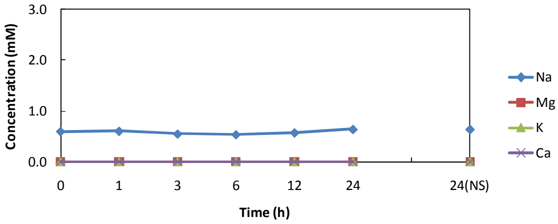

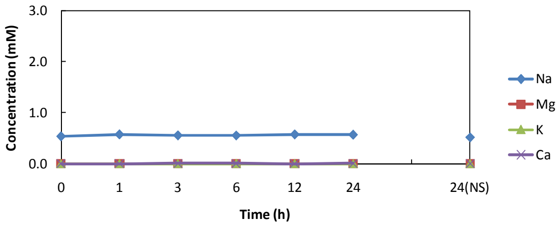

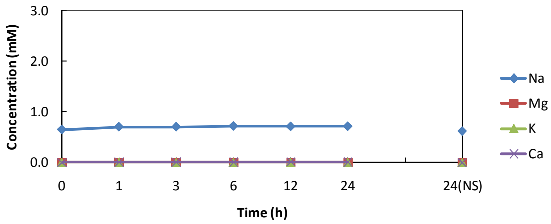

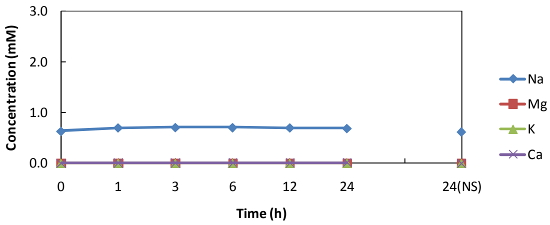

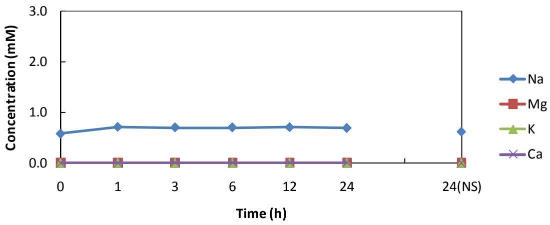

Ferrihydrite-As system: Na, Mg, K, and Ca concentration

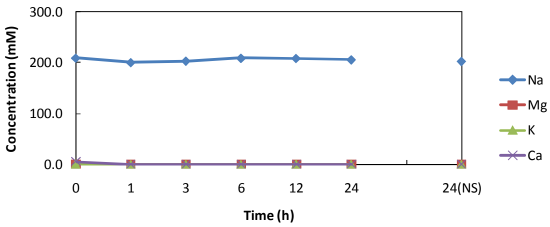

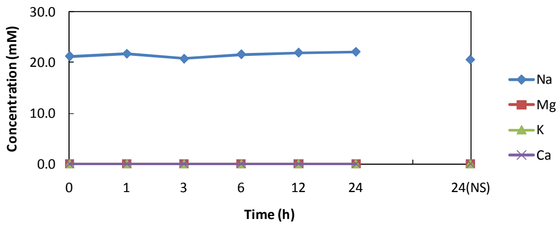

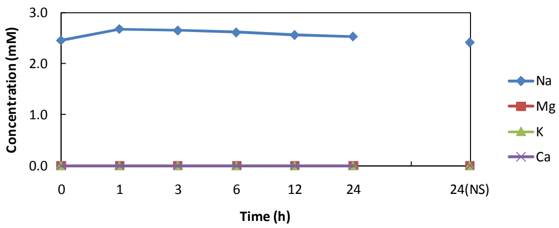

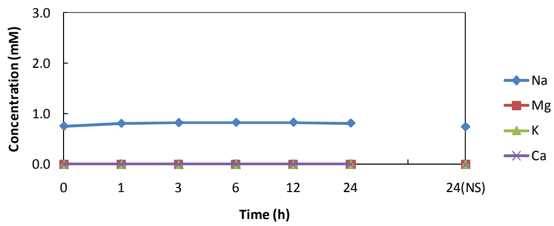

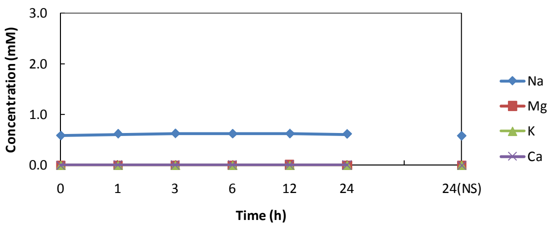

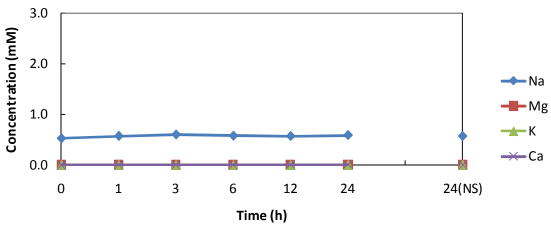

Ferrihydrite-Pb system: Na, Mg, K, and Ca concentration